

Systematic Investigation of Cuttings Transport Behavior in Horizontal and Inclined Drilling Operation

By

Mohammad Mojammel Huque

A Dissertation submitted to the School of Graduate Studies in partial fulfillment of the requirements for the degree of

Doctor of Philosophy

Faculty of Engineering and Applied Science

Memorial University of Newfoundland

May 2022

St. John's

Newfoundland, Canada

Abstract

Hole cleaning and cuttings transport play a vital role in the drilling operation. Various drilling problems such as a reduction in penetration rate, an increase in the torque and drag, and an increase in the potential of differential sticking are often related to poor cuttings transport from a wellbore. A variety of parameters, including the fluid rheology, mud velocity, cuttings size, and drill pipe inclination generally influence the cuttings transport performance. Although several experimental and modelling research investigations have been conducted in this area, there are controversial findings about the effect of different parameters on cuttings transport. For instance, the interactions among the parameters during cuttings transport which have not been adequately investigated. In this thesis, we systematically study the effect of drilling parameters on cuttings transport, especially interaction effects of the drilling parameters through experiments and Computational Fluid Dynamics (CFD) method.

An extensive experimental study was conducted to investigate the flow behavior of solid cuttings based on Newtonian and non-Newtonian Herschel Bulkley fluid models. Experiments were performed to simulate solid transport behavior in horizontal and near horizontal well trajectories. A high-speed imaging technology was used to visualize the cuttings transport behavior in the annulus section. This visualization tool validates the mechanistic three-layer model of cuttings transport and transition from a stagnant solid bed to a homogeneous single layer model of cuttings transport mechanism. An Electrical Resistance Tomography (ERT) system was used to observe the cutting transport which is capable of providing instantaneous cuttings volume fraction in the annular section of the experimental system.

ERT data shows cuttings concentration versus with change in fluid rheology, fluid velocity, eccentricity, drill pipe rotation, rate of penetration, and inclination angle. Experimental studies in the horizontal wells show that cuttings transport capability of non-Newtonian fluid increases upon an increase in fluid velocity, and drill pipe rotation. A higher viscous fluid carries more cuttings in the dispersed phase; however, transport capability reduces significantly through suspension mechanism with increasing fluid velocity and drill pipe rotation. A comparison of four different non-Newtonian fluid cases shows that turbulence plays a key role in cuttings transport in the horizontal well regardless of fluid rheology. This experimental study reveals that a higher ‘Minimum Transport Velocity (MTV)’ is required to move a solid dune in the annulus for a highly viscous fluid.

CFD modeling approach is employed to simulate the cuttings transport behaviors in the horizontal and inclined wellbore cases. Cuttings transport in the wellbore annulus represents a solid-liquid multiphase flow phenomenon. The Eulerian-Eulerian multiphase flow model is adopted to describe the flow characteristics in the wellbore annular section. A proper Design of Experiments (DOE) is used to systematically study the interactions among the independent variables. A comprehensive parametric sensitivity analysis is then conducted to obtain a better understanding of the relationship between the input variables and the target parameters (cutting transport performance). It is found that the mud viscosity, mud velocity, and drill pipe rotation have a positive impact on cuttings transport, whereas the cuttings size and annular clearance show a significant adverse effect on cuttings transport performance in the horizontal wells. Although both drilling mud viscosity and velocity exhibit the positive effect, the interaction among them shows a negative influence on cuttings transport. Analysis shows that the cuttings with a size of 1 to 2 mm are difficult to be cleaned, compared to larger cuttings. According to the CFD investigation,

the critical inclination angle prone to hole clogging is a function of a wide range of flow rates and fluid rheologies. Also, this study investigated two factor interaction of fluid rheology and velocity for the inclined wellbore orientation. Finally, a generalized expression of cutting transport efficiency is proposed for the inclined well considering two factor and three factor interactions.

Acknowledgements

I want to take the opportunity to thank my supervisors Dr. Syed Imtiaz, Dr. Stephen Butt and Dr. Sohrab Zendeboudi for all of their generous help, support, and valuable suggestions throughout my academic voyage. They encouraged and supported me with appropriate directions, spending hours with me over various stages of the research work.

I would also like to thank Dr. Mohammad Azizur Rahman for his magnificent support to conduct my experimental work at Texas A&M University at Qatar. I would also like to thank Dr. Faisal Khan for his leadership and administrative support during the crucial transition time of my Ph.D. program in 2018.

I gratefully acknowledge and thank Equinor Canada, School of Graduate Studies, Memorial University, Faculty of Engineering and Applied Science, InnovateNL, Natural Sciences and Engineering Research Council of Canada (NSERC) and Compute Canada for supporting my research work. I would like to thank Qatar National Research Fund (QNRF) a member of the Qatar Foundation, to support my experimental work at Texas A&M University at Qatar.

I would like to thank Dr. Muhammad Saad Khan and Mr. Abinash Barooah for their enormous support during my experimental work at Texas A&M University at Qatar. Also special thanks to other team members Dr. Hicham Ferroudji, Muhammad Yousuf Khan, and Dr. M. Fahed Qureshi at Texas A&M University at Qatar.

I would like to thank my research colleagues and friends in Memorial University who helped me through the journey with the share of their knowledge and expertise. I would like to thank the staff of Faculty of Engineering and Applied Science, Colleen Mahoney and Tina Dwyer, for their

endless support throughout my Ph.D. I would also thank to the Engineering Computing Service to provide me enormous assistance during my academic program at Memorial University.

I would like to express the highest gratitude to my family in St. John's and in Bangladesh, especially my wife Farhana Akter who supported me from the very beginning of my academic life. Farhana supported me in all critical discussions in my research and helped me by reviewing and proof reading of my manuscripts. I also thank my siblings and relatives for their encouragement and support. Finally, I express my greatest gratitude to my mother Aysha Begum and dedicate this thesis to my father late Abdul Huque.

Co-authorship Statement

I, **Mohammad Mojammel Huque**, hold the primary author status for all the Chapters in this thesis. However, each manuscript is co-authored by my supervisors, co-supervisors, and external research collaborators. Contributions of each of the co-authors are listed below:

1. Mohammad Mojammel Huque, Stephen Butt, Sohrab Zendehboudi, Syed Imtiaz, **“Systematic Sensitivity Analysis of Cuttings Transport in Drilling Operation Using Computational Fluid Dynamics Approach”** has been published in Journal of Natural Gas Science and Engineering. <https://doi.org/10.1016/j.jngse.2020.103386>

Statement: The research was conducted by Mohammad Mojammel Huque as the first author. He prepared the manuscript. Other authors supervised the student, reviewed the manuscript, and provided feedback.

2. Mohammad Mojammel Huque, Syed Imtiaz, Stephen Butt, Sohrab Zendehboudi, Mohammad Azizur Rahman, **“Experimental Study of Drill Cuttings Transport in Horizontal Well with Newtonian Fluid”** Proceedings of the ASME 2020, 39th International Conference on Ocean, Offshore & Arctic Engineering, OMAE2020, August 3 -August 7, 2020, Virtual, online. <https://doi.org/10.1115/OMAE2020-18751>

Statement: The research was conducted by Mohammad Mojammel Huque as the first author. He prepared the manuscript based on the experimental data. Mohammad Azizur Rahman supervised the student in the experimental work. Other authors supervised the first author, reviewed the manuscript, and provided feedback.

3. Mohammad Mojammel Huque, Mohammad Azizur Rahman, Sohrab Zendehboudi, Stephen Butt and Syed Imtiaz, “**Investigation of Cuttings Transport in a Horizontal Well with High-Speed Visualization and Electrical Resistance Tomography Technique**” manuscript has been published in the Journal of Natural Gas Science and Engineering. <https://doi.org/10.1016/j.jngse.2021.103968>

Statement: The research was conducted by Mohammad Mojammel Huque as the first author. He prepared the manuscript based on the experimental phase. Mohammad Azizur Rahman supervised the experimental work. Other authors supervised the student, reviewed the manuscript, and provided feedback.

4. Mohammad Mojammel Huque, Syed Imtiaz, Sohrab Zendehboudi, Stephen Butt, Mohammad Azizur Rahman and Priyank Maheshwari, “**Experimental Study of Cuttings Transport with Non-Newtonian Fluid in an Inclined Well Using Visualization and Electrical Resistance Tomography Techniques**” has been published in SPE Drilling & Completion. SPE-201709-PA. <https://doi.org/10.2118/201709-PA>

Statement: The research was conducted by Mohammad Mojammel Huque as the first author. He prepared the manuscript based on the results of the experimental work. Mohammad Azizur Rahman supervised the experimental work. Other authors supervised him, reviewed the manuscript, and provided feedback.

5. Mohammad Mojammel Huque, Mohammad Azizur Rahman, Sohrab Zendehboudi, Stephen Butt and Syed Imtiaz, “**Experimental and Numerical Study of Cuttings Transport in The Inclined Drilling Well**” manuscript has been published in the Journal of Petroleum Science and Engineering. <https://doi.org/10.1016/j.petrol.2021.109394>

Statement: The research was conducted by Mohammad Mojammel Huque as the first author. He prepared the manuscript. Other authors supervised the student, reviewed the manuscript, and provided feedback.

*The manuscripts presented in this thesis is slightly different than the published version.

Table of Contents

Chapter 1 Introduction.....	1
1.1 Background and motivation.....	1
1.2 Literature Review.....	3
1.3 Knowledge Gaps.....	10
1.4 Objectives.....	11
1.5 Research Tools and Expected Outcomes	12
1.6 Organization of Thesis	14
Chapter 2 : Systematic Sensitivity Analysis of Cuttings Transport in Drilling Operation Using Computational Fluid Dynamics Approach	28
2.1 Introduction.....	29
2.2 Theory and Background	32
2.2.1 Solid-Liquid Flow	32
2.2.2 Performance Measurement.....	38
2.2.3 Statistical Analysis	39
2.3 Methodology.....	40
2.3.1 Design of Experiment.....	40
2.3.2 Simulation Setup	41
2.3.3 Simulation Algorithm.....	45
2.3.4 Limitations of the Implemented Model.....	47
2.4 Results and Discussion.....	47
2.4.1 Model Validation.....	47
2.4.2 DOE for Fluid Rheology	50
2.4.3 DOE for Operational Parameters.....	53
2.4.4 DOE for Cuttings Size, Annular Space, and Eccentricity.....	57
2.4.5 Comparison of Significant Parameters.....	63
2.5 Conclusions	66
Chapter 3 : Experimental Study of Drill Cuttings Transport in Horizontal Well with Newtonian Fluid	77
3.1 Introduction.....	78
3.2 Experimental Procedure	79

3.2.1 Methodology.....	81
3.3 Results and Discussion.....	83
3.3.1 Effect of Mud Flow Rate and Inner Pipe Rotation.....	83
3.3.2 Effect of Eccentricity.....	86
3.3.3 Dune Movement Time.....	89
3.3.4 Annular Solid Volume Fraction Analysis.....	91
3.3.5 Effect of Rate of Penetration (ROP).....	93
3.3.6 Visualization of Cuttings Transport.....	96
3.4 Conclusions.....	97
Chapter 4 : Investigation of Cuttings Transport in a Horizontal Well with High-Speed Visualization and Electrical Resistance Tomography Technique	102
4.1 Introduction.....	103
4.2 Materials and Methods.....	108
4.2.1 Flow Loop.....	108
4.2.2 Instrumentation	110
4.2.3 Fluid Rheology Analysis.....	113
4.2.4 Design of Experiment.....	114
4.2.5 Repeatability Tests	116
4.3 Results and Discussion.....	117
4.3.1 Cuttings Movement Mechanism.....	117
4.3.2 Analysis of High-Speed Video Images	118
4.3.3 ERT Analysis.....	123
4.3.4 Moving Bed Velocity Estimation	127
4.3.5 Flow Regime Analysis.....	129
4.4 Conclusions.....	134
Chapter 5 : Experimental Study of Cuttings Transport with Non-Newtonian Fluid in Inclined Well Using Visualization and Electrical Resistance Tomography Techniques.....	148
5.1 Introduction.....	149
5.2 Materials and Method.....	153
5.2.1 ERT System.....	157
5.2.2 High-Speed Visualization	164
5.2.3 Fluid Rheology.....	165
5.2.4 Experimental Matrix.....	167

5.3 Results and Discussion.....	169
5.3.1 Visualization Study.....	169
5.3.2 Analysis of ERT Data.....	179
5.4 Conclusions.....	183
Chapter 6 : Experimental and Numerical Study of Cuttings Transport in the Inclined Drilling Operation.....	194
6.1 Introduction:.....	196
6.2 Materials and Methods:.....	202
6.2.1 Methodology.....	202
6.2.2 CFD model development.....	204
6.2.3 Mesh Size and Grid Study:.....	206
6.2.4 Experimental Procedure:.....	207
6.2.5 Fluid Rheology Estimation:.....	211
6.2.6 Design of Experiment:.....	213
6.2.7 Performance measurement:.....	213
6.2.8 Novelty and Limitations:.....	214
6.3 Result:.....	215
6.3.1 ERT analysis and visualization:.....	215
6.3.2 Validation of CFD Model:.....	217
6.3.3 Sensitivity Analysis: Transient solid dune movement.....	221
6.3.4 Factorial Design – Response Table:.....	223
6.3.5 Interaction Effects:.....	226
6.3.6 Parametric Analysis:.....	227
6.3.7 Analysis of Variance - ANOVA:.....	229
6.3.8 Artificial Neural Network (ANN) for model validation.....	233
6.4 Summary and Conclusions:.....	238
Chapter 7 : Conclusions and Future Recommendations.....	257
7.1 Conclusions.....	257
7.2 Recommendations.....	259
Appendix A.....	261
Appendix B.....	284

List of Tables

Table 1-1: Research tools and expected outcomes.....	13
Table 2-1: Key parameters selected for DOE.....	41
Table 2-2: Mesh properties.....	44
Table 2-3: Error analysis based on the comparison of predictions and experimental data.	49
Table 2-4: Design matrix of fluid rheology.	50
Table 2-5: Design matrix for operational parameters.	53
Table 2-6: Design matrix for cuttings size and annular space.	58
Table 2-7: Two-level DOE for the influential parameters on the basis of three subgroups.....	64
Table 3-1: Experimental test matrix details	82
Table 3-2: Improvement in dune propagation time with fluid velocity.....	91
Table 4-1: Summary of fluid rheology tests.....	114
Table 4-2: Matrix of experimental tests.....	115
Table 4-3: Flow regime analysis for input solid of 4%.....	130
Table 5-1: Fluid rheology test summary.....	167
Table 5-2: Experimental test matrix.....	168
Table 5-3: Experimental set up and cuttings properties.....	169
Table 6-1: Summary of fluid rheology tests (Huque et al., 2021a).....	212
Table 6-2: Factors used in the simulation with their ranges.....	213
Table 6-3: Factorial design for 5 factors interaction study.....	224
Table 6-4: ANOVA for the selected model	230
Table 6-5: The model fit statistics.....	231
Table 6-6: MSE and R ² values based on different numbers of neurons used for CTE model. .	234
Table 6-7: MSE and R ² correlations for different neurons used for DOE data.....	237
Table 6-8: ANOVA for annular cuttings concentration.....	250
Table 6-9: ANOVA for pressure drop.....	254

List of Figures

Figure 1-1: Rotary drilling and mud circulation system	2
Figure 1-2: Organization of the thesis.....	14
Figure 2-1: Cuttings transport in the annular section with concentric and eccentric profile.....	33
Figure 2-2: Computational mesh for different annular configurations.....	42
Figure 2-3: Grid independence study for all three annular configurations.....	43
Figure 2-4: Flow chart of CFD simulation.....	46
Figure 2-5: Frictional pressure drop comparison based on predictions and real data.....	48
Figure 2-6: Cuttings velocity as a function of fluid velocity.....	48
Figure 2-7: Total pressure drop comparison with managed pressure drilling experiment.....	49
Figure 2-8: Main effects and parameter interactions of drilling mud on CTE.....	51
Figure 2-9: Effect of two-factor interaction of a) k and n ; b) n and τ_0 on CTE.....	52
Figure 2-10: Cuttings transport efficiency as a function of a) n and k ; b) yield stress (τ_0)	52
Figure 2-11: The main effects and interaction of field parameters on CTE.	54
Figure 2-12: Effect of drill pipe rotation on CTE.....	55
Figure 2-13: Influence of mud circulation rate on the hole cleaning performance.	56
Figure 2-14: Stationary cuttings bed movement with increasing the mud velocity.	57
Figure 2-15: Main effects and interactions of cuttings size, annular clearance, eccentricity.....	58
Figure 2-16: Effect of cuttings size.....	59
Figure 2-17: Effect of annular orientation	61
Figure 2-18: Mud velocity streamlines in a) a concentric annulus; b) an eccentric annulus.....	62
Figure 2-19: Mud velocity contour and cuttings volume fraction for different eccentricities. ...	63
Figure 2-20: Main effects and two-factor interactions of significant parameters.	64
Figure 2-21: Interaction effect of mud velocity and cuttings size with yield stress	65
Figure 3-1: Flow loop experimental set up located at TAMUQ, Qatar.....	80
Figure 3-2: Schematic of flow loop experimental set up	80
Figure 3-3: Visualization section showing solid dune, annulus section, and inner pipe.....	82
Figure 3-4: Effect of annular fluid velocity on solid bed height ($e = 0$).....	84
Figure 3-5: Low rolling bed height at low fluid velocity.....	84
Figure 3-6: High rolling bed height at high fluid velocity	85
Figure 3-7: Rolling bed height variation with fluid velocities and drill pipe rotations ($e = 0$)....	86
Figure 3-8: Different eccentric annular position used in this study.	87
Figure 3-9: Effect of eccentricity on annular bed height at 40 RPM.....	88
Figure 3-10: Annular velocity profile for a highly eccentric annulus.....	88
Figure 3-11: Sand dune propagation time for stationary inner pipe (RPM = 0)	89
Figure 3-12: Sand dune propagation time for drill pipe rotation of 40 rpm	90
Figure 3-13: Sand dune propagation time for drill pipe rotation of 80 rpm	90
Figure 3-14: Annular volume fraction for concentric annulus ($e = 0$)	92
Figure 3-15: Annular volume fraction for highly eccentric annulus ($e = 0.6$).....	93
Figure 3-16: Effect of rate of penetration (ROP) on bed height ($e = 0$)	94
Figure 3-17: Effect of rate of penetration (ROP) on annular solid vol fraction ($e = 0$).....	95

Figure 3-18: Effect of rate of penetration (ROP) on dune propagation time ($e = 0.3$).....	95
Figure 3-19: Rolling particles and stationary bed.	96
Figure 3-20: Suspended solid particles in the annulus.....	97
Figure 3-21: Visualization of helical motion of solid particles due to inner pipe rotation.	97
Figure 4-1: Schematic of cuttings transport in horizontal well	105
Figure 4-2: TAMUQ multiphase flow loop experimental schematic.....	108
Figure 4-3: Experimental workflow.....	109
Figure 4-4: ERT output.....	112
Figure 4-5: ERT concentration tomogram.....	113
Figure 4-6: Shear stress vs. shear rate behavior for fluids FZ 1, FZ 2, FZ 3 and FZ 4.....	114
Figure 4-7: Repeatability test results for a slurry pump rate of 270 LPM (≈ 71 GPM).....	116
Figure 4-8: Front view of schematic of dune movement in a horizontal section	118
Figure 4-9: A cross-sectional view of three-layer model of cuttings transport.....	118
Figure 4-10: Visualization of the high-speed camera for different fluid rheology.....	119
Figure 4-11: High-speed camera image and corresponding schematic of three-layer model. ..	121
Figure 4-12: Transition of a stationary solid bed to fully suspended flow.	122
Figure 4-13: Forces acting on solid particles.	123
Figure 4-14: Annular solid volume fraction for four different fluids based on ERT data.	124
Figure 4-15: Minimum transport velocity (MTV) for different fluids	125
Figure 4-16: Maximum solid bed height for different mud velocities and drill pipe rotation...	126
Figure 4-17: Variations of bed thickness for different fluid rheologies and mud velocities.	127
Figure 4-18: Solid dune velocity versus fluid velocity at different drill pipe rotations.....	128
Figure 4-19: Solid bed propagation time reported in the ERT system.....	129
Figure 4-20: Flow regime map showing three different regions of solid transport.....	132
Figure 4-21: Transport performance number for FZ 1, FZ 2, and FZ 3	134
Figure 5-1: Schematic of experimental test section.....	154
Figure 5-2: Actual lab image during an experiment.....	154
Figure 5-3: Visualization section	155
Figure 5-4: Particle size distribution	156
Figure 5-5 : Pump mass flow rate at different slurry pump rates and drill pipe rotations	157
Figure 5-6: Schematic of ERT sensor	158
Figure 5-7: Solid dune movement inside the annular section.....	161
Figure 5-8: Conductivity and concentration profile	162
Figure 5-9: ERT conductivity tomogram	163
Figure 5-10: ERT concentration tomogram of solid and liquid phases.....	164
Figure 5-11: High speed image processing interface.....	165
Figure 5-12: Fluid rheology analysis.....	166
Figure 5-13: Effect of fluid velocity on cuttings transport in 10° inclined well.	170
Figure 5-14: Schematic of solid transport in inclined well with change in mud velocity.....	172
Figure 5-15: High-speed camera visualization of solid particles movement (RPM = 0).....	173
Figure 5-16: Cuttings moving in inclined well with no inner pipe rotation.	174
Figure 5-17: Inclined well with inner pipe rotation.....	175
Figure 5-18: Schematic of cuttings transport in inclined well with inner pipe rotation	175

Figure 5-19: Change in solid bed height with drill pipe rotation for fluid LV	176
Figure 5-20: Solid bed height at different inclination angles with fluid LV.....	177
Figure 5-21: Dune moving time recorded by ERT system for fluid LV.	178
Figure 5-22: Repeatability test for different operating conditions with fluid MV at 0.7 m/s....	179
Figure 5-23: Effect of mud velocity at different inclination angles.....	180
Figure 5-24: Effect of inclination on fluid rheology.....	182
Figure 6-1: Schematic of cuttings transport in inclined drilling operation.....	197
Figure 6-2: Overall methodology to study effect of drilling parameters on cutting transport. .	203
Figure 6-3: Grid study for concentric annular section	207
Figure 6-4: Experimental section schematic.....	208
Figure 6-5: Experimental set up image at 5° inclination.....	209
Figure 6-6: Simplified experimental procedure flowchart.....	210
Figure 6-7: Schematic of ERT sensor (Huque et al., 2021b)	211
Figure 6-8 : Shear stress vs. shear rate behavior for fluids FZ 1, FZ 2, FZ 3 and FZ 4	212
Figure 6-9 : Effect of inclination and fluid rheology on annular solid volume fraction.....	215
Figure 6-10: High-speed image (2000 fps) visualization of solid particle movement.....	217
Figure 6-11: CFD model validation. Experimental data vs. Simulation result.....	218
Figure 6-12: CFD Simulation contour vs. ERT Tomogram.....	218
Figure 6-13: Solid dune movement along the annular section	220
Figure 6-14: Solid dune profile at different time interval.....	221
Figure 6-15: CTE response against inclination for fluid FZ 1 and FZ 4	222
Figure 6-16: Half - Normal and Normal Plot.....	225
Figure 6-17: Mean dependency of CTE on other parameters	225
Figure 6-18: Interaction between mud velocity and cuttings size	226
Figure 6-19: Effect of fluid velocity on cutting transport efficiency.	227
Figure 6-20: Effect of inclination on cutting transport efficiency.	228
Figure 6-21: Effect of cuttings size.....	229
Figure 6-22: Factors and interactions contributions in the model	231
Figure 6-23: Actual vs. Predicted value of CTE for the selected model.....	232
Figure 6-24: ANN architecture for 25 neurons in hidden layer.....	233
Figure 6-25: Regression analysis for N =25	234
Figure 6-26: CTE versus data index for N=25.....	235
Figure 6-27: Error in trained ANN model for N =25	235
Figure 6-28: Comparison of ANN model with DOE outcome.....	236
Figure 6-29: Comparison of DOE test data, CTE model based on ANOVA and ANN model..	238
Figure 6-30: Factors and interaction contribution in annular solid concentration.....	251
Figure 6-31: Half normal plot for annular cuttings concentration.....	251
Figure 6-32: Mean dependency of annular concentration on other parameters.....	252
Figure 6-33: Two factor interaction in annular cuttings concentration.....	253
Figure 6-34: Factors and interaction contribution in pressure drop.	255
Figure 6-35: Half normal plot for pressure drop.	255
Figure 6-36: Mean dependency on annular pressure drop.	256
Figure 6-37: Velocity-Cuttings size interaction on pressure drop.....	256

Chapter 1 Introduction

1.1 Background and motivation

Due to technological development in the petroleum industry and continuous increase in demand of fossil fuels, petroleum industry explores offshore marine and geologically harsh environments with directional, horizontal, and extended reach drilling, where traditional drilling operations are less feasible. Horizontal drilling has become popular in recent years due to more contact with the pay zone, increase in production rate, less pressure drop, and increase in the ultimate recovery.

In a typical rotary drilling method, the hole is drilled by a rotating drill bit. The drill bit is attached with a drill string up to surface. A downward weight on bit is applied from the surface to the bit and a rotation is also imposed to the drill bit from the surface. The interaction of drill bits with geological formation, for example, sandstone generates numerous rock chips with different sizes. In conventional drilling fluid circulation system, a circulating drilling mud is injected into the well bore through the drill bit which removes the cuttings out of the hole through transport in the annular section. Drill cuttings are then separated at surface using shale shakers (vibrating screens), desanders and desilters; and then the drilling mud is recirculated to the well bore. **Figure 1-1** illustrates the simplified drilling system with mud circulation. For an efficient drilling operation, it is essential to remove the generated drill cuttings from the bottomhole effectively.

The success of a drilling operation depends on an efficient hole cleaning operation. Hole cleaning refers to the ability of a circulating drilling mud to transport the drill cuttings out of the wellbore during a drilling operation. Inadequate hole cleaning may cause some cost extensive problems with dreadful consequences including stuck pipe, excessive torque and drag, rapid bit wear, and slow

rate of penetration leading to lost operational time in drilling. Therefore, special care should be taken during drilling operations to avoid these complications.

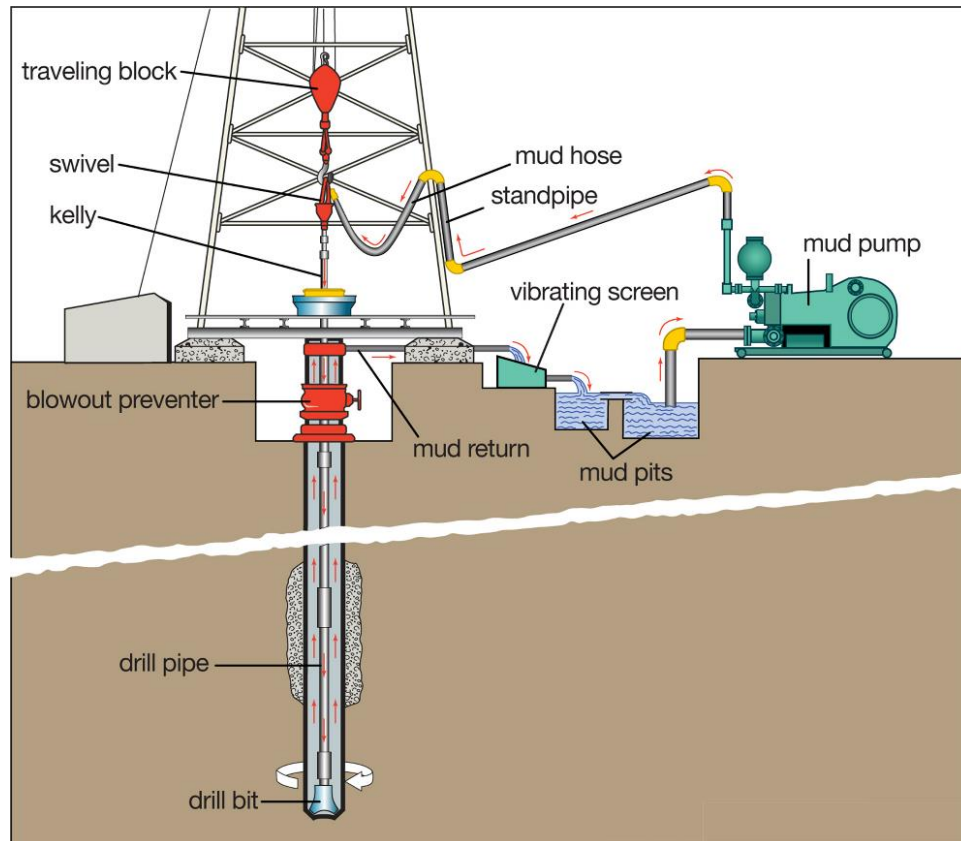


Figure 1-1: Rotary drilling and mud circulation system
(Encyclopaedia Britannica, 2017)

Field experience and laboratory investigations show that hole cleaning problems become severe in a directional or horizontal well where drill cuttings tend to settle in the lower annular section. A well with deviation of approximately 30 degrees from vertical shows serious issues in cuttings removal that are not encountered in a vertical or near vertical well. Thus, proper hole cleaning should be implemented during the entire drilling operation for horizontal, near horizontal, extended reach, and directional wells. An appropriate drilling fluid design and determining the

transport capabilities of the drilling fluid could be the solution to improve cuttings transport capability of horizontal or inclined wells drilling operation.

Several experimental studies have been performed by many researchers to investigate the cuttings transport behavior and flow pattern in the annular section. However, there are some diverse judgements on the effect of some of the crucial parameters such as drill pipe rotation, eccentricity, cuttings size and fluid viscosity on cuttings transport performance. Also, previous studies have not focused on the interaction behavior among the drilling parameters.

These knowledge gaps motivate us to study the effect of drilling parameters and their interaction effect on transport of cuttings in the annular section of horizontal and inclined wells using computational and experimental methods.

1.2 Literature Review

The rapid removal of drill cuttings from the borehole with an appropriate drilling mud assists in achieving a higher drilling penetration rate by continuous contact of a drill bit with fresh rock surfaces in the formation (Sanchez et al., 1999). An effective/accurate design of drilling mud and adequate mud circulation are necessary to remove the cuttings from the borehole. Other vital factors such as formation type, wellbore inclination, cuttings size, rate of penetration, and drill pipe eccentricity considerably affect the performance of drilling operation. Therefore, it is a challenging task to develop an optimum hole cleaning strategy considering all these factors.

The hydrodynamic behaviors of solid and liquid transport through pipe and annulus represent a complex phenomenon that has been analyzed by some experimental work, mechanistic modeling, and CFD simulation studies (Espinosa-paredes et al., 2007; Guo et al., 2010; Kelessidis and Bandelis, 2004; Nazri et al., 2010; Sun et al., 2017). The experimental investigations of cuttings

transport have been reported in the literature since 1970. The earlier experimental works were mainly conducted on vertical wells (Hussaini and Azar, 1983; Sifferman et al., 1973a). Vertical well experiments primarily deal with the fluid rheology. These studies showed that the fluid rheology has a significant impact on cuttings transport in the vertical well.

Experimental study of cuttings transport in inclined wells: Tomren et al. (1986) first experimentally investigated cuttings transport in the directional well and unveiled the problem of cuttings bed formation in the inclined/non-vertical wells. Their study showed that a cuttings bed is formed in the inclined well even at high mud flow rates in the annulus. Later, a number of experimental studies (Ford et al., 1990; Martin et al., 1987; Masuda et al., 2000; Okrajni and Azar, 1986; Peden et al., 1990; Sanchez et al., 1997; Sifferman and Becker, 1992; Walker and Li, 2000) were performed in the directional well to investigate the effects of fluid rheology, drill pipe rotation, fluid velocity, and eccentricity on the cuttings transport. For instance, Sifferman and Becker (1992) work showed that 50% of annular space (as the maximum amount) can be filled with cuttings under normal drilling conditions. However, cuttings bed size substantially decreased by a small increase in the mud weight. The experimental work conducted by Ford et al. (1996, 1990) revealed that a Minimum Transport Velocity (MTV) is required to commence cuttings transport by both rolling and suspension mechanisms. Peden et al. (1990) and Tomren et al. (1986) concluded that both high fluid viscosity and turbulence in flow regimes are beneficial in cuttings transport in the directional well. However, the Peden et al. (1990) experimental study showed that turbulence has a greater influence on MTV compared to the fluid viscosity. A similar observation was found by Okrajni and Azar (1986). They observed that cuttings transport is generally not affected by mud rheological properties under turbulent flow regimes for any inclination angle. Masuda et al. (2000) investigated the critical flow rate for effective cuttings transport in inclined

wells. They defined the critical flow rate as the minimum flow rate when a solid dune is formed in the annular section. Walker and Li (2000) concluded that a low-viscous fluid with turbulent flow regime offers best hole cleaning; however, they recommended a gel or multiphase flow system to maximize the solid carrying capacity.

Martin et al. (1987) concluded that drill pipe rotation is favorable in cuttings transport in inclined wells. According to their research outputs, drill pipe rotation can help in periodic reinserting of solid cuttings from the upper layer of the solid bed back into the fluid flow. Sanchez et al. (1997) also investigated the effect of drill pipe rotation on cuttings transport. They noticed that annular cuttings concentration is a function of rotary speed, hole inclination, and mud flow rate. It was also found that high drill pipe rotation is beneficial with low mud velocity in horizontal wells and the opposite is true for high flow rates. According to the past experimental works (Azar and Sanchez, 1997; Martin et al., 1987) an unsteady cuttings bed is formed and cuttings are transported like dune shape for a low inner pipe rotation. In such cases, drill pipe rotation helps to minimize the unsteady dune formation with improved cuttings transport capability.

In recent years, researchers have mainly focused on improving the cuttings transport behavior by using enhanced fluid rheology (Boyou et al., 2019; Gul et al., 2017; Hakim et al., 2018; Heshamudin et al., 2019; Hirpa and Kuru, 2020; Rodriguez Corredor et al., 2016; Yeu et al., 2019) and transport mechanism (Kim et al., 2014; Naganawa et al., 2017; Rasul et al., 2020). Boyou et al. (2019) investigation showed that nano silica based aqueous solution provide an improved cuttings transport efficiency for any inclination. It was found that addition of nano silica can be an alternative solution to the oil-based drilling mud. Hirpa and Kuru (2020) experimentally investigated the solid bed erosion using polymer solution. Their study showed that fluid elasticity significantly affects the solid bed erosion dynamics behavior. Several other research studies

(Hakim et al., 2018; Heshamudin et al., 2019; Yeu et al., 2019) used improved water based mud with polyethylene and polypropylene. It was concluded that addition of polyethylene beads can improve the transport ratio by approximately 16%. The impact of drag reducing polymer was also investigated in the literature (Gul et al., 2017; Rodriguez Corredor et al., 2016). It was revealed that addition of drag reducing polymer considerably reduce the minimum transport velocity to initiate the movement of coarse cuttings in the horizontal wells.

Sayindla et al.(2016) investigated the solid transport capability with different oil-based muds. Their study showed that fluid yield stress has a significant impact on holding cuttings at low shear rate. Other studies (Gul et al., 2017; Ozbayoglu et al., 2012; Rasul et al., 2020) investigated cuttings transport behavior with air-water system, and aerated mud. It was suggested that increasing gas volume fraction in the aerated mud can improve cuttings transport by increasing the local fluid velocity in the annular section.

Experimental study of cuttings transport in horizontal wells: With the advancement of extended reach well drilling in the petroleum industry, researchers further studied cuttings transport in the horizontal or near horizontal wells (Chen et al., 2007; Duan et al., 2008; Garcia-Hernandez et al., 2007; Kelessidis et al., 2007; Kelessidis and Bandelis, 2004; Ozbayoglu et al., 2008; Pilehvari et al., 2007; Yu et al., 2007). It has been revealed that the fluid rheology plays a significant role in cuttings transport in horizontal wells similar to the inclined wells. Kelessidis et al (2007), Kelessidis and Bandelis (2004), and Pilehvari et al (2007) suggested a turbulent flow regime for effective hole cleaning in the horizontal annular section. Based on fluid rheology study, Duan et al (2008) showed that non-Newtonian fluid exhibits better cuttings transport capability for smaller cuttings. Philip et al (1998) reported that flow behavior index ‘n’ of a power law fluid impacts the

solid lifting capability. A decrease in flow behavior index indicates more non-Newtonian flow behavior and improves cuttings lifting capability. In contrast, consistency index 'k' affects the solid suspension potential. A higher 'k' values indicates a more viscous behavior by the drilling mud. Piroozian et al (2012) also showed that an increase in plastic viscosity increases the solid transport capability as long as the flow regime is turbulent.

The critical deposition velocity and minimum transport velocity in horizontal well were also investigated by several researchers (Chen et al., 2007; Cho et al., 2000a; Dabirian et al., 2016; Duan et al., 2009; Garcia-Hernandez et al., 2007). Garcia-Hernandez et al. (2007) described that the solid transport capability of the moving layer is a resultant of three mechanisms as rolling, saltation, and suspension. They also revealed that a significant fraction of the solid bed in horizontal sections is transported by a moving layer, and the solid concentration of the moving layer is much higher than that in a suspended layer. Chen et al.(2007) reported that cuttings accumulated in the annular section are not sensitive to flow velocity until a minimum velocity is reached. Duan et al (2009) claimed that the minimum fluid velocity to prevent solid deposition is almost three times higher than the minimum velocity to initiate a solid bed erosion and start particle rolling. Cho et al. (2000) suggested a critical velocity of 3.5 to 4.5 ft/s to avoid solid deposition. However, the literature shows that the critical fluid velocity is a function of other drilling parameters such as fluid rheology, pressure gradient, and velocity profile near the cuttings bed. Dabirian et al. (2016)'s study found that the critical solid deposition velocity is affected by cuttings size; an increase in cuttings size increases the critical sand deposition velocity. Ozbayoglu et al. (2008) concluded that drill pipe rotation has a significant impact on hole cleaning in horizontal wells and reduces the MTV of drilling mud. However, an increase in drill pipe rotation diminishes the fluid viscosity effect.

Gul et al. (2017) investigated the solid-liquid flow regime map in their studies and compared the flow pattern with aerated mud. They observed four different flow regimes as bubble flow, elongated bubble flow, slug flow and wavy annular flows. Although their study could not distinguish performance variation in all four types of flow regimes, they concluded that wavy annular flow regime is more effective in cuttings transport in horizontal well.

In previous research studies, there are no adequate systematic experimental works with visualization techniques to verify “Three-Layer” and “Two-Layer” flow regimes in a horizontal well. A few of past studies (Cho et al., 2000b, 2000a; Dabirian et al., 2016, 2015; Fajemidupe et al., 2019; Gul et al., 2017; Kelessidis and Mpandelis, 2003; Li and Luft, 2014; Nguyen and Rahman, 1998; Zhu et al., 2010) reported the flow pattern; however, a systematic experimental visualization of two layer and three layer model of cuttings transport is still missing. Thus, a detailed analysis of flow behavior through using visualization methods is essential to further understand the flow patterns in the horizontal annular section. An appropriate visualization technique can identify the different layers of cuttings, solid movement pattern, and flow regimes in the annulus section. A few researchers (Fajemidupe et al., 2019; Kelessidis et al., 2007; Kelessidis and Bandelis, 2004; Kelessidis and Mpandelis, 2003; Li and Luft, 2014; Philip et al., 1998b) reported a low number of images of two-layer and three-layer models with experimental visualization. However, due to the low resolution of the images, the movement pattern of solid cuttings was indistinguishable.

Only a few studies (Kelessidis and Bandelis, 2004; Ozbayoglu and Osgouei, 2012; Wei et al., 2013; F. Zhang et al., 2018) were conducted to visualize the flow behavior of cuttings in the annular section. Due to the technical and equipment limitations, previous experimental studies on

cuttings transport visualization were not adequate to investigate solid movement patterns and flow behavior in the annular section.

Application of computational fluid dynamics in cuttings transport: Computational fluid dynamics (CFD) studies on cuttings transport have become popular in recent years. Most of the CFD studies (Busch and Johansen, 2020; Erge and van Oort, 2020; Huque et al., 2020; Pang et al., 2019, 2018a; Sun et al., 2014) used Eulerian-Eulerian multiphase flow modelling, and some other studies (Akhshik et al., 2015; Barbosa et al., 2019; Shao et al., 2019) used CFD- coupled with discrete element methods (DEM) or commonly known as CFD-DEM methods. Also, researchers have focused on the impact of drill pipe rotation, whirling and orbital motion (Busch and Johansen, 2020; Pang et al., 2018a), drill string eccentricity (Erge and van Oort, 2020; GhasemiKafrudi and Hashemabadi, 2016; Heydari et al., 2017), flow pattern map and hydraulic behavior (Pang et al., 2018b; Sayindla et al., 2019; Vaziri et al., 2020; C. Zhang et al., 2018), and complex wellbore (Epelle and Gerogiorgis, 2019) on cuttings transport. Very few studies used CFD-DEM methods (Akhshik et al., 2015; Barbosa et al., 2019; Shao et al., 2019) to investigate the solid particles movement; however these computational studies did not include experimental validation on solid particle movement patterns.

Mechanistic model: Due to stable cuttings dune formation in the horizontal section of a wellbore, cuttings transport mechanism in a horizontal well significantly differs from a vertical well. Several mechanistic models were introduced including ‘Three-Layer’ and ‘Two-Layer’ models of cuttings transport (Doron and Barnea, 1993; Kamp et al., 1999; Masuda et al., 2000; Ramadan et al., 2001). Doron and Barnea (1996, 1993) investigated solid-liquid flow patterns in the horizontal section through the mechanistic model, experimental tests, and flow regime map. They proposed a 3-layer

model as a stationary solid bed, a sliding bed, and heterogeneous suspension. Their flow regime map is based on superficial velocities of the liquid phase and solid phase, cuttings size, and density. However, their model did not consider the annular pipe, drill pipe rotation, and eccentricity effect of a horizontal drilling operation. Also, the effect of fluid rheology was not taken into account in their flow regime map (Doron and Barnea, 1996), though fluid viscosity plays a vital role in cuttings transport. Kamp et al. (1999) proposed a two-layer mechanistic model consisting of a moving bed of packed solid cuttings and heterogeneous mud and cuttings. Their model did not consider the solid deposition rate with varying mud velocity. Furthermore, they ignored the drill pipe rotation effect, which has a significant contribution in cuttings transport in a horizontal well. Masuda et al. (2000) also proposed a two-layer model (deposited bed and suspension layer) for inclined wells. Ramadan et al. (2001) proposed a mechanistic layer model based on the momentum balance of fluid and solid particles. Their study revealed that there is a specific particle size, which gives the highest cuttings removal from the solid bed by lifting and rolling mechanisms. However, this optimum size depends on other parameters such as fluid velocity, viscosity, and inclination angle.

1.3 Knowledge Gaps

Although researchers have confirmed that an increase in the fluid velocity and drill pipe rotation increases the cuttings transport efficiency, there are several diverse views on some crucial parameters. For example, Sorgun et al. (2011) and Walker and Li (2000) concluded that a low viscous mud shows a better hole cleaning performance, which contradicts the earlier findings by Sifferman et al. (1973b) and Tomren et al. (1986). A study in the slim hole annulus revealed that pressure drop in the annulus increases with increasing inner pipe rotation (Han et al., 2010), which is opposite to the findings of previous works (McCann et al., 1995; Ozbayoglu et al., 2008).

Focusing on the impact of cutting size, Sanchez et al. (1999) concluded that smaller cuttings are difficult to transport, whereas Walker et al. (2000) found that fine solid particles are easier to clean. One of the main reasons of such contradictions is that a variety of experimental setups with different pipe diameters, annular clearances, orientations, and fluid/mud types (or rheology) have been used in the previous research investigations.

Most of the experimental methods commonly consider "one factor at a time" (OFAT) so that all factors except one factor are kept constant. Thus, only one parameter varies each time. The OFAT technique is inefficient when multiple factors change simultaneously. Also, the ranges of input parameters have not been wide enough to capture all important behaviors in cuttings transport. In real-time drilling, many parameters directly interact with each other, which considerably affect the performance of cuttings transport operation. Due to the experimental limitations, all parameters might not be investigated simultaneously. Hence, the interaction between influential parameters is another vital aspect which has been ignored in most of the previous experimental studies. Similar drawbacks also exist in the relevant modelling works as discussed.

These limitations motivate us to study the effect of drilling parameters and their interactions on cutting transport performance using computational and experiment methods. The detailed goal and expected outcomes are presented in the next section.

1.4 Objectives

This research investigated the cuttings transport behavior in the horizontal and inclined annular section. A large number of parameters (e.g., fluid rheology, velocity, inclination, pipe rotation, cuttings size, eccentricity, and annular clearance) directly affect cuttings transport and consequently the drilling performance. This work focused on the impact of drilling parameters on cuttings transport performance. The objectives of this research work are given below:

- ❖ Investigate the cuttings transport behavior in the horizontal annulus section using Computational Fluid Dynamics (CFD) through introducing a robust multiphase flow model and then validating the computational model with published experimental results. This phase also includes identifying two factor interactions in the horizontal well.
- ❖ Experimentally investigate the of cuttings transport behavior in the horizontal and inclined annular sections with Newtonian and non-Newtonian fluids.
- ❖ Extend the CFD model for the inclined well and validate the predictions with experimental data. This phase also includes the two-factor interaction for the inclined well and develops a statistical model to optimize cuttings transport behavior in the inclined well.

1.5 Research Tools and Expected Outcomes

Experimental studies and numerical models reported in the literature are mainly case specific and designed for a specific drilling operation. These studies do not clearly delineate the optimization strategies in a drilling operation. A comprehensive parametric sensitivity analysis is required to overcome the shortcomings discussed in the literature review. The core research objectives, investigation tools, case study and expected outcomes are listed in **Table 1-1**. These tools can be grouped into two categories:

Simulation and statistical analysis: Design modular tools were used for drawing wellbore geometry. Ansys Fluent v.17.2 was used for computational simulation. Compute Canada ACENET supercomputer: Graham, Cedar and Beluga were used for transient simulation. RStudio and Design Expert v.11 were used for statistical analysis, and MATLAB ANN tool were employed for artificial neural network development.

Experimental investigation: Beside the annular flow loop experimental set up, the following specialized tools were used. High-speed visualization camera for particle movement tracking,

Digital Single-Lens Reflex (DSLR) for bed height and dune moving velocity estimation, Electrical Resistance Tomography (ERT) system for annular solid volume estimation and viscosity meter for fluid rheology estimation were employed.

Table 1-1: Research tools and expected outcomes.

Core Objectives	Features	Description
Investigate the cuttings transport behavior in the horizontal annulus section using CFD.	Tool Used	Ansys Fluent v 17.2, Design Modular, ACENET, RStudio
	Case Study	Horizontal well with different eccentric conditions and factor interactions.
	Expected Outcome	Two factor interaction study and parametric analysis of cuttings transport in horizontal well.
Experimental investigation of cuttings transport behavior in horizontal and inclined annular section with Newtonian and non-Newtonian fluids.	Tool Used	High speed visualization, electrical resistance tomography, viscosity meter.
	Case Study	Horizontal and inclined well with different eccentric conditions and interaction study with Newtonian and non-Newtonian fluids.
	Expected Outcome	Investigating the flow pattern of cuttings transport, visualization, in-situ solid volume estimation at different operating conditions such as eccentricity, fluid rheology, mud flow rate, rate of penetration, drill pipe rotation and inclination.
Two-factor interaction study for inclined well and develop a statistical model to optimize cuttings transport behavior in inclined well.	Tool Used	Experimental data, Ansys Fluent 17.2, Design Expert v 11.0, ACENET, MATLAB.
	Case Study	Two-factor interaction study in inclined well and identify the critical inclination prone to cuttings transport
	Expected Outcome	A statistical model to optimize cuttings transport behavior for inclined well.

1.6 Organization of Thesis

The thesis is written in manuscript format. Three published journal articles, one conference manuscript and one article under review are included in the thesis. A co-authorship statement is provided at the beginning of the thesis. Overall organization of the thesis is shown in **Figure 1-2** and a brief overview of each chapter is described below.

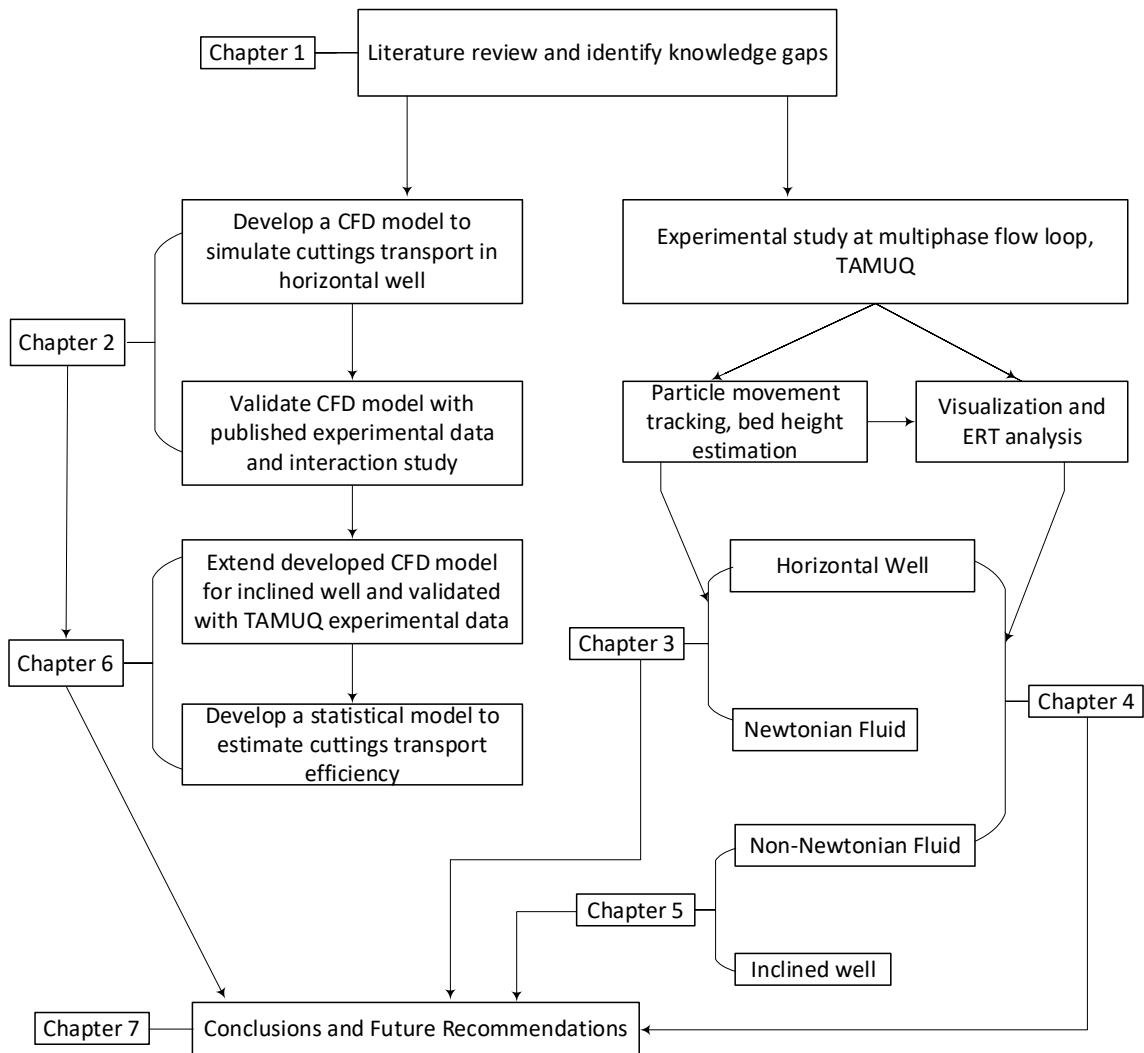


Figure 1-2: Organization of the thesis

Chapter 1 of the thesis describes the motivations and objectives of the research. This chapter also includes a brief review of the related previous studies.

Chapter 2 presents computational fluid dynamics model (CFD) of cuttings transport in a horizontal well. This chapter also discusses about the two-factor interaction behavior among drilling parameters.

Chapter 3 describes the experimental work on cuttings transport in the horizontal well with a Newtonian fluid. The chapter also includes the visualization of solid bed height during cuttings transport in the horizontal well with a Newtonian fluid.

Chapter 4 reports the experimental work on cuttings transport in the horizontal well with a non-Newtonian fluid. The chapter presents the visualization of mechanistic three-layer model of cuttings transport and flow regime map.

Chapter 5 investigates cuttings transport behavior in the inclined well. Different solid transport mechanisms in inclined well are described in this chapter through high-speed visualization. Also, an overview of electrical resistance tomography method is explained.

Chapter 6 demonstrates transient solid transport behaviors in the inclined well. Interactions among the parameters with respect to inclination are explained. A statistical cuttings transport efficiency (CTE) model is proposed for the inclined well.

Chapter 7 presents the conclusions of the study and the possible scopes of future work.

Appendices This section includes supplementary materials for this research work. **Appendix A** shows the solid transport behavior in the inclined bend section using CFD method. **Appendix B** includes some images and videos from the experimental work.

REFERENCES

- Akhshik, S., Behzad, M., Rajabi, M., 2015. CFD-DEM approach to investigate the effect of drill pipe rotation on cuttings transport behavior. *J. Pet. Sci. Eng.* 127, 229–244. <https://doi.org/10.1016/j.petrol.2015.01.017>
- Azar, J., Sanchez, R.A., 1997. Important Issues in Cuttings Transport for Drilling Directional Wells, in: Fifth Latin American and Caribbean Petroleum Engineering Conference and Exhibition. Rio de Janeiro, Brazil 30 August -3 September. <https://doi.org/10.2118/39020-MS>
- Barbosa, M. V., De Lai, F.C., Junqueira, S.L.M., 2019. Numerical Evaluation of CFD-DEM Coupling Applied to Lost Circulation Control: Effects of Particle and Flow Inertia. *Math. Probl. Eng.* 2019. <https://doi.org/10.1155/2019/6742371>
- Boyou, N.V., Ismail, I., Wan Sulaiman, W.R., Sharifi Haddad, A., Husein, N., Hui, H.T., Nadaraja, K., 2019. Experimental investigation of hole cleaning in directional drilling by using nano-enhanced water-based drilling fluids. *J. Pet. Sci. Eng.* 176, 220–231. <https://doi.org/10.1016/j.petrol.2019.01.063>
- Busch, A., Johansen, S.T., 2020. Cuttings transport: On the effect of drill pipe rotation and lateral motion on the cuttings bed. *J. Pet. Sci. Eng.* 191, 107136. <https://doi.org/10.1016/j.petrol.2020.107136>
- Chen, Z., Ahmed, R.M., Miska, S.Z., Takach, N.E., Yu, M., Pickell, M.B., Hallman, J.H., 2007. Experimental Study on Cuttings Transport With Foam Under Simulated Horizontal Downhole Conditions. *SPE Drill. Complet.* 22, 304–312. <https://doi.org/10.2118/99201-PA>
- Cho, H., Shah, S.N., Osisanya, S.O., 2000a. A three-segment hydraulic model for cuttings

- transport in horizontal and deviated wells, in: SPE/CIM International Conference on Horizontal Well Technology. Calgary, Alberta, Canada, pp. 1–16.
<https://doi.org/10.2118/65488-MS>
- Cho, H., Shah, S.N., Osisanya, S.O., 2000b. A three-layer modeling for cuttings transport with coiled tubing horizontal drilling, in: SPE Annual Technical Conference and Exhibition. Dallas, Texas, U.S.A, pp. 905–918. <https://doi.org/10.2118/63269-ms>
- Dabirian, R., Mohan, R.S., Shoham, O., Kouba, G., 2016. Solid-Particles Flow Regimes in Air/Water Stratified Flow in a Horizontal Pipeline. Oil Gas Facil. 5, 1–14.
<https://doi.org/10.2118/174960-pa>
- Dabirian, R., Mohan, R.S., Shoham, O., Kouba, G., 2015. Sand transport in stratified flow in a horizontal pipeline, in: Proceedings - SPE Annual Technical Conference and Exhibition. pp. 3222–3239. <https://doi.org/10.2118/174960-ms>
- Doron, P., Barnea, D., 1996. Flow pattern maps for solid-liquid flow in pipes. Int. J. Multiph. Flow 22, 273–283. [https://doi.org/10.1016/0301-9322\(95\)00071-2](https://doi.org/10.1016/0301-9322(95)00071-2)
- Doron, P., Barnea, D., 1993. A Three-Layer Model for Solid-Liquid Flow in Horizontal Pipes. Int. J. Multiph. Flow 19, 1029–1043. [https://doi.org/10.1016/0301-9322\(93\)90076-7](https://doi.org/10.1016/0301-9322(93)90076-7)
- Duan, M., Miska, S., Yu, M., Takach, N., Ahmed, R., Zettner, C., 2009. Critical conditions for effective sand-sized-solids transport in horizontal and high-angle wells. SPE Drill. Complet. 24, 229–238. <https://doi.org/10.2118/106707-PA>
- Duan, M., Miska, S.Z., Yu, M., Takach, N.E., Ahmed, R.M., Zettner, C.M., 2008. Transport of Small Cuttings in Extended-Reach Drilling. SPE Drill. Complet. 23, 258–265.

<https://doi.org/10.2118/104192-PA>

Encyclopaedia Britannica, 2017. Drilling Mud [WWW Document]. Encycl. Br. URL <https://www.britannica.com/technology/drilling-mud> (accessed 3.6.21).

Epelle, E.I., Gerogiorgis, D.I., 2019. Drill cuttings transport and deposition in complex annular geometries of deviated oil and gas wells: A multiphase flow analysis of positional variability. *Chem. Eng. Res. Des.* 151, 214–230. <https://doi.org/10.1016/j.cherd.2019.09.013>

Erge, O., van Oort, E., 2020. Modeling the effects of drillstring eccentricity, pipe rotation and annular blockage on cuttings transport in deviated wells. *J. Nat. Gas Sci. Eng.* 79, 103221. <https://doi.org/10.1016/j.jngse.2020.103221>

Espinosa-paredes, G., Salazar-mendoza, R., Cazarez-candia, O., 2007. Averaging model for cuttings transport in horizontal wellbores. *J. Pet. Sci. Eng.* 55, 301–316. <https://doi.org/10.1016/j.petrol.2006.03.027>

Fajemidupe, O.T., Aliyu, A.M., Baba, Y.D., Archibong, A.E., Okeke, N.E., Ehinmowo, A.B., Yeung, H., 2019. Minimum sand transport conditions in gas-solid-liquid three-phase stratified flow in horizontal pipelines. *Soc. Pet. Eng. - SPE Niger. Annu. Int. Conf. Exhib. 2019, NAIC 2019.* <https://doi.org/10.2118/198726-MS>

Ford, J.T., Gao, E., Oyenehin, M.B., Peden, J.M., Larrucia, M.B., Parker, D., 1996. A New MTV Computer Package for Hole-Cleaning Design and Analysis. *SPE Drill. Complet.* <https://doi.org/10.2118/26217-PA>

Ford, J.T., Peden, J.M., Oyenehin, M.B., Gao, E., Zarrouh, R., 1990. Experimental Investigation of Drilled Cuttings Transport in Inclined Boreholes, in: *SPE Annual Technical Conference*

and Exhibition. pp. 197–206. <https://doi.org/10.2118/20421-MS>

Garcia-Hernandez, A.J., Miska, S.Z., Yu, M., Takach, N.E., Zettner, C.M., 2007. Determination of Cuttings Lag in Horizontal and Deviated Wells, in: SPE Annual Technical Conference and Exhibition. Anaheim, California, U.S.A., 11–14 November. <https://doi.org/10.2118/109630-MS>

GhasemiKafrudi, E., Hashemabadi, S.H., 2016. Numerical study on cuttings transport in vertical wells with eccentric drillpipe. *J. Pet. Sci. Eng.* 140, 85–96. <https://doi.org/10.1016/j.petrol.2015.12.026>

Gul, S., Kuru, E., Parlaktuna, M., 2017. Experimental investigation of cuttings transport in horizontal wells using aerated drilling fluids, in: SPE Abu Dhabi International Petroleum Exhibition and Conference. <https://doi.org/10.2118/188901-ms>

Guo, X. le, Wang, Z. ming, Long, Z. hui, 2010. Study on Three-Layer Unsteady Model of Cuttings Transport for Extended Reach Well. *J. Pet. Sci. Eng.* 73, 171–180. <https://doi.org/10.1016/j.petrol.2010.05.020>

Hakim, H., Katende, A., Sagala, F., Ismail, I., Nsamba, H., 2018. Performance of polyethylene and polypropylene beads towards drill cuttings transportation in horizontal wellbore. *J. Pet. Sci. Eng.* 165, 962–969. <https://doi.org/10.1016/j.petrol.2018.01.075>

Han, S.M., Hwang, Y.K., Woo, N.S., Kim, Y.J., 2010. Solid-Liquid Hydrodynamics in a Slim Hole Drilling Annulus. *J. Pet. Sci. Eng.* 70, 308–319. <https://doi.org/10.1016/j.petrol.2009.12.002>

Heshamudin, N.S., Katende, A., Rashid, H.A., Ismail, I., Sagala, F., Samsuri, A., 2019.

- Experimental investigation of the effect of drill pipe rotation on improving hole cleaning using water-based mud enriched with polypropylene beads in vertical and horizontal wellbores. *J. Pet. Sci. Eng.* 179, 1173–1185. <https://doi.org/10.1016/j.petrol.2019.04.086>
- Heydari, O., Sahraei, E., Skalle, P., 2017. Investigating the Impact of Drillpipe's Rotation and Eccentricity on Cuttings Transport Phenomenon in Various Horizontal Annuluses using Computational Fluid Dynamics (CFD). *J. Pet. Sci. Eng.* 156, 801–813. <https://doi.org/10.1016/j.petrol.2017.06.059>
- Hirpa, M.M., Kuru, E., 2020. Hole cleaning in horizontal wells using viscoelastic fluids-an experimental study of drilling fluid properties on the bed erosion dynamics, in: *SPE/IADC Drilling Conference*. Galveston, Texas. <https://doi.org/10.2118/199636-pa>
- Huque, M.M., Butt, S., Zendejboudi, S., Imtiaz, S., 2020. Systematic Sensitivity Analysis of Cuttings Transport in Drilling Operation Using Computational Fluid Dynamics Approach. *J. Nat. Gas Sci. Eng.* 81, 103386. <https://doi.org/10.1016/j.jngse.2020.103386>
- Hussaini, S.M., Azar, J.J., 1983. Experimental Study of Drilled Cuttings Transport Using Common Drilling Muds. *Soc. Pet. Eng. J.* 23, 11–20. <https://doi.org/10.2118/10674-PA>
- Kamp, A.M., Rivero, M., Intevap, P., 1999. Layer Modeling for Cuttings Transport in Highly Inclined Wellbores, in: *SPE Latin American and Caribbean Petroleum Engineering Conference*. Caracas, Venezuela, 21-23 April. <https://doi.org/10.2118/53942-MS>
- Kelessidis, V.C., Bandelis, G.E., 2004. Flow Patterns and Minimum Suspension Velocity for Efficient Cuttings Transport in Horizontal and Deviated Wells in Coiled-Tubing Drilling. *SPE Drill. Complet.* <https://doi.org/10.2118/81746-PA>

- Kelessidis, V.C., Bandelis, G.E., Li, J., 2007. Flow of Dilute Solid-liquid Mixtures in Horizontal Concentric and Eccentric Annuli. *J. Can. Pet. Technol.* 46, 56–61. <https://doi.org/10.2118/07-05-06>
- Kelessidis, V.C., Mpandelis, G.E., 2003. Flow Patterns and Minimum Suspension Velocity for Efficient Cuttings Transport in Horizontal and Deviated Wells in Coiled-Tubing Drilling, in: *Proceedings of the SPE/ICoTA Coiled Tubing Roundtable Conf.* pp. 180–193. <https://doi.org/10.2523/81746-ms>
- Kim, Y.J., Woo, N.S., Hwang, Y.K., Kim, J.H., Han, S.M., 2014. Transport of small cuttings in solid-liquid flow with inclined slim hole annulus. *J. Mech. Sci. Technol.* 28, 115–126. <https://doi.org/10.1007/s12206-013-0952-7>
- Li, J., Luft, B., 2014. Overview of solids transport studies and applications in oil and gas industry - Experimental work. *Soc. Pet. Eng. - SPE Russ. Oil Gas Explor. Prod. Tech. Conf. Exhib. 2014, RO G 2014 - Sustain. Optimising Prod. Challenging Limits with Technol. 2*, 1365–1401. <https://doi.org/10.2118/171285-ms>
- Martin, M., Georges, C., Bisson, P., Konirsch, O., 1987. Transport of Cuttings in Directional Wells, in: *SPE/IADC Drilling Conference*. New Orleans, Louisiana, USA, 15-18 March. <https://doi.org/10.2118/16083-MS>
- Masuda, Y., Doan, Q., Oguztoreli, M., Naganawa, S., Yonezawa, T., Kbayashi, A., Kamp, A., 2000. Critical Cuttings Transport Velocity in Inclined Annulus: Experimental Studies and Numerical Simulation, in: *SPE/CIM International Conference on Horizontal Well Technology*. Calgary, Alberta, Canada, 6-8 November. <https://doi.org/10.2118/65502-MS>
- McCann, R.C., Quigley, M.S., Zamora, M., Slater, K.S., 1995. Effects of High-Speed Pipe

- Rotation on Pressures in Narrow Annuli. SPE Drill. Complet. 10, 96–103.
<https://doi.org/10.2118/26343-PA>
- Naganawa, S., Sato, R., Ishikawa, M., 2017. Cuttings-transport simulation combined with large-scale-flow-loop experimental results and logging-while-drilling data for hole-cleaning evaluation in directional drilling. SPE Drill. Complet. 32, 194–207.
<https://doi.org/10.2118/171740-PA>
- Nazri, T., Hareland, G., Azar, J., 2010. Review of Cuttings Transport in Directional Well Drilling: Systematic Approach, in: SPE Western Regional Meeting. Anaheim, California, USA, 27–29 May, p. 15. <https://doi.org/10.2118/132372-MS>
- Nguyen, D., Rahman, S.S., 1998. A Three-Layer Hydraulic Program for Effective Cuttings Transport and Hole Cleaning in Highly Deviated and Horizontal Wells. SPE Drill. Complet. 68, 78–82.
- Okrajni, S., Azar, J.J., 1986. The Effects of Mud Rheology on Annular Hole Cleaning in Directional Wells. SPE Drill. Eng. 1, 297–308. <https://doi.org/10.2118/14178-PA>
- Ozbayoglu, E.M., Etehad Osgouei, R., Ozbayoglu, M.A., Yuksel, E.H., 2012. Hole-Cleaning Performance of Gasified Drilling Fluids in Horizontal Well Sections. SPE J. 17, 912–923.
<https://doi.org/10.2118/131378-PA>
- Ozbayoglu, E.M., Osgouei, R.E. et al., 2012. Hole-Cleaning Performance of Gasified Drilling Fluids in Horizontal Well Sections. SPE J. <https://doi.org/10.2118/131378-PA>
- Ozbayoglu, M.E., Saasen, A., Sorgun, M., Svanes, K., 2008. Effect of Pipe Rotation on Hole Cleaning for Water-Based Drilling Fluids in Horizontal and Deviated Wells, in: IADC/SPE

- Asia Pacific Drilling Technology Conference and Exhibition. Jakarta, Indonesia. 25–27 August. <https://doi.org/10.2118/114965-MS>
- Pang, B., Wang, S., Jiang, X., Lu, H., 2019. Effect of orbital motion of drill pipe on the transport of non-Newtonian fluid-cuttings mixture in horizontal drilling annulus. *J. Pet. Sci. Eng.* 174, 201–215. <https://doi.org/10.1016/j.petrol.2018.11.009>
- Pang, B., Wang, S., Wang, Q., Yang, K., Lu, H., Hassan, M., Jiang, X., 2018a. Numerical prediction of cuttings transport behavior in well drilling using kinetic theory of granular flow. *J. Pet. Sci. Eng.* 161, 190–203. <https://doi.org/10.1016/j.petrol.2017.11.028>
- Pang, B., Wang, S., Wang, Q., Yang, K., Lu, H., Hassan, M., Jiang, X., 2018b. Numerical Prediction of Cuttings Transport Behavior in Well Drilling Using Kinetic Theory of Granular Flow. *J. Pet. Sci. Eng.* 161, 190–203. <https://doi.org/10.1016/j.petrol.2017.11.028>
- Peden, J.M., Ford, J.T., Oyeneyin, M.B., 1990. Comprehensive Experimental Investigation of Drilled Cuttings Transport in Inclined Wells Including the Effects of Rotation and Eccentricity, in: European Petroleum Conference. The Hague, The Netherlands, 22-24 October. <https://doi.org/10.2118/20925-MS>
- Philip, Z., Sharma, M.M., Chenevert, M.E., 1998a. Role of Taylor vortices in the transport of drill cuttings. *Proc. SPE India Oil Gas Conf. Exhib.* 77–83.
- Philip, Z., Sharma, M.M., Chenevert, M.E., 1998b. The Role of Taylor Vortices in the Transport of Drill Cuttings, in: SPE India Oil and Gas Conference and Exhibition. New Delhi, India, 7-9 April. <https://doi.org/10.2118/39504-MS>
- Pilehvari, A.A., Azar, J.J., Shirazi, S.A., 2007. State-of-the-Art Cuttings Transport in Horizontal

- Wellbores. SPE Drill. Complet. 14, 196–200. <https://doi.org/10.2118/57716-pa>
- Piroozian, A., Ismail, I., Yaacob, Z., Babakhani, P., Ismail, A.S.I., 2012. Impact of Drilling Fluid Viscosity, Velocity And Hole Inclination On Cuttings Transport In Horizontal And Highly Deviated Wells. J. Pet. Explor. Prod. Technol. 2, 149–156. <https://doi.org/10.1007/s13202-012-0031-0>
- Ramadan, A., Skalle, P., Johansen, S.T., Svein, J., Saasen, A., 2001. Mechanistic Model for Cuttings Removal From Solid Bed in Inclined Channels. J. Pet. Sci. Eng. 30, 129–141. [https://doi.org/10.1016/S0920-4105\(01\)00108-5](https://doi.org/10.1016/S0920-4105(01)00108-5)
- Rasul, G., Qureshi, M.F., Ferroudji, H., Butt, S., Hasan, R., Hassan, I., Rahman, M.A., 2020. Analysis of cuttings transport and flow pattern in nearly horizontal extended reach well. J. Adv. Res. Fluid Mech. Therm. Sci. 71, 69–86. <https://doi.org/10.37934/arfmts.71.2.6986>
- Rodriguez Corredor, F., Bizhani, M., Kuru, E., 2016. Experimental investigation of cuttings bed erosion in horizontal wells using water and drag reducing fluids. J. Pet. Sci. Eng. 147, 129–142. <https://doi.org/10.1016/j.petrol.2016.05.013>
- Sanchez, R.A., Azar, J.J., Bassal, A.A., Martins, A.L., 1999. Effect of Drillpipe Rotation on Hole Cleaning During Directional-Well Drilling. SPE J. 4(2), 101–108. <https://doi.org/10.2118/56406-PA>
- Sanchez, R.A., Azar, J.J., Bassal, A.A., Martins, A.L., 1997. The Effect of Drillpipe Rotation on Hole Cleaning During Directional Well Drilling, in: SPE/IADC Drilling Conference. Amsterdam, The Netherlands, 4-6 March. <https://doi.org/10.2118/37626-MS>
- Sayindla, S., Lund, B., Taghipour, A., Werner, B., Ytrehus, J.D., 2016. Experimental investigation

- of cuttings transport with oil based drilling fluids, in: 35th International Conference on Ocean, Offshore and Arctic Engineering. pp. 1–9. <https://doi.org/10.1115/OMAE2016-54047>
- Sayindla, S., Lund, B., Ytrehus, J.D., Saasen, A., 2019. CFD modeling of hydraulic behavior of oil- and water-based drilling fluids in laminar flow. *SPE Drill. Complet.* 34, 207–215. <https://doi.org/10.2118/184660-PA>
- Shao, B., Yan, Y., Yan, X., Xu, Z., 2019. A study on non-spherical cuttings transport in CBM well drilling by coupled CFD-DEM. *Eng. Appl. Comput. Fluid Mech.* 13, 579–590. <https://doi.org/10.1080/19942060.2019.1615553>
- Sifferman, T.R., Becker, T.E., 1992. Hole Cleaning in Full-Scale Inclined Wellbores. *SPE Drill. Eng.* 7, 115–120. <https://doi.org/10.2118/20422-PA>
- Sifferman, T.R., Myers, G.M., Haden, E.L., Wahl, H.A., 1973a. Drill Cuttings Transport in Full Scale Vertical Annuli, in: 48th Annular Fall Meeting of the Society of Petroleum Engineers of AIME. Las Vegas, 30 Sept- 3 Oct. <https://doi.org/10.2118/4514-MS>
- Sifferman, T.R., Myers, G.M., Haden, E.L., Wahl, H.A., 1973b. Drill Cutting Transport in Full Scale Vertical Annuli, in: Society of Petroleum Engineers of AIME. Las Vegas, p. 5.
- Sorgun, M., Aydin, I., Ozbayoglu, M.E., 2011. Friction Factors for Hydraulic Calculations Considering Presence of Cuttings and Pipe Rotation in Horizontal/Highly-Inclined Wellbores. *J. Pet. Sci. Eng.* 78, 407–414. <https://doi.org/10.1016/j.petrol.2011.06.013>
- Sun, B., Xiang, H., Li, H., Li, X., 2017. Modeling of the Critical Deposition Velocity of Cuttings in an Inclined-Slimhole Annulus. *SPE J.* 22, 1213–1224. <https://doi.org/10.2118/185168-PA>
- Sun, X., Wang, K., Yan, T., Shao, S., Jiao, J., 2014. Effect of drillpipe rotation on cuttings transport

- using computational fluid dynamics (CFD) in complex structure wells. *J. Pet. Explor. Prod. Technol.* 4, 255–261. <https://doi.org/10.1007/s13202-014-0118-x>
- Tomren, P.H., Iyoho, A.W., Azar, J.J., 1986. Experimental Study of Cuttings Transport in Directional Wells. *SPE Drill. Eng.* 43–56. <https://doi.org/10.2118/12123-PA>
- Vaziri, E., Simjoo, M., Chahardowli, M., 2020. Application of foam as drilling fluid for cuttings transport in horizontal and inclined wells: A numerical study using computational fluid dynamics. *J. Pet. Sci. Eng.* 194, 107325. <https://doi.org/10.1016/j.petrol.2020.107325>
- Walker, S., Li, J., 2000. The Effects of Particle Size, Fluid Rheology, and Pipe Eccentricity on Cuttings Transport, in: *SPE/ICoTA Coiled Tubing Roundtable*. Houston, TX, USA, 5–6 April. <https://doi.org/10.2118/60755-MS>
- Wei, N., Meng, Y., Li, G., Wan, L., Xu, Z., Xu, X., Zhang, Y., 2013. Cuttings transport models and experimental visualization of underbalanced horizontal drilling. *Math. Probl. Eng.* 2013. <https://doi.org/10.1155/2013/764782>
- Yeu, W.J., Katende, A., Sagala, F., Ismail, I., 2019. Improving hole cleaning using low density polyethylene beads at different mud circulation rates in different hole angles. *J. Nat. Gas Sci. Eng.* 61, 333–343. <https://doi.org/10.1016/j.jngse.2018.11.012>
- Yu, M., Takach, N.E., Nakamura, D.R., Shariff, M.M., 2007. An Experimental Study of Hole Cleaning Under Simulated Downhole Conditions, in: *SPE Annual Technical Conference and Exhibition*. <https://doi.org/10.2118/109840-MS>
- Zhang, C., Tang, J., Wang, L., Zhang, G., 2018. Flow pattern maps for particle-fluid mixture transport in a horizontal pipe - application of a three-layer model. *J. Dispers. Sci. Technol.*

39, 1664–1674. <https://doi.org/10.1080/01932691.2018.1461640>

Zhang, F., Miska, S., Yu, M., Ozbayoglu, E., 2018. A unified transient solid-liquid two-phase flow model for cuttings transport- modelling part. *J. Pet. Sci. Eng.* 166, 146–156. <https://doi.org/10.1016/j.petrol.2018.03.027>

Zhu, Z., Sand, K. W., Teevens, P. J., 2010. Effects of flow regime on solids deposition in multiphase petroleum flow, in: *NACE - International Corrosion Conference Series*. pp. 1–19.

Chapter 2 : Systematic Sensitivity Analysis of Cuttings Transport in Drilling Operation Using Computational Fluid Dynamics Approach

Mohammad Mojammel Huque, Stephen Butt, Sohrab Zendehboudi, Syed Imtiaz
Department of Process Engineering, Memorial University, St. John's, NL, Canada

ABSTRACT

Hole cleaning and cuttings transport play a vital role in the drilling operation. Various drilling problems such as a reduction in penetration rate, increase in the torque and drag, and an increase in the potential of differential sticking are often related to poor cuttings transport from a wellbore. Multiple parameters, including the fluid rheology, mud velocity, cuttings size, and drill pipe inclination generally influence the cuttings transport performance. Although several experimental and modelling research works have been conducted in this area, the interactions among the parameters during cuttings transport have not been adequately investigated. This study focuses on interactions between the drilling parameters. Cuttings transport in the wellbore represents a solid-liquid multiphase flow phenomenon. In this research work, Computational Fluid Dynamics (CFD) is employed to simulate the cuttings transport behaviors in a horizontal wellbore. The Eulerian-Eulerian multiphase flow model is adopted to describe the flow characteristics in the wellbore annular section. A statistical method, Design of Experiment (DOE), is used to systematically monitor the interactions among the independent variables. A comprehensive parametric sensitivity analysis is then conducted to obtain a better understanding of the relationship between input variables and target parameter (cutting transport performance). It is found that the mud viscosity, mud velocity, and drill pipe rotation have a positive impact, whereas the cuttings size and annular clearance show a significant adverse effect on cuttings transport performance. Although both drilling mud viscosity and velocity show the positive effect, the interaction among them exhibits

a negative influence on cuttings transport. According to the results, the cuttings with a size of 1 mm to 2 mm are difficult to be cleaned, compared to larger cuttings. Due to operational limitations, optimization of all drilling parameters is not feasible. Thus, a two-factor interaction study can assist in determining the most significant factors and implementing an optimized drilling strategy.

Keywords: Drilling; Cuttings Transport; Two-Factor Interaction; Design of Experiment; CFD Sensitivity Analysis; Two-Phase Flow

2.1 Introduction

Cuttings removal from the borehole is a critical step in the drilling process, especially for horizontal, extended reach, and inclined wells. An improper hole cleaning can cause serious issues such as stuck pipe, reduced penetration rate, faster bit wear, lost circulation, and excessive torque and drag. A rapid removal of drill cuttings from the borehole with an appropriate drilling mud assists in achieving a higher drilling penetration rate by continuous contact of a drill bit with fresh rock surface in the formation (Sanchez et al., 1999). An effective/accurate design of drilling mud and adequate mud circulation is necessary to remove the cuttings from the borehole. Other vital factors such as formation type, wellbore inclination, cuttings size, rate of penetration, and drill pipe eccentricity considerably affect the performance of drilling operation. It is challenging to develop an optimum hole cleaning strategy considering all these factors.

Investigating cuttings transport behavior in the annular section of the drilling system is of great interest to researchers for the last few decades. Early studies on solid transport were mostly experimental. More recently, researchers carried out CFD simulation for detailed sensitivity analysis, scale-up, and optimization purposes. There are several experimental studies in the literature that investigated the effect of fluid rheology and velocity in cuttings transport (Ahmed

and Miska, 2008; Avila et al., 2004; Capo et al., 2004; Chen et al., 2007; Duan et al., 2010; Hemphill and Ravi, 2006; Naganawa and Nomura, 2006; Ozbayoglu and Sorgun, 2010; Pereira et al., 2007; Sifferman and Becker, 1992; Tormen et al., 1986). Almost all of the experimental studies revealed that non-Newtonian fluid plays a vital role in cuttings transport. The CFD studies also emphasized on the effect of fluid rheology (Bilgesu et al., 2007; Demiralp, 2014; Epelle and Gerogiorgis, 2017; GhasemiKafrudi and Hashemabadi, 2016; Heydari et al., 2017; Ozbayoglu and Sorgun, 2010; Pang et al., 2018; Rooki et al., 2015, 2014; Sorgun et al., 2011; Wang et al., 2009). However, the cuttings transport capability of a viscous fluid is diminished by an increase in the mud velocity and drill pipe rotation (Pang et al., 2018). Both experimental and CFD studies revealed that an increase in the drill pipe rotation effectively reduces the minimum transport velocity of drilling mud and cuttings bed thickness in the horizontal annular section. However, there is no improvement in cuttings transport beyond a threshold limit of drill pipe rotation (Demiralp, 2014; Heydari et al., 2017; Ofei et al., 2014). The effect of cuttings size on solid transport was investigated in some experimental studies, which revealed that an increase in cuttings size decreases the cuttings transport capability (Ford et al., 1996; Sanchez et al., 1999; Tormen et al., 1986; Walker and Li, 2000). Some of the past CFD also claimed that an increase in eccentricity and cuttings size has adverse impacts on cuttings transport investigations (GhasemiKafrudi and Hashemabadi, 2016; Pang et al., 2018). Transport of drill cuttings in the annulus has also been studied considering mechanistic models (Clark and Bickham, 1994; Doron and Barnea, 1993; Guo et al., 2010; Larsen et al., 1997; Li et al., 2007; Mao et al., 2012; Naganawa and Nomura, 2006; Nguyen. D., Rahman, 1996; Osunde and Kuru, 2008; Ozbayoglu et al., 2005; Philip et al., 1998; Ramadan et al., 2001; Sun et al., 2017; Wei et al., 1998). Most of the mechanistic models focused on the prediction of critical fluid velocity to avoid cuttings deposition

in the annulus. Due to complexity in the numerical solution, almost all steady-state and unsteady-state models consider only one or two vital parameters for estimation and evaluation purposes.

Although several researchers have claimed that an increase in the fluid velocity and drill pipe rotation increases the cuttings transport efficiency, there are some diverse views on a part of crucial parameters. For example, a low viscous mud shows a better hole cleaning performance (Sorgun et al., 2011; Walker and Li, 2000) that contradicts the past finding (Sifferman et al., 1973; Tormen et al., 1986). A study in the slim hole annulus revealed that pressure drop in the annulus increases with increasing inner pipe rotation (Han et al., 2010), which is opposite to the findings of previous works (McCann et al., 1995; Ozbayoglu et al., 2008). Sanchez et al. (1999) concluded that smaller cuttings are difficult to transport, whereas Walker and Li (2000) found that fine solid particles are easier to clean.

One of the main reasons for such contradictions is that a variety of experimental setups with different pipe diameters, annular clearances, orientations, and fluid/mud types (or rheology) have been used in the previous research investigations. Many of the experimental methods commonly consider "One Factor At a Time" (OFAT) so that all factors except one factor are kept constant. Thus, only one parameter varies each time. The OFAT technique is inefficient when multiple factors change simultaneously.

Based on our literature review, all experimental studies and numerical models developed so far are mainly case-specific. Due to the experimental limitations, not all parameters may be varied simultaneously. Since a large number of parameters such as viscosity, velocity, cuttings size, drill pipe rotation, and eccentricity have direct influence on cuttings transport, the interaction between influential parameters is a vital aspect, which is ignored in the majority of the previous experimental studies.

The objective of this work is to investigate two-factor interactions among the parameters that have a combined effect on drilling performance. A computational two-phase (solid-liquid) model is presented, and the model is validated using available experimental data. A two-level statistical DOE is introduced to check interactions between several variables considered in this study. Furthermore, a parametric study is performed to find the optimum cuttings transport scenario.

This manuscript is organized as follows: **Section 3.2** includes an overview of solid-liquid two-phase flow modelling and statistical Design of Experiment (DOE). **Section 3.3** describes the methodology presented in the current work. Limitations of the proposed model are given in **Section 3.4**. The experimental validation, and results and discussion are found in **Section 3.5**. Finally, the main remarking points are listed in conclusions.

2.2 Theory and Background

This section covers an overview of solid-liquid multiphase flow modelling, assumptions, and governing equations used to simulate two-phase flow behaviors. A brief on performance measurement and fundamentals of statistical DOE are also provided in this section.

2.2.1 Solid-Liquid Flow

Cuttings transport in the annulus represents a two-phase flow of solid cuttings and drilling mud. In this study, the Eulerian-Eulerian multiphase flow model (Inc. ANSYS, 2013) is used to model the two-phase flow system. The drilling mud is considered as the primary fluid and the cuttings as the secondary fluid. In the Eulerian-Eulerian model, solid cuttings are treated as a continuum. A typical drilling cuttings transport system is demonstrated in **Figure 2-1** that provides a simple schematic of concentric and eccentric drill pipe configurations.

The following assumptions are considered for the two-phase model:

- Drilling fluid is an incompressible non-Newtonian fluid. A Herschel-Bulkley model is used to represent the fluid properties/behaviors.
- All drill cuttings are sphere with a mean diameter.
- The density of drill cuttings is constant.
- No interfacial mass transfer occurs between the drilling mud and cuttings.
- Pressure distribution is uniform among all phases, both phases have the same pressure.
- An isothermal condition is maintained.

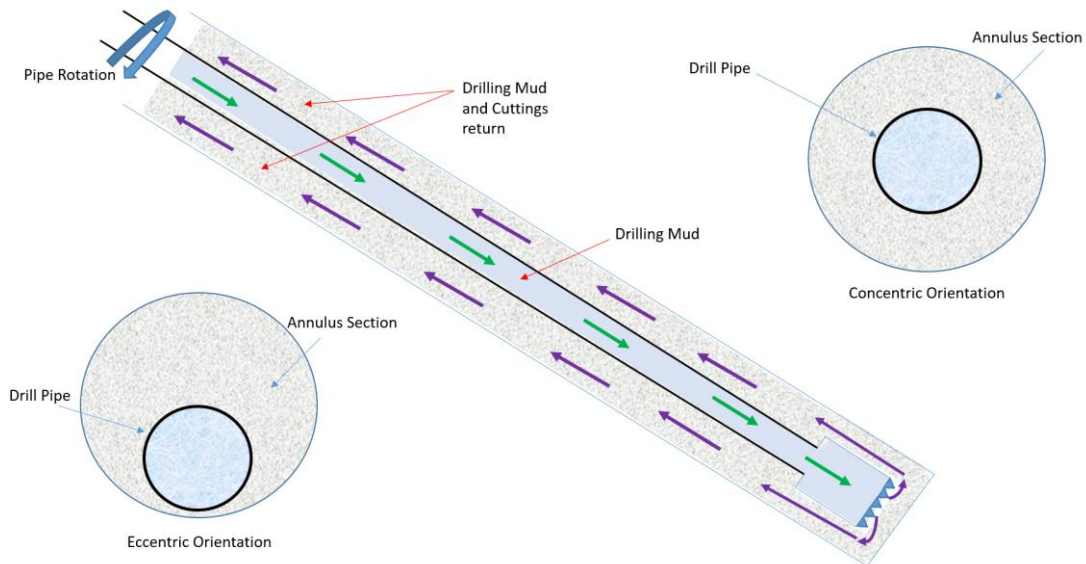


Figure 2-1: Cuttings transport in the annular section with concentric and eccentric profile.

The pipe eccentricity is defined as follows (Wei et al., 1998):

$$e = \frac{2\delta}{D_{hole} - D_{pipe}} \quad (2-1)$$

where e stands for the eccentricity of the annulus and δ represents the offset from the centre. D_{hole} and D_{pipe} are the hole and pipe diameters, respectively.

Mass conservation. The continuity equation for the drilling mud (liquid) is given below (Fluent, 2015):

$$\frac{\partial}{\partial t}(\alpha_l \rho_l) + \nabla \cdot (\alpha_l \rho_l \vec{v}_l) = \Sigma(\dot{m}_{ls} - \dot{m}_{sl}) = 0 \quad (2-2)$$

in which, v_l is the velocity of the liquid phase; ρ_l denotes the density of the liquid phase; \dot{m}_{ls} refers to the mass transfer from the liquid phase to the solid phase; and \dot{m}_{sl} resembles the mass transfer from the solid phase to the liquid phase. Since there is no mass transfer among the phases, the summation on the right-hand side of Equation (2-2) is assumed to be zero. The annular volume is comprised of only two phases. The volume fraction is defined as α_l for the mud phase and α_s for the cuttings, where $\alpha_l + \alpha_s = 1$. The subscripts l and s are used for the mud (liquid) and cuttings (solid) phases, respectively.

Similarly, the continuity equation for the solid phase is represented by the following relationship (Fluent, 2015):

$$\frac{\partial}{\partial t}(\alpha_s \rho_s) + \nabla \cdot (\alpha_s \rho_s \vec{v}_s) = \Sigma(\dot{m}_{sl} - \dot{m}_{ls}) = 0 \quad (2-3)$$

in which, v_s is the velocity of the solid phase; and ρ_s stands for the density of the solid phase.

Momentum conservation. The momentum balance for the liquid phase is given by the following equation (Fluent, 2015):

$$\frac{\partial}{\partial t}(\alpha_l \rho_l \vec{v}_l) + \nabla \cdot (\alpha_l \rho_l \vec{v}_l \vec{v}_l) = -\alpha_l \nabla p + \nabla \cdot \bar{\tau}_l + \alpha_l \rho_l \vec{g} + \Sigma(\vec{R}_{sl} + \dot{m}_{sl} \vec{v}_{sl} - \dot{m}_{ls} \vec{v}_{ls}) + (\vec{F}_l + \vec{F}_{lift,l} + \vec{F}_{wl,l} + \vec{F}_{vm,l} + \vec{F}_{td,l}) \quad (2-4)$$

in which, F_l is an external body force; $\vec{F}_{lift,l}$ represents a lift force; $\vec{F}_{wl,l}$ symbolizes the wall lubrication force; $\vec{F}_{vm,l}$ is the virtual mass force; $\vec{F}_{td,l}$ stands for a turbulent dispersion force; p introduces the pressure shared by both solid and liquid phases; and \vec{v}_{sl} is the interphase velocity defined as: $\vec{v}_{sl} = \vec{v}_s$ if $\dot{m}_{sl} < 0$.

$\bar{\tau}_l$ also introduces the stress-strain tensor for the liquid phase, as defined below (Fluent, 2015):

$$\bar{\tau}_l = \alpha_l \mu_l (\nabla \vec{v}_l + \nabla \vec{v}_l^T) + \alpha_l (\lambda_l - \frac{2}{3} \mu_l) \nabla \cdot \vec{v}_l \bar{I} \quad (2-5)$$

In Equation (2-5), μ_l and λ_l denote the shear and bulk viscosity of liquid phase, respectively.

The conservation of momentum for the solid phase is expressed as follows (Fluent, 2015):

$$\frac{\partial}{\partial t} (\alpha_s \rho_s \vec{v}_s) + \nabla \cdot (\alpha_s \rho_s \vec{v}_s \vec{v}_s) = -\alpha_s \nabla p - \nabla p_s + \nabla \cdot \bar{\tau}_s + \alpha_s \rho_s \vec{g} + \sum (K_{ls} (\vec{v}_l - \vec{v}_s)) + \dot{m}_{ls} \vec{v}_{ls} - \dot{m}_{sl} \vec{v}_{sl}) + (\vec{F}_s + \vec{F}_{lift,s} + \vec{F}_{wl,s} + \vec{F}_{vm,s} + \vec{F}_{td,s}) \quad (2-6)$$

where p_s stands for the solid phase pressure. \vec{R}_{sl} is the interaction force between the solid and liquid phases. This force mainly depends on the friction and pressure cohesion and is subject to the condition that $\vec{R}_{sl} = -\vec{R}_{ls}$ and $\vec{R}_{ll} = 0$ (Fluent, 2015), as given below:

$$\sum \vec{R}_{sl} = \sum K_{sl} (\vec{v}_s - \vec{v}_l) = 0 \quad (2-7)$$

Here, K_{sl} ($= K_{ls}$) introduces the interphase momentum exchange coefficient; and \vec{v}_s and \vec{v}_l are the solid and liquid phase velocities, respectively.

Solid shear stress. The solid stress tensor contains the shear and bulk viscosities resulted from particle momentum exchange due to the translation and collision among the particles in a two-phase flow. Solid shear viscosity (μ_s) can be properly defined as a combination of the collisional, kinetic, and frictional components as follows (Fluent, 2015):

$$\mu_s = \mu_{s,col} + \mu_{s,kin} + \mu_{s,fr} \quad (2-8)$$

Gidaspow (1994) proposed the following equation for the collisional part of the shear viscosity ($\mu_{s,col}$):

$$\mu_{s,col} = \frac{4}{5} \alpha_s \rho_s d_s g_{0,ss} (1 + e_{ss}) \left(\frac{\theta_s}{\pi} \right)^{1/2} \alpha_s \quad (2-9)$$

in which, d_s is the solid diameter; θ_s denotes the granular temperature of solid phase; e_{ss} refers to the coefficient of restitution; and $g_{0,ss}$ represents a distribution function.

The kinetic viscosity ($\mu_{s,kin}$) of the solid is introduced as follows (Gidaspow, 1994):

$$\mu_{s,kin} = \frac{10 \rho_s d_s \sqrt{\theta_s \pi}}{96 \alpha_s (1 + e_{ss}) g_{0,ss}} \left[1 + \frac{4}{5} g_{0,ss} \alpha_s (1 + e_{ss}) \right]^2 \alpha_s \quad (2-10)$$

Schaeffer (1987) proposed the following expression for the frictional viscosity ($\mu_{s,fr}$):

$$\mu_{s,fr} = \frac{p_s \sin \phi}{2 \sqrt{I_{2D}}} \quad (2-11)$$

where p_s resembles the solids pressure; ϕ is the angle of internal friction; and I_{2D} introduces the second invariant of deviatoric stress tensor.

The solid bulk viscosity (λ_s) accounts for the resistance of the granular particles to the compression and expansion. Lun et al. (1984) expressed the solid bulk viscosity in terms of other important parameters such as solid density and mean diameter, as given below:

$$\lambda_s = \frac{4}{5} \alpha_s^2 \rho_s d_s g_{0,ss} (1 + e_{ss}) \left(\frac{\theta_s}{\pi} \right)^{1/2} \quad (2-12)$$

Particle drag model. The momentum exchange between the solid and liquid phases is based on the interphase exchange coefficient (K_{sl}). Gidaspow (1994) introduced the following equations (for K_{sl}), which are combinations of Wen and Yu (1966) and the Ergun correlations.

When $\alpha_l > 0.8$, the fluid-solid exchange coefficient (K_{sl}) is obtained as follows (Fluent, 2015):

$$K_{sl} = \frac{3}{4} C_D \frac{\alpha_s \alpha_l \rho_l |\bar{v}_s - \bar{v}_l|}{d_s} \alpha_l^{-2.65} \quad (2-13)$$

In Equation (2-13), C_D is the drag coefficient that can be defined as follows:

$$C_D = \frac{24}{\alpha_l Re_s} [1 + 0.15(\alpha_l Re_s)^{0.687}] \quad , \quad \text{for } Re_s < 1000 \quad (2-14)$$

and $C_D = 0.44$ for $Re_s > 1000$

Where,

$$Re_s = \frac{\rho_l d_s |\vec{v}_s - \vec{v}_l|}{\mu_l} \quad (2-15)$$

in which, Re_s symbolizes the relative Reynolds number.

When $\alpha_l < 0.8$, the fluid-solid exchange coefficient is determined by the following expression:

$$K_{sl} = 150 \frac{\alpha_s(1-\alpha_l)\mu_l}{\alpha_l d_s^2} + 1.75 \frac{\alpha_l \alpha_s |\vec{v}_s - \vec{v}_l|}{d_s} \quad (2-16)$$

Particle lift model. The Saffman-Mei particle lift model is used in the ANSYS Fluent. Saffman (1965) defined the lift coefficient (C_l) for low Reynolds number flow past a spherical particle as given below:

$$C_l = \frac{3}{2\pi\sqrt{Re_\omega}} C'_l \quad (2-17)$$

where C'_l is the lift coefficient; Re_p is the particle Reynolds number; and Re_ω refers to the vorticity Reynolds number. According to Equation (2-17), $C'_l = 6.46$ and $0 \leq Re_p \leq Re_\omega \leq 1$.

Mei and Klausner (1994) extended the model to a higher range of particle Reynolds number (Re_p).

The Saffman-Mei model is empirically expressed as follows:

$$C_l = \begin{cases} 6.46 \times f(Re_p, Re_\omega) & Re_p \leq 40 \\ 6.46 \times 0.0524 (\beta Re_p)^{1/2} & 40 < Re_p \leq 100 \end{cases} \quad (2-18)$$

where,

$$\beta = 0.5 \left(\frac{Re_\omega}{Re_p} \right) \quad (2-19)$$

$$f(Re_p, Re_\omega) = (1 - 0.3314\beta^{0.5})e^{-0.1Re_p} + 0.3314\beta^{0.5} \quad (2-20)$$

For a denser packing of the solid phase at low shear rates, the generation of stress is only due to the friction between the particles.

2.2.2 Performance Measurement

To evaluate the effectiveness of different parameters involved in the transport of cuttings, two quantitative measures are used; including, Cuttings Transport Efficiency (CTE) and Annular Cuttings Percentage (ACP). The CTE is defined as follows (Sifferman et al., 1973):

$$CTE = \frac{v_c}{v_m} \times 100 \quad (2-21)$$

where v_c refers to the average velocity of the cuttings and v_m stands for the average velocity of the drilling mud in the annular section. A higher CTE value means that more cuttings are transported out of the hole, and fewer cuttings are accumulated in the annular hole section.

Annular cuttings volume fraction is defined as the ratio of the volume of cuttings to the total annular volume in the annulus where the total volume is comprised of mud volume and cuttings volume (Kleinstreuer, 2003). Thus, ACP is expressed as follows:

$$ACP = \frac{\text{Volume occupied by solids}}{\text{Volume occupied by mixture}} \times 100 \quad (2-22)$$

A low annular cuttings percentage implies that fewer cuttings are accumulated in the annulus, leading to efficient cuttings transport.

Continuous measurements and control of annular pressure loss are essential for safer drilling operations without fracturing the porous rock formation. The rheological properties of drilling fluid, annular fluid velocity, and two-phase mixture densities greatly influence the annular pressure loss variation. For performance measurement, the variation of annular pressure is also estimated with the aid of parametric analysis.

2.2.3 Statistical Analysis

A statistical approach, “Design of Experiments (DOE)”, is used in this study. DOE is an efficient and rigorous method for a variety of engineering applications. This method can simultaneously explore the effect of various factors and facilitate design optimization. DOE helps to identify the relationships between the cause and effect of a system or process. It can also evaluate which process inputs have significant effects on process output. DOE can also identify the input level for the desired process output. In this study, a two-level DOE is used. Two levels are ‘low’ and ‘high’. The two-level design is selected due to the small size of the experiments. Also, the interactions of the factors can be easily detected with a two-level design. The general two-level factorial experiment is also known as 2^k design where k represents the number of factors being investigated. For example, a two-level experiment with four factors requires $2 \times 2 \times 2 \times 2 = 2^4 = 16$ runs to explore the interactions among the factors.

During a drilling and hole cleaning operation, a higher cuttings transport efficiency (CTE) is always desirable along with minimum solid deposition in the annular section. In this study, the outcomes of DOE expressed as “positive effect” and “negative effect” in hole cleaning operation. A “positive effect” implies that increasing a factor value (such as mud velocity, viscosity etc.) increase the CTE with a reduced annular solid cuttings percentage. The “negative effect” shows the opposite trend, e.g., an increase in factor values decrease CTE and increase annular solid concentration.

In this study, the simulated results are compared with the experimental data. We then obtain the error percentage to examine model reliability. The error percentage is defined as the difference between a real value and a predicted value over the actual value, which is written below:

$$\% \text{ of error} = \frac{|Prediction - Experimental \text{ value}|}{Experimental \text{ value}} \times 100 \quad (2-23)$$

2.3 Methodology

The complete workflow is comprised of four tasks: appropriate DOE, simulation set up, experimental validation, and sensitivity analysis. In the DOE, all parameters used in this study are grouped according to their respective categories where their ranges are given. The simulation set up includes drawing the geometry, meshing, and running the simulation based on proper boundary conditions. The validation section compares the experimental data with simulation results. The parametric sensitivity analysis section shows the effect of each parameter on the cuttings transport performance.

2.3.1 Design of Experiment

To capture the effects of main factors as well as significant interactions among the parameters, a comprehensive list of parameters affecting the fluid transport is made based on the previous studies. Subsequently, the DOE method is employed before conducting the simulation runs. A carefully planned experimental design can explore important interactions between multiple input factors.

Referring to the previous hole-cleaning studies, it is evident that a large number of parameters affect the transport of the cuttings. **Table 2-1** lists the vital parameters and their ranges seen in past studies (Ahmed and Miska, 2008; Han et al., 2010; Ozbayoglu et al., 2008; Sifferman et al., 1973; Tormen et al., 1986). The targeted output is the maximization of the cuttings transport capability.

A two-level factorial design of experiment is performed. All parameters are classified into three sub-groups based on domain knowledge, as shown in **Table 2-1**.

Table 2-1: Key parameters selected for DOE.

Subgroup	Category	Parameter	Tested Range	
			Minimum	Maximum
1	Fluid Rheology	Consistency Index (k), Pa.s ⁿ	0.3	0.7
		Flow Behavior Index (n)	0.3	0.7
		Yield Stress (τ_o), Pa	0	4
2	Operational Parameters	Inner Pipe Rotation, rpm	10	80
		Mud Velocity, m/s	0.494	0.988
3	Cuttings Size and Annular Space	Cuttings Size, mm	1	5
		Diameter Ratio, (D_p/D_h)	0.44	0.89
		Eccentricity	0	0.8

Initially, experiments are carried out by varying parameters within each group to identify the parameter which has the most impact (or significance) on cuttings transport. The most important parameters from all subgroups are then selected, and another set of experiments are conducted by selected parameters to find the optimal operating and process conditions. Also, a sensitivity analysis is presented to discuss the effect of each parameter separately on cuttings transport.

2.3.2 Simulation Setup

In this study, a 6.4-meter (≈ 21 ft) horizontal annular test section is considered. This includes an outer pipe with a diameter of 2.91 in and an inner pipe with a diameter of 1.85 in. The length of the test section length is selected based on the hydrodynamic entrance length (L_h), i.e. the minimum length required for a fully developed flow in the test section for all tested fluid flow rates and fluid rheology. There is no well-established entrance length found in the literature for solid-liquid flow

in the annulus section. Thus, the entrance length is estimated based on the single-phase flow model, as given below (Bergman and Incropera, 2011; Çengel and Cimbala, 2006).

$$L_{h,lam} = 0.05 R_e D \quad (2-24)$$

$$L_{h,turb} = 4.4 D R_e^{1/6} \quad (2-25)$$

An eccentric annulus might be observed in horizontal drilling due to the weight of the drill pipe. The eccentric position is shown by the relative position of the drill pipe with respect to the borehole wall for a horizontal annulus (see **Figure 2-2**). Three different annular orientations, concentric ($e = 0$) and two eccentric ($e = 0.5, 0.8$) conditions, are examined in this study.

Mesh size and mesh quality play a significant role in CFD study. The structured hexahedral mesh is used in this simulation study due to simple annular geometry. To determine the optimal number of mesh sizes that can produce an acceptable result with a certain degree of accuracy and minimum computational resources requirement, a grid independency study is performed for all geometric conditions. Water with a velocity of 1.0 m/s is used to check the grid study for the horizontal annulus section and the corresponding pressure drop is estimated.

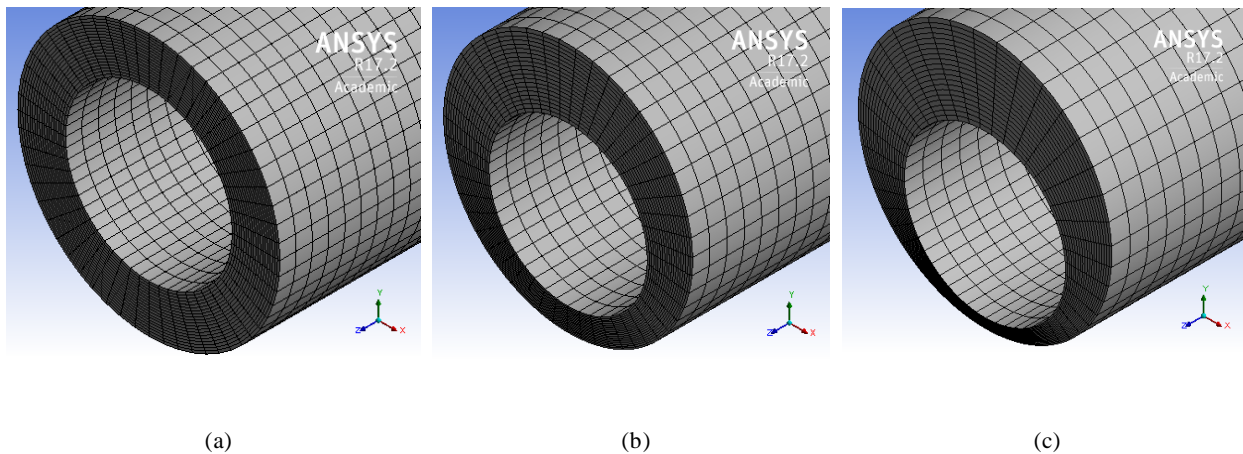


Figure 2-2: Computational mesh for different annular configurations

(a) Fully concentric annulus, $e = 0$, (b) Moderately eccentric annulus, $e = 0.5$, and (c) Highly eccentric annulus, $e = 0.8$.

Out of several meshing methodologies, the edge sizing and face meshing are implemented at the inlet and outlet boundaries to capture boundary condition with reasonable resolution. Different combinations of face division and edge sizing are tested to identify the optimal mesh properties. The grid independence analysis shows that there is no improvement in mesh quality above face division of 20 for this annular diameter. However, increasing edge sizing exhibits gradual improvement in mesh quality in terms of skewness and orthogonal quality.

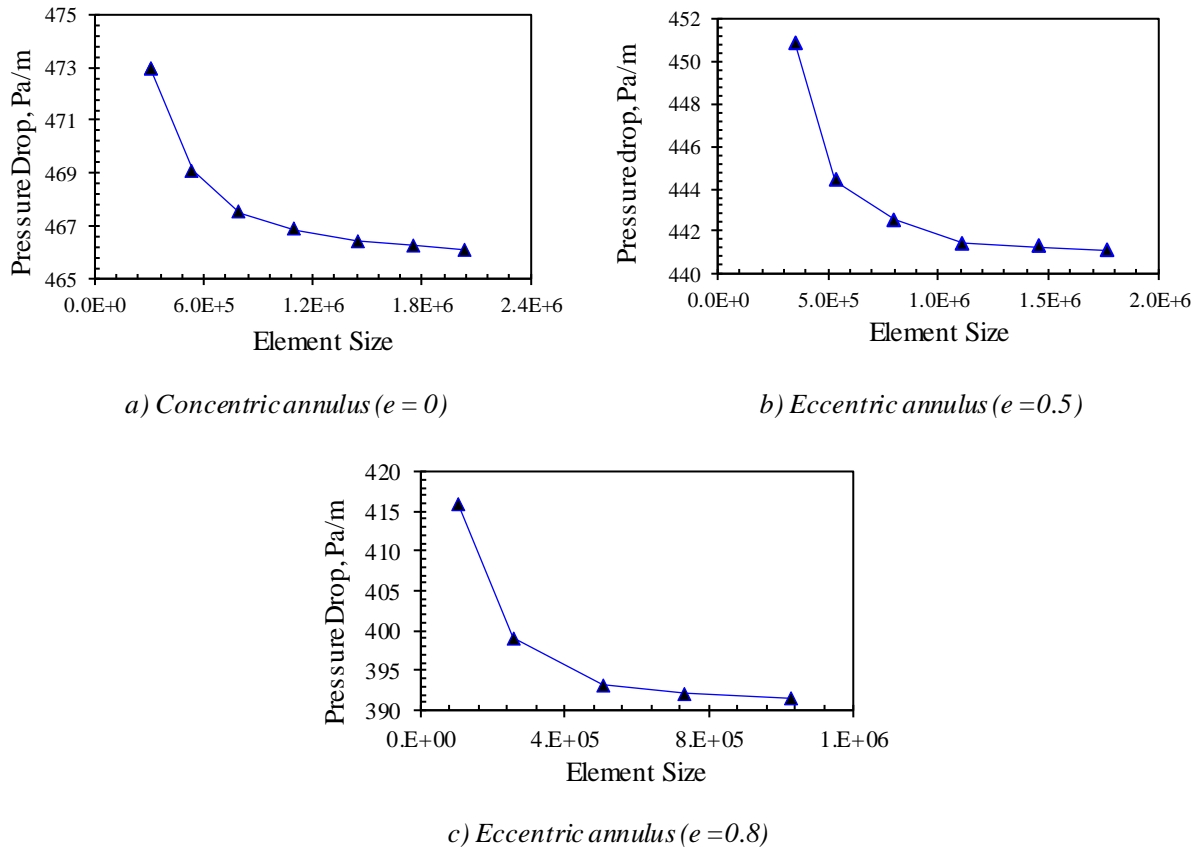


Figure 2-3: Grid independence study for all three annular configurations.

The grid independence analysis for all three geometric conditions is illustrated in **Figure 2-3**. The results show that approximately 1.5 million elements for a concentric system, 1.1 million elements

for eccentricity 0.5, and 1.0 million elements for eccentricity 0.8 are required to make the simulation free from the mesh size dependency. The maximum, minimum, and average orthogonal quality and skewness for the selected mesh size are reported in **Table 2-2**. A high orthogonal quality (~ 1.0) and low skewness (< 0.25) are ensured for all geometric conditions, implying a decent mesh quality.

For an acceptable prediction of multiphase flow behavior with CFD, accurate fluid and solid properties are required along with appropriate initial and boundary conditions. Two different drilling fluids [$(\tau_o=2 \text{ Pa}, K =0.65 \text{ Pa}\cdot\text{s}^n, n =0.42)$ & $(\tau_o= 0 \text{ Pa}, K =0.25 \text{ Pa}\cdot\text{s}^n, n =0.61)$] (Ahmed and Miska, 2008) and uniform 3-mm spherical cuttings are utilized for the parametric sensitivity analysis study. The densities of cuttings and fluids are 2650 kg m^{-3} and 1030 kg m^{-3} , respectively. In the Eulerian-Eulerian model of multiphase flow, cuttings are being treated as a continuum, as discussed in **Section 2.2.1**.

Table 2-2: Mesh properties

	e = 0	e = 0.5	e = 0.8
Radial face divisions	20	20	20
Edge division	60	50	50
Total face divisions	1200	1000	1000
Number of elements	1,444,800	1,109,200	1,030,240
Number of nodes	5,999,392	4,606,094	4,278,410
Minimum orthogonality	0.99496	0.97456	0.8453
Maximum orthogonality	0.99854	0.99878	0.99824
Average orthogonality	0.99706	0.99217	0.9584
Minimum skewness	0.03495	0.0325	0.032
Maximum skewness	0.065138	0.1436	0.1907
Average skewness	0.049024	0.0755	0.0982

2.3.3 Simulation Algorithm

The simulation procedure begins from a selection of geometry, followed by meshing and grid independence study. The Eulerian model is adopted in this work, which is the most complex multiphase flow model employed in ANSYS Fluent. This model can solve a set of 'n' momentum and continuity equations for each phase. Interphase coupling is achieved through pressure and interphase exchange coefficient. For the solid-liquid granular flow, the properties are obtained from the application of kinetic theory (Fluent, 2015). The solution convergence is checked for each simulation run. A simple schematic of the simulation algorithm is depicted in **Figure 2-4**.

The simulation study is carried out with the finite volume technique for the discretization of flow equation using commercial simulator Ansys Fluent v. 17.2. Phase Coupled SIMPLE scheme is employed for pressure-velocity coupling and the momentum equations are discretized using the QUICK scheme. These schemes are chosen due to their robust capability of solving mass and momentum conservation equations with reasonable stability and convergence for a particular control volume and full grid under investigation. The convergence criteria for residuals are set as 10^{-4} for the continuity and 10^{-3} for other residuals. Also, solution convergence speed depends on under relaxation factors. Therefore, under relaxation factors for the continuity and solid volume fraction are tweaked to obtain a quicker solution.

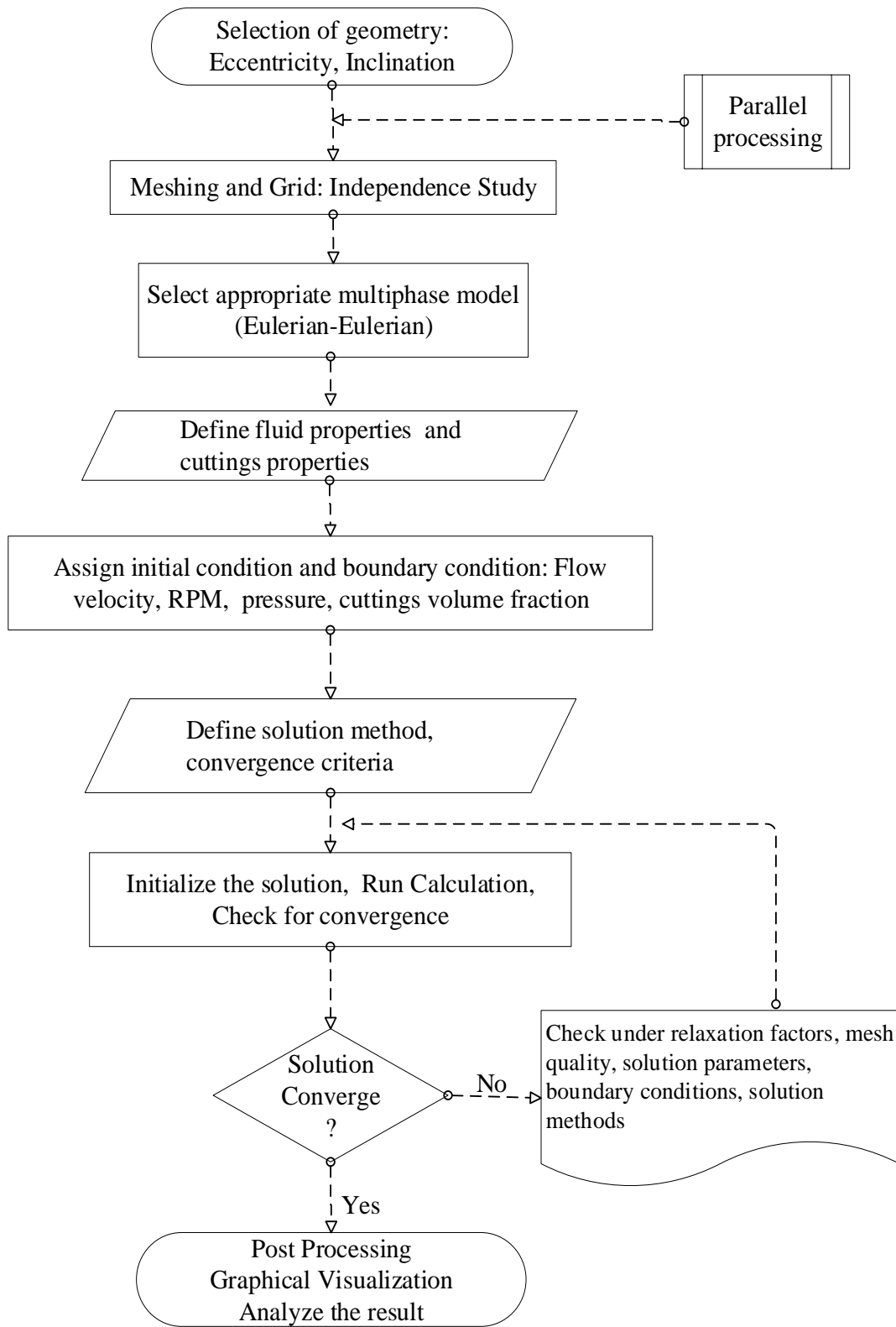


Figure 2-4: Flow chart of CFD simulation.

2.3.4 Limitations of the Implemented Model

The proposed Eulerian-Eulerian multiphase flow model can be utilized in various engineering and science cases, though it has a few limitations. For instance, the Reynolds stress turbulence model is not available per phase basis. Also, the inviscid flow is not allowed/applicable in the Eulerian model. To minimize the run time of the simulation, eight drilling parameters are investigated under three DOE subgroups. Most influential parameters from each group are used to form a new DOE. It allows assessing the interactions among the prominent parameters from each group. However, the interactions between the less influential parameters from different groups are ignored.

2.4 Results and Discussion

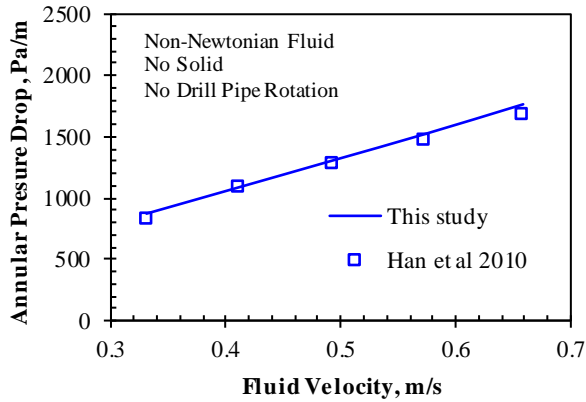
This section presents the results and discussion on the model validation and parametric sensitivity analysis where cuttings transport in the drilling operation is comprehensively studied through employing a CFD strategy.

The complete parametric study is grouped into three subgroups with eight parameters, as tabulated in **Table 2-1**. Each subgroup includes a full factorial design of experiment (DOE) and individual parametric sensitivity analysis. Finally, the most influential outcomes from three subgroups are combined to form a new DOE structure for checking (and exploring) the interactions among the parameters.

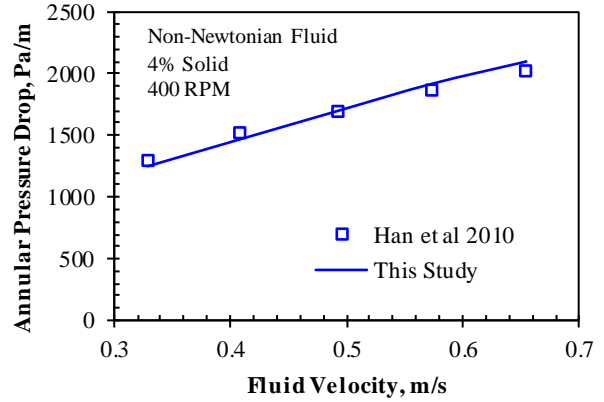
2.4.1 Model Validation

The developed model is validated against several experimental cases (Garcia-Hernandez et al., 2007; Han et al., 2010). **Figure 2-5a** depicts the frictional pressure drop comparison for a non-Newtonian fluid, excluding any solid cuttings and inner pipe rotation. **Figure 2-5b** shows the frictional pressure drop versus flow rate where a case including a fluid with 4% sand and an inner

pipe rotation is assessed. **Figure 2-6a** and **Figure 2-6b** illustrate the change of average cuttings velocity with average fluid velocity in a vertical and a horizontal annular section, respectively.

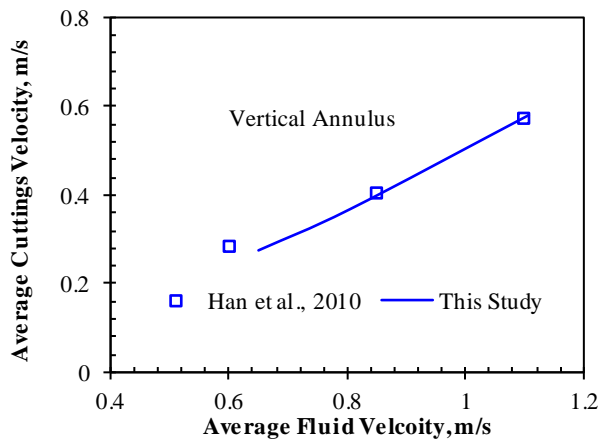


(a) Single-phase flow case

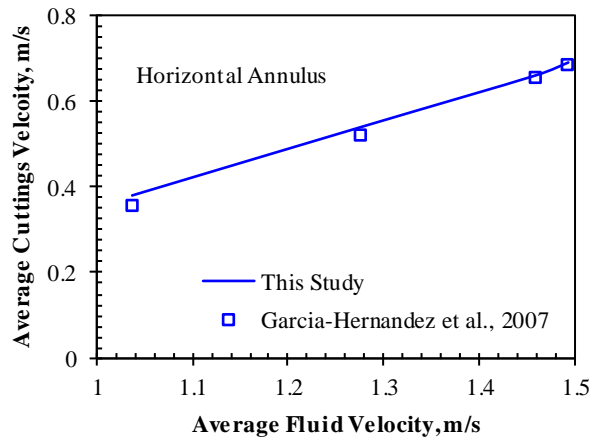


(b) Two-phase flow case

Figure 2-5: Frictional pressure drop comparison based on predictions and real data.



(a) Vertical annulus section



(b) Horizontal annulus section

Figure 2-6: Cuttings velocity as a function of fluid velocity

Figure 2-7 presents the total pressure drop comparison with experimental investigation performed at the Managed Pressure Drilling (MPD) lab at Memorial University. The experimental phase is carried out in a vertical annulus flow loop using water. Also, the total pressure drop is compared

with the results obtained from analytical Lamb’s equation(Lamb, 1945), showing a good match between the simulation and correlation results.

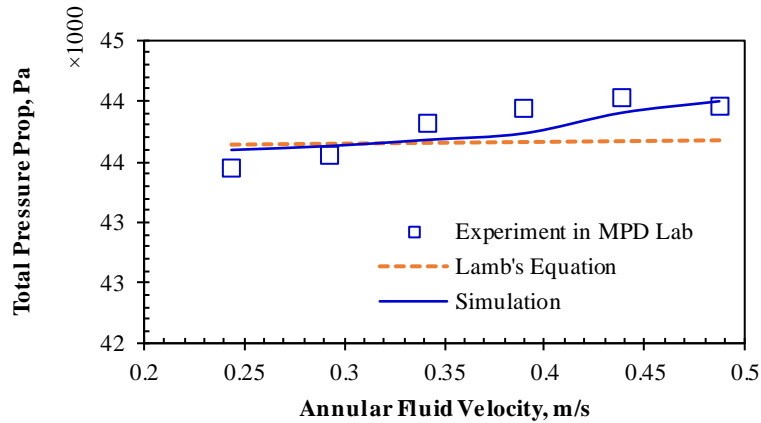


Figure 2-7:Total pressure drop comparison with managed pressure drilling experiment.

The relative errors (showing the difference between the predictions and real data) are quantitatively reported in **Table 2-3**. The average errors are less than 4%. This indicates good agreement between the model outputs and experimental data, implying the accuracy and reliability of the introduced model.

Table 2-3: Error analysis based on the comparison of predictions and experimental data.

Compared Parameter	Experimental Conditions	Error (%)		
		Min.	Max.	Avg.
Annular Pressure Drop (Han et al., 2010)	Non-Newtonian Fluid No Solid, No RPM	0.53%	5.41%	3.28%
Annular Pressure Drop (Han et al., 2010)	Non-Newtonian Fluid 4% Solid, 400 RPM	0.73%	4.42%	2.97%
Cuttings Velocity vs. Liquid Velocity (Han et al., 2010)	Vertical Annulus Water + Sand, No RPM	1.8%	8.0%	3.87%
Cuttings Velocity vs. Liquid Velocity (Garcia-Hernandez et al., 2007)	Horizontal Annulus Water + Sand, No RPM	1.03%	7.16%	3.51%
Total Pressure Drop - Managed Pressure Drilling (MPD) Lab – Flow Loop Experimental Set Up at Memorial University	Closed Loop Annulus Water Only, No RPM	0.10 %	1.38%	0.44%

2.4.2 DOE for Fluid Rheology

A non-Newtonian Herschel-Bulkley fluid is used as the drilling mud in this study. A Herschel-Bulkley fluid is expressed as follows:

$$\tau = \tau_o + k\dot{\gamma}^n \quad (2-26)$$

where τ introduces shear stress; $\dot{\gamma}$ is the shear rate; τ_o represents the yield stress or yield point; k refers to the consistency index; and n stands for the flow index. The three parameters $n, k,$ and τ_o are needed to characterize the Herschel-Bulkley fluid. In this study, a full factorial design for three factors with two levels is implemented to investigate the effects of $n, k,$ and τ_o on CTE, as shown in **Table 2-4**

A (–) sign indicates the minimum value and a (+) sign represents the maximum value of the examined parameter (see **Table 2-1**). In this phase of the study, parameters related to the fluid flow and drill pipe are maintained at constant values. The drill pipe is rotated at 50 rpm with a cuttings size of 3 mm and 5% solids by volume. The mud velocity is set to be 0.494 m/s.

Table 2-4: Design matrix of fluid rheology.

Run No	Factor 1: Consistency Index (k)	Factor 2: Flow Behavior Index (n)	Factor 3: Yield Stress, Pa	Response: CTE
1	–	–	–	45%
2	+	–	–	69%
3	–	+	–	62%
4	+	+	–	93%
5	–	–	+	88%
6	+	–	+	90%
7	–	+	+	89%
8	+	+	+	94%

The results from the simulated model and DOE approach are given in **Table 2-4** and **Figure 2-8**. All three parameters ($k, n,$ and τ_o) used in this analysis indicate a positive influence on cuttings transport. The analysis illustrates that yield stress (τ_o) or yield point contributes more to the cutting transport behavior/effectiveness, compared to the other two parameters. Yield point can be used

to evaluate the ability of drilling mud to transport cuttings out of the annulus. For a non-Newtonian fluid, a high yield stress implies that fluid carries cuttings better than fluids with the same density but with a lower yield stress or yield point.

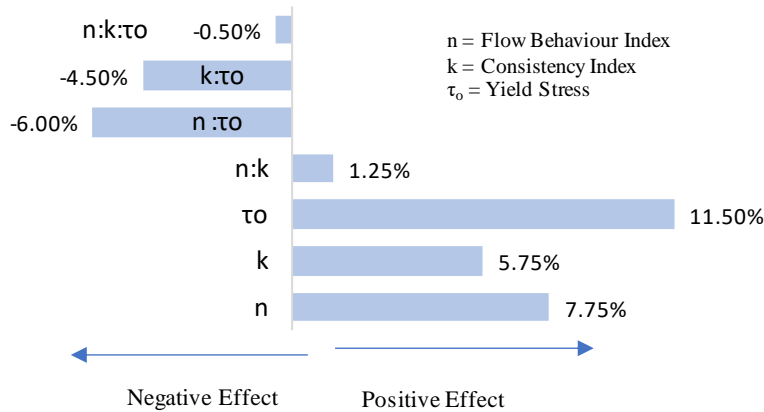


Figure 2-8: Main effects and parameter interactions of drilling mud on CTE

The two-factor interactions, $k: \tau_0$ and $n:\tau_0$, exhibit significant negative effects, whereas $n: k$ represents a slight positive interaction. The contribution of the three-factor interaction ($n: k: \tau_0$) to the cuttings transport is negligible, compared to the individual effects and two-factor interactions (see **Figure 2-8**). The next parts of the manuscript explain the two-factor interactions in detail in a graphical manner.

The impact of the interaction between k and n on CTE is demonstrated in **Figure 2-9a**. For both cases, $k = 0.3$ and $k = 0.7$, an increase in the value of n increases the CTE. This indicates a positive interaction between k and n in terms of hole cleaning efficiency. **Figure 2-9b** shows that, for $n = 0.3$, the CTE increases significantly as the yield stress increases from 0 to 4 Pa. However, for $n = 0.7$, it remains almost constant. This implies that there is a negative interaction between n and τ_0 .

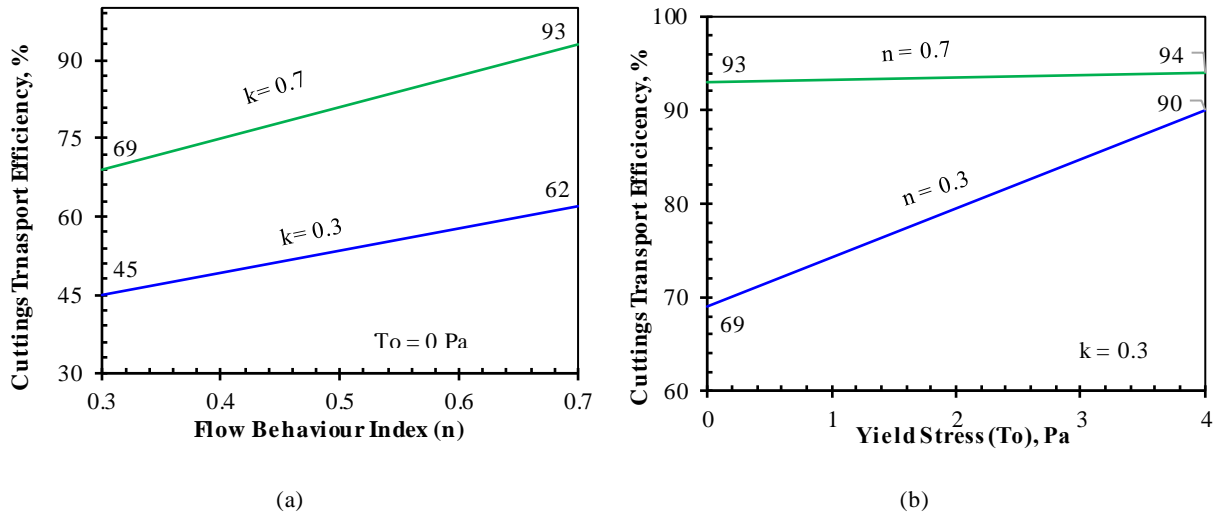


Figure 2-9: Effect of two-factor interaction of a) k and n ; b) n and τ_0 on CTE

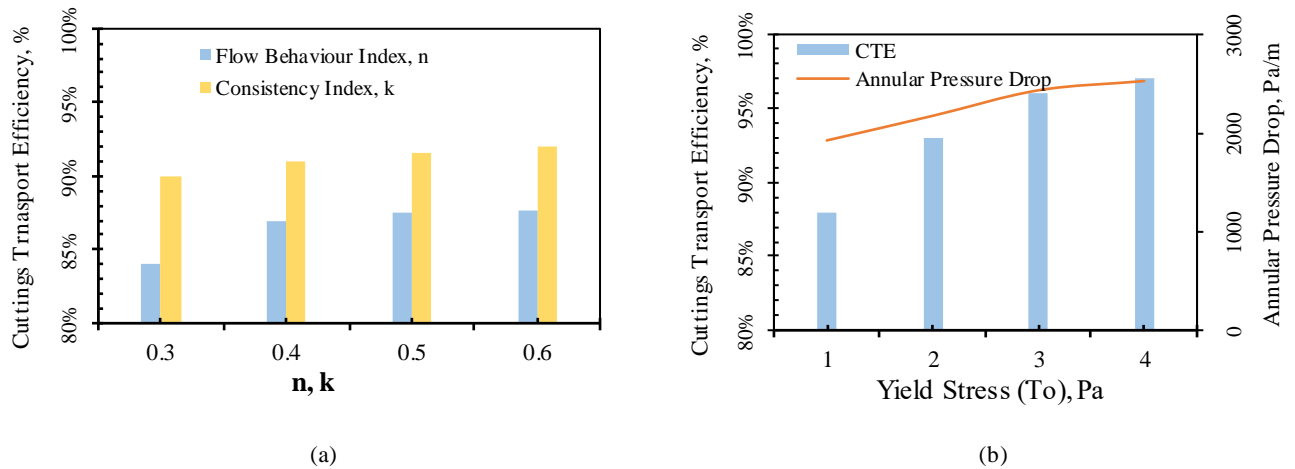


Figure 2-10: Cuttings transport efficiency as a function of a) n and k ; b) yield stress (τ_0)

The effect of n and k on cuttings transport is depicted in **Figure 2-10a**. As n increases from 0.3 to 0.4, CTE increases by about 4%. No significant improvement in CTE is observed beyond $n = 0.4$ (see **Figure 2-10a**). A negligible enhancement in CTE is found by increasing the consistency index (k). **Figure 2-10b** presents the influence of yield stress on the cuttings transport and annular pressure drop. With increasing yield stress, both CTE and annular pressure drop increase

significantly. Thus, the annular pressure drop can be used as an indicator or a limiting factor for cutting transport capabilities.

2.4.3 DOE for Operational Parameters

In this study, only the major field parameters such as drilling mud velocity and drill pipe rotation are considered in the factorial design. The drilling penetration rate is not included since this parameter is a function of input cuttings fraction. A greater rate of penetration (ROP) indicates a higher input cuttings fraction only in the simulation study. Information/data of the operational parameter matrix are listed in **Table 2-5** along with outcome (e.g. CTE) for each case.

Table 2-5: Design matrix for operational parameters.

Run No	Factor 1: Drill Pipe Rotation	Factor 2: Mud Velocity	Response: CTE
1	–	–	35.8%
2	+	–	42.3%
3	–	+	45.9%
4	+	+	44.6%

To minimize the effect of fluid rheology, the rheological parameters are set at constant values ($\tau_y = 0$ Pa, $n = 0.61$, and $k = 0.25$) (Ahmed and Miska, 2008). It is clear from **Table 2-4** and **Table 2-5** that the rheological properties have a greater effect on cuttings transport, compared to the operational parameters. According to **Figure 2-11**, both drill pipe rotation and mud velocity have a positive influence on cuttings transport. However, the interaction between the mud velocity and drill pipe rotation negatively affects the hole cleaning operation. In the next subsections, the influence of each parameter is discussed separately.

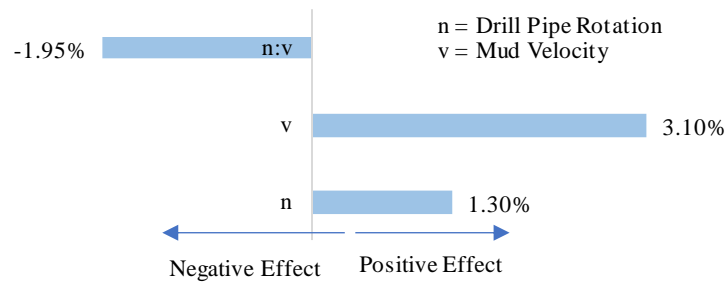


Figure 2-11: The main effects and interaction of field parameters on CTE.

Effect of drill pipe rotation. Pipe rotation introduces a centrifugal force to the cuttings, which causes a rapid variation in the drill cuttings position in the annulus. Drill pipe rotation applies a drag force to the stationary cuttings bed at the bottom and disperses the cuttings into the mud around the annulus. Hence, it helps in reducing the stationary cuttings bed thickness in the annulus.

Figure 2-12a demonstrates the annular cuttings concentration and cuttings transport efficiency for a concentric annular section in terms of drill pipe rotation. The analysis shows that if the drill pipe rotation is increased from 0 to 120 rpm, the annular cuttings volume fraction is decreased by approximately 19%. The pressure drop in the horizontal annular section against the drill pipe rotation is plotted in **Figure 2-12b**.

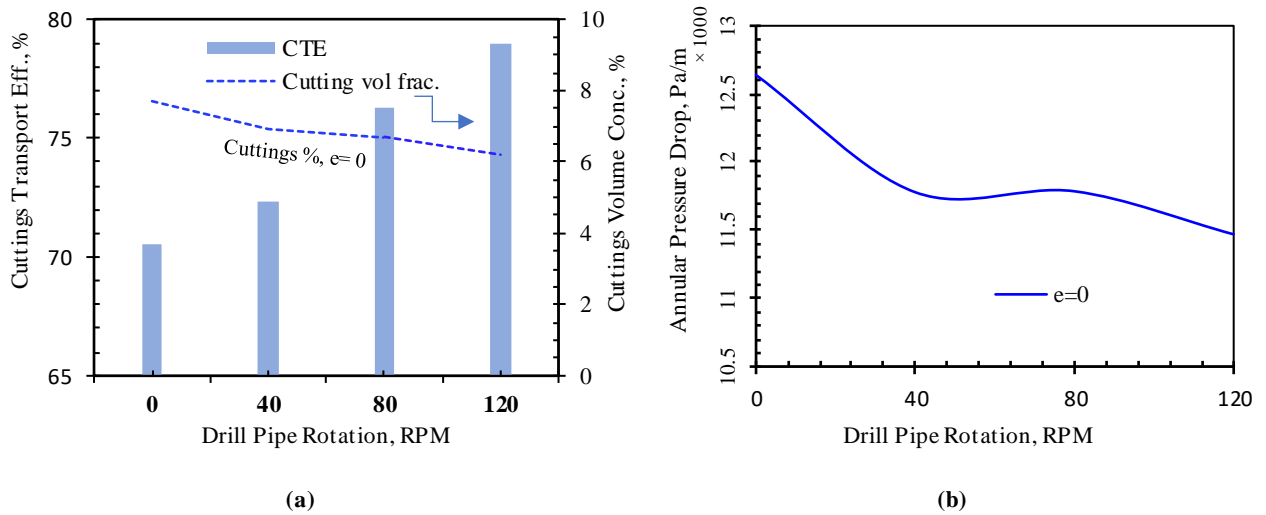


Figure 2-12: Effect of drill pipe rotation on CTE

a) Annular cutting concentration and CTE versus RPM; b) Change in pressure drop with RPM

Based on **Figure 2-12b**, an increase in the drill pipe rotation (from a stationary condition) leads to a reduction in the annular pressure drop in the concentric annulus. Also, the fluid viscosity decreases due to an increase in the internal pipe rotation. The pressure drop decline is due to a reduction in the annular cutting's concentration and a lower fluid viscosity. However, between 40 to 80 rpm, the annular pressure drop shows a slightly increasing trend. This might be attributed to a decrease in the frictional pressure drop because of fewer cuttings in the annular section, which is counterbalanced by an increase in frictional pressure loss due to pipe rotation. Further increase in the pipe rotation above 80 rpm leads to a decrease in the annular pressure drop, indicating less frictional pressure loss due to the cuttings.

Effect of mud circulation rate. Variations of annular pressure drop and cuttings concentration with mud velocity are shown in **Figure 2-13**. For a concentric annulus, by increasing mud velocity, the annular cuttings concentration gradually decreases, and the annular pressure drop increases.

Figure 2-13 also reveals that the mud flow rate of approximately 1.6 m/s is sufficient to clean the concentric section with an input-cuttings of 5% for this concentric annular section.

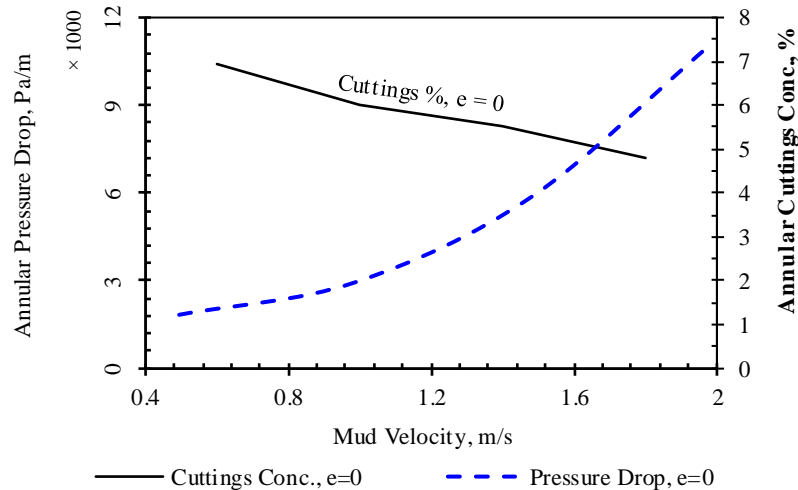


Figure 2-13: Influence of mud circulation rate on the hole cleaning performance.

A contour map clearly illustrates the role of the mud circulation rate in hole cleaning, as shown in **Figure 2-14**. For the visualization purpose, the contour map cuttings volume fraction is selected for the lower annular section of an eccentric annulus ($e = 0.8$), which is more prone to the cuttings accumulation. At a mud velocity of 0.494 m/s, three distinct layers of cuttings are formed (see **Figure 2-14**); namely, stationary bed at the bottom, moving cuttings bed in the middle region, and cuttings suspended in the flowing mud at the top. At a mud velocity of 0.988 m/s, a slight change in the thickness of top and middle beds is observed, whereas the stationary bed thickness remains unchanged. Further increase in the mud velocity causes a significant change in the thickness of the cuttings bed. When the magnitudes of mud velocity are 1.482 m/s and 1.976 m/s, no stationary cuttings bed is observed. Increasing the mud velocity enlarges the moving bed domain, which carries a significant volume of cuttings in the annulus.

For a mud velocity of 0.494 m/s, a very low local Reynolds number ($Re = 59$) indicates a laminar flow regime at the lower annular section of an eccentric annulus. This is due to a very small average fluid velocity (≈ 0.105 m/s) in the bottom part. Increasing the fluid velocity increases the local Reynolds number, improves the cuttings transport, and hence lowers the annular cuttings concentration. It can be concluded that the flow regime toward the turbulent condition improves the cuttings transport efficiency. However, the interactions of other parameters need to be considered for better evaluation, as well.

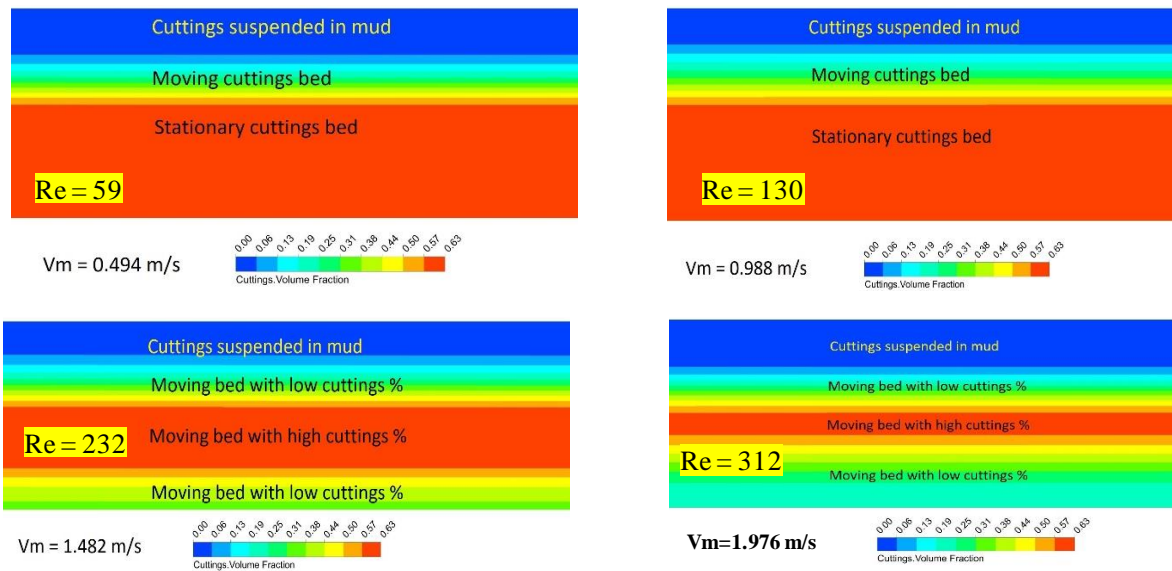


Figure 2-14: Stationary cuttings bed movement with increasing the mud velocity.

2.4.4 DOE for Cuttings Size, Annular Space, and Eccentricity

Some simulation runs based on DOE are performed to investigate the cutting transport efficiency in terms of the annular clearance and cuttings size, as listed in **Table 2-6**. The runs are planned to explore the effect of cuttings size on the transport efficiency upon various diameter ratios and drill pipe eccentricities. Two different cuttings sizes of 1 mm and 5 mm are used to represent the small cuttings and large cuttings sizes, respectively. Annular clearance is defined as the difference

between the hole diameter and pipe diameter. A high annular clearance indicates a low diameter ratio (D_p/D_h) of the drill pipe and hole. The annular clearance is chosen in the way to keep the annular area and volumetric mud flow rate constant for all cases. A concentric ($e = 0$) and an eccentric ($e = 0.8$) condition are used in this study.

Table 2-6: Design matrix for cuttings size and annular space.

Run No	Factor 1: Cuttings Size	Factor 2: Diameter Ratio, (D_p/D_h)	Factor 3: Eccentricity	Response: CTE
1	-	-	-	98%
2	+	-	-	73%
3	-	+	-	91%
4	+	+	-	38%
5	-	-	+	98%
6	+	-	+	80%
7	-	+	+	96%
8	+	+	+	44%

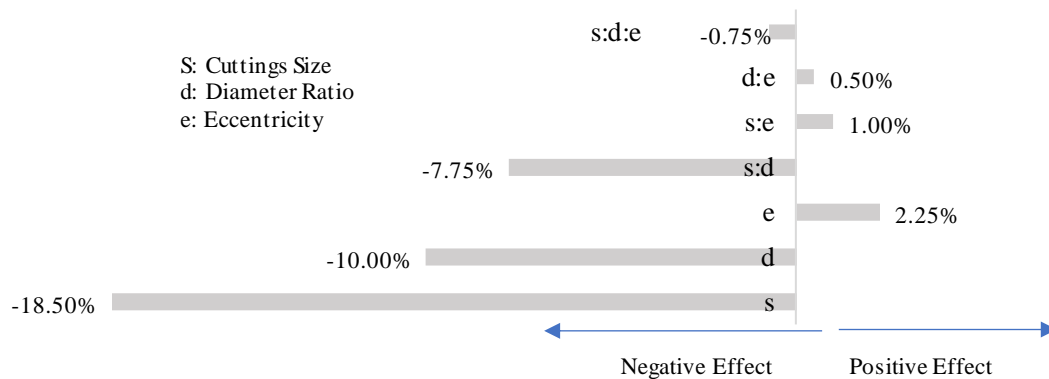
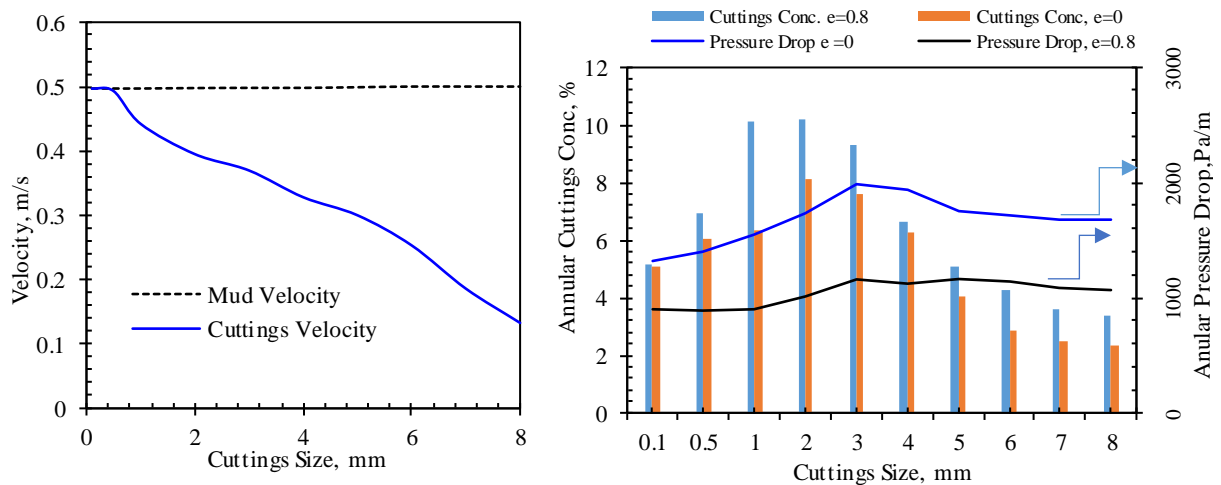


Figure 2-15: Main effects and interactions of cuttings size, annular clearance, eccentricity.

According to **Figure 2-15**, the size of the cuttings exhibits the most significant adverse effect on cuttings transport efficiency. An increase in the diameter ratio (D_p/D_h) leads to a remarkable negative impact on cuttings transport, whereas the eccentricity shows a slightly positive influence on CTE. Moreover, the cuttings size and diameter ratio exhibit a substantial negative interaction.

Other two-factor and three-factor interactions have negligible contributions, compared to the main effects. In the next subsection, all three main factors are further discussed.

Effect of cuttings size. During a drilling operation, the drill bit may encounter various types of rocks towards its destination. Different formation rock characteristics (lithology and porosity), overburden pressures, and drill bit interactions may cause rock chips to break down into smaller pieces with different sizes. Numerical simulations are conducted in the horizontal concentric annulus to investigate the effect of cuttings size ranging from 0.1 to 8 mm on the annular cuttings concentration and pressure drop (see panels (a) and (b) of **Figure 2-16**). A low mud velocity is selected to minimize the effect of mud velocity in the cuttings transport event.



(a) Mud velocity versus cuttings velocity and size

(b) Annular cuttings concentration and pressure drop for different cuttings sizes.

Figure 2-16: Effect of cuttings size

The cuttings and mud velocity versus cuttings size is depicted in **Figure 2-16a**. For very small cuttings sizes (≤ 0.5 mm), the cuttings travel with almost the same velocity as the drilling mud. Thus, the current drilling mud viscosity ($\tau_o=2$ Pa, $k =0.65$ Pa.sⁿ, $n =0.42$) is adequate to offer nearly 100% efficient hole cleaning. It seems that small size cuttings are suspended in the drilling

mud at this condition. Therefore, the cuttings deposition due to the gravity effect is negligible. By increasing the size of the cuttings above 0.5 mm, the average cuttings transport velocity in the annulus gradually decreases. Upon an increase in the grain size, the mass of the cutting grains increases; gravity force exceeds the drag force; this causes more cuttings to be deposited on the annulus bed, leading to a reduction in the transport efficiency. An increase in cuttings size from 1 mm to 6 mm lowers the cuttings transport efficiency by 43%.

For all cuttings sizes, the eccentric annulus case shows a higher annular cuttings concentration. Cuttings size from 1 mm to 3 mm has a higher cuttings concentration in the annulus, as demonstrated in **Figure 2-16b**. This cuttings accumulation restricts the fluid flow in the lower annular section and causes an increase in the pressure drop. A noticeable decrease in the cuttings concentration is observed for cuttings size greater than 3 mm. **Figure 2-16b** also reveals that there is a particular cutting size that seems most difficult to clean with this specific drilling mud. According to the current study's results, the size of the critical cuttings is 2 mm. This conclusion is consistent with the finding obtained from the study of slurry flow in a single pipe by Wilson and Judge (1978) as well as experimental data on cuttings transport by Walker and Li (2000). It was found that smaller particles are more difficult to clean out than larger ones when the particle size is greater than 0.5 mm. However, for the particle size smaller than 0.5 mm, the hole cleaning operation is easier. The annular pressure drop is slightly declined up to a cutting size of 5 mm; but, above this particular size, the pressure drop remains almost unchanged.

Effect of annular clearance. Four different values of annular clearance are studied to explore the effect of this key parameter on the cutting transport efficiency. Annular clearance is chosen by the equivalent annular area to ensure the same velocity for all cases. The 3 mm cuttings size is used in the analysis for all annular geometries.

A narrow slot or high diameter ratio (D_p/D_h) shows a higher pressure drop and a lower cuttings transport efficiency, as seen in **Figure 2-17a**. This is due to the high friction/contact of solid cuttings and drilling mud with the pipe wall in the narrow space. **Figure 2-17b** demonstrates that increasing eccentricity results in an increase in the cuttings concentration and a reduction in the annular pressure drop. However, eccentricity has no appreciable effect on CTE.

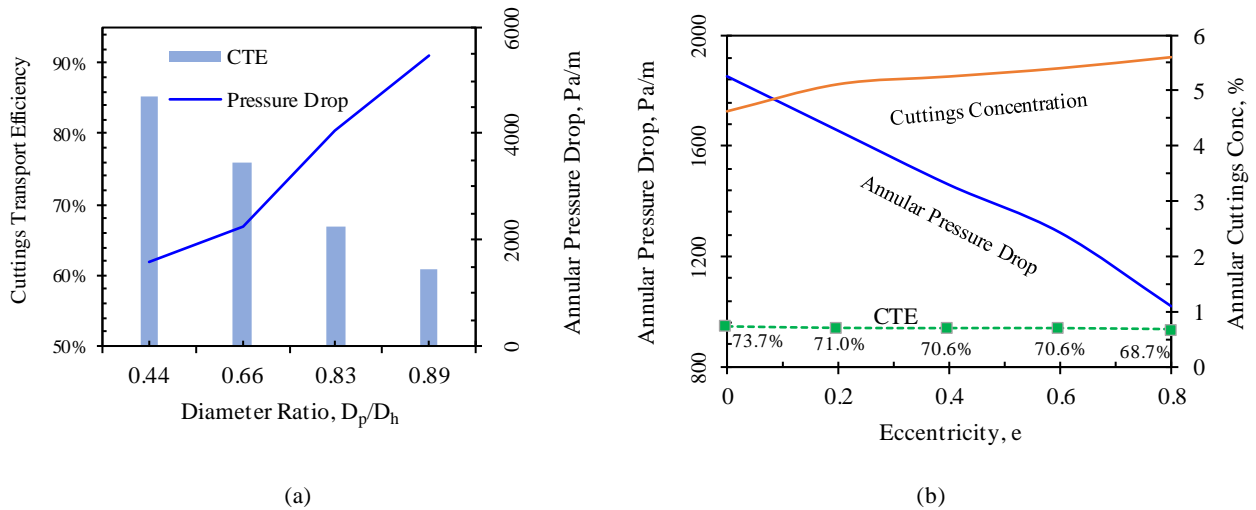


Figure 2-17: Effect of annular orientation

a) CTE and pressure drop for different magnitudes of D_p/D_h ; b) Variations of cuttings concentration, CTE, and pressure drop with eccentricity.

Effect of pipe eccentricity. In a horizontal drilling operation, both fluid and rock chips with different sizes and shapes move in the axial direction. The velocity distribution along the pipe varies from zero at the wall to the maximum at the annulus center. The fluid hydrodynamics become more complex when the drill pipe rotation is applied. An inner pipe rotation introduces a complex helical motion of fluid inside the annulus as shown in **Figure 2-18a** by velocity streamline of the drilling mud. Pipe rotation introduces a centrifugal motion to the cuttings, which causes a rapid change in the drill cuttings location within the annulus. However, the velocity distribution is

not uniform for an eccentric annular orientation case. For an eccentric annulus system, the situation becomes extreme with a non-uniform velocity distribution as demonstrated by velocity streamline in panel (b) of **Figure 2-18**.

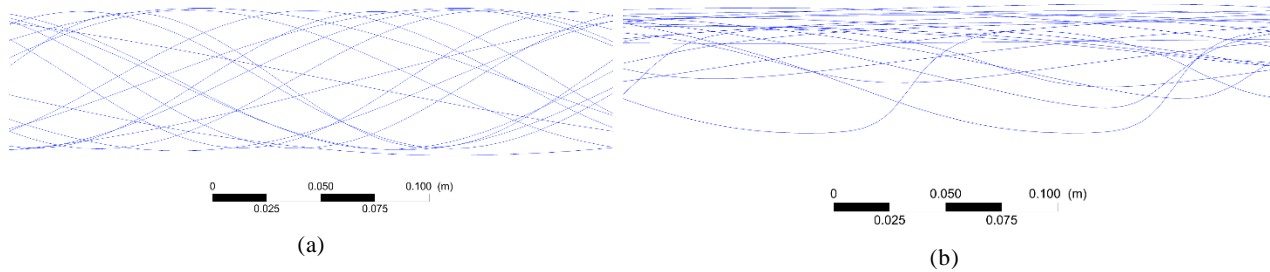


Figure 2-18: Mud velocity streamlines in a) a concentric annulus; b) an eccentric annulus.

Five different orientations are considered to simulate the pipe eccentricity ranging from concentric annulus ($e = 0$) to an extreme eccentric annulus ($e = 0.8$), as illustrated in **Figure 2-17b**. At a penetration rate of 100 ft/hr, an increase in the eccentricity leads to a gradual increase in the annular cuttings fraction. The most remarkable feature of eccentricity is the rapid reduction in the pressure drop with increasing eccentricity. This change in the annular pressure drop should be compensated to maintain the Equivalent Circulation Density (ECD) during a drilling operation. The simulation runs also show a slight decrease in cuttings transport efficiency with increasing eccentricity.

Mud velocity contour maps for different forms of the eccentric annulus and corresponding annular cuttings fractions are presented in **Figure 2-19**. An increase in the eccentricity causes an offset of a drill pipe position from the center and creates an asymmetric distribution of mud velocity profile. Based on the velocity contour, the higher the eccentricity, the less flow of mud in the lower annular part. For a eccentric annular section, the average velocity in the narrow part of the annulus is reduced since narrow annular section provide a higher resistance to the fluid flow. As a result, most of the fluid flow occurs at upper annular section with wide annular space and least resistance

to fluid flow. Thus, upper annular section shows a higher mud velocity compared to a lower annular section. This leads to less efficient hole cleaning in the lower section of the eccentric annulus, as illustrated by the higher sand volume fraction contour (see **Figure 2-19**).

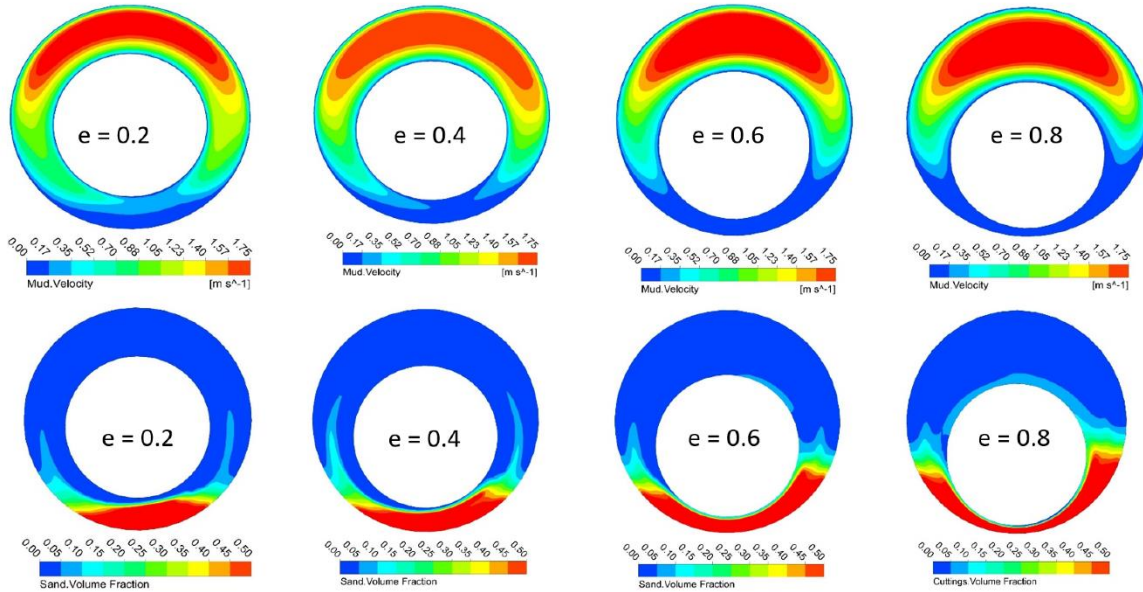


Figure 2-19: Mud velocity contour and cuttings volume fraction for different eccentricities.

2.4.5 Comparison of Significant Parameters

Due to the complex behaviors of solid-drill mud hydrodynamics, drilling engineers and personnel typically rely on the field observations and experience while determining the cuttings transport capability of drilling mud. To improve the hole cleaning, drillers may either increase the mud circulation rate or increase the drilling mud viscosity or pipe rotation. Increasing the mud circulation rate and fluid viscosity often increases the annular pressure drop and decreases the footage drill per hour. However, pore pressure and formation pressure windows limit the operating pressure and annular pressure drop. Hence, there should be a trade-off between the drilling window and available drilling parameters to be used for hole cleaning analysis.

In this section, a separate three-factor design of experiment is conducted based on the most significant parameters from all three subgroups (see **Table 2-1**). The most vital parameters from all subgroups are the yield stress (τ_o), mud velocity (V), and cuttings size (S) obtained from Sections 5.2, 5.3 and 5.4. The detailed design matrix and outcomes (CTE) are listed in **Table 2-7**. In this DOE approach, the yield stress varies from 0 to 4 Pa, the mud velocity changes between 0.494 m/s and 1.976 m/s, and the size of the cuttings is within the range of 2 mm - 5 mm.

Table 2-7: Two-level DOE for the influential parameters on the basis of three subgroups.

Run No	Yield Stress (τ_o), Pa	Mud Velocity, m/s	Cuttings Size, mm	Response: CTE
1	-	-	-	57%
2	+	-	-	88%
3	-	+	-	66%
4	+	+	-	76%
5	-	-	+	18%
6	+	-	+	62%
7	-	+	+	33%
8	+	+	+	52%

The objective of this DOE is to investigate the impact of interactions among all three influential parameters on the cuttings transport performance. The relative importance of all parameters is given in **Figure 2-20**.

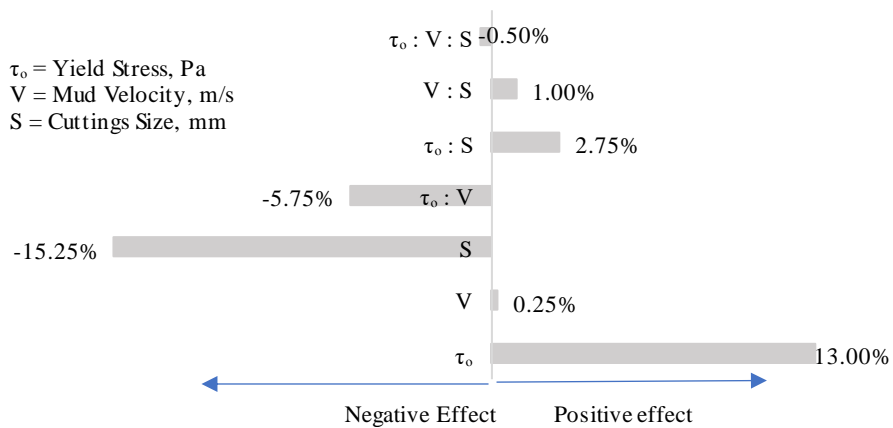
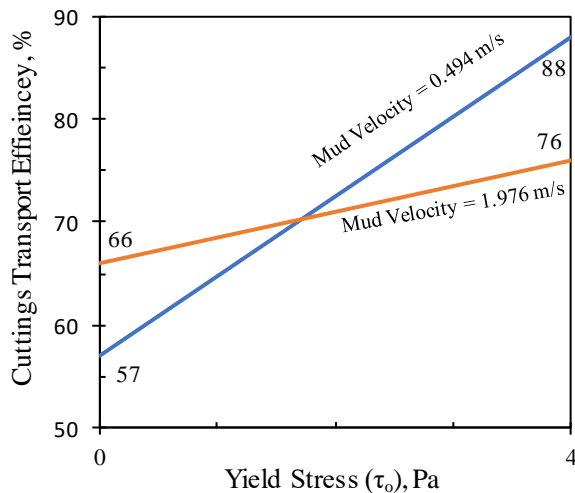


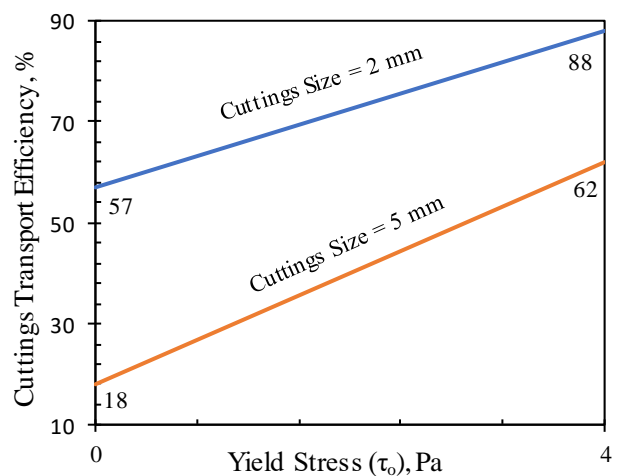
Figure 2-20: Main effects and two-factor interactions of significant parameters.

Cuttings size shows a considerable negative impact, while the yield stress exhibits the maximum positive contribution. Fluid velocity has a minor positive impact, compared to the yield stress and cuttings size. Although both yield stress and mud velocity have a positive impact, the interaction between them causes a remarkable negative influence on cuttings transport. The reverse trend is observed for the cuttings size such that it has the highest negative impact. However, its interaction with mud velocity and yield stress exhibits a positive influence on cuttings transport. Therefore, it can be concluded that a larger cuttings size requires a high mud velocity or high viscous fluid for an effective hole cleaning.

As **Figure 2-21a** shows, at low yield stress ($\tau_o = 0$), increasing the fluid velocity from 0.494 m/s to 1.976 m/s increases the cuttings transport efficiency by 9%. However, at high yield stress ($\tau_o = 4$ Pa), increasing the fluid velocity causes a reduction in cuttings transport efficiency by 12%. This reveals a negative interaction between fluid velocity and yield stress.



(a) Interaction between yield stress and fluid velocity in terms of cuttings transport efficiency change



(b) Impact of interaction between yield stress and cuttings size on the cuttings transport.

Figure 2-21: Interaction effect of mud velocity and cuttings size with yield stress

Figure 2-21b presents the CTE as a function of yield stress and cuttings size. At the size of a small cutting (2 mm), increasing yield stress from 0 to 4 Pa causes an increase in transport efficiency by 39%. However, at large cuttings size (5 mm), the improvement is 26%. It is found that there is a slight positive interaction between the cuttings size and yield stress. Multiple factors discussed in this study directly affect the drilling performance in a horizontal or extended-reach well. DOE and parametric sensitivity analysis revealed that some factors have a significant impact on cuttings transport, while the rest of the variables show less significance. However, during a drilling operation, all factors cannot be optimized at the same time due to operating constraints and geological uncertainties. A two-factor interaction study can assist the drilling personnel in proposing a suitable drilling plan and hole cleaning strategy.

2.5 Conclusions

In this paper, we carried out a comprehensive study of drilling parameters using CFD model. A large set of variables related to the cutting transport were classified into three categories: (i) fluid rheology; (ii) operational variables; (iii) design parameters (i.e., cutting size and annular space). The effect of each parameter in the group, their interactions within the group as well as interactions between the groups were studied systematically. Below we summarize the important findings:

- From the parametric study, it was found that yield stress, mud circulation rate, and drill pipe rotation are the most significant parameters that can be controlled to improve the cutting transport. All three parameters are positively correlated with cuttings transport.
- It was observed that mid-size particles (i.e., 1 mm and 2 mm) were more challenging to transport. Smaller size particles remain suspended in the fluid and are carried along with the fluid, and larger size particles have enough drag force acting on them to transport the

particles. This is a new observation and consistent with other research fields; for example, in medicine, it is well known that the mid-size cholesterol particles are the most difficult to transport and typically deposits on the blood vessel (Campos et al., 1992)

- The DOE results showed a significant negative interaction effect when mud velocity and yield stress are changed simultaneously. Therefore, increasing fluid yield stress and mud velocity simultaneously may not improve the cutting transport efficiency.
- Mud velocity and drill pipe rotation separately have a positive impact on drilling efficiency. However, DOE results revealed that there is a sufficient negative interaction effect to offset the individual positive effects.
- Three-factor interactions (i.e., the interaction between fluid yield stress, mud velocity, and cuttings size) are not significant in comparison to two-factor interactions.
- It was observed that a minimum transport velocity is required to move the stationary bed into a moving bed. In our study, the minimum transport velocity to avoid cuttings bed formation is 1.482 m/s.

ACKNOWLEDGEMENTS

The financial support of the Memorial University, Equinor Canada, InnovateNL, and the Natural Sciences and Engineering Research Council of Canada (NSERC) is acknowledged.

NOMENCLATURES

Acronyms

1-D	-	One dimensional
ACP	-	Annular cuttings percentage
CFD	-	Computational fluid dynamics
CTE	-	Cuttings transport efficiency
CMC	-	Carboxymethyl cellulose

DOE	-	Design of experiment
OFAT	-	One factor at a time
ROP	-	Rate of penetration
RPM	-	Revolutions per minute
Re	-	Reynolds number
Rep	-	Particles Reynolds number
Re_S	-	Relative Reynolds number
mm	-	Millimeter

Variables/Symbols

I_{2D}	-	second variant of deviatoric stress tensor	(-)
e_{ss}	-	coefficient of restitution	(-)
F	-	external body force	(N, lb _f)
F_{lift}	-	lift force	(N, lb _f)
F_{wl}	-	wall lubrication force	(N, lb _f)
F_{vm}	-	virtual mass force	(N, lb _f)
F_{td}	-	turbulent dispersion force	(N, lb _f)
C_D	-	drag coefficient	(-)
$g_{0,ss}$	-	distribution function	(-)
v	-	velocity	(ms ⁻¹)
p	-	pressure	(Pa)
g	-	gravitational acceleration	(m/s ² , ft/s ²)
\dot{m}	-	mass flow rate	(kg/s, lb _m /s)
C_l	-	lift coefficient	(-)
R	-	interaction force between phases	(-)
K	-	interphase momentum exchange coefficient	(-)
K	-	consistency index	(Pa.s ⁿ)
v_c	-	average velocity of the cuttings	(ms ⁻¹)
v_m	-	average velocity of the drilling mud	(ms ⁻¹)
D_h	-	hole diameter	(mm, inch)
D_p	-	pipe diameter	(mm, inch)
n	-	flow behavior index	(-)
e	-	eccentricity	(-)
Lh	-	hydrodynamic entrance length	(mm, feet)

Greek Letters

α	-	volume fraction	(-)
π	-	mathematical constant	3.1417
τ_o	-	yield stress	(Pa)
τ	-	shear stress	(Pa)
$\dot{\gamma}$	-	shear rate	(s ⁻¹)

δ	-	offset from the centre	(mm, inch)
∇	-	derivative	(-)
β	-	ratio of vorticity Reynolds number to particle	(-)
$\bar{\tau}$	-	stress strain tensor	(-)
ρ	-	density	(kg.m ⁻³)
μ	-	shear viscosity	(ms ⁻¹)
λ	-	bulk viscosity	(ms ⁻¹)
Θ	-	granular temperature	(m ² /s ²)
\emptyset	-	angel of internal friction	(rad)

Subscripts

l	-	liquid phase
s	-	solid phase
kin	-	kinetic component
col	-	collisional component
fr	-	frictional component
ls	-	liquid to solid
sl	-	solid to liquid
h	-	hole
p	-	pipe

REFERENCES

- Ahmed, R.M., Miska, S.Z., 2008. Experimental Study and Modeling of Yield Power-Law Fluid Flow in Annuli with Drillpipe Rotation, in: IADC/SPE Drilling Conference. Orlando, Florida, U.S.A, 4–6 March. <https://doi.org/10.2118/112604-MS>
- Avila, R., Pereira, E., Miska, S., Takach, N., 2004. Correlations and Analysis of Cuttings Transport with Aerated Fluids in Deviated Wells, in: IADC/SPE Drilling Conference. Dallas, Texas, U.S.A., 2 – 4 March. <https://doi.org/10.2118/87180-MS>
- Bergman, T., Lavine, A., Incropera, F.P., Dewitt, D., 2011. Fundamentals of Heat and Mass Transfer, 7th ed. John Wiley & Sons, Inc.
- Bilgesu, H.I., Mishra, N., Ameri, S., 2007. Understanding the Effects of Drilling Parameters on Hole Cleaning in Horizontal and Deviated Wellbores Using Computational Fluid Dynamics,

- in: SPE Eastern Regional Meeting. Lexington, Kentucky, U.S.A., 17–19 October.
<https://doi.org/10.2118/111208-MS>
- Campos, H., Genest, J.J., Blijlevens, E., McNamara, J.R., Jenner, J.L., Ordovas, J.M., Wilson, P.W.F., Schaefer, E.J., 1992. Low Density Lipoprotein Particle Size and Coronary Artery Disease. *Arterioscler. Thromb.* 12, 187–195. <https://doi.org/10.1161/01.atv.12.2.187>
- Capo, J., Yu, M., Miska, S.Z., Takach, N., Ahmed, R., 2004. Cuttings Transport with Aqueous Foam at Intermediate Inclined Wells, in: SPE/ICoTA Coiled Tubing Conference and Exhibition. Houston, Texas, U.S.A. <https://doi.org/10.2118/89534-MS>
- Çengel, Y.A., John M Cimbala, 2014. *Fluid Mechanics Fundamentals and Applications*, 3rd ed. New York, NY : McGraw-Hil.
- Chen, Z., Ahmed, R.M., Miska, S.Z., Takach, N.E., Yu, M., Pickell, M.B., Hallman, J.H., 2007. Experimental Study on Cuttings Transport With Foam Under Simulated Horizontal Downhole Conditions. *SPE Drill. Complet.* 22, 304–312. <https://doi.org/10.2118/99201-PA>
- Cl Kleinstreuer, 2003. *Two-Phase Flow Theory and Applications*. Routledge, New York. <https://doi.org/https://doi.org/10.1201/9780203734865>
- Clark, R.K., Bickham, K.L., 1994. A Mechanistic Model for Cuttings Transport, in: SPE 69th Annual Technical Conference and Exhibition. New Orleans, La, U.S.A., 25-28 September, pp. 139–154. <https://doi.org/10.2118/28306-MS>
- Demiralp, Y., 2014. *Effects of Drill-Pipe Whirling Motion on Cuttings Transport Performance for Horizontal Drilling*. Louisiana State University.
- Dimitri Gidaspow, 2012. *Multiphase Flow and Fluidization*, 1st ed. Academic Press.

- Ding, J., Gidaspow, D., 1990. A Bubbling Fluidization Model Using Kinetic Theory of Granular Flow. *AIChE J.* 36(40), 523–538. <https://doi.org/10.1002/aic.690360404>
- Doron, P., Barnea, D., 1993. A Three-Layer Model for Solid-Liquid Flow in Horizontal Pipes. *Int. J. Multiph. Flow* 19, 1029–1043. [https://doi.org/10.1016/0301-9322\(93\)90076-7](https://doi.org/10.1016/0301-9322(93)90076-7)
- Duan, M., Miska, S., Yu, M., Takach, N.E., Ahmed, R.M., Hallman, J.H., 2010. Experimental Study and Modeling of Cuttings Transport Using Foam With Drillpipe Rotation. *SPE Drill. Complet.* 25, 352–362. <https://doi.org/10.2118/116300-PA>
- Epelle, E.I., Gerogiorgis, D.I., 2017. A Multiparametric CFD Analysis of Multiphase Annular Flows for Oil and Gas Drilling Applications. *Comput. Chem. Eng.* 106, 645–661. <https://doi.org/10.1016/j.compchemeng.2017.08.011>
- Fluent, 2015. ANSYS FLUENT User 's Guide 15317, 2794.
- Ford, J.T., Gao, E., Oyeneyin, M.B., Peden, J.M., Larrucia, M.B., Parker, D., 1996. A New MTV Computer Package for Hole-Cleaning Design and Analysis. *SPE Drill. Complet.* <https://doi.org/10.2118/26217-PA>
- Garcia-Hernandez, A.J., Miska, S.Z., Yu, M., Takach, N.E., Zettner, C.M., 2007. Determination of Cuttings Lag in Horizontal and Deviated Wells, in: *SPE Annual Technical Conference and Exhibition*. Anaheim, California, U.S.A., 11–14 November. <https://doi.org/10.2118/109630-MS>
- GhasemiKafrudi, E., Hashemabadi, S.H., 2016. Numerical Study on Cuttings Transport in Vertical Wells with Eccentric Drillpipe. *J. Pet. Sci. Eng.* 140, 85–96. <https://doi.org/10.1016/j.petrol.2015.12.026>

- Guo, X. le, Wang, Z. ming, Long, Z. hui, 2010. Study on Three-Layer Unsteady Model of Cuttings Transport for Extended Reach Well. *J. Pet. Sci. Eng.* 73, 171–180.
<https://doi.org/10.1016/j.petrol.2010.05.020>
- Han, S.M., Hwang, Y.K., Woo, N.S., Kim, Y.J., 2010. Solid-Liquid Hydrodynamics in a Slim Hole Drilling Annulus. *J. Pet. Sci. Eng.* 70, 308–319.
<https://doi.org/10.1016/j.petrol.2009.12.002>
- Hemphill, T., Ravi, K., 2006. Pipe Rotation and Hole Cleaning in an Eccentric Annulus, in: IADC/SPE Drilling Conference. Miami, Florida, U.S.A., 21–23 February.
<https://doi.org/10.2118/99150-MS>
- Heydari, O., Sahraei, E., Skalle, P., 2017. Investigating the Impact of Drillpipe’s Rotation and Eccentricity on Cuttings Transport Phenomenon in Various Horizontal Annuluses using Computational Fluid Dynamics (CFD). *J. Pet. Sci. Eng.* 156, 801–813.
<https://doi.org/10.1016/j.petrol.2017.06.059>
- Inc. ANSYS, 2013. ANSYS FLUENT Theory Guide. Release 18.2 15317, 373–464.
[https://doi.org/10.1016/0140-3664\(87\)90311-2](https://doi.org/10.1016/0140-3664(87)90311-2)
- Lamb, H., 1945. *Hydrodynamics*. Dover Publications., New York City.
- Larsen, T.I., Pilehvari, A.A., Azar, J.J., 1997. Development of a New Cuttings-Transport Model for High-Angle Wellbores Including Horizontal Wells. *SPE Drill. Complet.* 12, 129–136.
<https://doi.org/10.2118/25872-PA>
- Li, Y., Bjorndalen, N., Kuru, E., 2007. Numerical Modelling of Cuttings Transport in Horizontal Wells Using Conventional Drilling Fluids. *J. Can. Pet. Technol.* 46, 9–15.

<https://doi.org/10.2118/07-07-TN>

Lun, C.K.K., Savage, S.B., Jeffrey, D.J., Chepurnyi, N., 1984. Kinetic Theories for Granular Flow: Inelastic Particles in Couette Flow and Slightly Inelastic Particles in a General Flowfield. *J. Fluid Mech.* <https://doi.org/10.1017/S0022112084000586>

Mao, Z., Yang, C., Kelessidis, V.C., 2012. Modeling and Numerical Simulation of Yield Viscoplastic Fluid Flow in Concentric and Eccentric Annuli. *Chinese J. Chem. Eng.* 20, 191–202. [https://doi.org/10.1016/S1004-9541\(12\)60379-6](https://doi.org/10.1016/S1004-9541(12)60379-6)

McCann, R.C., Quigley, M.S., Zamora, M., Slater, K.S., 1995. Effects of High-Speed Pipe Rotation on Pressures in Narrow Annuli. *SPE Drill. Complet.* 10, 96–103. <https://doi.org/10.2118/26343-PA>

Mei, R., Klausner, J.F., 1994. Shear Lift Force on Spherical Bubbles. *Int. J. Heat Fluid Flow* 15, 62–65. [https://doi.org/10.1016/0142-727X\(94\)90031-0](https://doi.org/10.1016/0142-727X(94)90031-0)

Naganawa, S., Nomura, T., 2006. Simulating Transient Behavior of Cuttings Transport Over Whole Trajectory of Extended Reach Well, in: *IADC/SPE Asia Pacific Drilling Technology Conference and Exhibition*. Bangkok, Thailand, 13-15 November. <https://doi.org/10.2118/103923-MS>

Nguyen. D., Rahman, S.S., 1996. A Three-Layer Hydraulic Program for Effective Cuttings Transport and Hole Cleaning in Highly Deviated and Horizontal Wells, in: *IADC/SPE Asia Pacific Drilling Technology Conference*. Kuala Lumpur, Malaysia, 9-11 September, pp. 163–173. <https://doi.org/10.2118/36383-MS>

Ofei, T.N., Irawan, S., Pao, W., 2014. CFD Method for Predicting Annular Pressure Losses and

- Cuttings Concentration in Eccentric Horizontal Wells. *J. Pet. Eng.* 2014, 1–16.
<https://doi.org/10.1155/2014/486423>
- Osunde, O., Kuru, E., 2008. Numerical Modelling of Cuttings Transport with Foam in Inclined Wells. *Open Fuels Energy Sci. J.* 1, 19–33. <https://doi.org/10.2118/2006-071>
- Ozbayoglu, E.M., Sorgun, M., 2010. Frictional Pressure Loss Estimation of Non-Newtonian Fluids in Realistic Annulus with Pipe Rotation. *J. Can. Pet. Technol.* 49, 57–64.
<https://doi.org/10.2118/141518-PA>
- Ozbayoglu, M.E., Miska, S.Z., Reed, T., Takach, N., 2005. Using Foam in Horizontal Well Drilling: A Cuttings Transport Modeling Approach. *J. Pet. Sci. Eng.* 46, 267–282.
<https://doi.org/10.1016/j.petrol.2005.01.006>
- Ozbayoglu, M.E., Saasen, A., Sorgun, M., Svanes, K., 2008. Effect of Pipe Rotation on Hole Cleaning for Water-Based Drilling Fluids in Horizontal and Deviated Wells, in: *IADC/SPE Asia Pacific Drilling Technology Conference and Exhibition*. Jakarta, Indonesia. 25–27 August. <https://doi.org/10.2118/114965-MS>
- Pang, B., Wang, S., Wang, Q., Yang, K., Lu, H., Hassan, M., Jiang, X., 2018. Numerical Prediction of Cuttings Transport Behavior in Well Drilling Using Kinetic Theory of Granular Flow. *J. Pet. Sci. Eng.* 161, 190–203. <https://doi.org/10.1016/j.petrol.2017.11.028>
- Pereira, F.A.R., Barrozo, M.A.S., Ataíde, C.H., 2007. CFD Predictions of Drilling Fluid Velocity and Pressure Profiles in Laminar Helical Flow. *Brazilian J. Chem. Eng.* 24, 587–595.
<https://doi.org/10.1590/S0104-66322007000400011>
- Philip, Z., Sharma, M.M., Chenevert, M.E., 1998. The Role of Taylor Vortices in the Transport of

- Drill Cuttings, in: SPE India Oil and Gas Conference and Exhibition. New Delhi, India, 7-9 April. <https://doi.org/10.2118/39504-MS>
- Ramadan, A., Skalle, P., Johansen, S.T., Svein, J., Saasen, A., 2001. Mechanistic Model for Cuttings Removal From Solid Bed in Inclined Channels. *J. Pet. Sci. Eng.* 30, 129–141. [https://doi.org/10.1016/S0920-4105\(01\)00108-5](https://doi.org/10.1016/S0920-4105(01)00108-5)
- Rooki, R., Ardejani, F.D., Moradzadeh, A., Norouzi, M., 2015. CFD Simulation of Rheological Model Effect on Cuttings Transport. *J. Dispers. Sci. Technol.* 36, 402–410. <https://doi.org/10.1080/01932691.2014.896219>
- Rooki, R., Doulati Ardejani, F., Moradzadeh, A., Norouzi, M., 2014. Simulation of Cuttings Transport with Foam in Deviated Wellbores Using Computational Fluid Dynamics. *J. Pet. Explor. Prod. Technol.* 4, 263–273. <https://doi.org/10.1007/s13202-013-0077-7>
- Saffman, P.G., 1965. The Lift on a Small Sphere in a Slow Shear Flow. *J. Fluid Mech.* 22, 385. <https://doi.org/10.1017/S0022112065000824>
- Sanchez, R.A., Azar, J. J., Bassal, A.A., Martins, A.L., 1999. Effect of Drillpipe Rotation on Hole Cleaning During Directional-Well Drilling. *SPE J.* 4(2), 101–108. <https://doi.org/10.2118/56406-PA>
- Schaeffer, D.G., 1987. Instability in The Evolution Equations Describing Incompressible Granular Flow. *J. Differ. Equ.* 66, 19–50. [https://doi.org/10.1016/0022-0396\(87\)90038-6](https://doi.org/10.1016/0022-0396(87)90038-6)
- Sifferman, T.R., Becker, T.E., 1992. Hole Cleaning in Full-Scale Inclined Wellbores. *SPE Drill. Eng.* 7, 115–120. <https://doi.org/10.2118/20422-PA>
- Sifferman, T.R., Myers, G.M., Haden, E.L., Wahl, H.A., 1973. Drill Cutting Transport in Full

- Scale Vertical Annuli, in: Society of Petroleum Engineers of AIME. Las Vegas, p. 5.
- Sorgun, M., Aydin, I., Ozbayoglu, M.E., 2011. Friction Factors for Hydraulic Calculations Considering Presence of Cuttings and Pipe Rotation in Horizontal/Highly-Inclined Wellbores. *J. Pet. Sci. Eng.* 78, 407–414. <https://doi.org/10.1016/j.petrol.2011.06.013>
- Sun, B., Xiang, H., Li, H., Li, X., 2017. Modeling of the Critical Deposition Velocity of Cuttings in an Inclined-Slimhole Annulus. *SPE J.* 22, 1213–1224. <https://doi.org/10.2118/185168-PA>
- Tormen, P.H., Iyoho, A.W., Azar, J.J., 1986. Experimental Study of Cuttings Transport in Directional Wells. *SPE Drill. Eng.* 43–56. <https://doi.org/10.2118/12123-PA>
- Walker, S., Li, J., 2000. The Effects of Particle Size, Fluid Rheology, and Pipe Eccentricity on Cuttings Transport, in: *SPE/ICoTA Coiled Tubing Roundtable*. Houston, TX, 5–6 April. <https://doi.org/10.2118/60755-MS>
- Wang, Z. ming, Guo, X. le, Li, M., Hong, Y. kui, 2009. Effect of Drillpipe Rotation on Borehole Cleaning for Extended Reach Well. *J. Hydrodyn.* 21, 366–372. [https://doi.org/10.1016/S1001-6058\(08\)60158-4](https://doi.org/10.1016/S1001-6058(08)60158-4)
- Wei, X., Miska, S.Z., Takach, N.E., Bern, P., Kenny, P., 1998. The Effect of Drillpipe Rotation on Annular Frictional Pressure. *J. Energy Resour. Technol.* ASME 1. <https://doi.org/10.1115/1.2795011>
- Wen. C.Y., Yu., Y., 1966. Mechanics of Fluidization. *Chem. Eng. Prog. Symp. Ser.* 62 (1), 100–111.
- Wilson, K., D.G. Judge, 1978. Analytically-Based Nomographic Charts for Sand-Water Flow, in: *Hydrotransport 5, Solids in Pipes*, BHRA Fluid Engineering. Cranfield, UK.

Chapter 3 : Experimental Study of Drill Cuttings Transport in Horizontal Well with Newtonian Fluid

Mohammad Mojammel Huque¹, Syed Imtiaz¹, Stephen Butt¹, Sohrab Zendehboudi¹, Mohammad Azizur Rahman²

¹Memorial University of Newfoundland

²Texas A & M University at Qatar

ABSTRACT

Transport of cuttings is crucial in horizontal drilling operation. An effective removal of cuttings is necessary for an efficient drilling. An experimental investigation has been carried out to analyze the flow behavior of solid cuttings in different drilling environment with visualization technique. This study investigates the cuttings transport mechanism in horizontal annulus section. A 6.16 m long and 4.5”x2.5” annulus section was used to model the real-time drilling behavior with different flow rates, drill pipe rotations and eccentric positions. Water as a Newtonian fluid was used as drilling mud and 2-3 mm solid glass beads was used to simulate the drill cuttings. The in-situ volume fraction of cuttings in the annulus was estimated by Electrical Resistivity Tomography (ERT) analyzer. Visualization technique used to estimate the moving bed velocity in the horizontal annulus section. A high-speed camera was used to capture the transport phenomena of the moving solid particle at 2000 frames per second. High speed camera can effectively track each particle in the system. Analysis of high-speed camera revealed different cuttings transport phenomena like rolling of cuttings, stationary cuttings bed and cuttings suspended into the drilling mud. A commercial software was used to simulate the multiphase flow behavior in the annulus section. Experimental investigation revealed that, drill pipe rotation helps in cuttings bed movement and resist the formation of large cuttings dune in the annulus formation. Also, this study revealed that,

eccentric annulus shows less annular solid volume in compared to a concentric annulus, however eccentric annulus is harder to clean compared to a concentric annulus section.

Keywords: Two phase flow, Cuttings Transport, Eccentricity, Drill Pipe Rotation, ERT Analysis

3.1 Introduction

Hole cleaning in a drilling operation is a key concern in the entire drilling activities. During a drilling process, as drill bit proceeds forward, it always generates rock chips of different size and shapes. These drill cuttings must be removed from the borehole so that drill bit can encounter fresh rock formation for subsequent drilling. The removal of these drill cuttings are accomplished by appropriate drilling mud which transporting cuttings to the surface through the annulus section. Inadequate hole cleaning may lead to several problem like stuck pipe, differential sticking, poor rate of penetration etc. A proper hole cleaning is a necessary step in entire drilling operation especially directional, horizontal, and extended reach well.

This research work focused on experimental study of cuttings transport in horizontal well. Several lab scale experimental investigations were performed by researchers in last few decades. Sifferman et al. 1973 and Tomren et al. 1986 were the very first experimental group who studied the cuttings transport behavior in vertical and inclined annulus respectively. Their study revealed that fluid velocity have a positive impact in cuttings transport in the annulus section. Cuttings transport in directional well(Avila et al., 2004; Capo et al., 2004; Ford et al., 1990; Larsen et al., 1997) and in horizontal well(Duan et al., 2010; Garcia-Hernandez et al., 2007; Ozbayoglu and Osgouei, 2012; Ozbayoglu et al., 2008) were also investigated with experimental work in past decade. Most of the past studies primarily focused on the effect of fluid rheology(Ahmed and Miska, 2008; Chen et

al., 2007; Hemphill and Ravi, 2006; Naganawa and Nomura, 2006) and drill pipe rotation (McCann et al., 1995; Sorgun et al., 2011). Very few experimental studies were conducted for the horizontal annulus section with advanced high definition visualization (Raza et al., 2019; Zahid et al., 2018) and instantaneous solid volume fraction estimation.

Drill cuttings transport study in horizontal well is a complex study of multiphase flow of solid and liquid in the annulus section. Due to significant density difference between solid cuttings and liquid, drill cuttings always tends to settle down in the annulus section at a low flow rate. Settlement of solid particles forms a solid bed which reduce the fluid flow area and makes the solid transport complicated. Eccentric annulus position causes an uneven velocity distribution of fluid flow and solid transport in the annulus section.

The goal of this study is to further investigate the cuttings transport behavior in a horizontal annulus section with advanced high-definition visualization technique for different drilling condition such as change in fluid velocity, inner pipe rotation, eccentricity, and rate of penetration. This study also used Electrical Resistance Tomography (ERT) system to estimate instantaneous cuttings volume fraction in the system. This can be used as an indicator of cuttings transport capability of the system.

3.2 Experimental Procedure

The experimental test section consists of 6.16-meter-long annulus system with transparent acrylic outer pipe and an aluminum inner pipe as shown in **Figure 3-1**. Diameter of the outer pipe is 4.5” and inner pipe is 2.5”. With a manual regulator, aluminum pipe can be placed in both concentric and eccentric condition with respect to the outer pipe. Inner pipe can also be rotated upto 150 RPM for any eccentric orientation. The complete set up can be inclined up to 15° from horizontal

position. The system can be operated with a maximum pressure 30 psig. in the annulus for liquid flowing condition only.

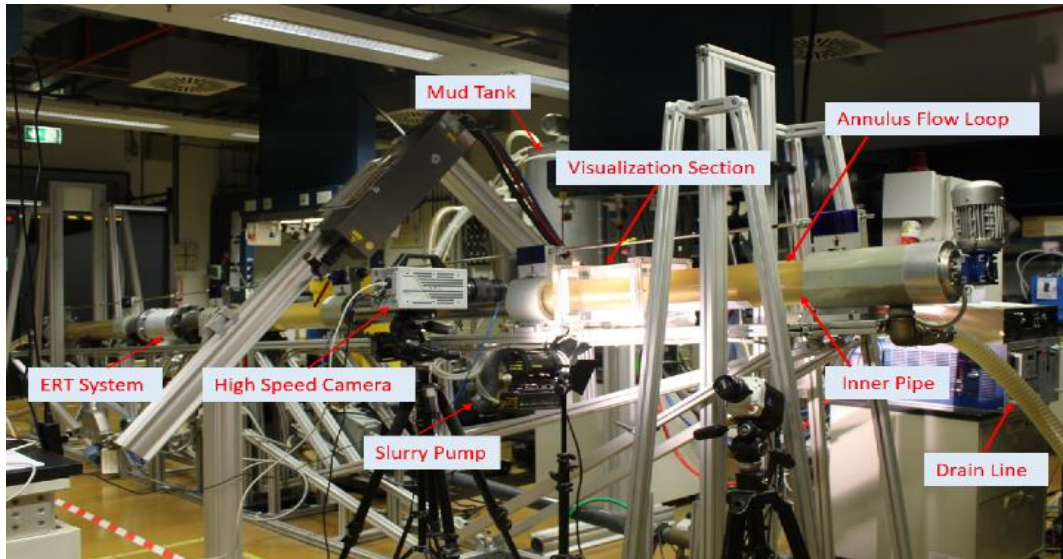


Figure 3-1: Flow loop experimental set up located at TAMUQ, Qatar.

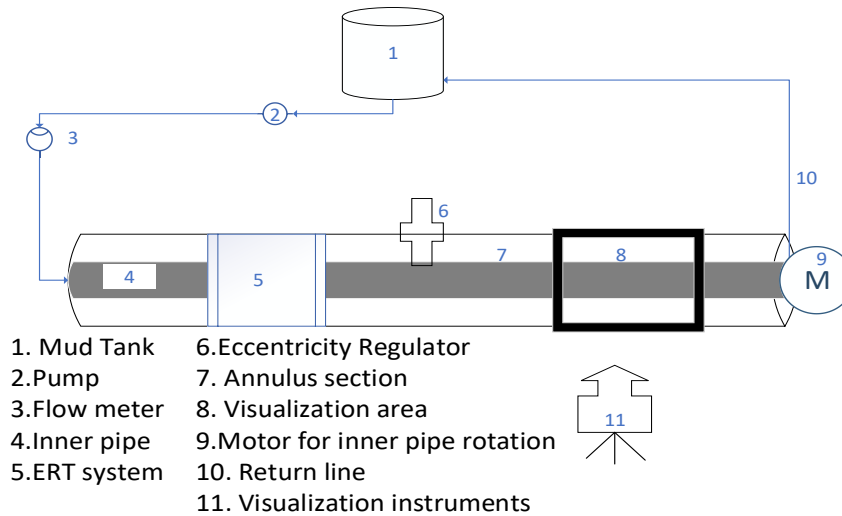


Figure 3-2: Schematic of flow loop experimental set up

Figure 3-2 shows a simple schematic of the test section. The complete experiment run in a closed loop experimental system where solid cuttings and liquid are mixed with a high-speed agitator in the mud tank. Once a homogenous slurry is formed, a slurry pump delivers the two-phase mixture to the annulus. A Coriolis meter measures the mass flow rate of the system. In the test section,

fluid and solid enter into the ERT (Raza et al., 2019) section which is about 2.5 meter away from the inlet. ERT system estimated the instantaneous solid volume fraction in the system and visualization section allows to estimate the bed height and solid bed movement patterns. Once the two-phase mixture passed ERT section, pressure sensor and visualization section, slurry return to the mud tank by a drain line from test section outlet.

3.2.1 Methodology

The experiment begins by filling up the main mud tank with 300 liters of water at room temperature. Sold glass beads of size ranging from 2.5mm to 3.0 mm were used as cuttings in this experiment. The density of the glass beads is about 2600 kg/m³. 4% solid by weight were used for first experiments set which corresponds rate of penetration of 85 ft/hr. The rate of penetration is estimated (Larsen et al., 1997) as

$$R_p \left(\frac{ft}{hr} \right) = Q_{inj} \left(\frac{ft^3}{sec} \right) \left(\frac{3600 \text{ sec}}{hr} \right) \left(\frac{1}{A_{hole}} \right) \left(\frac{1}{ft^2} \right) \quad (3-1)$$

Where R_p represents the rate of penetration, Q_{inj} is the volumetric injection of solid and A_{hole} denotes the area of the hole during a drilling operation.

For 300 liters of water, a total of 12 kg solid was added into the mud tank. The test was performed at different slurry pump rate starting from 500 RPM to 1000 RPM which corresponding to annular fluid velocity of 0.397 m/s to 0.818 m/s. For lower mud pump rate of 500 and 600 RPM, a non-moving sand bed were formed at the entrance of the test section and no solid dune reached upto the visualization section. So, the complete test matrix started from 700 RPM slurry pump rate. For each flow rate, the effect of inner pipe rotation was tested. The details of experimental matrix are tabulated in **Table 3-1**. A total of 48 experiments were performed with 4% solid with three different eccentricities ($e = 0, 0.3, 0.6$). Another 24 experiments were performed with 8% solid

with different mud pump rate and two annular orientations ($e = 0, 0.3$). For all experimental cases, ERT system estimated the annular volume fractions, visualization system captures the video of the solid bed height, bed movement time and solid particles movement pattern.

Table 3-1: Experimental test matrix details

Matrix No	Pump Rate, RPM	Eccentricity	Solid Vol. Frac,	Drill Pipe Rotation, RPM	Number of Test
1	700	0, 0.3, 0.6	4%	0, 40, 80, 120	12
	800	0, 0.3, 0.6	4%	0, 40, 80, 120	12
	900	0, 0.3, 0.6	4%	0, 40, 80, 120	12
	1000	0, 0.3, 0.6	4%	0, 40, 80, 120	12
2	800	0, 0.3	8%	0, 40, 80, 120	8
	900	0, 0.3	8%	0, 40, 80, 120	8
	1000	0, 0.3	8%	0, 40, 80, 120	8

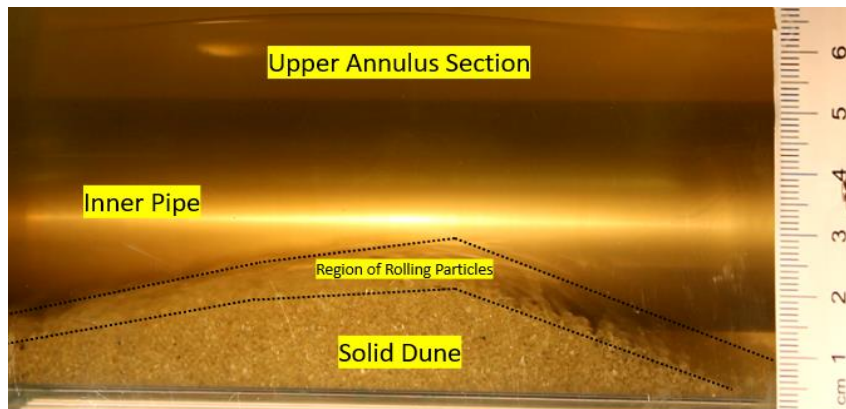


Figure 3-3: Visualization section showing solid dune, annulus section, and inner pipe.

The visualization section is 19 cm long with full height of annulus observation as shown in **Figure 3-3**. Solid dune height and solid movement pattern at different orientation were observed in this section and all movement patterns were recorded with a digital single lens reflex (DSLR) video camera. Also, the individual solid moving pattern was observed with a Photon Fastcam high-speed video camera at 2000 frames per second. Solid dune moving time at different operating condition were calculated. In this study, the dune movement time was estimated as the time required by a sand dune crossing the test section only.

3.3 Results and Discussion

Four different drilling parameters were investigated during this study, these are change in flow rate, change in inner pipe rotation, change in eccentricity and effect of rate of penetration. These are discussed in **section 3.3.1** to **3.3.5**. Effect of liquid flow rate or fluid velocity in cuttings transport are discussed in **section 3.3.1**. **Section 3.3.2** explains the effect of eccentricity, **section 3.3.3** discusses the dune propagation time for various experimental condition and **section 3.3.4** describes the annular solid volume fraction. The effect of rate of penetration is discussed in **section 3.3.5**. Finally, **section 3.3.6** shows the visualization of different cuttings transport phenomena for different flow conditions.

3.3.1 Effect of Mud Flow Rate and Inner Pipe Rotation

Drilling mud carries all cuttings to the surface from borehole. So, mud flow rate has significant influence in cuttings transport in the drilling system since **Figure 3-4** represents the solid bed height in the annulus for different fluid velocities and inner pipe rotations. It is clearly observed that, a stationary position of inner pipe (no drill pipe rotation, RPM = 0) indicates a higher bed height compared to a case of rotating inner pipe. It shows almost 4 cm bed height for fluid velocity from 0.57 m/s to 0.72 m/s. At higher fluid velocity (0.82 m/s), solid bed height shows a decreasing trend for all inner pipe rotation. Imposing an inner pipe rotation 40 RPM shows a significant decrease in solid bed height by approximately 1 cm.

Drill pipe rotation imposes an inertial force to the stationary solid bed that are in contact with the inner pipe wall. This inertial force assists the solid particles to flow with the moving liquid in the test section. There is further improvement in solid bed height by 0.5 cm when inner pipe rotation increased to 80 RPM. However, no significant improvement is observed when inner pipe rotation

increased from 80 RPM to 120 RPM. It can be concluded that, inner pipe rotation has significant impact on reducing the solid bed height in the annulus section.

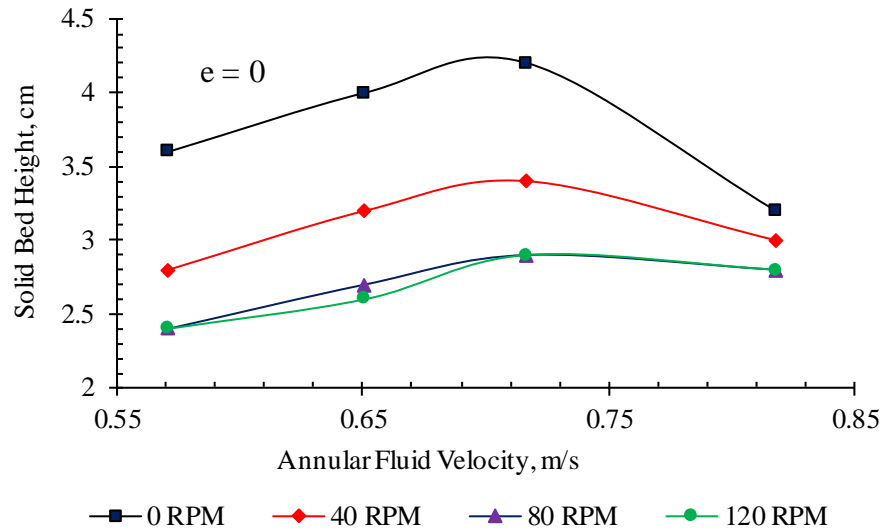


Figure 3-4: Effect of annular fluid velocity on solid bed height ($e = 0$)

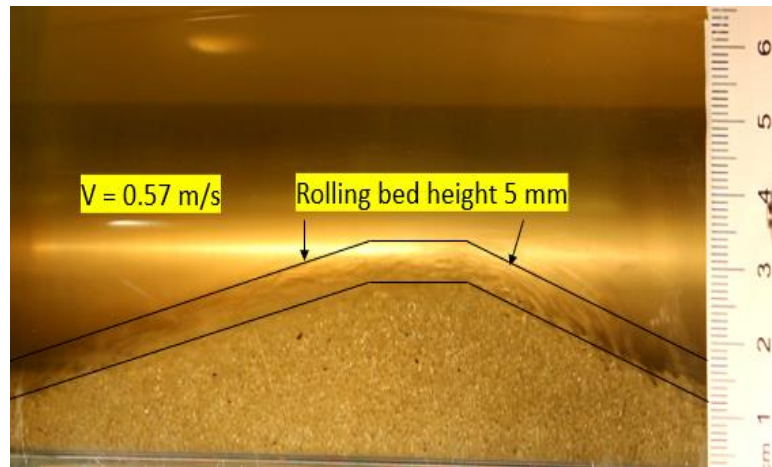


Figure 3-5: Low rolling bed height at low fluid velocity

In addition to inner pipe rotation and fluid velocity, with increasing the fluid velocity, solid bed height slightly increases for all flowrates upto 0.72 m/s, beyond this point a downward trend in solid bed height was observed for fluid velocity of 0.82m/s. This trend can be explained by the

solid transport mechanism. Visual observation shows that, sand dune is moving due to the rolling particles at the top of the sand dune. Rolling sand bed thickness over the static sand dune depends on the fluid velocity. **Figure 3-5** shows the thickness of bed rolling bed height of approximately 4-5 mm for the effect of low fluid velocity in the annulus. **Figure 3-6** shows an increase in rolling bed height upto 10-15 mm with increase in fluid velocities in the annulus section.

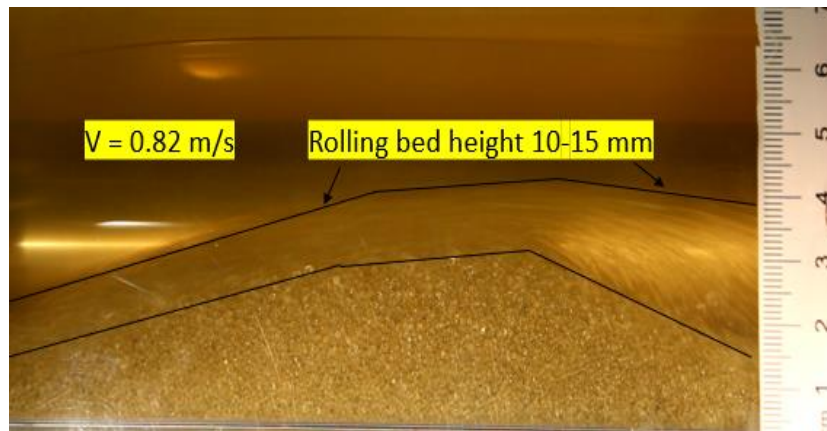


Figure 3-6: High rolling bed height at high fluid velocity

Sand particles are moving due to resultant of two forces acting upon the particles. The fluid velocity drags the particles in the axial direction whereas rotating inner pipe drag the particles in the radial direction. The axial force drags the rolling particles over the stationary solid bed and hence gradually increase in rolling bed thickness is observed with increasing fluid velocity. Though increasing the fluid velocity increases solid bed height, it decreases the dune length in the annulus which reflects with the dune movement time as shown in **Section 3.3.3**. In absence of inner pipe rotation, only axial force acts on the solid particles. This is the reason for high solid bed height in absence of inner pipe rotation.

Figure 3-7 shows rolling bed height in mm with different fluid velocities and inner pipe rotation for a concentric annulus section. A higher rolling bed thickness indicates more solid are being

transported along with the liquid at higher velocities and hence reduces the stationary sand dune height. An increase in fluid velocity increases the rolling bed height for all inner pipe rotations. Comparing **Figure 3-4** and **Figure 3-7**, it can be concluded that a rolling bed increases corresponding to a low sand dune size since rolling sand particles are travelling at a higher speed compared to the sand dune movement in the annulus.

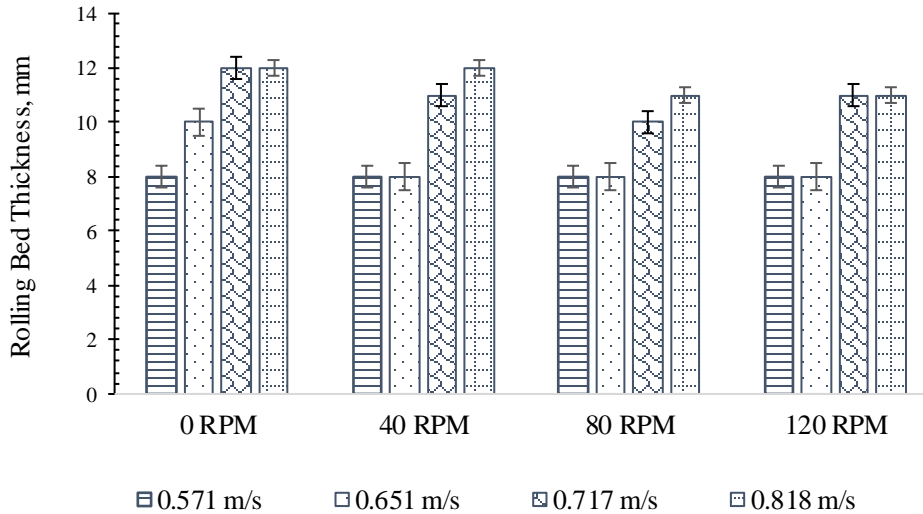


Figure 3-7: Rolling bed height variation with fluid velocities and drill pipe rotations ($e = 0$)

3.3.2 Effect of Eccentricity

In a horizontal drilling operation, due to the self-weight of the drillpipe, it might show an eccentric position in the annulus. Eccentricity is defined as the degree of offset of inner drill pipe from its concentric annular position. Eccentricity is a most common scenario observed in a horizontal or extended reach well. Mathematically, eccentricity is defined as

$$e = \frac{2\delta}{D_o - D_i} \quad (3-2)$$

Where "e" is defined as the eccentricity, D_o and D_i are defined as the diameter of outer pipe and inner pipe respectively and " δ " is defined as the offset of center of the inner circle from outer circle. **Figure 3-8** shows three different eccentric positions of the drill pipe- annulus orientation.

Three different annular orientations ($e = 0, 0.3, 0.6$) were tested where $e = 0$ represents a concentric annulus and $e = 0.3$ represent a moderate eccentric and 0.6 represents a highly eccentric annulus condition for this test section. Experimental work limited to eccentricity value of 0.6 due to safety issue. **Figure 3-9** describes the effect of eccentricity on solid bed height for different fluid velocities. It is clearly showing that a concentric annulus exhibits a higher solid bed height in the annulus section compared to the eccentric annulus. Increase in the eccentricity from 0 to 0.3 slightly decreases the annulus bed height, however more than 50% decrease in solid bed height was observed when eccentricity increases to 0.6 . Eccentric annulus clearly shows a significantly low bed thickness due to less annulus space in the lower annulus section. Also, inner pipe has a very close contact with the solid dune. Inner pipe rotation drags the stationary solid particles from the sand dune to the upper annulus section where sand particles can flow together with the moving liquid in the test section.

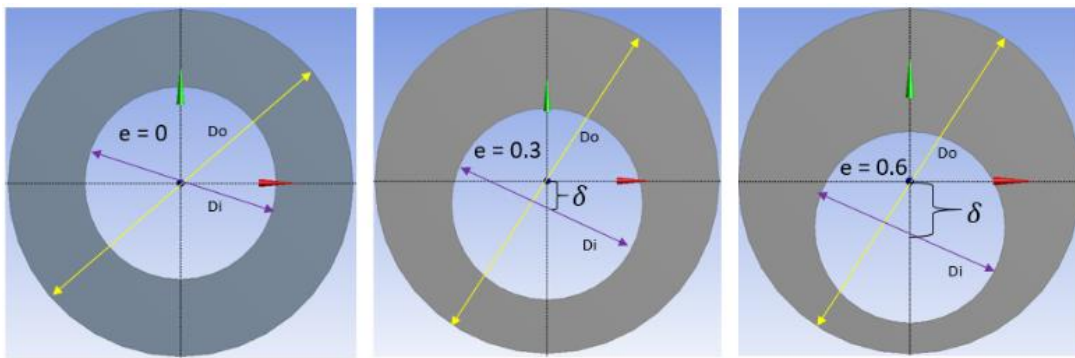


Figure 3-8: Different eccentric annular position used in this study.

Figure 3-10 shows the annular velocity profile for an highly eccentric annular section using two phase flow behaviour. Simulation was carried out using Ansys Fluent v.17.2 with Eulerian - Eulerian multiphase flow model. Water was considered as primary fluid and solid cuttings were simulated as secondary medium. Simulation study shows that the velocity profile in the lower annular section is significantly low compared to the upper annular section. This is due to the fact

that the narrow annular gap creates more resistance to flow in the lower annular section. Also, solid bed formed in the lower annular section obstruct the mud flow within the lower section. This can be correlated with the low bed height and high dune movement time for a highly eccentric annulus as discussed in **section 3.3.1** and **3.3.3** respectively.

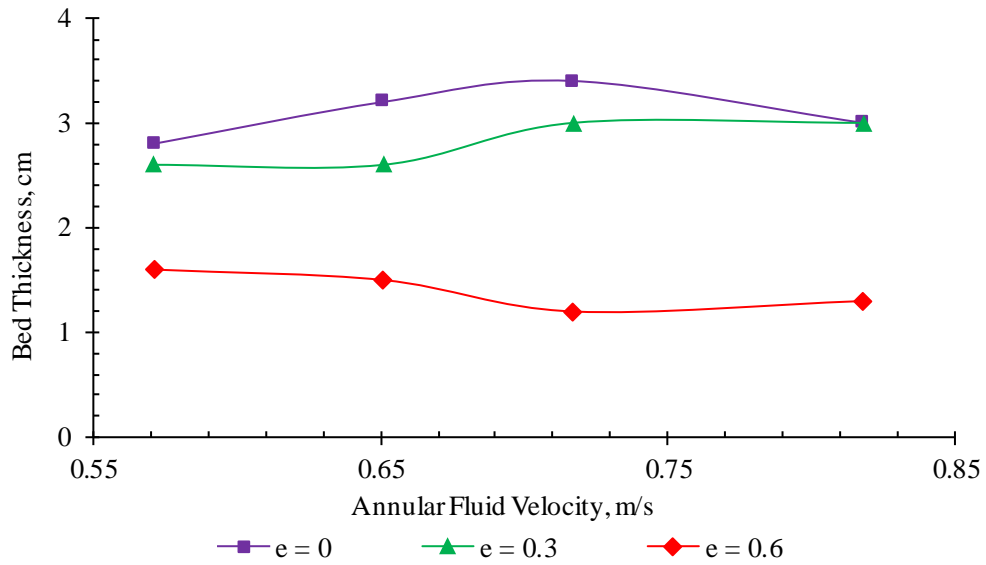


Figure 3-9: Effect of eccentricity on annular bed height at 40 RPM

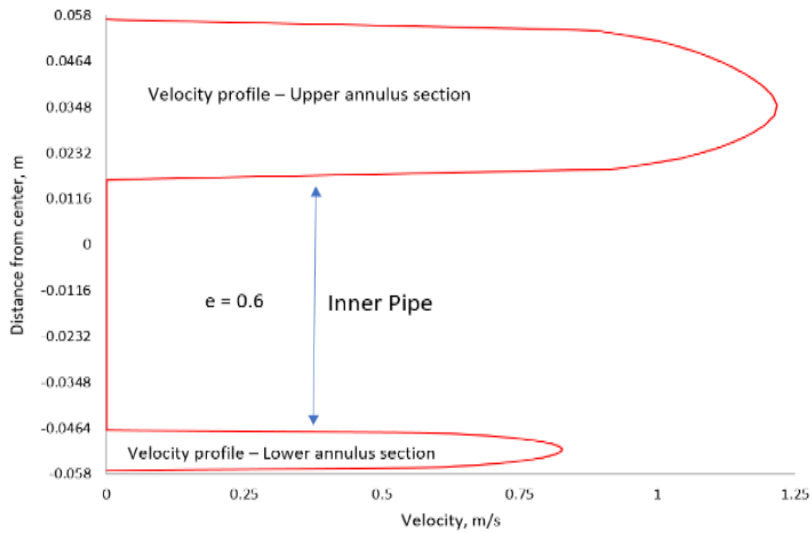


Figure 3-10: Annular velocity profile for a highly eccentric annulus

3.3.3 Dune Movement Time

In this experimental work, the sand dune movement time has been studied for both fluid velocities and inner pipe rotations from the visualization section. Elapsed time is measured as total time for a sand dune to enter the visualization section and leave the visualization section. A low dune movement time indicates a high solid moving velocity in the annulus section and hence a good hole cleaning.

Sand dune propagation time for different fluid velocities and eccentric conditions are shown in **Figure 3-11** for the inner pipe rotation of 0 RPM. Study shows that with increasing the eccentricity, dune propagation time significantly increased. For example, for a flow rate of 0.57 m/s, eccentricity, $e = 0.6$ shows a dune propagation time of 280 seconds whereas it was 84 seconds for eccentricity, $e = 0.3$ and only 48 seconds for a concentric annulus configuration.

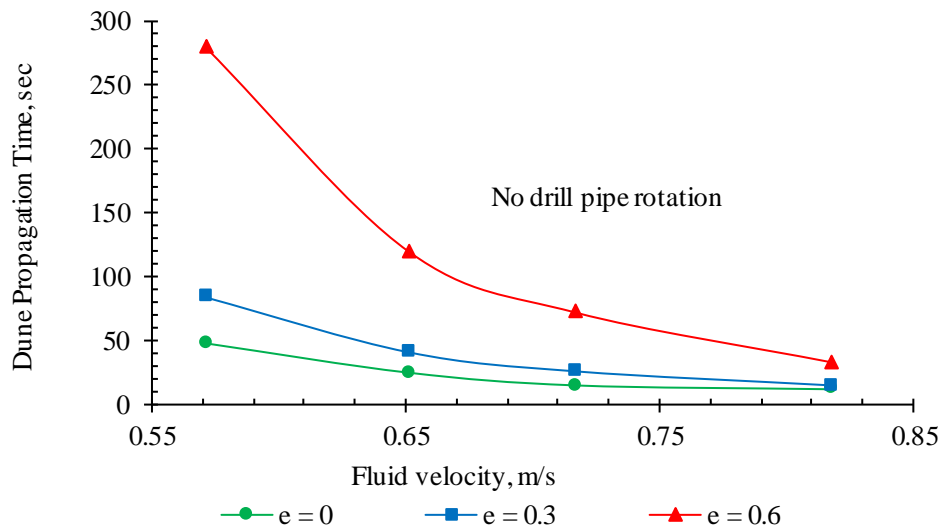


Figure 3-11: Sand dune propagation time for stationary inner pipe (RPM = 0)

Figure 3-12 and **Figure 3-13** shows dune propagation time for inner pipe rotation of 40 and 80 RPM respectively. Comparing **Figure 3-11** with **Figure 3-12** and **Figure 3-13** shows that, imposing inner pipe rotation significantly reduce the dune propagation time for all cases. For

example, for a highly eccentric case of $e = 0.6$, dune propagation time was 280 sec, 210 sec and 90 sec for the inner pipe rotation of 0, 40 and 80 RPM respectively.

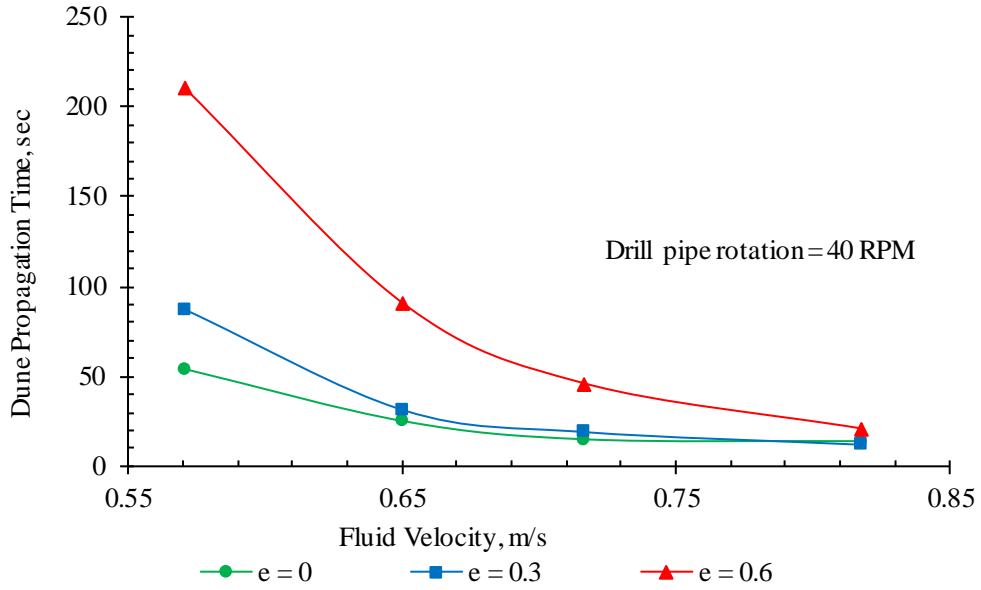


Figure 3-12: Sand dune propagation time for drill pipe rotation of 40 rpm

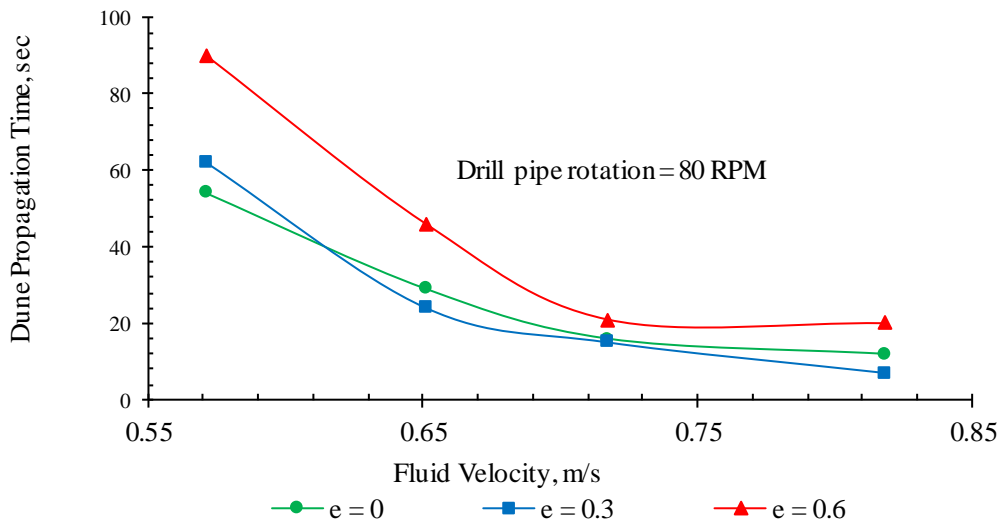


Figure 3-13: Sand dune propagation time for drill pipe rotation of 80 rpm

Table 3-2: Improvement in dune propagation time with fluid velocity

Eccentricity	Base case	Improvement in dune propagation time, %		
	0.571 m/s	0.651 m/s	0.717 m/s	0.818 m/s
e = 0	48 sec	47.9%	68.8%	75.0%
e = 0.3	84 sec	51.2%	69.0%	82.1%
e = 0.6	280 sec	57.1%	74.3%	88.2%

Table 3-2 shows improvement in dune propagation time compared to a base case of fluid velocity 0.571 m/s for all eccentric condition. It shows that increase in fluid velocity from 0.571 m/s to 0.818 m/s significantly improves the dune propagation time. Improvement is upto 75% for a concentric annulus and 88% for a highly eccentric annulus. It can be concluded that fluid velocity has positive effect on sand dune propagation time. However, a highly eccentric annulus shows significant negative impact on dune propagation time compared with a concentric annulus. This revealed that, eccentric annulus is harder to clean compared to a concentric annulus.

3.3.4 Annular Solid Volume Fraction Analysis

ERT system identifies the instantaneous solid volume fraction when solid dune passes the ERT section. Integrating whole solid volume fraction over time implies annular volume fraction in the annulus section. **Figure 3-14** shows annular solid volume fraction obtained from the ERT system for different fluid velocities and different inner pipe rotations. It shows that, a stationary inner pipe rotation with low fluid velocity indicates a higher annular solid volume fraction which can also be correlated from the high bed height condition from **Figure 3-4**. Increase in the inner pipe rotation decreases the overall solid volume fraction in the annulus section. A less annular solid volume fraction indicates a good hole cleaning condition. And hence it can be concluded that, for a horizontal concentric drilling condition, an inner pipe rotation and high fluid velocity improve cuttings transport significantly. A significant improvement of annular solid volume fraction was observed for all condition of inner pipe rotations when fluid velocity is 0.82m/s.

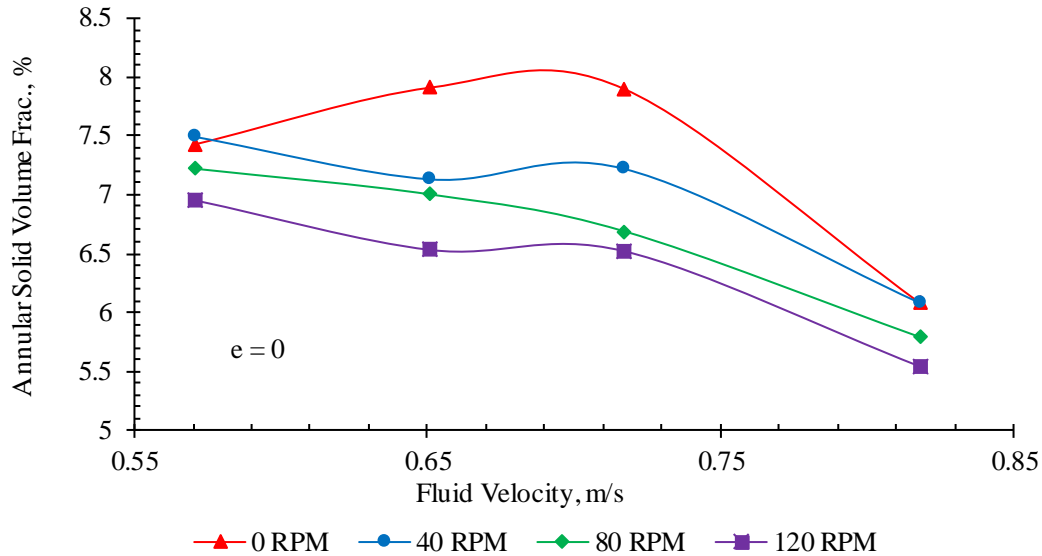


Figure 3-14: Annular volume fraction for concentric annulus ($e = 0$)

For a highly eccentric annulus, ERT analysis shows a contrary scenario in annular solid volume fraction compared to a concentric annulus as shown in **Figure 3-15**. For all inner pipe rotations, ERT analysis of a highly eccentric annulus shows a significantly less annular solid volume fraction compared to a concentric annulus. However, for an eccentric annulus, annular solid volume fraction slightly increases with increase in liquid flow rate up to 0.72 m/s and beyond this a decreasing trend is observed for all inner pipe rotation except for stationary case of 0 RPM. High speed visualization shows that solid cuttings are mainly transported as rolling mechanism at low mud velocities until a threshold mud velocity reached. The rolling bed height gradually increased with an increasing in mud velocity. For this reason, an increase in solid volume fraction is observed until velocity reached to 0.72 m/s. Once the threshold velocity reached, the dominating transport mechanism switches from rolling to suspension mechanism. Therefore, most of the solid cuttings are transported in the suspended form after fluid velocity of 0.72 m/s. As a result, ERT section estimates a less solid volume fraction in the sand dune after fluid velocity of 0.72 m/s with a drill

pipe rotation. However, the situation becomes worst with stationary drill pipe and highly eccentric condition. Fluid velocity is not enough to clean the hole section for a highly eccentric annular section and a drill pipe rotation is recommended. It is an evident that, for a horizontal drilling, eccentric annulus with inner pipe rotation helps in improving the cuttings transport. This is due to the higher contact area of inner pipe with solid cuttings bed in the lower annular section and dragging of the solid cuttings by the inner pipe rotation to the fluid region.

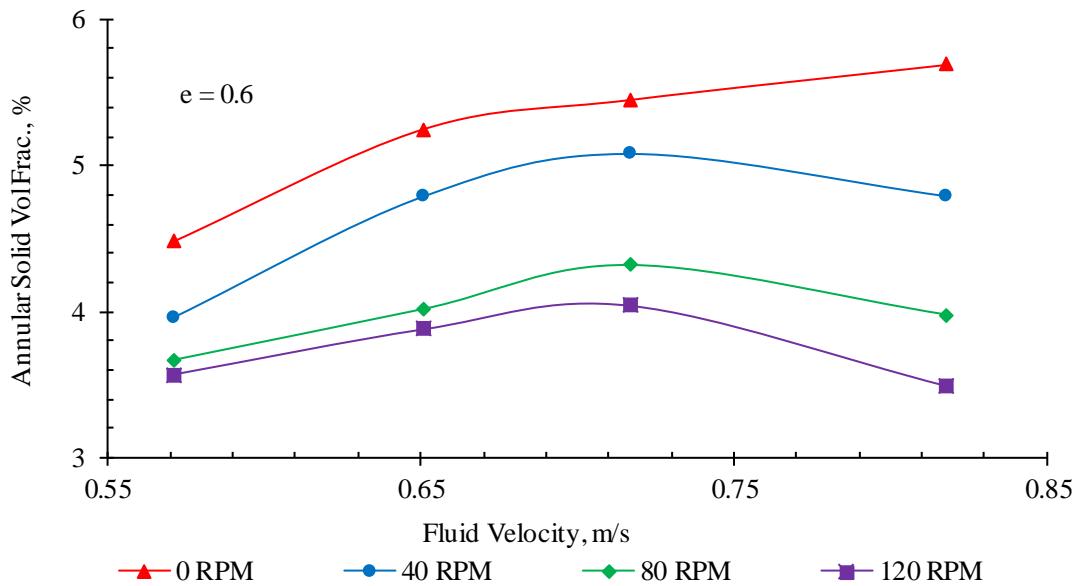


Figure 3-15: Annular volume fraction for highly eccentric annulus ($e = 0.6$)

3.3.5 Effect of Rate of Penetration (ROP)

Drilling rate of penetration is one of the major parameters to evaluate drilling performance. A higher drilling rate of penetration is always desirable in terms of rig time and overall drilling project cost. Drilling rate of penetration can be attributed by input solid volume fraction in the flow loop experimental set up. Two different rate of penetration 85 ft/hr. and 170 ft/hr. were compared in this section which corresponds to input solid fraction of 4% and 8% respectively. The

effect of ROP in terms of bed height in the annulus, ERT analysis and dune movement time was compared in this section.

Figure 3-16 shows a comparison of solid bed height for ROP of 85 ft/hr. and 170 ft/hr. for both stationary inner pipe and a rotation of 80 RPM. A higher ROP indicates a higher solid bed height in the annulus section. For a stationary inner pipe, it shows a 50% increase in solid bed height in the annulus section when ROP increase from 85 ft/hr. to 170 ft/hr. **Figure 3-17** shows the effect of rate of penetration on annular solid volume fraction for a concentric annulus orientation. It shows that increase in the ROP by 100% shows increase in annular solid volume fraction by approximately 50% for both 0 and 80 RPM.

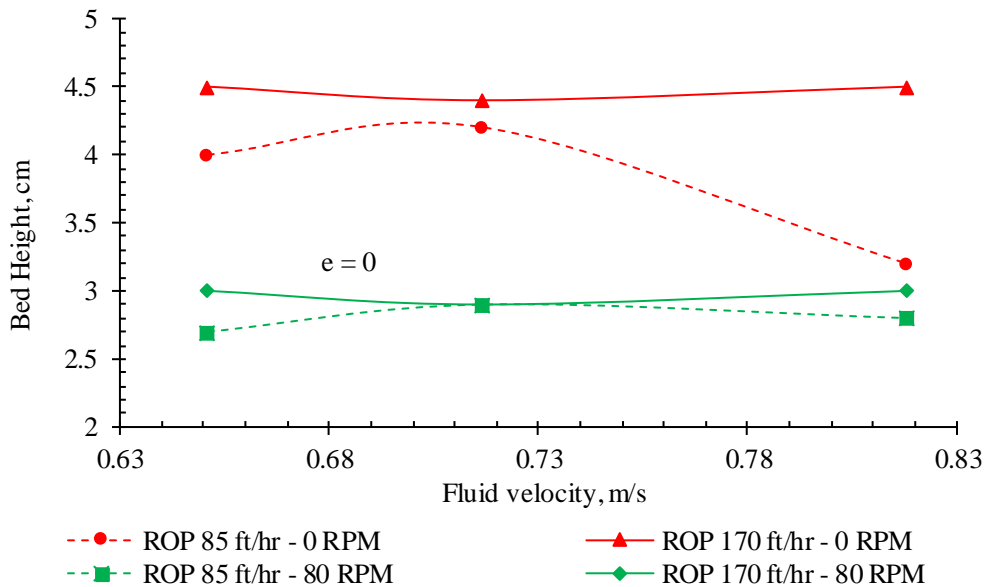


Figure 3-16: Effect of rate of penetration (ROP) on bed height ($e = 0$)

The effect of rate of penetration can be significantly expressed by dune propagation time as shown in **Figure 3-18**. For both stationary and rotatory inner pipe condition, dune propagation time significantly increased with increase in the rate of penetration. For a fluid velocity of 0.65 m/s and

a ROP of 170 ft/hr. showed sand dune was 150 seconds to pass the visualization section whereas ROP of 85 ft/hr. shows only 41 seconds in the case of no inner pipe rotation. Similar situation is observed with 80 RPM as shown in **Figure 3-18**.

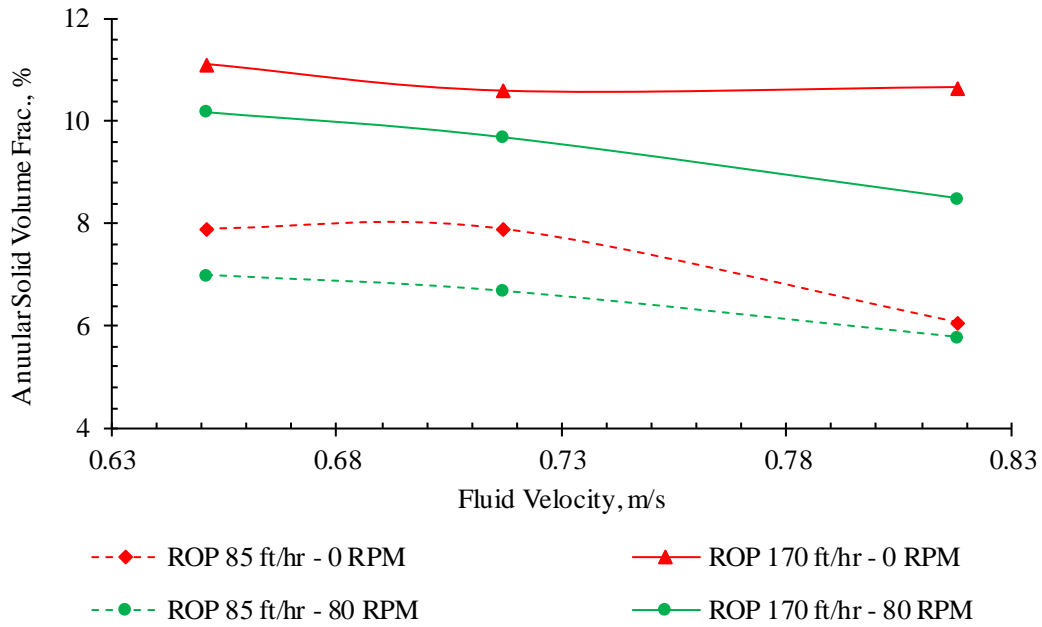


Figure 3-17: Effect of rate of penetration (ROP) on annular solid vol frac (e = 0)

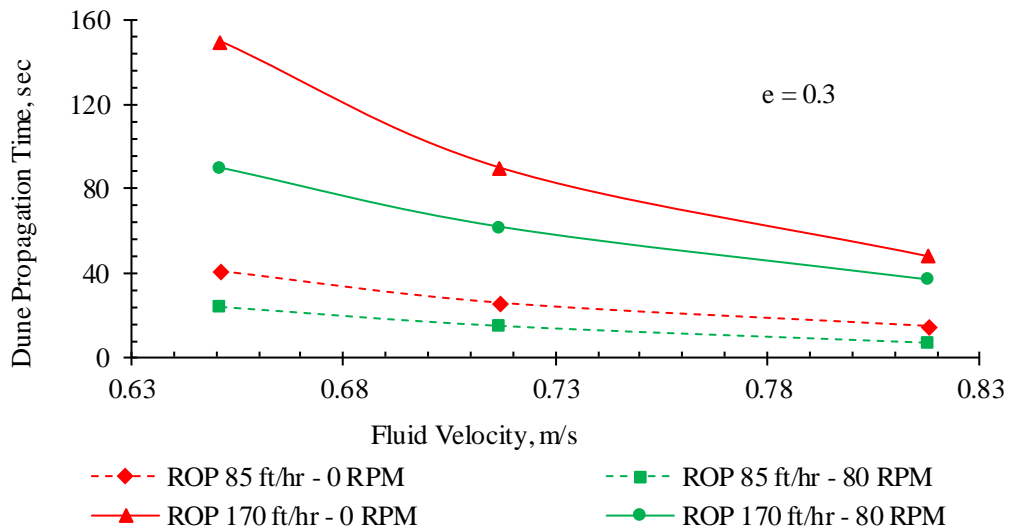


Figure 3-18: Effect of rate of penetration (ROP) on dune propagation time (e = 0.3)

3.3.6 Visualization of Cuttings Transport

Visualization technique reveals three distinct solid movement patterns during cuttings transport in the horizontal section. This camera captures the particles movement at 2000 frames per second. At a low fluid velocity, almost stationary bed is formed in the lower annulus with very few solid particles rolling over the stationary bed as shown in the **Figure 3-19**.

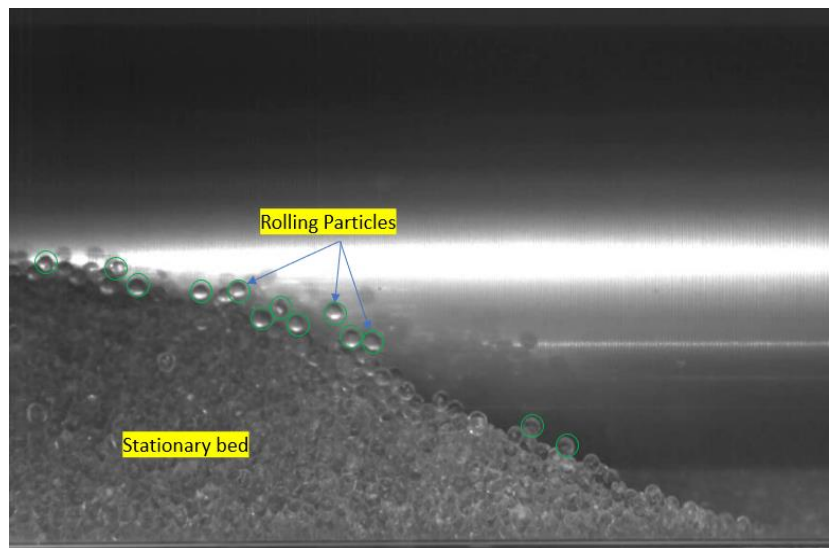


Figure 3-19: Rolling particles and stationary bed.

At higher fluid velocity, due to high turbulence, some of the solid particles were suspended into the liquid at the upper section of the annulus and axial force dominates the solid transport along the pipe as shown in the **Figure 3-20**.

A helical motion of solid particles in the eccentric annulus section also observed due to inner pipe rotation as shown in **Figure 3-21**. This helical motion of solid particles is introduced from resultant of two driving forces. The combined effect of the axial motion of liquid and rotational motion of inner pipe are responsible for this helical motion of solid particles.

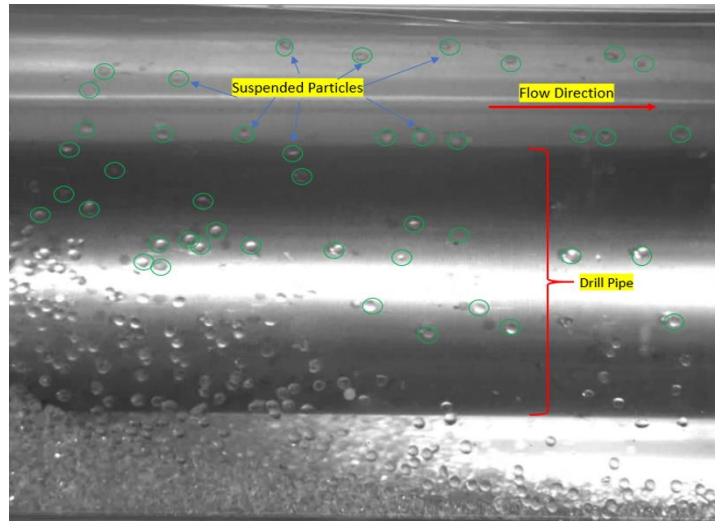


Figure 3-20: Suspended solid particles in the annulus.

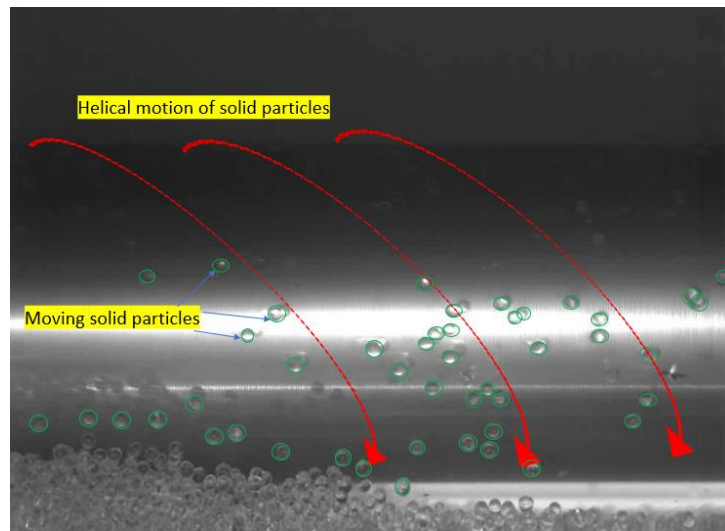


Figure 3-21: Visualization of helical motion of solid particles due to inner pipe rotation.

3.4 Conclusions

An experimental study has been performed to investigate the annular flow behavior of solid liquid flow with different drilling conditions. Visualization technique of solid bed height and ERT analysis are in good agreement with annular solid volume estimation. For all annular configuration, a stationary inner pipe shows a maximum highest solid volume fraction compared to the eccentric annulus condition. The following conclusion can be drawn from this experimental work.

- a) Imposing inner pipe rotation along with high fluid velocities improved cuttings transport significantly for concentric horizontal annular condition.
- b) Sand dune propagation time and solid bed height significantly reduce with increase in the inner pipe rotation. This implies the improved cuttings transport capability.
- c) Though eccentric annulus shows less solid fraction in the annulus, it is harder to clean.
- d) Increase in the rate of penetration or input solid volume fraction, considerably increases the due propagation time in the annulus section.
- e) Visual observation from high-speed camera indicates an additional motion of solid particles in highly eccentric annulus condition. A helical motion of solid particles was observed when rotating drill pipe are in contact with solid cuttings.

ACKNOWLEDGEMENTS

The researchers gratefully acknowledge and thank Equinor, Memorial University, InnovateNL, and NSERC to support this research work. This publication was also made possible by the grant NPRP10-0101-170091 from Qatar National Research Fund (a member of the Qatar Foundation). Statements made herein are solely the responsibility of the authors.

NOMENCLATURE

e	eccentricity
D_o	diameter of outer pipe, inch
D_i	diameter of inner pipe, inch
δ	offset of center of two circles, inch
R_p	rate of penetration, ft/hr

Q_{inj}	solid injection rate, cubic feet/sec
A_{hole}	area of the hole, sq. ft
RPM	revolution per minute
ROP	rate of penetration, ft/hr

REFERENCES

- Ahmed, R.M., Miska, S.Z., 2008. Experimental Study and Modeling of Yield Power-Law Fluid Flow in Annuli with Drillpipe Rotation, in: IADC/SPE Drilling Conference. Orlando, Florida, U.S.A, 4–6 March. <https://doi.org/10.2118/112604-MS>
- Avila, R., Pereira, E., Miska, S., Takach, N., 2004. Correlations and Analysis of Cuttings Transport with Aerated Fluids in Deviated Wells, in: IADC/SPE Drilling Conference. Dallas, Texas, U.S.A., 2 – 4 March. <https://doi.org/10.2118/87180-MS>
- Capo, J., Yu, M., Miska, S.Z., Takach, N., Ahmed, R., 2004. Cuttings Transport with Aqueous Foam at Intermediate Inclined Wells, in: SPE/ICoTA Coiled Tubing Conference and Exhibition. Houston, Texas, U.S.A. <https://doi.org/10.2118/89534-MS>
- Chen, Z., Ahmed, R.M., Miska, S.Z., Takach, N.E., Yu, M., Pickell, M.B., Hallman, J.H., 2007. Experimental Study on Cuttings Transport With Foam Under Simulated Horizontal Downhole Conditions. SPE Drill. Complet. 22, 304–312. <https://doi.org/10.2118/99201-PA>
- Duan, M., Miska, S., Yu, M., Takach, N.E., Ahmed, R.M., Hallman, J.H., 2010. Experimental Study and Modeling of Cuttings Transport Using Foam With Drillpipe Rotation. SPE Drill. Complet. 25, 352–362. <https://doi.org/10.2118/116300-PA>
- Ford, J.T., Peden, J.M., Oyenyin, M.B., Gao, E., Zarrouh, R., 1990. Experimental Investigation

- of Drilled Cuttings Transport in Inclined Boreholes, in: SPE Annual Technical Conference and Exhibition. pp. 197–206. <https://doi.org/10.2118/20421-MS>
- Garcia-Hernandez, A.J., Miska, S.Z., Yu, M., Takach, N.E., Zettner, C.M., 2007. Determination of Cuttings Lag in Horizontal and Deviated Wells, in: SPE Annual Technical Conference and Exhibition. Anaheim, California, U.S.A., 11–14 November. <https://doi.org/10.2118/109630-MS>
- Hemphill, T., Ravi, K., 2006. Pipe Rotation and Hole Cleaning in an Eccentric Annulus, in: IADC/SPE Drilling Conference. Miami, Florida, U.S.A., 21–23 February. <https://doi.org/10.2118/99150-MS>
- Larsen, T.I., Pilehvari, A.A., Azar, J.J., 1997. Development of a New Cuttings-Transport Model for High-Angle Wellbores Including Horizontal Wells. SPE Drill. Complet. 12, 129–136. <https://doi.org/10.2118/25872-PA>
- McCann, R.C., Quigley, M.S., Zamora, M., Slater, K.S., 1995. Effects of High-Speed Pipe Rotation on Pressures in Narrow Annuli. SPE Drill. Complet. 10, 96–103. <https://doi.org/10.2118/26343-PA>
- Naganawa, S., Nomura, T., 2006. Simulating Transient Behavior of Cuttings Transport Over Whole Trajectory of Extended Reach Well, in: IADC/SPE Asia Pacific Drilling Technology Conference and Exhibition. Bangkok, Thailand, 13-15 November. <https://doi.org/10.2118/103923-MS>
- Ozbayoglu, E.M., Osgouei, R.E. et al., 2012. Hole-Cleaning Performance of Gasified Drilling Fluids in Horizontal Well Sections. SPE J. <https://doi.org/10.2118/131378-PA>

- Ozbayoglu, M.E., Saasen, A., Sorgun, M., Svanes, K., 2008. Effect of Pipe Rotation on Hole Cleaning for Water-Based Drilling Fluids in Horizontal and Deviated Wells, in: IADC/SPE Asia Pacific Drilling Technology Conference and Exhibition. Jakarta, Indonesia. 25–27 August. <https://doi.org/10.2118/114965-MS>
- Raza, S., Zahid, A.A., Hasan, A., Hassan, I., 2019. Experimental Investigation of Volume Fraction in an Annulus Using Electrical Resistance Tomography. SPE J. 1–10. <https://doi.org/10.2118/194211-PA>
- Sifferman, T.R., Myers, G.M., Haden, E.L., Wahl, H.A., 1973. Drill Cuttings Transport in Full Scale Vertical Annuli, in: 48th Annular Fall Meeting of the Society of Petroleum Engineers of AIME. Las Vegas, 30 Sept- 3 Oct. <https://doi.org/10.2118/4514-MS>
- Sorgun, M., Aydin, I., Ozbayoglu, M.E., 2011. Friction Factors for Hydraulic Calculations Considering Presence of Cuttings and Pipe Rotation in Horizontal/Highly-Inclined Wellbores. J. Pet. Sci. Eng. 78, 407–414. <https://doi.org/10.1016/j.petrol.2011.06.013>
- Tomren, P.H., Iyoho, A.W., Azar, J.J., 1986. Transport in Directional Wells. SPE Drill. Eng. 43–56.
- Zahid, A.A., ur Rehman, S.R., Rushd, S., Hasan, A., Rahman, M.A., 2018. Experimental investigation of multiphase flow behavior in drilling annuli using high speed visualization technique. Front. Energy 13–17. <https://doi.org/10.1007/s11708-018-0582-y>

Chapter 4 : Investigation of Cuttings Transport in a Horizontal Well with High-Speed Visualization and Electrical Resistance Tomography Technique

Mohammad Mojammel Huque¹, Mohammad Azizur Rahman², Sohrab Zendehboudi¹, Stephen Butt¹, and Syed Imtiaz^{1*}

¹Memorial University, St. John's, NL, Canada

²Texas A&M University at Qatar

*email: simtiaz@mun.ca

ABSTRACT

In a horizontal well drilling operation, a part of generated drill cuttings tends to settle down at a lower annular section. Formation of sand bed causes several operational issues such as low rate of penetration and stuck drill pipe. In this study, a lab-scale experimental work is carried out to investigate hole cleaning in the extended reach and horizontal drilling operation. This work focuses on the visualization of the flow behavior of drill cuttings in the horizontal annular section. A 6.16 m-long horizontal well test section with an outer diameter of 4.5 inch (11.43 cm) and an inner diameter of 2.5 inch (6.35 cm) is used in this study. Four non-Newtonian Herschel-Bulkley fluids are tested as the drilling mud. Solid glass beads of 2.5-3.0 mm with a density of 2650 kg/m³ are utilized as the drill cuttings with two different solid concentrations. The flow behavior in the horizontal annular section is analysed with a high-speed imaging technology at 2000 frames/second and electrical resistance tomography (ERT) technique. The effects of fluid rheology, fluid velocity, drill pipe rotation, and eccentricity on the cuttings transport are investigated. This study showed that an optimum drill pipe rotation of 80 RPM and a minimum transport performance number (TPN) of 70 is required for efficient hole cleaning in horizontal well section. This study also reveals that fluid rheology has a significant effect on the minimum

transport velocity (MTV). A flow regime analysis revealed that a turbulent flow regime is required for effective hole cleaning without sand bed formation. The mechanistic three-layer model of cuttings transport is experimentally verified with high-speed visualization techniques. Furthermore, this study introduces the concept of estimating the instantaneous annular solid volume fraction by the ERT system as well as visualization of solid bed distribution in the annulus section.

Keyword: Cutting transport; Horizontal drilling, Sand bed formation; High-speed visualization; Electrical resistance tomography; Minimum transport velocity.

4.1 Introduction

Horizontal and extended reach well have widened the capability of exploring the key geological formations and improving the productivity of reservoirs. An extended reach well has a long horizontal section, which differs significantly from a conventional vertical well. Since a horizontal well has access to a larger section in the reservoir, it can offer substantial enhanced production compared to a vertical well. In general, horizontal well are high-angle wells (inclination greater than 85°) drilled to enhance reservoir performance in terms of greater exposure to pay zone, higher production rate and reduced pressure drop around the wellbore. Horizontal well trajectories are complicated and cuttings transport from a horizontal well is substantially complex from the vertical well (Eren and Polat, 2020; Huanget al., 2020; Muecke et al., 2018; Wang et al., 2019). Designing an extended reach well (ERW) or horizontal well always associated with challenges in all aspects such as bottom hole assembly (BHA) design, equivalent circulation density (ECD) optimization, casing design, trajectory planning, and hole cleaning (Asef Hashmi et al., 2020). In recent decades, there is significant improvement in horizontal well drilling operation that can drill even thousand meters of horizontal section with improved fluid rheology, advanced drilling tools and engineering

expertise(Abbas et al., 2014; Aladsani et al., 2018; Asef Hashmi et al., 2020; Kenupp et al., 2017; Miguel et al., 2015). However, despite of technological advancement, drilling industry still experiencing hole cleaning issue in the horizontal and highly deviated well (Bulgachev and Pouget, 2006; Czuprat et al., 2020; Vadinal et al., 2019; Vanpuymbroeck, 2013).

The success of extended reach drilling is greatly affected by the cuttings transport mechanism. In horizontal wells, generated cuttings tend to deposit in the lower side of the annular section as shown in **Figure 4-1**. Cuttings generated in the bottomhole must be carried to the surface by appropriate drilling fluids. A poor cleaning of solid cuttings leads to build up of a stationary cuttings bed. Development of a stationary solid bed often cause some operational issue such as excessive torque and drag, low rate of penetration, stuck pipe, lost circulation and loss off well control(Bilgesu et al., 2002; Bradley et al., 1991; Brown et al., 1989; Gulrud et al., 2009; Ozbayoglu et al., 2012, 2003; Rodriguez Corredor et al., 2016). As a remedial action, drilling operation need to be ceased intermittently for a dedicated hole cleaning operation with an increase in non-productive time.

Cuttings transport in the annular section is complicated process with many parameters involved such as fluid rheology, drill pipe rotation, flow rate, cuttings size, inclination. The hydrodynamic behaviors of solid cuttings and drilling mud transport through annulus represent a multiphase flow behavior that has been analyzed through experimental work, mechanistic modeling, and computational fluid dynamics simulation studies. Tomren et al. (1986) first experimentally investigated cuttings transport in the directional well and unveiled the problem of cuttings bed formation in inclined/non-vertical wells. Their study showed that a cuttings bed is formed in the inclined well even at high flow rates in the annulus. Later, a number of experimental studies (Ford et al., 1990; Martin et al., 1987; Masuda et al., 2000; Okrajni and Azar, 1986; Peden et al., 1990;

Sanchez et al., 1997; Sifferman and Becker, 1992; Walker and Li, 2000) were performed in the directional well to investigate the effects of fluid rheology, drill pipe rotation, fluid velocity, and eccentricity on the cuttings transport.

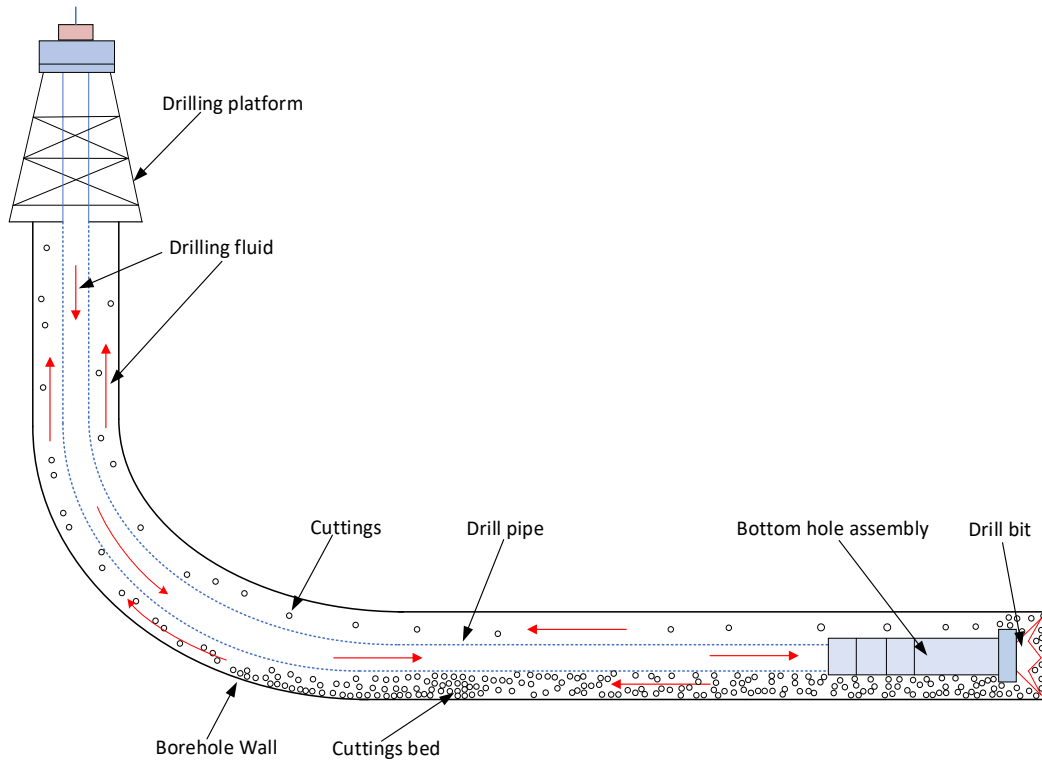


Figure 4-1: Schematic of cuttings transport in horizontal well

With the advancement of extended reach well drilling in the petroleum industry, researchers further studied cuttings transport in the horizontal or near horizontal well (Chen et al., 2007; Duan et al., 2008b; Garcia-Hernandez et al., 2007; Kelessidis et al., 2007; Kelessidis and Bandelis, 2004; Ozbayoglu et al., 2008; Pilehvari et al., 2007; Yu et al., 2007). These experimental tests revealed that the fluid rheology plays a significant role in cuttings transport in horizontal wells similar to the inclined wells; and these studies recommended a turbulent flow regime for effective hole cleaning. Several other studies (Chen et al., 2007; Cho et al., 2000a; Dabirian et al., 2016; Duan et al., 2009; Garcia-Hernandez et al., 2007) investigated the critical deposition velocity and minimum

transport velocity (MTV) in horizontal. Chen et al.(2007) reported that cuttings accumulated in the annular section are not sensitive to flow velocity until a minimum velocity is reached. Ozbayoglu et al. (2008) concluded that drill pipe rotation has a significant impact on hole cleaning in horizontal wells and it reduces the minimum transport velocity (MTV).

Garcia-Hernandez et al. (2007) described that the solid transport capability of the moving layer is a resultant of three mechanisms: rolling, saltation, and suspension. They also revealed that a significant percentage of the solid bed in horizontal section is transported by a moving layer, and the solid concentration of the moving layer is much higher than solid in a suspended layer. Doron and Barnea (1996, 1993) investigated solid-liquid flow patterns in horizontal section through mechanistic model, experimental studies, and flow regime map. They proposed a 3-layer model including a stationary solid bed, a sliding bed, and heterogeneous suspension. Kamp et al. (1999) and Masuda et al., (2000) proposed a two-layer mechanistic model consisting of a moving bed of packed solid cuttings and a heterogeneous solid mud and cuttings.

Though there are few mechanistic models proposed for cuttings transport in horizontal well, there are no adequate systematic experimental studies with visualization techniques to verify “Three-Layer” and “Two-Layer” flow regimes in a horizontal well. Few of past studies (Cho et al., 2000b, 2000a; Dabirian et al., 2016, 2015; Fajemidupe et al., 2019; Gul et al., 2017; Kelessidis and Mpandelis, 2003; Li and Luft, 2014; Nguyen and Rahman, 1998; Zhu et al., 2010) reported the flow pattern, however, a systematic experimental visualization of two-layer and three-layer model of cuttings transport is still missing. Thus, a detailed investigation of flow behavior through visualization methods is essential to further understand the flow patterns in the horizontal annular section. An appropriate visualization technique can identify the different layers of cuttings, solid movement pattern, and flow regimes in the annulus section. Few researchers (Fajemidupe et al.,

2019; Kelessidis et al., 2007; Kelessidis and Bandelis, 2004; Kelessidis and Mpandelis, 2003; Li and Luft, 2014; Philip et al., 1998) reported a few images of two-layer and three-layer models with experimental visualization. However, due to poor image resolution, the movement pattern of solid cuttings was indistinguishable.

This manuscript focuses on a comprehensive experimental study of cuttings transport in a horizontal well with an advanced visualization approach to identify different cuttings transport mechanisms proposed in the literature. A high-speed camera is employed to track the cuttings in the annular section and precisely identify the different layers of cuttings such as stable bed, rolling bed, and suspended cuttings.

In addition to the visualization of cuttings transport, this study uses the electrical resistance tomography (ERT) analysis to investigate the effect of drilling parameters on cuttings transport performance. The result from the ERT analysis is used for parametric study to show the impact of each drilling parameters. Experimental data obtained from this study is used to generate a flow regime analysis for cuttings transport behavior. This study also explores the effect of fluid rheology, eccentricity, and flow regimes on cuttings transport in the horizontal well. This study also assesses (and validates) some of the previous findings obtained from the mechanistic models.

This manuscript is organized as follows: **Section 4.2** covers a brief overview of experimental methods; this section also contains instrumentation, fluid rheology, and design of experiments. **Section 4.3** includes the result obtained from high-speed video camera, ERT system, and a flow regime analysis. **Section 4.4** summarizes the main remarks/findings of this study.

4.2 Materials and Methods

4.2.1 Flow Loop

An extensive experimental work is carried out in the multiphase flow loop located in the Texas A & M University at Qatar (TAMUQ). The test section consists of a 6.16-meter-long annulus system with a transparent acrylic outer pipe and an aluminum inner pipe. The diameter of the outer pipe is 4.5 inch (ID), and the inner pipe is 2.5 inch (OD). The aluminum inner pipe can be placed in both concentric and eccentric conditions with respect to the outer pipe. The inner pipe can also be rotated up to 150 RPM for any eccentric condition. A simplified schematic of the test section is illustrated in **Figure 4-2**.

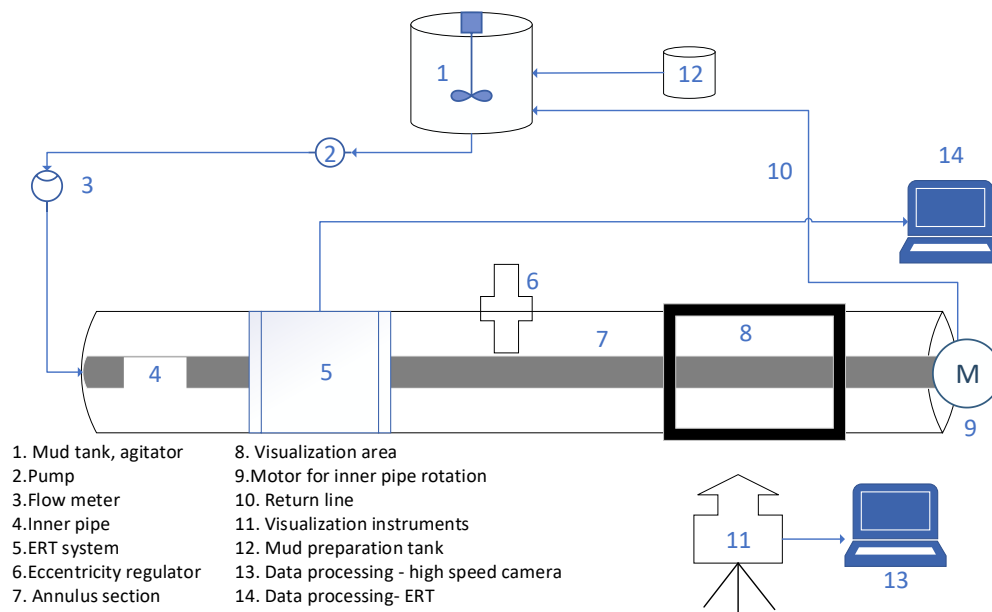


Figure 4-2: TAMUQ multiphase flow loop experimental schematic

The experiment starts with filling the mud tank with an appropriate drilling fluid and solid cuttings. The slurry is then pumped into the test section, where it passes through the ERT system and visualization section. Finally, this slurry returns to the mud tank and ends an experimental run.

A simple workflow of the complete experimental work is shown in **Figure 4-3** with six major tasks involved. The experiment begins with the fluid rheology test, mud preparation and experimental design. Experimental matrix is designed for different drill pipe rotation, eccentricity, flow rate, fluid rheology and input solid concentration.

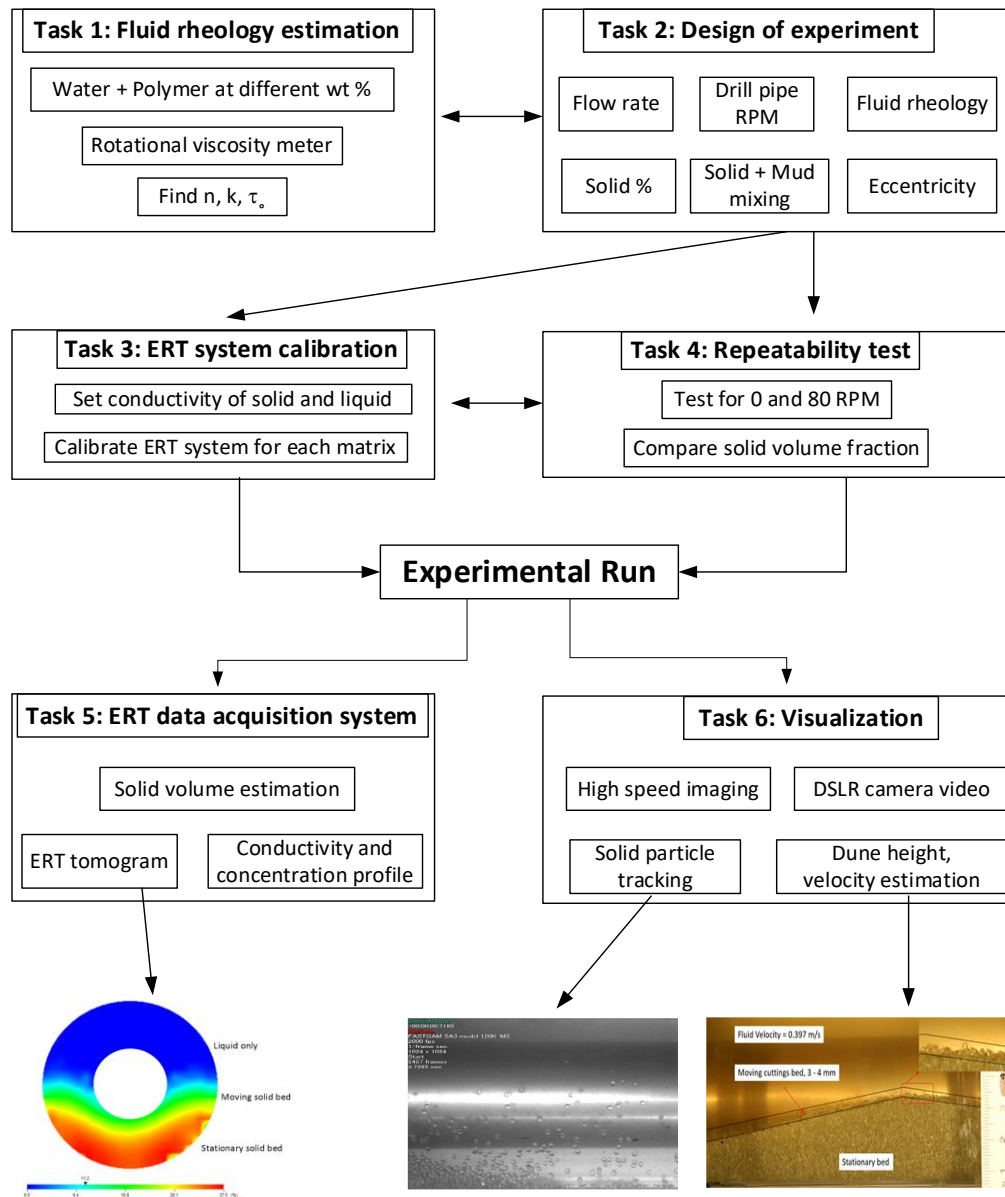


Figure 4-3: Experimental workflow

Several repeatability tests were performed to check the consistency of the experiments. For each change in annular configuration and fluid rheology, ERT system was calibrated. Experimental data were collected by three different channels as a DSLR camera, a high-speed camera and ERT system.

4.2.2 Instrumentation

The setup is equipped with visualization and analysis tools, as described below:

- i. The instantaneous solid volume fraction is estimated and visualized by the ERT system. Detailed description of the ERT system is provided in the next subsection.
- ii. Solid bed height and dune moving velocity are determined using a DSLR camera.
- iii. Solid particle movement pattern is investigated using a high-speed imaging video camera. This camera captures images at 2000 frame per second for this experimental study.
- iv. Fluid rheology were estimated by a rotational viscosity meter.

Solid volume percentage estimation with ERT system. In this experimental study, the modern electrical resistance tomography (ERT) system is used to measure the in-situ solid volume fraction while running an experiment. The ERT principle is to detect any change in electrical voltage from the periphery of a pipe or annular system. Simultaneously, it converts this change in electrical voltage into a meaningful electrical signal, which can be later translated into physical measurements such as conductivity, concentration, and resistivity of the flowing materials inside the pipe or annulus section (Huque et al., 2020b). The ERT system can be applied to the multiphase flow system to visualize the flow behavior of a secondary solid phase in the presence of a primary flowing liquid. The ERT system allows the use of conductivity-concentration model through the Maxwell equation as given below (Beck and Williams, 1995):

$$\alpha = \frac{2\sigma_1 + \sigma_2 - 2\sigma_{mc} - \frac{\sigma_{mc}\sigma_2}{\sigma_1}}{\sigma_{mc} - \frac{\sigma_2}{\sigma_1}\sigma_{mc} + 2(\sigma_1 - \sigma_2)} \quad (4-1)$$

where α is the volume fraction of the dispersed material; σ_1 refers to the conductivity of the continuous phase, mS/cm; σ_2 represents the conductivity of the dispersed phase, mS/cm; and σ_{mc} is the reconstructed measured conductivity, mS/cm.

For a non-conducting solid material, Equation (4-1) can be simplified into the following form:

$$\alpha = \frac{2\sigma_1 - 2\sigma_{mc}}{\sigma_{mc} + 2\sigma_1} \quad (4-2)$$

When the conductivity is estimated for the system using Equation (4-2), the concentration or volume fraction of the secondary phase can be calculated. The ERT system continuously monitors the electrical conductivity of the primary fluid phases passing through the test section. In this experimental study, drilling mud is the primary phase and solid glass beads (as the secondary phase) are used to simulate the cuttings behavior. The conductivity values are set to 0.1 mS/cm (measured in the laboratory) and 0 mS/cm for the liquid phase and solid phase, respectively. A simple method of secondary phase estimation is explained **Figure 4-4**.

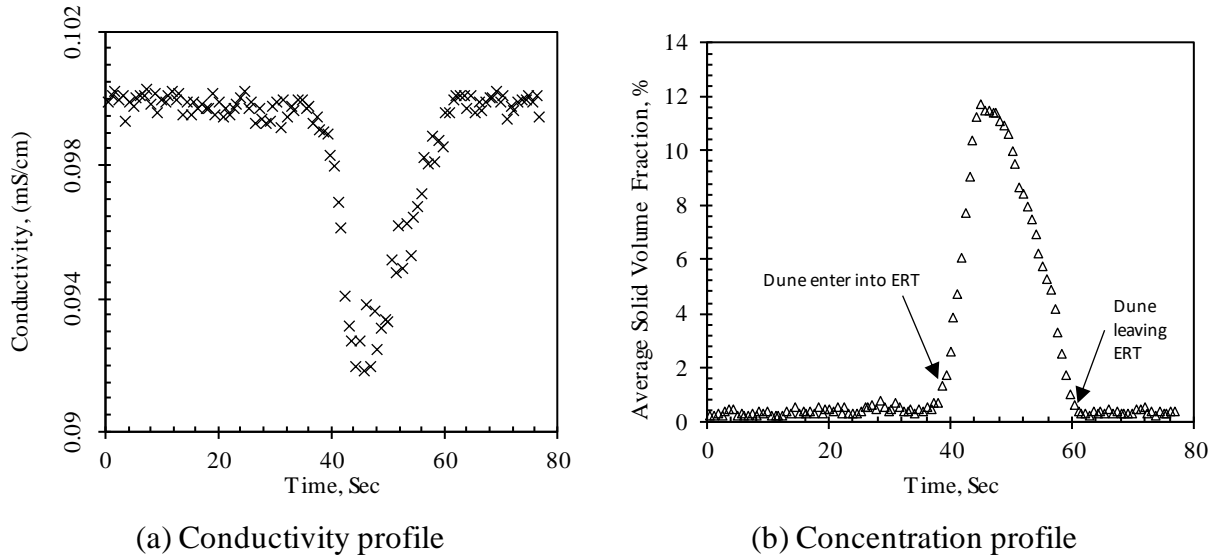


Figure 4-4: ERT output

Figure 4-4 (a) shows that conductivity remains almost constant up to 35 seconds from the beginning of the measurement where no solid dune enters into the ERT system. When a solid dune passes the ERT system, the overall conductivity of the two-phase mixture gradually decreases in the system as depicted in **Figure 4-4** (a) from the time of 35 to 65 seconds with an inverted bell shape trend of conductivity. This is due to the higher volume of non-conductive solid glass beads passing the ERT section, which reduces the overall conductivity of the system under investigation. Once the solid dune left the ERT system, the conductivity again increases to the base level. The corresponding average instantaneous solid volume fraction against time is illustrated in **Figure 4-4** (b). The area under the bell shape curve in **Figure 4-4** (b) gives the annular solid volume fraction of the cuttings for a particular experiment.

ERT Tomography. The ERT system generates a color 2-D plot showing stationary cuttings bed region, liquid region, and interphase of the solid and liquid regions. The interface is represented by a moving cuttings bed in the test section. A visual representation of the three-layer cuttings transport model from the ERT system is illustrated in **Figure 4-5**. Solids settling in the lower

annular section at a higher concentration indicates a stationary bed by a red contour. The green contour shows a lower concentration of solids, which demonstrates a moving cuttings bed. The blue color represents a cuttings free mud in the annulus.

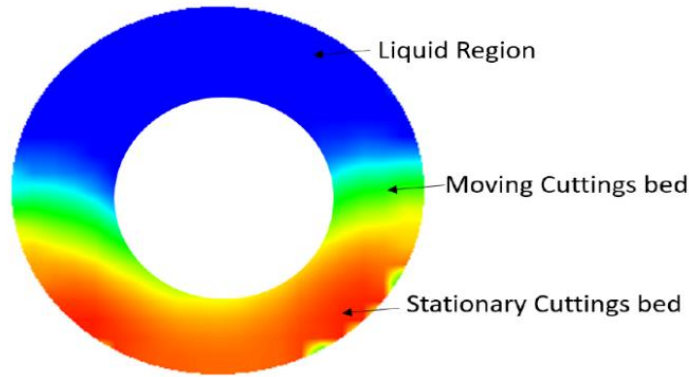


Figure 4-5: ERT concentration tomogram

4.2.3 Fluid Rheology Analysis

A commercial grade biopolymer (Xanthan Gum) with different concentrations is used to prepare different non-Newtonian fluids FZ 1, FZ 2, FZ 3, and FZ 4. Fluid rheology was tested in the laboratory with a lab scale rotational viscosity meter. Shear stress vs. shear rate curve for all four fluids are shown in **Figure 4-6**.

All four fluids follow a power-law trend with an intercept at shear stress axis, showing a non-Newtonian Herschel-Bulkley fluid behavior. A Herschel-Bulkley fluid is expressed as follows:

$$\tau = \tau_o + k\dot{\gamma}^n \quad (4-3)$$

where τ is the shear stress; $\dot{\gamma}$ stands for the shear rate; τ_o refers to the yield stress of the fluid; k is known as a consistency index; and ' n ' introduces the flow behavior index.

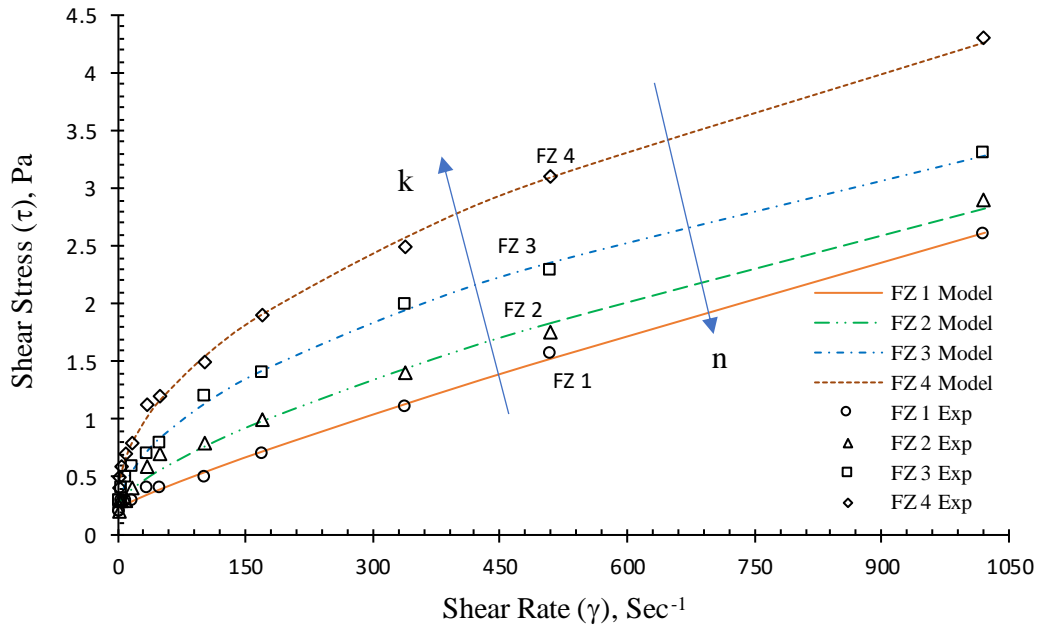


Figure 4-6: Shear stress vs. shear rate behavior for fluids FZ 1, FZ 2, FZ 3 and FZ 4

Table 4-1: Summary of fluid rheology tests

Fluid Properties	FZ 1	FZ 2	FZ 3	FZ 4
Polymer Concentration (wt./wt.), %	0.050	0.075	0.100	0.125
Yield Stress, τ_0 (pa)	0.229	0.234	0.269	0.308
Consistency Index, k (Pa-s ⁿ)	0.005	0.020	0.064	0.116
Flow Behavior Index, n	0.878	0.702	0.557	0.510
R^2	0.997	0.998	0.999	0.999

The summary of the curve fitting model and fluid rheology is reported in **Table 4-1** and the respective models are plotted in **Figure 4-6**. A comparative analysis of fluid rheology shows that the fluid yield stress and consistency index gradually increase with an increase in polymer concentration, but the flow behavior index decreases, implying more non-Newtonian behavior.

4.2.4 Design of Experiment

The experiments are conducted with four different fluids (e.g., FZ 1, FZ 2, FZ 3 and FZ 4) and two different solid weight concentrations (e.g., 4% and 8%). Spherical solid glass beads with a size ranging from 2.5 mm to 3.0 mm are employed as the cuttings in this experimental work. The

density of the glass beads is about 2650 kg/m³. A 4% solid by weight is used in the first experimental matrices (Matrix 1, 2, 3, and 4 in **Table 4-2**) which corresponds to a penetration rate of 85 ft/hr. For the second phase, 8% solid (w/w) is used, corresponding to a rate of penetration of 170 ft/hr. The rate of penetration is estimated as follows (Larsen et al., 1997):

$$ROP \left(\frac{ft}{hr} \right) = Q_{inj} \left(\frac{ft^3}{sec} \right) \left(\frac{3600 \text{ sec}}{hr} \right) \left(\frac{1}{A_{hole} \text{ ft}^2} \right) \quad (4-4)$$

where ROP represents the rate of penetration; Q_{inj} is the volumetric injection of solid; and A_{hole} denotes the area of the hole during a drilling operation.

Table 4-2: Matrix of experimental tests

Matrix No	Fluid Name	Solid %	Drill Pipe Rotation	Mud velocity, (m/s)	Eccentricity	Number of Experiments	Range of Re
1	FZ 1	4%	0, 40, 80, 120	0.397, 0.482, 0.571, 0.651, 0.717, 0.818	0, 0.3, 0.6	72	2630-8260
2	FZ 3	4%	0, 40, 80, 120	0.397, 0.482, 0.571, 0.651, 0.717, 0.818	0, 0.3, 0.6	72	1853-5695
3	FZ 2	4%	0, 40, 80, 120	0.571, 0.651, 0.717, 0.818	0, 0.3, 0.6	48	3282-4695
4	FZ 4	4%	0, 40, 80, 120	0.651, 0.717, 0.818	0, 0.3, 0.6	36	1939-2790
5	FZ 4	8%	0, 40, 80, 120	0.651, 0.717, 0.818	0, 0.3	24	1939-2790
6	FZ 1	8%	0, 40, 80, 120	0.651, 0.717, 0.818	0, 0.3	24	5790-8206
7	FZ 2	8%	0, 40, 80, 120	0.651, 0.717, 0.818	0, 0.3	24	4020-5695
8	FZ 3	8%	0, 40, 80, 120	0.651, 0.717, 0.818	0, 0.3	24	2685-3852

Mud velocity was calculated neglecting the solid volume and assuming that the annular space is completely filled with mud ($velocity = \frac{volumetric \text{ flow rate}}{Annular \text{ area}}$). Slurry pump can operate as low as 500 RPM which is equivalent to a flow rate of 165 LPM (\approx 44 GPM) and corresponding mud velocity is 0.397 m/s. Other mud velocities were set for different slurry pump rate at 100 RPM interval from 500 RPM to 1000 RPM. For each experimental matrix, four inner pipe rotational condition were used 0, 40, 80 and 120 RPM. Where a 0 RPM corresponds to a stationary inner pipe condition. Three different eccentric conditions (0, 0.3, 0.6) were chosen for this study. Due to higher amount of solid content in matrix, eccentricity was limited to 0.3 for experimental matrix

5 – 8. Reynolds number were calculated for Herschel Bulkley fluid for annular flow proposed by Tang et al., (2016). Details of Reynolds number calculation is presented in section 3.5.

4.2.5 Repeatability Tests

Several repeatability tests were performed to check the deliverability of the mud pump and the mixing capability of the agitator at different operating conditions. Fluid FZ 1 with a flow rate 270 LPM (\approx 71 GPM) is tested for the repeatability test in the horizontal well configuration with the stationary inner pipe and a drill pipe rotation of 80 RPM. The input solid fraction is estimated as 4% (wt./wt.), which corresponds to a volume fraction of 1.51% (vol./vol.). The solid volume fraction is measured by the ERT system for three successive tests, as reported in **Figure 4-7**.

The magnitudes of standard deviation are 0.077 and 0.0416 for the stationary inner pipe condition and 80 RPM drill pipe rotation, respectively. These low standard deviations indicate that the agitator can deliver a representative solid volume for rest of the experiment.

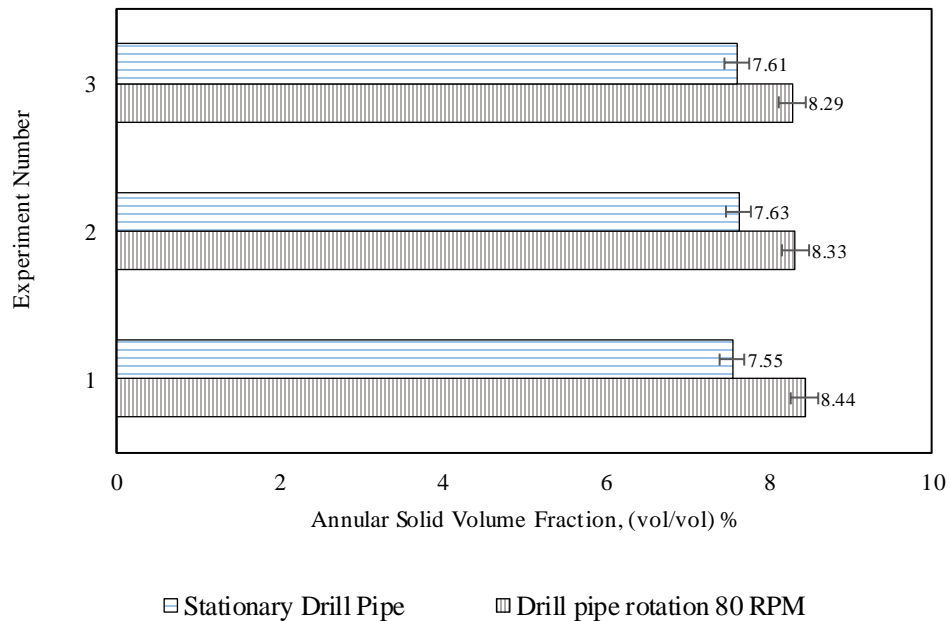


Figure 4-7: Repeatability test results for a slurry pump rate of 270 LPM (\approx 71 GPM)

4.3 Results and Discussion

Experimental observations and results from the DSLR camera, and high-speed video camera images are presented in this section. Also, a summary of ERT analysis for different operating conditions as well as flow regime analysis is provided.

4.3.1 Cuttings Movement Mechanism

The cuttings removal from a stationary bed can be explained by a critical bed shear stress concept (Ozbayoglu et al., 2007). In order to lift a solid particle or cutting from a stationary cuttings bed, a minimum shear stress should be applied on cuttings bed by the fluid. Apart from the fluid velocity and viscosity, cutting lift force is also a function of cuttings size, shape, and solid bed compaction (Kjøsnes et al., 2003). For a highly porous rock and loosely consolidated solid cuttings, a small amount of shear stress is required to remove a single cutting. Thus, it is relatively easy to clean the cuttings deposition. A simple schematic of dune movement in the horizontal section is also depicted in **Figure 4-8**. It shows that solid cuttings from the outer layer of the sand dune is transported by the rolling mechanism at low mud velocity. A cross sectional schematic of a three-layer cuttings transport model is depicted in **Figure 4-9** with a stationary bed, a moving dune, and a cutting free zone.

In contrary, for a well packed and densely consolidated cuttings bed, solid cuttings are attached together by internal cohesive forces. Thus, a higher shear stress is required to break the cohesive forces and roll the solid cuttings. Moreover, drilling mud shows certain gel strength. The gel formation increases the tendency of solid cuttings bonding. High gel strength increases the particle-particle bonding forces (Saasen and Løklingholm, 2002). In this case, a higher shear stress is required to break the gel strength and erode the solid bed.

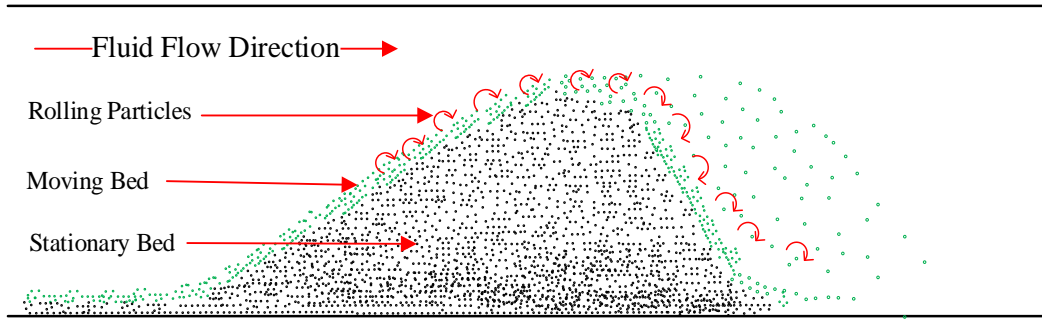


Figure 4-8: Front view of schematic of dune movement in a horizontal section

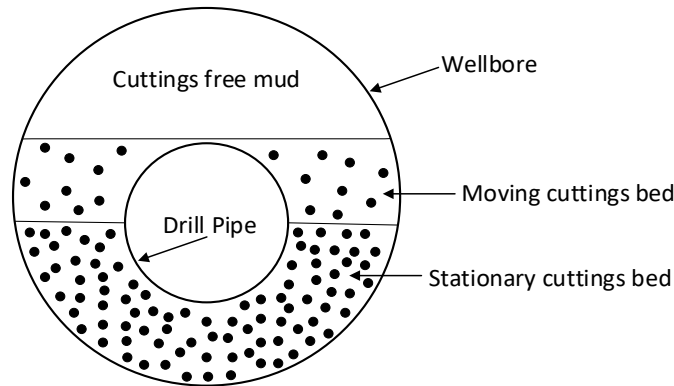


Figure 4-9: A cross-sectional view of three-layer model of cuttings transport

4.3.2 Analysis of High-Speed Video Images

Fluid rheology effect. This section presents the solid transport behaviors for fluid FZ 1, FZ 2, FZ 3, and FZ 4 based on the images taken by the high-speed camera (see **Figure 4-10**). All images shown in **Figure 4-10** are obtained for a slurry pump rate of 270 LPM (\approx 71 GPM) and an inner pipe rotation of 80 RPM.

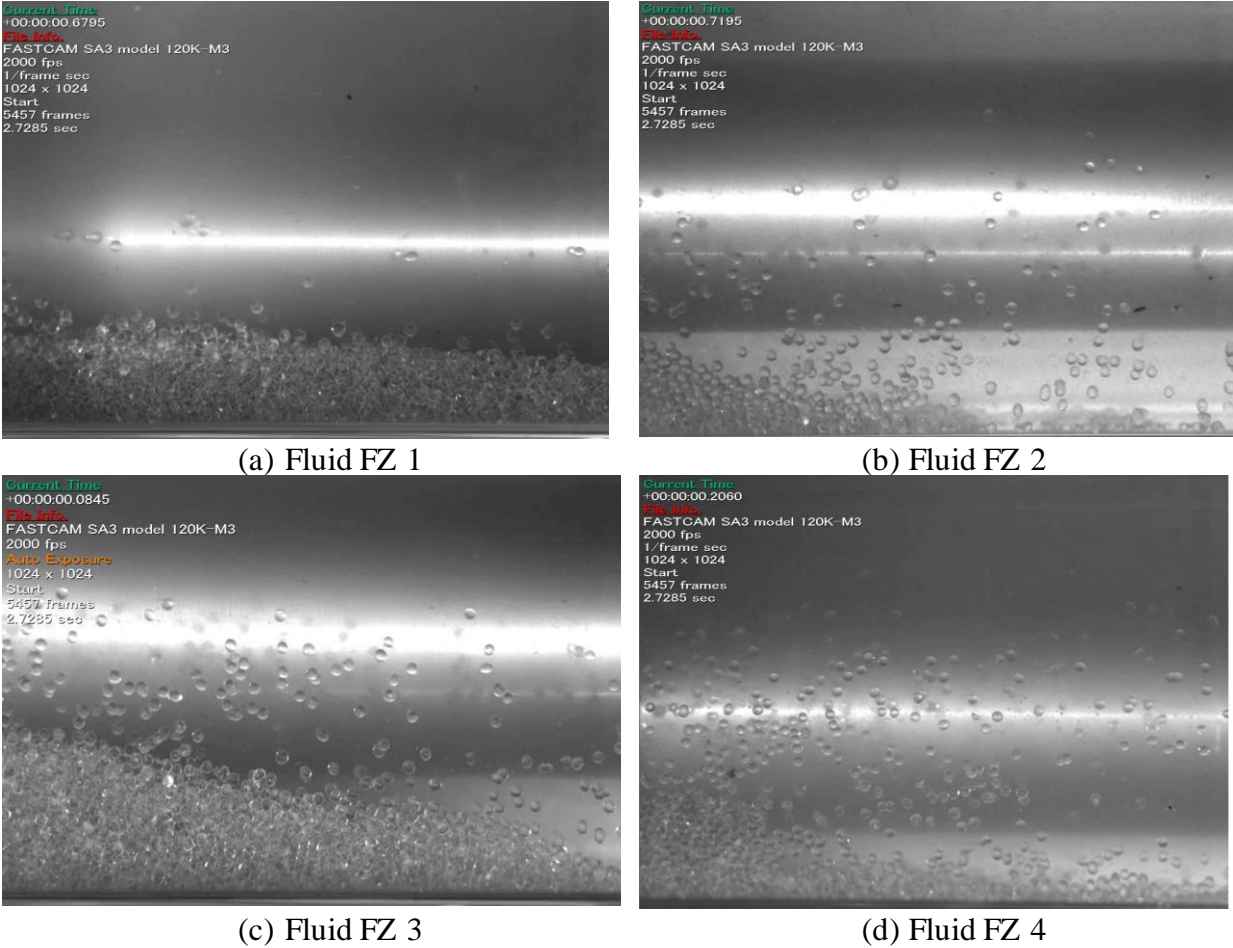


Figure 4-10: Visualization of the high-speed camera for different fluid rheology.

Increasing the fluid viscosity shows a higher solid content in a suspended form in the mud

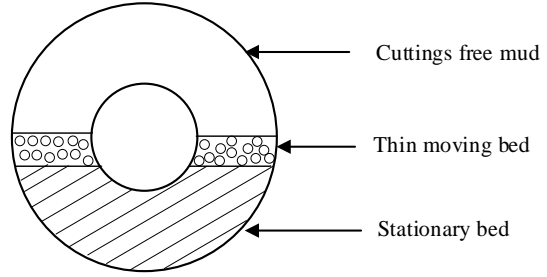
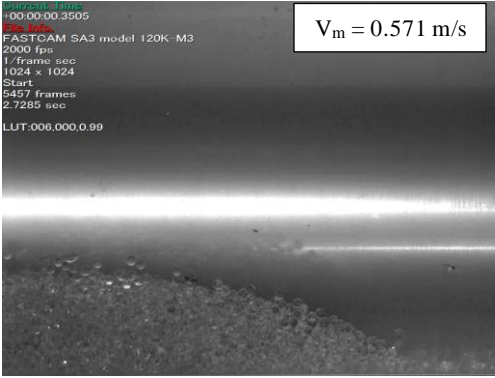
$$(\mu_{FZ1} < \mu_{FZ2} < \mu_{FZ3} < \mu_{FZ4}).$$

High-speed camera shows that fluid FZ 1 (least viscous) contains a relatively smaller number of solid particles as the dispersed phase. Only a few suspended solids move above the stationary bed region. A gradual increase in the fluid viscosity from FZ 1 to FZ 4 results in a higher amount of dispersed solids in the fluid, as shown in panels (b), (c), and (d) of **Figure 4-10** for fluids FZ 2, FZ 3, and FZ 4, respectively. It should be noted that dispersed solid particles cover almost the entire region of the wellbore for the case of fluid FZ 4.

Fluid velocity effect. **Figure 4-11** illustrates three different images from high-speed camera and corresponding schematic for fluid FZ 2 without inner pipe rotation. At a fluid velocity 0.571 m/s, almost a stationary bed is formed with very few rolling particles, as illustrated in **Figure 4-11** (a). High speed image visualization shows that a very thin layer of rolling solid bed is noticed over the stationary cuttings bed and fluid does not carry any suspended solid particles. This situation is improved with a fluid velocity of 0.651 m/s (see **Figure 4-11** (b)). It follows that the suspended solid portion gradually increases in the annulus section and moves with the drilling mud while leaving a small stationary bed in the annulus.

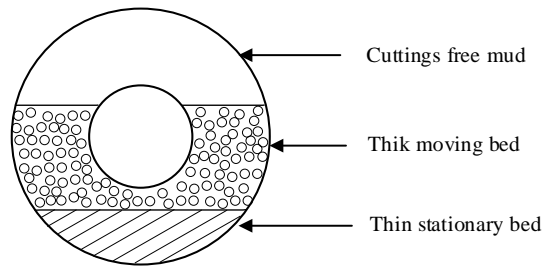
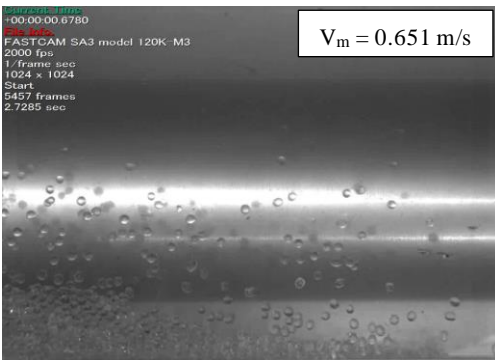
Another important observation is that the suspended solids do not cover the complete annulus section. The phase distribution in the layer is as follows: *a) solid free mud at the top, b) dispersed solids in the middle, and c) stationary solid bed in the bottom*. This confirms the mechanistic three-layer cuttings transport model for the horizontal well.

A further increase in the fluid velocity causes the solid particles to be distributed almost all over the horizontal annulus section, as shown in **Figure 4-11**(c) for the fluid velocity of 0.818 m/s. This scenario also shows the presence of a very thin layer of stationary bed in the annulus. This can be justified by the two-layer cuttings transport model where a large number of suspended solids and a thin stationary bed are observed.



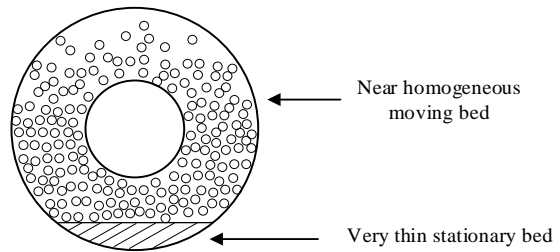
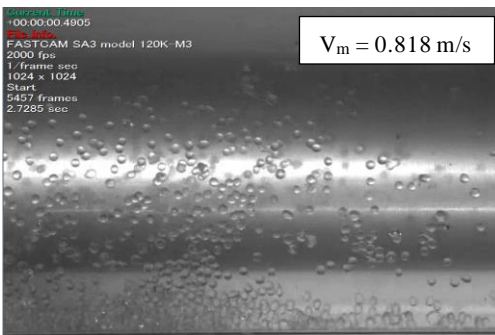
Thin moving layer, thick stationary bed: Three-layer model

(a) $V_m = 0.571 \text{ m/s}$



Thick moving layer, thin stationary bed: Three-layer model

(b) $V_m = 0.651 \text{ m/s}$



Near homogeneous moving bed: Two-layer model

(c) $V_m = 0.818 \text{ m/s}$

Figure 4-11: High-speed camera image and corresponding schematic of three-layer model.

Increasing the fluid velocity results in a higher solid content in the suspended form.

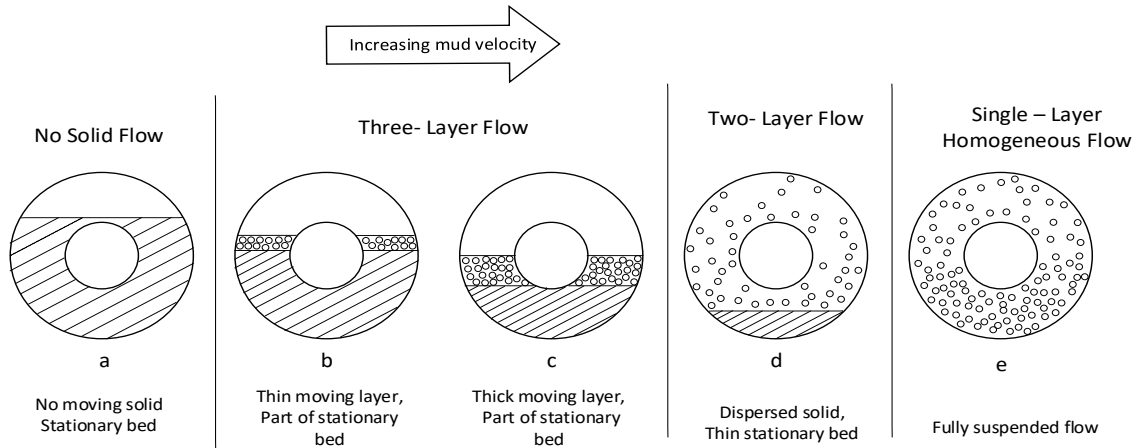


Figure 4-12: Transition of a stationary solid bed to fully suspended flow.

Due to the operational limitation, the experimental study limits the mud velocity upto 0.818 m/s. However, it can be expected that a further increase in the slurry pump rate might lead to an approximately homogeneous distribution of solids in the annulus with no stationary bed in the lower side of the annular section. A conceptual sketch to represent distribution of cuttings in the fluid starting from a stable stationary bed to a single layer homogeneous flow is demonstrated in **Figure 4-12** upon an increase in the mud velocity.

Visualization of particles movement. Solid particles are transported into the horizontal annulus where solid particle is in equilibrium between the drag force by the fluid, gravity force due to the weight of the solid particles, and the lift force. However, inner pipe rotation introduces an additional motion to the fluid, particularly at high eccentric positions (see **Figure 4-13(a)**).

In a highly eccentric condition, the drill pipe is in close contact with the stable solid bed in the lower annular section. Any inner pipe rotation drags some of the solid particles from the lower annular section to the upper annular section where the solid particles can flow with the drilling

mud in the axial direction. The high-speed camera shows a helical motion of solid particles, which is the resultant of the axial motion of drilling mud and a rotational effect of the inner pipe. This might lead to movement of some of the stationary solids from the lower annular section. The helical motion of solid particles is depicted in **Figure 4-13(b)**. This helical motion of flow pattern was previously reported in a horizontal well, but no visual evidence was provided (Garcia-Hernandez et al., 2007).

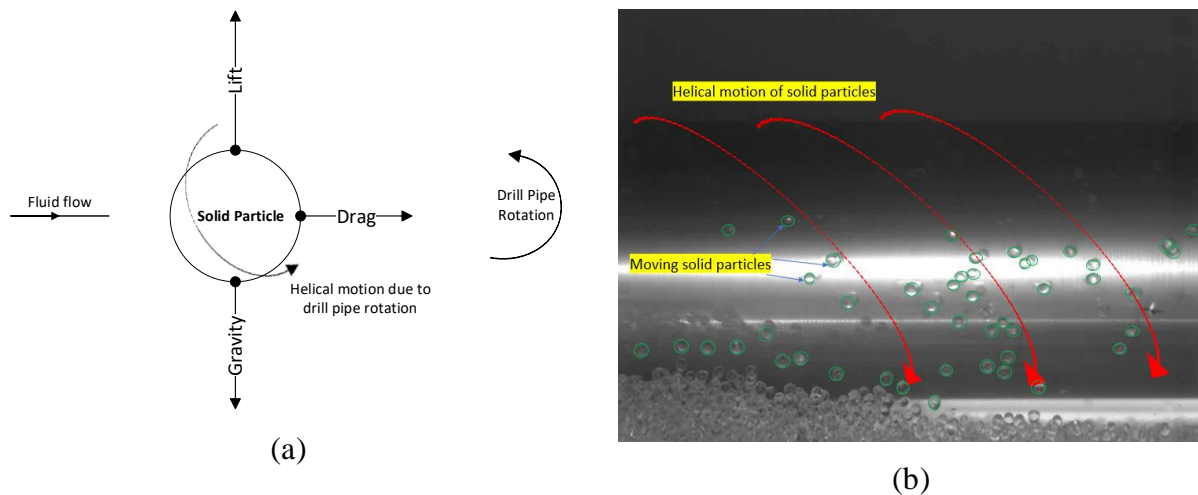


Figure 4-13: Forces acting on solid particles.

(a) Simplified free body diagram showing different forces acting on a solid particle, and (b) Helical motion of solid particles captured from high-speed camera at a drill pipe rotation of 80 RPM.

4.3.3 ERT Analysis

Effect of fluid rheology. The annular solid volume fraction data obtained from the ERT system for all four fluids at various fluid velocities is presented in **Figure 4-14**. Fluid FZ 1 exhibits the highest annular solid percentage (an average 9.5%). A low-viscous fluid generates a higher local velocity compared to a high viscous fluid, which in turn develops a stronger hydrodynamic force near the solid bed. These strong hydrodynamic forces aid in solid transport by rolling and lifting

mechanisms; they eventually help cuttings in moving through the main flow stream of the annular section. However, low- viscous fluid cannot transport the solid particles in suspension for an extended period of time and solid cuttings are re-deposited again. For this reason, a low-viscous fluid like FZ 1 shows a higher amount of annular solid volume fraction for a particular mud velocity as shown in **Figure 4-14** from ERT data.

In contrary, high-viscous fluid shows a high transport capability, it can hold the solid particles for long time and facilitate solid transport by suspension mechanism. For a higher viscous fluid, the solid dune volume is gradually decreased, and it shows as low as 6% for FZ 4 with a mud velocity of 0.818 m/s. It confirms the high solid transport capabilities of viscous fluid at dispersed condition and hence less solid settle down in the annular section. It can be concluded that increasing fluid viscosity facilitates cuttings transport in the annulus section with a higher fluid velocity.

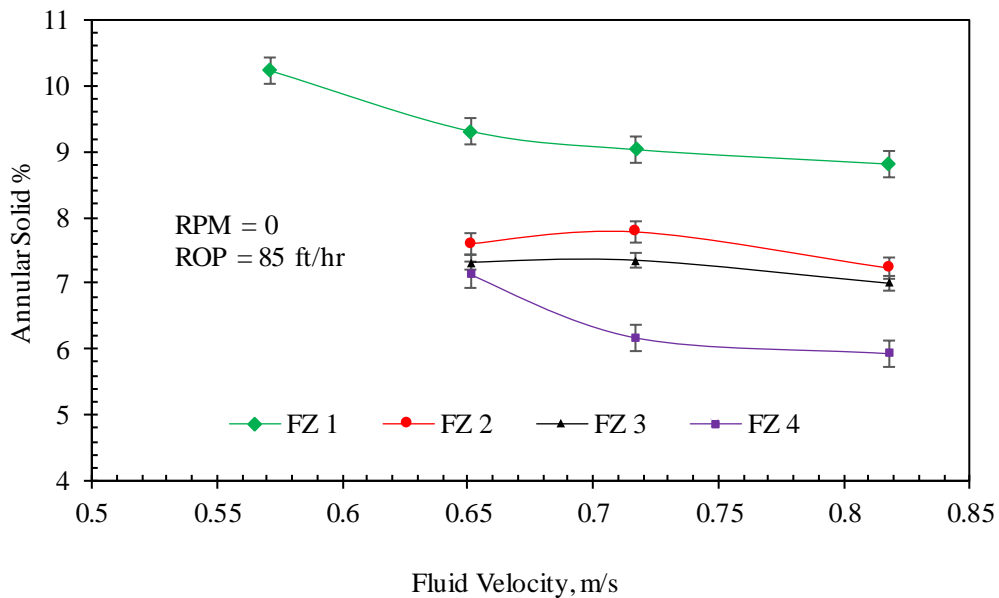


Figure 4-14: Annular solid volume fraction for four different fluids based on ERT data.

Increasing fluid viscosity decreases the solid volume in the sand dune ($\mu_{FZ1} < \mu_{FZ2} < \mu_{FZ3} < \mu_{FZ4}$).

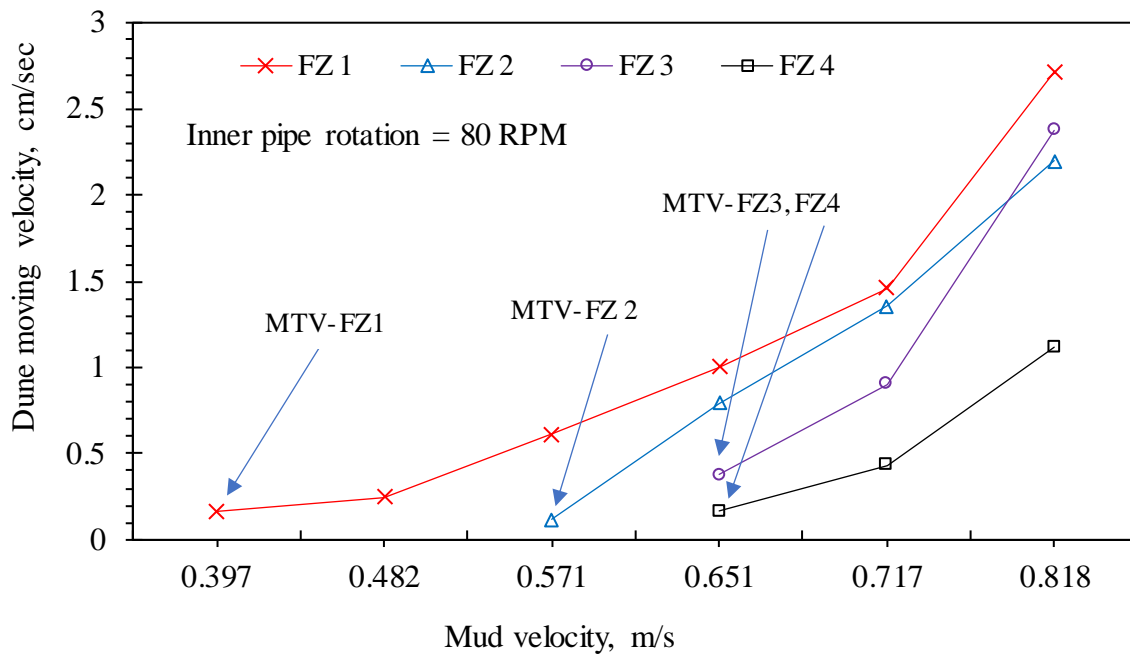


Figure 4-15: Minimum transport velocity (MTV) for different fluids

Increasing fluid viscosity requires a higher MTV ($\mu_{FZ1} < \mu_{FZ2} < \mu_{FZ3} < \mu_{FZ4}$).

Figure 4-15 shows solid dune moving velocity versus mud velocity for all 4 fluids at inner pipe rotation of 80 RPM. For a given mud flow rate, the least viscous fluid (FZ 1) results in the maximum dune movement velocity, whereas the highest viscous fluid (FZ 4) exhibits the lowest dune movement velocity. Fluid FZ 1 shows a slowly moving dune at mud velocity of 0.397 m/s, as depicted in **Figure 4-15**. However, for fluid FZ 2, a long horizontal stationary bed is formed in the entrance of the test section and no moving bed is observed for the mud until mud velocity reach 0.571 m/s. Transport of cuttings by rolling or sliding mechanism along the wellbore requires a drag force that should exceed the gravitational and frictional forces. Hence, 0.571 m/s is the minimum transport velocity (MTV) for the fluid FZ 2. For fluid FZ 3 and FZ 4, no moving dune is observed until the mud velocity reach to 0.651 m/s. Although a higher viscous mud carries more solid cuttings, it requires a higher fluid velocity (or higher MTV) to transport solid cuttings.

Effect of inner pipe rotation on bed thickness. Figure 4-16 shows a comparative study of maximum bed height for different velocities and drill pipe rotation with fluid FZ 1 in a concentric annular condition. It shows that increase in drill pipe rotation decrease the solid bed height significantly for all mud velocities. The most interesting phenomena is that with increase in mud velocity, a slight increase in solid bed height was observed at mud velocity 0.651 m/s and 0.717 m/s for all condition of drill pipe rotations. At comparatively higher mud velocity (0.651 m/s and 0.717 m/s), more solid cuttings are transported as rolling mechanism that makes the bed height high and with a short length, compare to a low mud velocity. Further increase in mud velocity add significant momentum to the solid particles on stationary sand bed and a large portion of solid are transported as suspended or slurry form. For this reason, the maximum solid bed height again decreases at mud velocity 0.818 m/s where solid transport by suspension is more prominent than rolling mechanism.

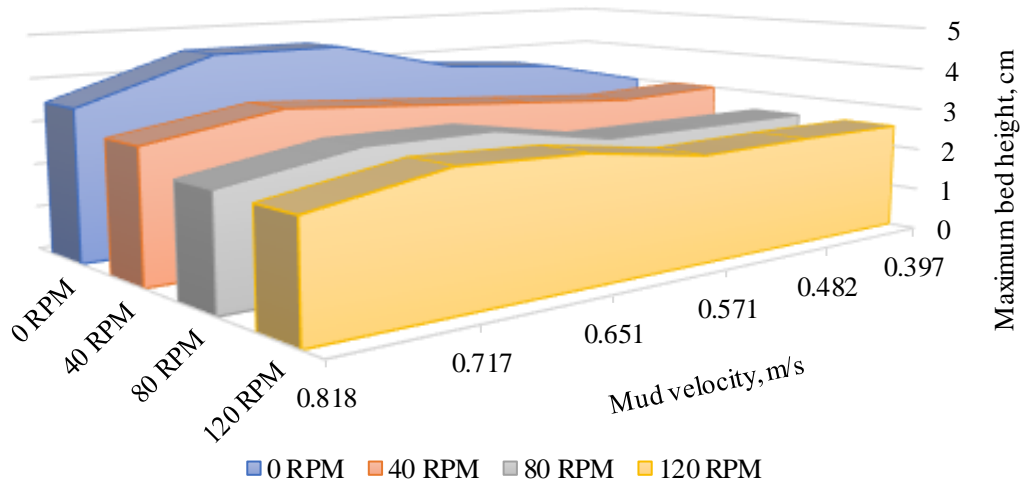


Figure 4-16: Maximum solid bed height for different mud velocities and drill pipe rotation

Effect of fluid rheology on bed thickness. Figure 4-17 shows the variation of dimensionless bed thickness with fluid FZ 1, FZ 2, FZ 3 and FZ 4 at an inner pipe rotation of 80 RPM and different

mud velocities. Fluid FZ 1 shows the highest bed thickness among all four fluids. An increase in fluid velocity gradually decreases the bed thickness for fluid FZ 1. Increasing the fluid viscosity leads to a decreasing trend in the bed thickness for FZ 2, FZ 3, and FZ 4 respectively. This indicates that a viscous fluid can carry more solid cuttings in suspended form. This causes a less bed height in the annular section for a higher viscous fluid. However, no moving dune is observed unless a velocity of 0.65 m/s is reached for fluid FZ 3 and FZ 4. For fluid FZ 1, this is 0.57 m/s.

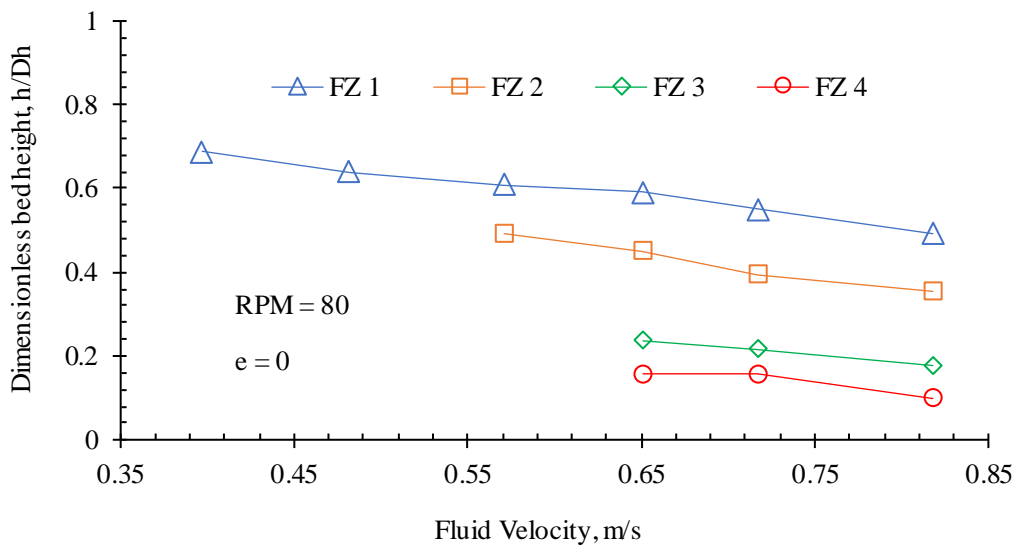


Figure 4-17: Variations of bed thickness for different fluid rheologies and mud velocities.

4.3.4 Moving Bed Velocity Estimation

Variations of cuttings dune velocity with changes in the mud velocity and drill pipe rotation in the concentric annulus are described in **Figure 4-18**. It is found that solid dune moving velocity increases exponentially with increasing mud velocity in the annulus. The effect of drill pipe rotation on dune moving velocity is nominal at low fluid velocities. However, at higher mud velocity above 0.65 m/s, an improvement in dune moving velocity is noticed due to the drill pipe rotation. It is worth noting that the effect of fluid velocity in the dune movement velocity surpasses the effect of drill pipe rotation.

In this study, beside the solid bed height, solid bed length movement with respect to time is also estimated with the ERT system for different annular configurations. **Figure 4-19** illustrates the influence of eccentricity on solid bed movement time. It shows the time spent by a solid bed in the ERT system at different fluid velocities and eccentricities for fluid FZ 1 where the inner pipe rotation is 80 RPM. Eccentric annulus ($e > 0$) represents a longer time required for the solid bed in the horizontal section, compared to the concentric annulus ($e = 0$). The mud velocity profile in the annular section is not uniform for an eccentric annular section. According to the past studies (Duan et al., 2008a; Erge et al., 2015; Huque et al., 2020a; Kamp et al., 1999; Pereira et al., 2011, 2007), the fluid shows a higher axial mud velocity in the upper annular section compared to lower annular section. This low axial velocity in the lower annular section affects movement rate in the eccentric condition, compared to a fully concentric annular section.

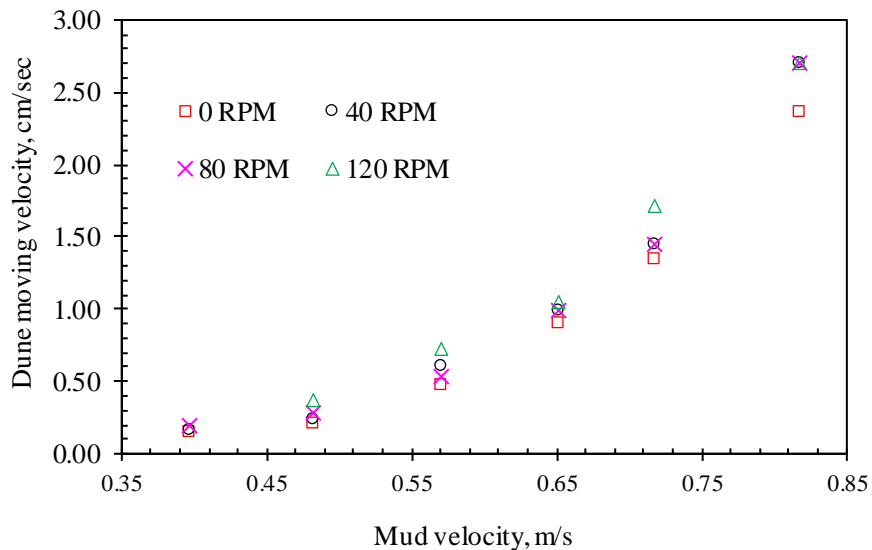


Figure 4-18: Solid dune velocity versus fluid velocity at different drill pipe rotations (4 % solid with FZ 1)

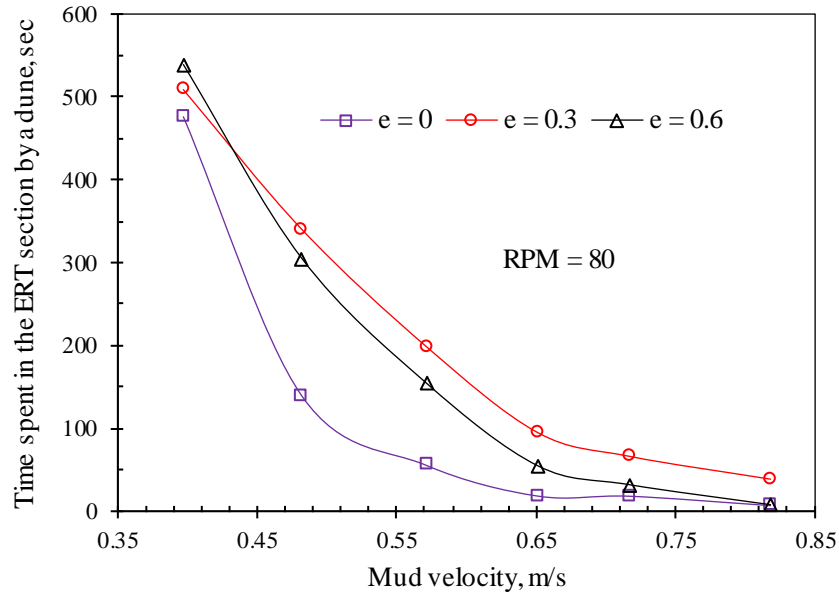


Figure 4-19: Solid bed propagation time reported in the ERT system.

Although the eccentric annulus has less bed height (see *Figure 4-19*), it takes a longer time to clean the eccentric annular section, compared to the concentric one. Also, it is observed that bed movement time would be a better indication of hole cleaning rather than estimation of moving bed height alone. Surprisingly, slightly eccentric annulus ($e = 0.3$) needs longer time, compared to a highly eccentric annulus ($e = 0.6$). For a highly eccentric annulus, solid dune stays in a close contact with the drill pipe; applying drill pipe rotation assists in moving the dune to the fluid flow region by strong orbital motion. This leads to faster dune movement in a highly eccentric annulus, compared to a slightly eccentric condition.

4.3.5 Flow Regime Analysis

Fluid velocity and rheology play vital role in solid transport capability. To generalize the solid transport capabilities at various fluid rheology and velocities, a dimensionless group (Reynolds

number) is calculated at different flow conditions. Tang et al.(2019, 2016) proposed expression of Reynolds number for the annular flow with stationary inner pipe condition as

$$Re_{Ann-HB} = \frac{\rho \bar{u}^{2-n} D^n}{\left(\frac{\tau_o}{8}\right) \left(\frac{D}{\bar{u}}\right)^n + K \left(\frac{a_f + b_f m}{m}\right)^n 8^{n-1}} \quad (4-5)$$

$$\text{Where } m = \frac{nk \left(\frac{8v}{D}\right)^n}{\tau_o + K \left(\frac{8v}{D}\right)^n}, \text{ for power law fluid, } m = n \quad (4-6)$$

In the above equation, ρ and \bar{u} are the density and velocity of the fluid, and D stands for the hydraulic diameter of the test section. The remaining parameters are related to the Herschel-Bulkley fluid properties. Annular parameters (a_f and b_f) can be approximated as: $a_f \approx 0.5$ and $b_f \approx 1$ for the annular diameter ratio greater than 0.3. Tang et al.(2019) reported the maximum errors of 3% will be caused by using the approximated values for a_f and b_f . The annular diameter ratio for this experimental set up is 0.55. Therefore, the approximation of $a_f \approx 0.5$ and $b_f \approx 1$ can produce representative values of Reynolds number for annular flow with a reasonable error limit.

Table 4-3: Flow regime analysis for input solid of 4%.

Viscosity ↓	Fluid	Reynolds Number						Transitional
	FZ 1	2049	2784	3616	4412	5097	6189	2300 < Re < 3250
	FZ 2	1463	1977	2564	3129	3618	4406	2670 < Re < 3650
	FZ 3	984	1341	1754	2156	2509	3083	2760 < Re < 3700
	FZ 4	713	973	1275	1571	1831	2255	2780 < Re < 3720

	<i>Stationary bed</i>
	<i>Stationary bed + moving dune</i>
	<i>Moving dune</i>

To minimize the effect of drill pipe rotation, all data are generated at the stationary inner pipe condition for a comparative analysis. **Table 4-3** presents a comparative summary of the Reynolds number for different fluids tested in this study for 4% input solid fraction. Six column shows the Reynolds number for six different fluid velocities reported in **Table 4-2**. Fluid velocities are

increasing from left to right direction. **Table 4-3** also shows the critical range of transitional Reynolds number for all four fluids.

The critical Reynolds number (Zamora et al., 2005) defines the transitional range of laminar to turbulent flow. For a non Newtonian Herschel Buckley fluid, Vajargah et al. (2017) described the transitional flow boundary between lower limit (R_{e_1}) and upper limit (R_{e_2}) of Reynolds number.

R_{e_1} and R_{e_2} are defined as follows:

$$R_{e_1} = 3250 - 1150N \quad (4-7)$$

$$R_{e_2} = 4150 - 1150N \quad (4-8)$$

The Reynolds number lower than R_{e_1} represents the laminar flow regime; when the Reynolds number is greater than R_{e_2} , the flow regime is turbulent.

It should be noted that N is the generalized flow behavior index obtained from Equation (4-9). The transition flow regime is not constant; it is a function of N . The value of N can be calculated from the equations below:

$$\frac{1}{N} = A + B \quad (4-9)$$

Where,

$$A = \frac{(1-2n)\tau_w + 3n\tau_y}{n(\tau_w - \tau_y)} \quad (4-10)$$

$$B = \frac{2n(1+n)[(1+2n)\tau_w^2 + n\tau_y\tau_w]}{n(1+n)(1+2n)\tau_w^2 + 2n^2(1+n)\tau_w\tau_y + 2n^3\tau_y^2} \quad (4-11)$$

For each flow rate, there are two transitional Reynolds numbers, and the range of transitional Reynolds number decreases with increase in flow velocity. **Table 4-3** listed the lowest critical Reynolds number R_{e_1} for the lowest flow rate (0.397 m/s) and highest critical Reynolds number

R_{e2} for the highest mud velocity (0.818 m/s) to cover the entire transitional range for the tested domain for a given fluid rheology.

Figure 4-20 shows a graphical representation of fluid velocity and generalized Reynolds number for HB fluid with respect to the solid dune flow characteristics. Fluid FZ 1 shows a transitional range of Reynolds number between 2300 and 3250. The yellow zone with $Re = 2049$ and 2784 indicates a stationary bed and a moving dune. However, for turbulent flow regimes $Re > 3250$, fluid FZ 1 shows a fully moving dune. Fluid FZ 3 and FZ 4 both shows stationary bed at lower order Reynolds number and a combination of stationary bed and moving dune close to the lower transitional limit of Reynolds number (R_{e1})

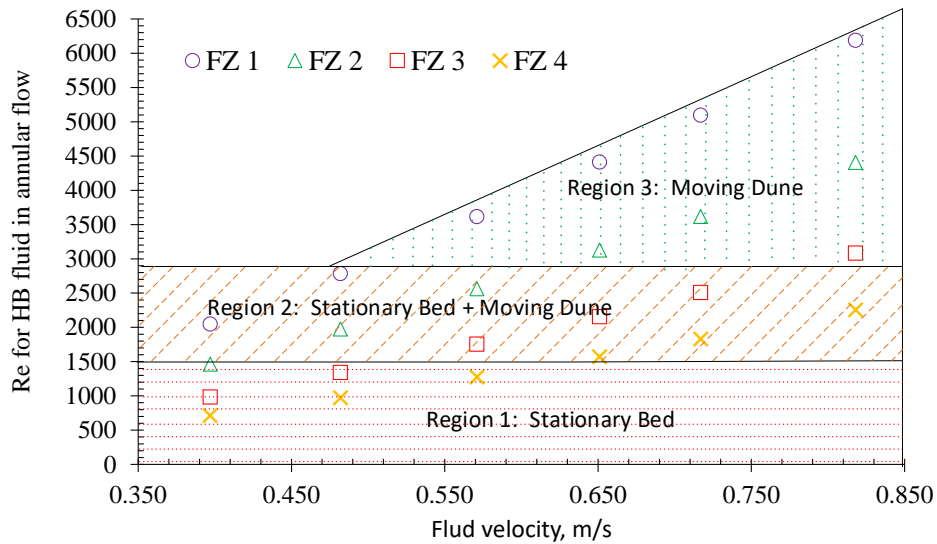


Figure 4-20: Flow regime map showing three different regions of solid transport.

Reynolds number range of 1500 to 2900 identified as generalized transitional zones (region 2) for all four fluid and it includes both stationary bed and moving dune. Any Reynolds number less than 1500 (region 1) indicates a completely stationary bed of cutting. The flow regime analysis in horizontal well indicates that a turbulent flow regime (Region 3) works best for an efficient hole

cleaning with out forming any stationary bed. The flow regime analysis and critical Reynolds number range indicate that a turbulence zone with a low viscous fluid is more beneficial for an efficient hole cleaning in the horizontal annular section even at low mud velocity. Similar observations are found in the past experimental studies (Kelessidis and Bandelis, 2004; Piroozian et al., 2012; Walker and Li, 2000) .

In this study, we also introduce a non-dimensional number named as ‘*Transport Performance Number*’ that includes the relationship between the solid bed height and sand dune moving velocity. **Figure 4-17** and **Figure 4-18** reveal that apart from the fluid rheology, the solid bed height is also impacted by the dune moving velocity in the annular section.

Transport performance number (TPN) includes the relationship between the dune velocity, dune height in the annular section, and fluid kinematic viscosity.

$$\textit{Transport performance number} = \frac{\textit{solid bed height (m)} \times \textit{solid dune velocity (m/sec)}}{\textit{kinematic viscosity of fluid (m}^2\text{/sec)}}$$

The transport performance number (TPN) versus mud velocity is plotted in **Figure 4-21** for fluids FZ 1, FZ 2, and FZ 3. According to **Figure 4-21**, there are two distinct regions: i) stationary bed and moving dune region and ii) Moving dune region. The experimental study and flow regime analysis show that a minimum TPN value of 70 is required to have a fully moving dune in the horizontal annular section for all three fluids. A TPN value less than 70 indicates a poor cuttings transport with stationary bed formation.

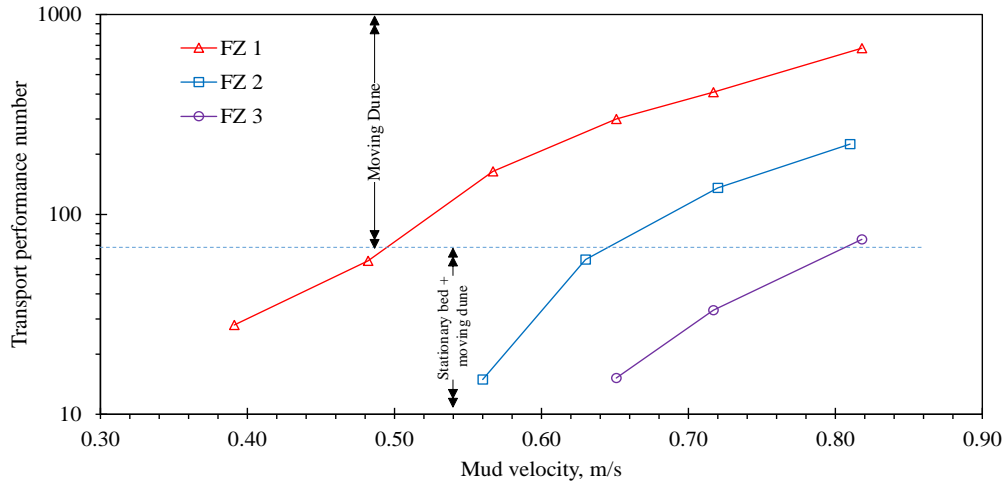


Figure 4-21: Transport performance number for FZ 1, FZ 2, and FZ 3

4.4 Conclusions

This study estimates the annular solid volume fraction through the ERT analysis that enables easier and faster data processing and interpretation in cuttings transport. The transient dune propagation analysis can be used to identify dune propagation time; it can also identify any stable solid bed formation in the horizontal section. Beside the quantitative estimation, ERT tomography provides a qualitative distribution solid cutting in the annular section where visual inspection is not feasible.

This study distinguishes the different zones (stable solid bed, moving layer, and cuttings free zone) of the mechanistic three-layer model using high speed visualization methods. Visualization study also shows the transition of stationary cuttings bed to a three-layer model followed by a two-layer model and a homogeneous fully suspended solid transport mechanism (single layer) upon an increase in the fluid velocity. Beside ERT analysis and visualization study, the following conclusion can be drawn from this study.

- A flow regime analysis show that turbulent flow regime provides a better hole cleaning without developing a stationary solid bed. A transitional flow regime shows a combination of moving

bed with stationary bed, however; a laminar flow shows a completely stationary bed in the annular section.

- This study also introduces a concept of transport performance number (TPN) that includes the combined effect of solid bed height and solid dune moving velocity for a horizontal annular section. It is concluded that a minimum TPN value of 70 is required for a proper hole cleaning.
- The eccentric annular section exhibits a less solid bed height, compared to a concentric annular section; however, it takes a longer time to clean the solid bed in the eccentric annulus.
- Inner pipe rotation significantly improves the stationary bed height in the annulus, though no significant improvement is observed for rotations above the range of 80 RPM-120 RPM.

Based on this experimental work, the following recommendations for future work can be listed:

- Particles with various sizes, shapes, color, and weight percentages can be used to simulate a more heterogeneous environment and further track particles movement to investigate the behavior of gravity and buoyancy effects on particle size and fluid rheology.
- Integration of particle image velocimetry (PIV) system can help to explore the effect of drill pipe rotation on fluid streamline and further investigate the helical motion of cuttings.
- The concept of transport performance number (TPN) is still at early stages. A detailed investigation of this hypothesis through using a wide range of fluid rheology, cuttings size and cuttings shapes can help to develop a nomograph of cuttings transport behaviors.

ACKNOWLEDGEMENTS

The researchers gratefully acknowledge and thank Equinor Canada, Memorial University, InnovateNL, and the Natural Sciences and Engineering Research Council of Canada (NSERC) to support this research work. This publication was also made possible by the grant NPRP10-0101-170091 from Qatar National Research Fund (a member of the Qatar Foundation).

NOMENCLATURES

Acronyms

2-D	-	Two Dimensional
DSLR	-	Digital Single Lens Reflex
ERT	-	Electrical Resistance Tomography
FZ	-	Flowzan
GPM	-	Gallons Per Minute
ID	-	Inner Diameter
LPM	-	Liter Per Minute
MTV	-	Minimum Transport Velocity
OD	-	Outer Diameter
PIV	-	Particle Image Velocimetry
ROP	-	Rate of Penetration, ft/hr.
RPM	-	Revolution Per Minutes
TAMUQ	-	Texas A & M University at Qatar
TPN	-	Transport Performance Number

Variables/Symbols

A	-	Constant	(-)
B	-	Constant	(-)
N	-	Constant	(-)
A_{hole}	-	Area of the hole during a drilling operation	(ft ²)
a_f	-	Annular parameter	(-)
b_f	-	Annular parameter	(-)
e	-	Eccentricity	(-)
k	-	Consistency index	(Pa·s ⁿ)
n	-	Flow behavior index	(-)
Re_1	-	Lower Reynolds number limit	(-)
Re_2	-	Upper Reynolds number limit	(-)
Q_{inj}	-	Volumetric injection rate	(ft ³ /sec)
Re	-	Reynolds Number, a dimensionless number	(-)
HB	-	Herschel-Bulkley	(-)
Rh	-	Hydraulic Radius	(ft, m)
R^2	-	Coefficient of determination	(-)
v	-	Velocity	(m/s)

Greek Letters

α	-	Volume fraction of the dispersed material	(-)
----------	---	---	-----

σ	-	Conductivity	(mS/cm)
ρ	-	Density	(lbm/ft ³)
τ	-	Shear stress	(Pa)
τ_w	-	Wall shear stress	(Pa)
τ_o	-	Yield stress	(Pa)
τ_y	-	Yield stress	(Pa)
$\dot{\gamma}$	-	Shear rate	(s ⁻¹)

Subscripts

1	-	Continuous phase	(-)
2	-	Dispersed phase	(-)
mc	-	Reconstructed measured conductivity	(mS/cm)
m	-	Mud	(-)

REFERENCES

- Abbas, N., Al Nokhatha, J., Farouz, A., Mohamed, E., Abbas, S.H., Hui, W., 2014. The longest horizontal well drilled in the U.A.E., geosteered in a thin calcareous dolomite sublayer, in: 0th Abu Dhabi International Petroleum Exhibition and Conference. pp. 1579–1589. <https://doi.org/10.2118/171825-ms>
- Aladsani, A., Aranda, J., Ahmed, Mula, Qallabi, S.A.L., Bankole, I., Ahmed, Mubashir, Dutta, A., 2018. Successful Drilling Longest Horizontal Sour Gas Well, in: Abu Dhabi International Petroleum Exhibition & Conference. Abu Dhabi, UAE, 12-15 November 2018.
- Asef Hashmi, M., Salem, G., Morales, A., Banihammad, B., Al Yamani, S.M., 2020. Planning and challenges of longest complex 3D ERD well drilled in United Arab Emirates onshore field artificial island using slim casing design, in: Abu Dhabi International Petroleum Exhibition and Conference 2020, ADIP 2020. Abu Dhabi, UAE. <https://doi.org/10.2118/202717-ms>
- Beck, M.S., Williams, 1995. Process Tomography: Principles, Techniques and Applications, 1st ed. Butterworth-Heinemann. <https://doi.org/10.1016/C2009-0-24202-4>

- Bilgesu, H.I., Ali, M.W., Aminian, K., Ameri, S., 2002. Computational Fluid Dynamics (CFD) as a Tool to Study Cutting Transport in Wellbores, in: SPE Eastern Regional Meeting. <https://doi.org/10.2118/78716-MS>
- Bradley, W.B., Jarman, D., Plott, R.S., Wood, R.D., Schofield, T.R., Auflick, R.A., Cocking, D., 1991. A Task Force Approach to Reducing Stuck Pipe Costs. SPE/IADC Drill. Conf. <https://doi.org/10.2118/21999-MS>
- Brown, N.P., Bern, P.A., Weaver, A., 1989. Cleaning Deviated Holes: New Experimental and Theoretical Studies. SPE/IADC Drill. Conf. <https://doi.org/10.2118/18636-MS>
- Bulgachev, R. V., Pouget, P., 2006. New experience in monofilament fiber tandem sweeps hole cleaning performance on kharyaga cilfield, timan-pechora region of Russia, in: SPE Russian Oil and Gas Technical Conference and Exhibition. pp. 344–355. <https://doi.org/10.2523/101961-ms>
- Chen, Z., Ahmed, R.M., Miska, S.Z., Takach, N.E., Yu, M., Pickell, M.B., Hallman, J.H., 2007. Experimental Study on Cuttings Transport With Foam Under Simulated Horizontal Downhole Conditions. SPE Drill. Complet. 22, 304–312. <https://doi.org/10.2118/99201-PA>
- Cho, H., Shah, S.N., Osisanya, S.O., 2000a. A three-segment hydraulic model for cuttings transport in horizontal and deviated wells, in: SPE/CIM International Conference on Horizontal Well Technology. Calgary, Alberta, Canada, pp. 1–16. <https://doi.org/10.2118/65488-MS>
- Cho, H., Shah, S.N., Osisanya, S.O., 2000b. A three-layer modeling for cuttings transport with coiled tubing horizontal drilling, in: SPE Annual Technical Conference and Exhibition. Dallas, Texas, U.S.A, pp. 905–918. <https://doi.org/10.2118/63269-ms>

- Czuprat, O., Faugstad, A.M., Byrski, P., Schulze, K., 2020. Hole cleaning efficiency of sweeping pills in horizontal wells - Facts or philosophy?, in: SPE Annual Technical Conference and Exhibition. Denver, Colorado, USA. <https://doi.org/10.2118/201634-ms>
- Dabirian, R., Mohan, R.S., Shoham, O., Kouba, G., 2016. Solid-Particles Flow Regimes in Air/Water Stratified Flow in a Horizontal Pipeline. *Oil Gas Facil.* 5, 1–14. <https://doi.org/10.2118/174960-pa>
- Dabirian, R., Mohan, R.S., Shoham, O., Kouba, G., 2015. Sand transport in stratified flow in a horizontal pipeline, in: *Proceedings - SPE Annual Technical Conference and Exhibition*. pp. 3222–3239. <https://doi.org/10.2118/174960-ms>
- Doron, P., Barnea, D., 1996. Flow pattern maps for solid-liquid flow in pipes. *Int. J. Multiph. Flow* 22, 273–283. [https://doi.org/10.1016/0301-9322\(95\)00071-2](https://doi.org/10.1016/0301-9322(95)00071-2)
- Doron, P., Barnea, D., 1993. A Three-Layer Model for Solid-Liquid Flow in Horizontal Pipes. *Int. J. Multiph. Flow* 19, 1029–1043. [https://doi.org/10.1016/0301-9322\(93\)90076-7](https://doi.org/10.1016/0301-9322(93)90076-7)
- Duan, M., Miska, S., Yu, M., Takach, N., Ahmed, R., Tulsa, U., 2008a. The Effect of Drillpipe Rotation on Pressure Losses and Fluid Velocity Profile in Foam Drilling, in: *SPE Western Regional and Pacific Section AAPG Joint Meeting*. Bakersfield, California, U.S.A., 31 March–2 April 2008. <https://doi.org/10.2118/114185-MS>
- Duan, M., Miska, S., Yu, M., Takach, N., Ahmed, R., Zettner, C., 2009. Critical conditions for effective sand-sized-solids transport in horizontal and high-angle wells. *SPE Drill. Complet.* 24, 229–238. <https://doi.org/10.2118/106707-PA>
- Duan, M., Miska, S.Z., Yu, M., Takach, N.E., Ahmed, R.M., Zettner, C.M., 2008b. Transport of

- Small Cuttings in Extended-Reach Drilling. SPE Drill. Complet. 23, 258–265.
<https://doi.org/10.2118/104192-PA>
- Eren, T., Polat, C., 2020. Numerical investigation of the application of intelligent horizontal well completion. J. Nat. Gas Sci. Eng. 83, 103599. <https://doi.org/10.1016/j.jngse.2020.103599>
- Erge, O., Ozbayoglu, E.M., Miska, S.Z., Yu, M., Takach, N., Saasen, A., May, R., 2015. The effects of drillstring-eccentricity, -rotation, and -buckling configurations on annular frictional pressure losses while circulating yield-power-law fluids, in: SPE Drilling and Completion. Fort Worth, Texas, USA. <https://doi.org/10.2118/167950-PA>
- Fajemidupe, O.T., Aliyu, A.M., Baba, Y.D., Archibong, A.E., Okeke, N.E., Ehinmowo, A.B., Yeung, H., 2019. Minimum sand transport conditions in gas-solid-liquid three-phase stratified flow in horizontal pipelines. Soc. Pet. Eng. - SPE Niger. Annu. Int. Conf. Exhib. 2019, NAIC 2019. <https://doi.org/10.2118/198726-MS>
- Ford, J.T., Peden, J.M., Oyenehin, M.B., Gao, E., Zarrough, R., 1990. Experimental Investigation of Drilled Cuttings Transport in Inclined Boreholes, in: SPE Annual Technical Conference and Exhibition. pp. 197–206. <https://doi.org/10.2118/20421-MS>
- Garcia-Hernandez, A.J., Miska, S.Z., Yu, M., Takach, N.E., Zettner, C.M., 2007. Determination of Cuttings Lag in Horizontal and Deviated Wells, in: SPE Annual Technical Conference and Exhibition. Anaheim, California, U.S.A., 11–14 November. <https://doi.org/10.2118/109630-MS>
- Gul, S., Kuru, E., Parlaktuna, M., 2017. Experimental investigation of cuttings transport in horizontal wells using aerated drilling fluids, in: SPE Abu Dhabi International Petroleum Exhibition and Conference. <https://doi.org/10.2118/188901-ms>

- Gulrud, T.O., Nybø, R., Bjørkevoll, K.S., 2009. Statistical Method for Detection of Poor Hole Cleaning and Stuck Pipe. SPE Offshore Eur. Oil Gas Conf. Exhib. <https://doi.org/10.2118/123374-MS>
- Huang, Zhe, Huang, Zhongwei, Su, Y., Bi, G., Li, W., Liu, X., Jiang, T., 2020. A feasible method for the trajectory measurement of radial jet drilling laterals. SPE Drill. Complet. 35, 125–135. <https://doi.org/10.2118/192140-PA>
- Huque, M.M., Butt, S., Zendejboudi, S., Imtiaz, S., 2020a. Systematic sensitivity analysis of cuttings transport in drilling operation using computational fluid dynamics approach. J. Nat. Gas Sci. Eng. 81, 103386. <https://doi.org/https://doi.org/10.1016/j.jngse.2020.103386>
- Huque, M.M., Imtiaz, S., Zendejboudi, S., Butt, S., 2020b. Experimental Study of Cuttings Transport with Non-Newtonian Fluid in an Inclined Well Using Visualization and ERT Techniques, in: SPE Annual Technical Conference & Exhibition. Denver, Colorado, U.S.A. <https://doi.org/10.2118/201709-MS>
- Kamp, A.M., Rivero, M., Intevp, P., 1999. Layer Modeling for Cuttings Transport in Highly Inclined Wellbores, in: SPE Latin American and Caribbean Petroleum Engineering Conference. Caracas, Venezuela, 21-23 April. <https://doi.org/10.2118/53942-MS>
- Kelessidis, V.C., Bandelis, G.E., 2004. Flow Patterns and Minimum Suspension Velocity for Efficient Cuttings Transport in Horizontal and Deviated Wells in Coiled-Tubing Drilling. SPE Drill. Complet. <https://doi.org/10.2118/81746-PA>
- Kelessidis, V.C., Bandelis, G.E., Li, J., 2007. Flow of Dilute Solid-liquid Mixtures in Horizontal Concentric and Eccentric Annuli. J. Can. Pet. Technol. 46, 56–61. <https://doi.org/10.2118/07-05-06>

- Kelessidis, V.C., Mpandelis, G.E., 2003. Flow Patterns and Minimum Suspension Velocity for Efficient Cuttings Transport in Horizontal and Deviated Wells in Coiled-Tubing Drilling, in: Proceedings of the SPE/ICoTA Coiled Tubing Roundtable Conf. pp. 180–193. <https://doi.org/10.2523/81746-ms>
- Kenupp, R., Lourenço, A., Soltvedt, S., Thomson, I., Hughes, B., Simões, G., Morosov, D.L., Andrade, R., 2017. The longest horizontal section ever drilled in an extended-reach well in Brazil, in: Offshore Technology Conference. Rio de Janeiro, Brazil, pp. 1538–1547. <https://doi.org/10.4043/28091-ms>
- Kjøsnes, I., Laklingholm, G., Saasen, A., Syrstad, S.O., Agle, A., Solvang, K.A., 2003. Successful Water Based Drilling Fluid Design for Optimizing Hole Cleaning and Hole Stability. Proc. Drill. Conf. 339–346. <https://doi.org/10.2523/85330-ms>
- Larsen, T.I., Pilehvari, A.A., Azar, J.J., 1997. Development of a New Cuttings-Transport Model for High-Angle Wellbores Including Horizontal Wells. SPE Drill. Complet. 12, 129–136. <https://doi.org/10.2118/25872-PA>
- Li, J., Luft, B., 2014. Overview of solids transport studies and applications in oil and gas industry - Experimental work. Soc. Pet. Eng. - SPE Russ. Oil Gas Explor. Prod. Tech. Conf. Exhib. 2014, RO G 2014 - Sustain. Optimising Prod. Challenging Limits with Technol. 2, 1365–1401. <https://doi.org/10.2118/171285-ms>
- Martin, M., Georges, C., Bisson, P., Konirsch, O., 1987. Transport of Cuttings in Directional Wells, in: SPE/IADC Drilling Conference. New Orleans, Louisiana, USA, 15-18 March. <https://doi.org/10.2118/16083-MS>
- Masuda, Y., Doan, Q., Oguztoreli, M., Naganawa, S., Yonezawa, T., Kbayashi, A., Kamp, A.,

2000. Critical Cuttings Transport Velocity in Inclined Annulus: Experimental Studies and Numerical Simulation, in: SPE/CIM International Conference on Horizontal Well Technology. Calgary, Alberta, Canada, 6-8 November. <https://doi.org/10.2118/65502-MS>
- Miguel, D.L., Anh, P.L., Wittry, A., Vernizeau, B., Duy, C., Malpas, P., 2015. Setting new records for drilling the World's longest horizontal well in basement, in: SPE/IATMI Asia Pacific Oil and Gas Conference and Exhibition. <https://doi.org/10.2118/176324-ms>
- Muecke, N., Wroth, A., Zharkeshov, S., Anton, R., McCourt, I., Armstrong, N., 2018. Extended-reach drilling to maximize recovery from a mature asset: A case study. SPE Drill. Complet. 33, 385–401. <https://doi.org/10.2118/194000-PA>
- Nguyen, D., Rahman, S.S., 1998. A Three-Layer Hydraulic Program for Effective Cuttings Transport and Hole Cleaning in Highly Deviated and Horizontal Wells. SPE Drill. Complet. 68, 78–82.
- Okrajni, S., Azar, J.J., 1986. The Effects of Mud Rheology on Annular Hole Cleaning in Directional Wells. SPE Drill. Eng. 1, 297–308. <https://doi.org/10.2118/14178-PA>
- Ozbayoglu, E.M., Etehad Osgouei, R., Ozbayoglu, M.A., Yuksel, E.H., 2012. Hole-Cleaning Performance of Gasified Drilling Fluids in Horizontal Well Sections. SPE J. 17, 912–923. <https://doi.org/10.2118/131378-PA>
- Ozbayoglu, E.M., Miska, S.Z., Reed, T., Takach, N., 2003. Cuttings Transport with Foam in Horizontal & Highly-Inclined Wellbores, in: SPE/IADC Drilling Conference. <https://doi.org/10.2118/79856-MS>
- Ozbayoglu, E.M., Saasen, A., Sorgun, M., Svanes, K., 2007. Estimating critical velocity to prevent

- bed development for horizontal-inclined wellbores. Proc. SPE/IADC Middle East Drill. Technol. Conf. Exhib. 233–238. <https://doi.org/10.2118/108005-ms>
- Ozbayoglu, M.E., Saasen, A., Sorgun, M., Svanes, K., 2008. Effect of Pipe Rotation on Hole Cleaning for Water-Based Drilling Fluids in Horizontal and Deviated Wells, in: IADC/SPE Asia Pacific Drilling Technology Conference and Exhibition. Jakarta, Indonesia. 25–27 August. <https://doi.org/10.2118/114965-MS>
- Peden, J.M., Ford, J.T., Oyenehin, M.B., 1990. Comprehensive Experimental Investigation of Drilled Cuttings Transport in Inclined Wells Including the Effects of Rotation and Eccentricity, in: European Petroleum Conference. The Hague, The Netherlands, 22-24 October. <https://doi.org/10.2118/20925-MS>
- Pereira, F.A.R., Ataíde, C.H., Barrozo, M.A.S., 2011. CFD approach using a discrete phase model for annular flow analysis. Lat. Am. Appl. Res. 40, 53–60.
- Pereira, F.A.R., Barrozo, M.A.S., Ataíde, C.H., 2007. CFD Predictions of Drilling Fluid Velocity and Pressure Profiles in Laminar Helical Flow. Brazilian J. Chem. Eng. 24, 587–595. <https://doi.org/10.1590/S0104-66322007000400011>
- Philip, Z., Sharma, M.M., Chenevert, M.E., 1998. The Role of Taylor Vortices in the Transport of Drill Cuttings, in: SPE India Oil and Gas Conference and Exhibition. New Delhi, India, 7-9 April. <https://doi.org/10.2118/39504-MS>
- Pilehvari, A.A., Azar, J.J., Shirazi, S.A., 2007. State-of-the-Art Cuttings Transport in Horizontal Wellbores. SPE Drill. Complet. 14, 196–200. <https://doi.org/10.2118/57716-pa>
- Piroozian, A., Ismail, I., Yaacob, Z., Babakhani, P., Ismail, A.S.I., 2012. Impact of Drilling Fluid

Viscosity, Velocity And Hole Inclination On Cuttings Transport In Horizontal And Highly Deviated Wells. *J. Pet. Explor. Prod. Technol.* 2, 149–156. <https://doi.org/10.1007/s13202-012-0031-0>

Rodriguez Corredor, F., Bizhani, M., Kuru, E., 2016. Experimental investigation of cuttings bed erosion in horizontal wells using water and drag reducing fluids. *J. Pet. Sci. Eng.* 147, 129–142. <https://doi.org/10.1016/j.petrol.2016.05.013>

Saasen, A., Løklingholm, G., 2002. The Effect of Drilling Fluid Rheological Properties on Hole Cleaning. *Proc. Drill. Conf.* 683–687. <https://doi.org/10.2523/74558-ms>

Sanchez, R.A., Azar, J.J., Bassal, A.A., Martins, A.L., 1997. The Effect of Drillpipe Rotation on Hole Cleaning During Directional Well Drilling, in: *SPE/IADC Drilling Conference*. Amsterdam, The Netherlands, 4-6 March. <https://doi.org/10.2118/37626-MS>

Sifferman, T.R., Becker, T.E., 1992. Hole Cleaning in Full-Scale Inclined Wellbores. *SPE Drill. Eng.* 7, 115–120. <https://doi.org/10.2118/20422-PA>

Tang, M., Ahmed, R., Srivastav, R., He, S., 2016. Simplified surge pressure model for yield power law fluid in eccentric annuli. *J. Pet. Sci. Eng.* 145, 346–356. <https://doi.org/10.1016/j.petrol.2016.05.038>

Tang, M., He, L., Kong, L., He, S., Zhang, T., 2019. Simplified modeling of laminar helical flow in eccentric annulus with YPL fluid. *Energy Sources, Part A Recover. Util. Environ. Eff.* 0, 1–14. <https://doi.org/10.1080/15567036.2019.1649322>

Tomren, P.H., Iyoho, A.W., Azar, J.J., 1986. Experimental Study of Cuttings Transport in Directional Wells. *SPE Drill. Eng.* 43–56. <https://doi.org/10.2118/12123-PA>

- Vadinal, R.B., Perrout, S.R., de Campos Chuvas, R., dos Passos, A.G.L.G., da Silva, L.P., 2019. Influence of hole cleaning on the liner cement job in Papa terra field, in: Offshore Technology Conference. Rio de Janeiro, Brazil, pp. 1–13. <https://doi.org/10.4043/29786-ms>
- Vajargah, A.K., Sullivan, G., Johnson, M., Oort, E. Van, 2017. Transitional and Turbulent Flow of Drilling Fluids in Pipes : An Experimental Investigation, in: AADE National Technical Conference and Exhibition.
- Vanpuymbroeck, L., 2013. Increasing drilling performance using hydro-mechanical hole cleaning devices, in: SPE Middle East Unconventional Gas Conference and Exhibition. Muscat, Oman, pp. 544–561. <https://doi.org/10.2118/164005-ms>
- Walker, S., Li, J., 2000. The Effects of Particle Size, Fluid Rheology, and Pipe Eccentricity on Cuttings Transport, in: SPE/ICoTA Coiled Tubing Roundtable. Houston, TX, USA, 5–6 April. <https://doi.org/10.2118/60755-MS>
- Wang, Z., Gao, D., Yang, J., 2019. Design and calculation of complex directional-well trajectories on the basis of the minimum-curvature method. SPE Drill. Complet. 43, 173–188. <https://doi.org/10.2118/194511-PA>
- Yu, M., Takach, N.E., Nakamura, D.R., Shariff, M.M., 2007. An Experimental Study of Hole Cleaning Under Simulated Downhole Conditions, in: SPE Annual Technical Conference and Exhibition. <https://doi.org/10.2118/109840-MS>
- Zamora, M., Roy, S., Slater, K., 2005. Comparing a Basic Set of Drilling Fluid Pressure-Loss Relationships to Flow-Loop and Field Data, in: AADE National Technical Conference and Exhibition.

Zhu, Z., Sand, K. W., Teevens, P. J., 2010. Effects of flow regime on solids deposition in multiphase petroleum flow, in: NACE - International Corrosion Conference Series. pp. 1–19.

Chapter 5 : Experimental Study of Cuttings Transport with Non-Newtonian Fluid in Inclined Well Using Visualization and Electrical Resistance Tomography Techniques

Mohammad Mojammel Huque¹, Syed Imtiaz¹, Sohrab Zendehboudi¹, Stephen Butt¹
Mohammad Azizur Rahman², Priyank Maheshwari³

¹Department of Process Engineering, Memorial University, St. John's, NL, Canada

²Texas A&M University at Qatar

³Total Research Center-Qatar

ABSTRACT

Hole cleaning is a concern in directional and horizontal well drilling operation where drill cuttings tend to settle in the lower annulus section. A lab-scale experiments were performed with different non-Newtonian fluids in a 6.16-meter-long, 114.3 mm x 63.5 mm transparent annulus test section to investigate cuttings transport behavior. This experimental study focused on understanding the cuttings transport mechanism in the annulus section with high-speed imaging technology. The movement of cuttings in the inclined annular section was captured with a high-speed camera at 2000 frames per second. Also, cuttings bed movement patterns at different fluid velocity and inner pipe rotation were captured with a DSLR video camera. The electrical resistance tomography (ERT) system was used to quantify the cuttings volume fraction in the annulus. Different solid bed height and cuttings movement were observed based on fluid rheology, fluid velocity and inner pipe rotation. The mechanistic three layers cuttings transport model was visualized with the experimental procedure. This study showed that solid bed height is significantly reduced with an increase in the inner pipe rotation. This study also identified that cutting bed thickness largely depends on fluid rheology and wellbore inclination. The image from the high-speed camera identified a downward trend of some rolling particles in the annulus due to gravitational force at a

low mud velocity. Visual observation from high-speed camera identified a helical motion of solid particles when drill pipe is in contact with solid particles and rotating at higher RPM. Different cuttings movement patterns such as: rolling, sliding, suspension, helical movement, downward movement were identified from the visualization of a high-speed camera.

Keyword: Cuttings Transport, Inclined well, Visualization, Electrical Resistance Tomography, non-Newtonian Fluid, Annular Flow.

5.1 Introduction

Inadequate hole cleaning in a drilling operation often leads to some serious problems like high torque and drag, low rate of penetration, lost circulation, and poor ECD control (Sanchez et al., 1997). If these problems are not tackled appropriately, it may cause a potential risk of loss of the well and increase the non-productive time. Though investigation on cuttings transport has been carried out for many years, still poor hole cleaning remains one of the most critical issues in a drilling operation. Early experiments on cuttings transport studies were conducted on vertical wells only and focused on the terminal velocity requirement to lift the cuttings to the surface (Ozbayoglu et al., 2003). In recent decades, oil industries are more focused on exploring the directional, horizontal, and extended reach well to produce from the unconventional, harsh geological, and offshore environments. Cuttings transport mechanism differs significantly in the inclined and horizontal well than to the vertical well. In a vertical or near vertical well, cuttings settling velocity determines the cuttings transport capability. In contrast, in the intermediate inclined well, the observed moving cuttings bed is transported by the lifting mechanism of the drilling mud. However, for the horizontal and near-horizontal well, a significant cuttings bed forms, and cuttings are transported through the rolling mechanism (Clark and Bickham, 1994).

Tormen et al. (1986) experimental study showed that cuttings bed could be formed in the inclined well even at a higher mud flow rate. They also showed that fluid viscosity has a dominant effect on cuttings transport in the inclined well. Ford et al. (1990) show that a minimum transport velocity (MTV) is required to initiate a rolling mechanism of cuttings transport in the directional well. They also found that turbulent behavior shows a reduction in magnitude of MTV in the annular section. Azar and Sanchez (1997) studies showed that drill pipe rotation has a significant impact on hole cleaning in the horizontal and near-horizontal well. Kelessidis and Bandelis (2004) presented a flow pattern map of slurry flow in the annular section as a function of superficial liquid velocity and the effect of fluid rheology. Several other experimental studies (Ford et al., 1990; Garcia-Hernandez et al., 2007; Kelessidis et al., 2007; Martin et al., 1987; Masuda et al., 2000; Ozbayoglu et al., 2008; Piroozian et al., 2012; Shadizadeh and Zoveidavianpoor, 2012; Sifferman and Becker, 1992; Zahid et al., 2018) focused on cuttings transport in inclined/ directional well. These experimental studies revealed that mud flow rate and fluid viscosity show a significant impact on cuttings transport in the inclined well. The impact of drill pipe rotation on solid transport in inclined well was also investigated in several experimental studies. Heshamudin et al.(2019) and Zhang et al. (2018) investigations concluded that the impact of drill pipe rotation is more significant in the horizontal or near horizontal well though transport in horizontal well is more challenging. Yeu et al. (2019) experimental study shows that horizontal well (90°) is the worst for hole cleaning followed by inclination of 60°. Kim et al.(2014) study with inclined well shows that drill pipe rotation impeded the solid bed formation and improved the solid transport ratio in the slim hole annulus.

In recent years, researchers are more focused on improving the cuttings transport behavior by using enhanced fluid rheology(Boyoun et al., 2019; Gul et al., 2017; Hakim et al., 2018; Heshamudin et

al., 2019; Hirpa and Kuru, 2020; Rodriguez Corredor et al., 2016; Yeu et al., 2019) and transport mechanism (Kim et al., 2014; Naganawa et al., 2017; Rasul et al., 2020). Boyou et al. (2019) study with nano silica based aqueous solution shows an improved cuttings transport efficiency for any inclination. They proposed that addition of nano silica can be an alternative solution to the oil-based drilling mud. Hirpa and Kuru (2020) experimentally investigate the solid bed erosion using polymer solution. Their study shows that fluid elasticity significantly affects the solid bed erosion dynamics behavior. Several other investigations (Hakim et al., 2018; Heshamudin et al., 2019; Yeu et al., 2019) used improved water based mud with polyethylene and polypropylene. These studies concluded that addition of polyethylene beads can improved the transport ratio by approximately 16%. The impact of drag reducing polymer also investigated in some of the past studies (Gul et al., 2017; Rodriguez Corredor et al., 2016). These studies revealed that addition of drag reducing polymer considerably reduce the minimum transport velocity to initiate the movement of coarse cuttings in horizontal well.

Sayindla et al. (2016) investigated the solid transport capability with different oil-based mud. Their study showed that fluid yield stress has significant impact on holding cuttings at low shear rate. Several other studies (Gul et al., 2017; Ozbayoglu et al., 2012; Rasul et al., 2020) investigated cuttings transport with air-water, and aerated mud along. These studies suggested that an increase gas volume fraction in the aerated mud can improve cuttings transport by increasing the local fluid velocity in the annular section. Gul et al. (2017) investigated the solid-liquid flow regime map in their studies and compared the flow pattern with aerated mud. They observed four different flow regimes as bubble flow, elongated bubble flow, slug flow and wavy annular flows. Though, their study could not distinguish performance variation in all four types of flow regimes, however, they concluded that wavy annular flow regime is more effective in cuttings transport in horizontal well.

Computational fluid dynamics (CFD) study also becoming popular in recent years in cuttings transport studies. Most of the CFD studies (Busch and Johansen, 2020; Erge and van Oort, 2020; Huque et al., 2020; Pang et al., 2019, 2018a; Sun et al., 2014) used Eulerian-Eulerian multiphase flow modelling and some other studies (Akhshik et al., 2015; Barbosa et al., 2019; Shao et al., 2019) used CFD- coupled with discrete element methods (DEM) or commonly known as CFD-DEM methods. CFD-DEM method offers precise investigation of the effect of solid cutting size, shapes, sphericity, solid bed erosion and transport mechanism. Beside the conventional cuttings transport studies with different drilling parameters, researchers now focuses more precisely on the impact of drill pipe rotation, whirling and orbital motion (Busch and Johansen, 2020; Pang et al., 2018a), drill string eccentricity (Erge and van Oort, 2020; GhasemiKafrudi and Hashemabadi, 2016; Heydari et al., 2017), flow pattern map and hydraulic behavior (Pang et al., 2018b; Sayindla et al., 2019; Vaziri et al., 2020; C. Zhang et al., 2018), complex wellbore (Epelle and Gerogiorgis, 2019).

However, very few studies (Kelessidis and Bandelis, 2004; Ozbayoglu and Osgouei, 2012; Wei et al., 2013; F. Zhang et al., 2018) were conducted to visualize the flow behavior of cuttings in the annular section. Due to the technical and equipment limitations, previous experimental studies on cuttings transport visualization were not adequate to investigate solid movement patterns and flow pattern in the annular section are indistinguishable. Very few studies used CFD-DEM methods (Akhshik et al., 2015; Barbosa et al., 2019; Shao et al., 2019) to investigate the solid particles movement, however these computational study shows lack of experimental validation of solid particle movement patterns.

Moreover, most of the past experimental studies estimates solid volume fraction after separating the solid at the end of the experiment and measure the total solid volume. This estimation methods suffers from inline or instantaneous solid volume measurement while conducting an experiment.

These limitations motivate the authors to investigate the flow pattern of solid cuttings movement in a near-horizontal well using high-speed visualization methods along with inline tracking of solid volume fraction. The objective of this experimental study is to identify different solid transport mechanisms involved in an inclined well section. The movement of the solid cutting was captured at different drilling environments (inclination, fluid rheology, drill pipe rotation, and mud velocity) with a high-speed camera. This study also used the ERT data acquisition system to monitor instantaneous solid volume fraction in the annular section. High-speed camera images and ERT results at 5°, and 10° inclination from the horizontal position were compared in this study.

This manuscript is summarizing as follows: **Section 5.2** describes experimental materials and method, **Section 5.3** shows the result from the high-speed camera visualization and ERT system, and **Section 5.4** summarizes the conclusion from this study.

5.2 Materials and Method

An experimental study was conducted in the multiphase flow-loop at Texas A & M University at Qatar. The multiphase flow loop consists of a 6.16-meter-long annular section. It has an inner pipe of 63.5 mm made of aluminum and an outer pipe of 114.3 mm made by acrylic materials. A simplified schematic of the test section is shown in **Figure 5-1** and actual lab image is shown in **Figure 5-2**. The test section can be placed in horizontal and inclined position upto 15° from the horizontal position. The inner drill pipe can be rotate upto 150 RPM. The test section can also be used for different eccentric position of the inner pipe.

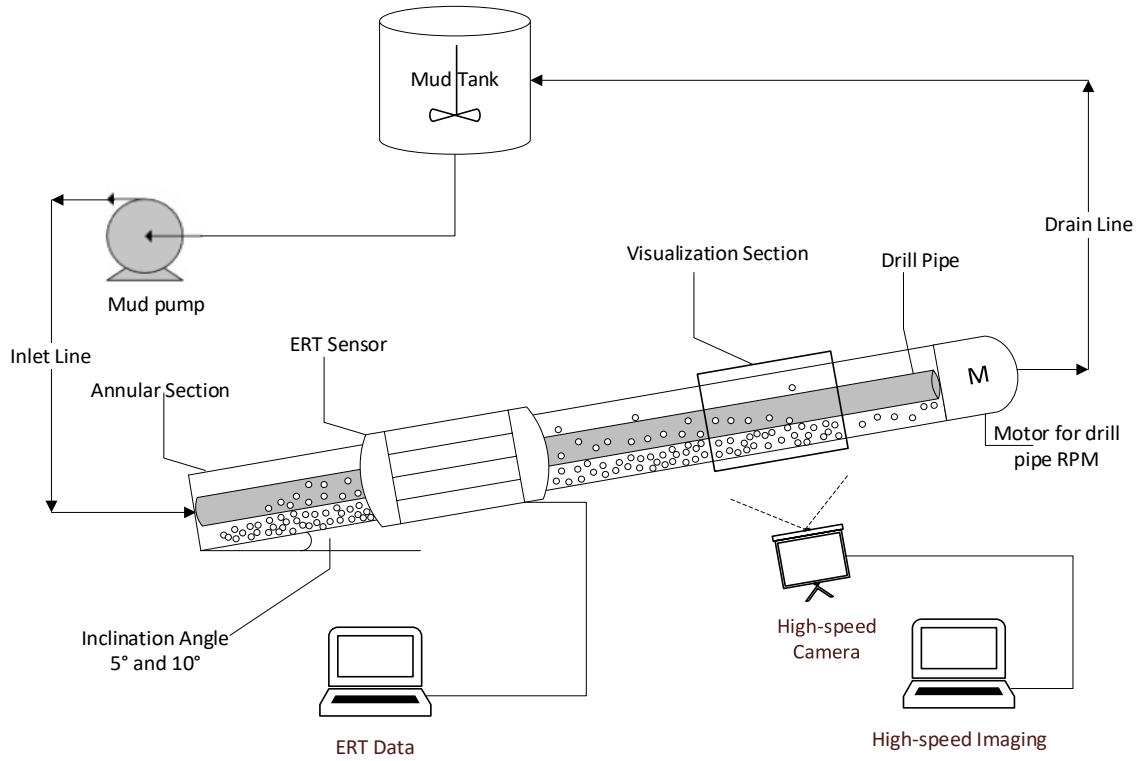


Figure 5-1: Schematic of experimental test section

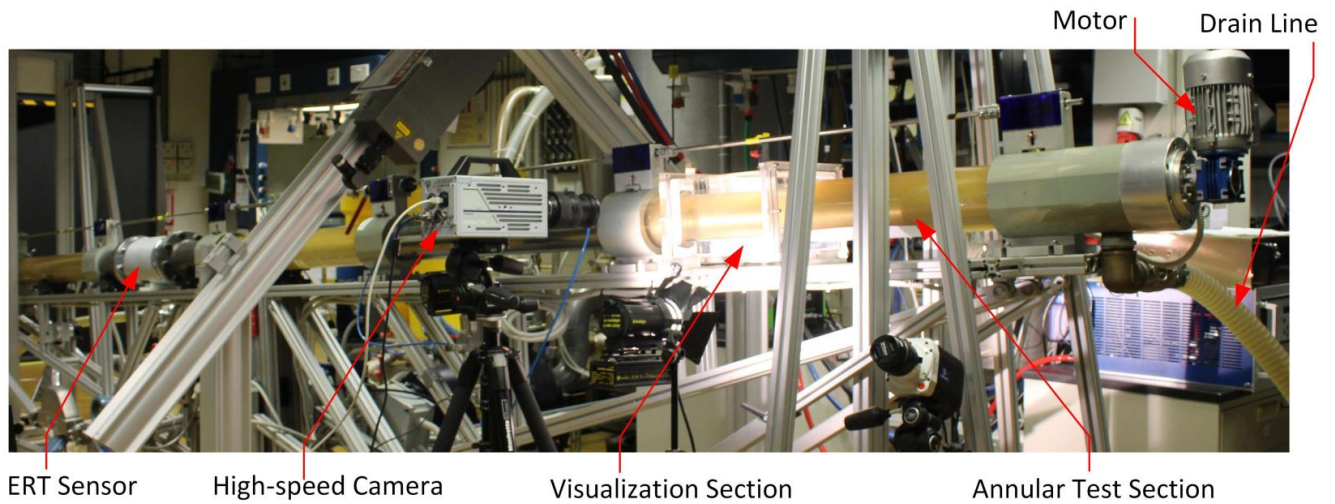


Figure 5-2: Actual lab image during an experiment

Figure 5-3 shows the visualization section. The visualization section is made of an acrylic chamber around the test section. The void space between the acrylic chamber and outer pipe is filled with

glycerin to minimize the parallax error and adjust refraction. Two measurement scale were set on the side of the visualization section to measure the solid bed height.

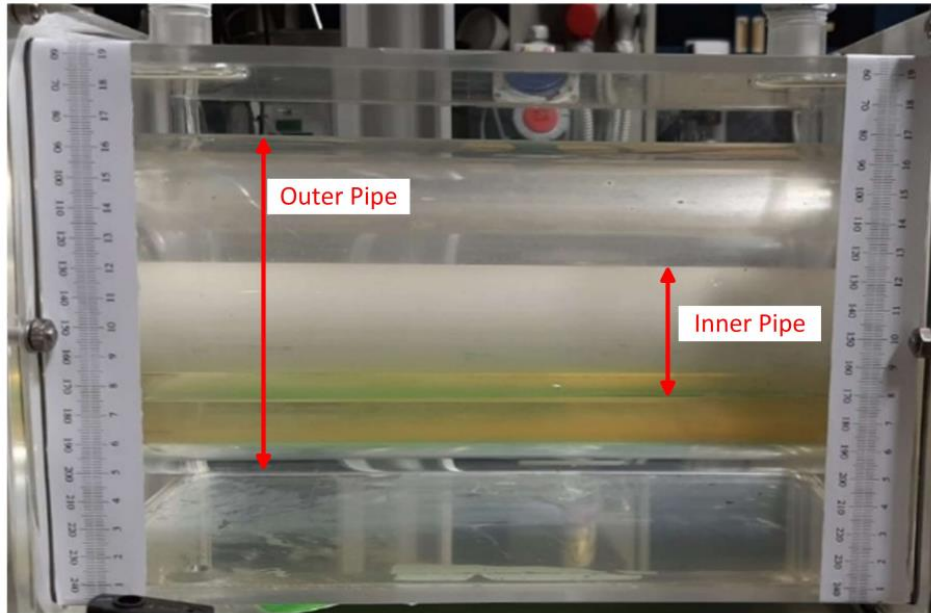


Figure 5-3: Visualization section

The experiment began with preparing the 80-litre of drilling mud with a commercial grade biopolymer at different concentrations (0.05, 0.075, 0.125 wt%) in a mud mixing tank. Once mud was prepared, then it was transferred to the main tank. This process was continued until a total of 300-litres of mud were transferred into the main tank. Solid cuttings were directly added into the main mud tank. Initial experimental work started with commercial grade spherical, well sorted solid glass beads of size 3.00 mm as drill cuttings. However, after a series of experimental study, it showed that solid glass beads size slightly decreased due to erosion. There is a slide variation among the cuttings size that cannot be distinguishable using a typical lab scale sieve analyzer. To mitigate this issue, high speed image processing and visual observation method were employed. Random sampling of 510 solid cuttings were captured from different experiment. Solid cuttings size distribution of 510 cuttings is shown in **Figure 5-4**. Since most of the particles fall within a

very narrow size window, so we have used a regular plot instead of typical semi-log representation of particle size distribution. Solid size distribution shows that almost two-third of the particles are within the size range of 2.8 mm to 3.00 mm.

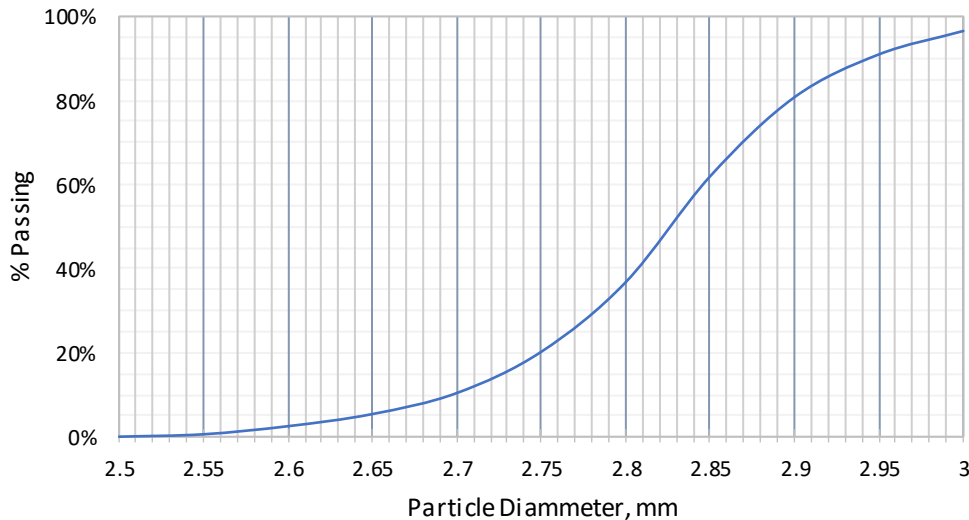


Figure 5-4: Particle size distribution

An agitator was used in the main tank to prepare a homogeneous mixture of cuttings and drilling fluid. The slurry was then pumped to the annular test section. A Coriolis flowmeter was used to measure the mass flow rate of slurries. The inline data acquisition system continuously monitors the mass flow rate of the slurry pump at different operating condition. A TightVNC viewer lab-view interface continuously record all operating conditions such as mass flow rate, agitator RPM, slurry pump RPM, inclination, eccentricity, temperature etc. for any experimental run. To ensure the repeatability of the system, several repeatability tests were performed to verify the pump mass flow rate and ERT data acquisition system. **Figure 5-5** shows a comparison of mass flow rate for at different mud pump RPM and inner pipe rotation. For all slurry pump rates, stationary drill pipe condition shows a slightly higher mass flow rate than compared to a rotating drill pipe condition.

Comparison of mass flow rate at different drill pipe rotation implies that slurry pump can deliver almost a constant throughput regardless of downstream condition. Another repeatability test on the ERT system at different inclination is discussed later in this manuscript in the ERT data analysis section.

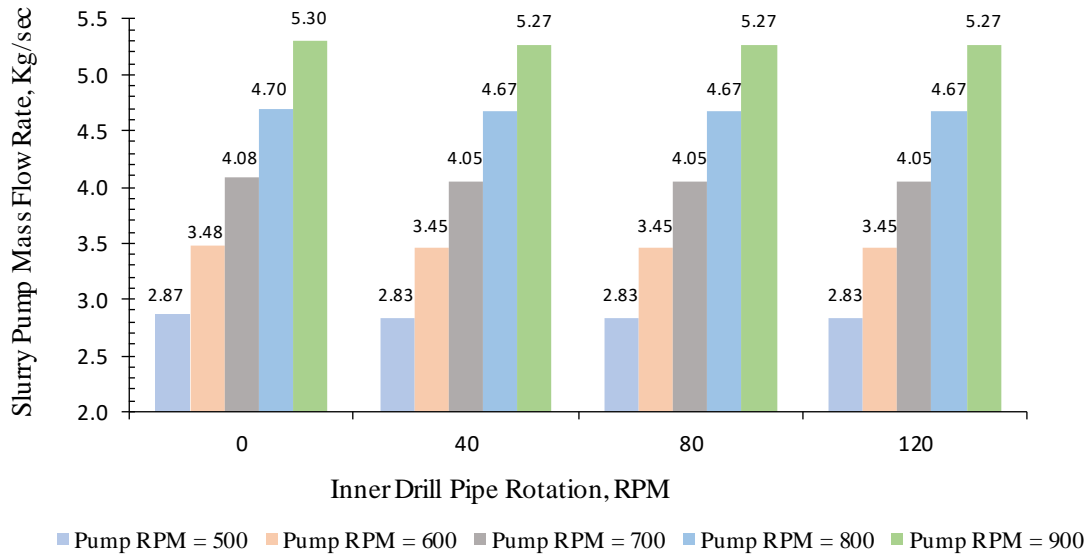


Figure 5-5 : Pump mass flow rate at different slurry pump rates and drill pipe rotations

As the slurry pump was continued running, the two-phase mixture was drained to the return line from the test section and sent back to the main mud tank. Solid are settled down at tank bottom due to gravity while agitator is turned off. Two principal apparatus were used for data acquisition in this study: i) ERT system and ii) High-speed camera.

5.2.1 ERT System

The ERT system (Qureshi et al., 2021, 2019; Raza et al., 2019) measures the in-situ solid cuttings volume fraction from the annular test section in the presence of drilling mud. Drilling mud is assumed as a conductive phase, and solid cuttings are the non-conducting phase of electrical

current. ERT system used a conductivity-concentration model (Beck and Williams, 1995) to obtain solid concentration from conductivity data of a flowing two-phase flow.

Figure 5-6 shows a schematic of the working principle of ERT system. ERT section consist of two parallel circular sensing electrode section with 16 electrodes per sensor. These circular cross sections are used to measure instantaneous real-time conductivity of the medium (air, liquid, solid etc.) flowing inside the ERT section. These electrodes can be used to inject and detect current and creates an electrical sensing field within the cross section. This electrical field does not interrupt the movement of solid or liquid inside the sensor hence the data acquisition with ERT is completely non-intrusive method.

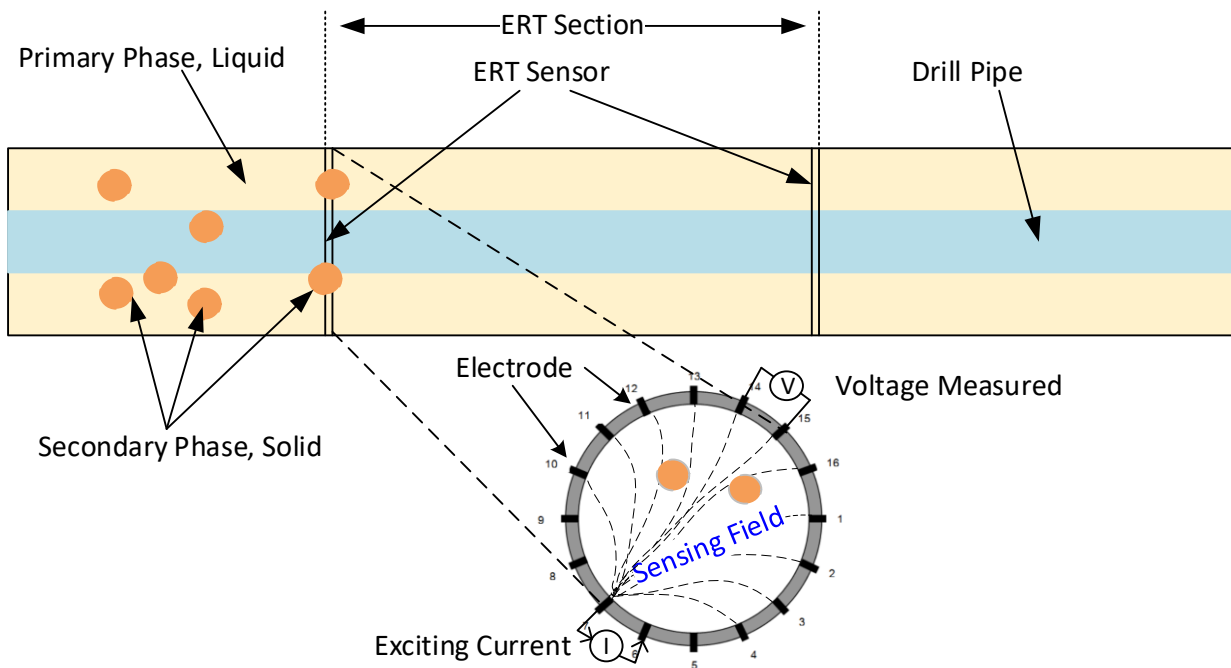


Figure 5-6: Schematic of ERT sensor

ERT sensor continuously measures the reference voltage difference between the electrodes for the primary phase (liquid). Any presence of secondary phase impact the electrical field within the ERT

section and cause a change in measured electrical voltage signal. A data acquisition software is used to control and visualize the output of ERT system.

A built-in algorithm in ERT system process electrical voltage signal into conductivity data. Finally, ERT system use the maxwell's equation to generate conductivity into concentration data by using the Equation (5-1).

$$\alpha = \frac{2\sigma_1 + \sigma_2 - 2\sigma_{mc} - \frac{\sigma_{mc}\sigma_2}{\sigma_1}}{\sigma_{mc} - \frac{\sigma_2}{\sigma_1}\sigma_{mc} + 2(\sigma_1 - \sigma_2)} \quad (5-1)$$

where α is the volume fraction of the dispersed material; σ_1 refers to the conductivity of the continuous phase, mS/cm; σ_2 represents the conductivity of the dispersed phase, mS/cm; and σ_{mc} is the reconstructed measured conductivity, mS/cm. For a non-conducting solid material, Equation (5-1) can be simplified into the following form:

$$\alpha = \frac{2\sigma_1 - 2\sigma_{mc}}{\sigma_{mc} + 2\sigma_1} \quad (5-2)$$

5.2.1.1 ERT System Calibration

Prior to data collection, ERT system requires a through calibration with the reference fluid. In this study, drilling mud was used as reference fluid or primary fluid. In the calibration process, the annular test section kept full of the drilling mud by continuously running the mud pump. Agitator was kept in shut down condition to allow only drilling mud in the annular section. Once liquid flow is stabilized, ERT system injects a reference current signal between a pair of electrodes and measure the resultant change in voltage between electrodes in the presence of primary fluid (drilling mud) and the inner pipe. This calibration process continued for at least three times to check for any discrepancy. The data processing system evaluates the reference current value and voltage value. Finally, ERT system saves the reference fluid data such as conductivity, voltage

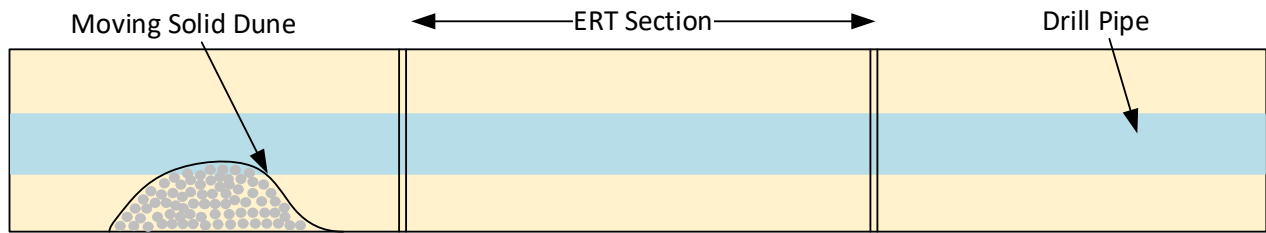
difference, injecting current, reference environment etc. for the subsequent experiment with two phase flow. Once the calibration is completed, the system is ready for secondary phase's conductivity and concentration measurement.

The conductivity of the drilling mud was tested in the laboratory and measured value was set as 0.1 mS/cm in the ERT system as reference fluid (or primary fluid) conductivity. Solid glass beads are non-conductor of electricity and hence conductivity of solid cuttings (secondary phase) set as 0 mS/cm. In absence of any solid cuttings, ERT system only record the conductivity of the reference fluid. When a two-phase mixture/ slurry crosses the ERT sensor, it shows a decrease in overall conductivity of the mixture/ slurry due to the presence of solid or non-conducting phases.

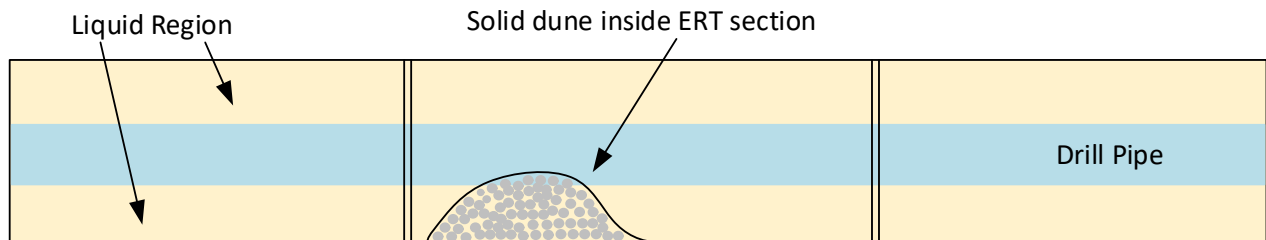
5.2.1.2 Estimating solids concentration using ERT Systems

Figure 5-7 shows a schematic of a solid dune crossing the ERT section with three distinct situations: solid dune prior to the ERT section, solid dune inside ERT section and solid dune left ERT section. **Figure 5-8** shows the corresponding conductivity and concentration profile of ERT data acquisition system for fluid LV. The conductivity profile is represented by a dotted line in the figure and concentration profile represented by a solid line. **Figure 5-7** and **Figure 5-8** shows three distinct situations.

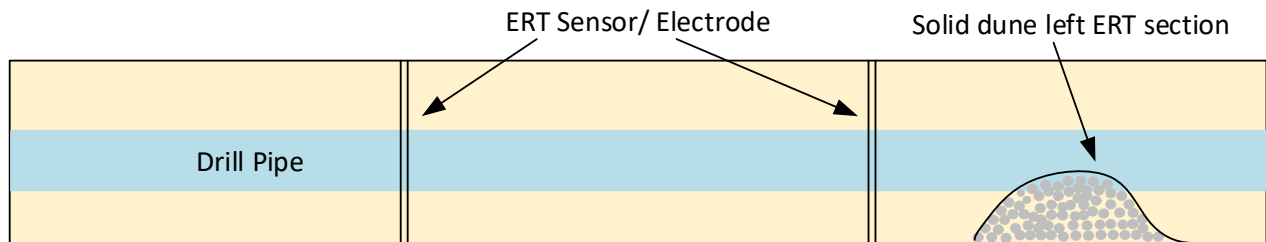
Case 1: A solid dune is formed prior to the ERT section and is moving towards the ERT. **Figure 5-8** shows that at the beginning of the data acquisition (time = 0 sec), there is only drilling fluid flowing inside the ERT sensor. ERT measured the conductivity of the drilling mud as 0.1 mS/cm. It shows almost a constant value of conductivity upto 40 seconds. **Figure 5-8** also shows that the secondary phase concentration is zero.



Case 1: Only liquid inside the ERT section. Solid dune did not reach to ERT.



Case 2: Both solid dune and liquid inside the ERT section.



Case 3: Solid dune left ERT section and only liquid inside the ERT section.

Figure 5-7: Solid dune movement inside the annular section

Case 2: Solid dune inside the ERT section. **Figure 5-8** shows that at 40 seconds, solid dune enters the ERT system. This cause steady decrease in conductivity of the medium upto 55 seconds and then again gradual increase in conductivity until 110 sec as dune leaving ERT section. ERT system measure the conductivity and generates the corresponding concentration of the secondary phase (solid). The concentration profile shows the mirror image of the conductivity profile. A decreasing the conductivity implies an increase in solid or non-conducting phase. Solid concentration start

increasing from 40 seconds to 55 seconds and then a gradual decrease upto 110 seconds. The area under the concentration curve implies the average solid concentration in the system.

Case 3: Solid dune left the ERT section **Figure 5-8** also shows that after 110 sec, solid dunes left the ERT system and conductivity becomes steady again like the initial conductivity. Solid concentration again dropped to zero.

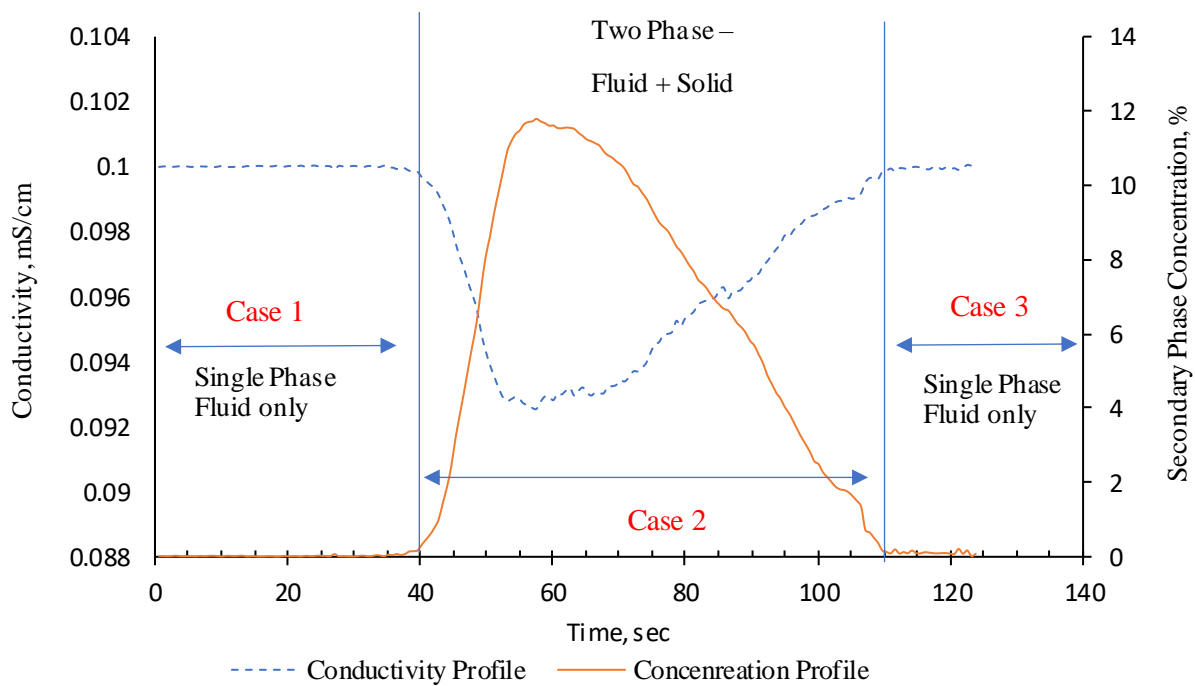


Figure 5-8: Conductivity and concentration profile

5.2.1.3 ERT Tomogram

Beside the numerical data acquisition, ERT system also generates instantaneous conductivity and concentration tomogram. The tomographic image can be used to identify the approximate location of primary and secondary phase. This is extremely beneficial where a direct visual observation or visualization method is not available. **Figure 5-9** shows the conductivity tomogram. The

transport mechanism. It shows that a thick stationary solid bed is formed at the bottom with red colour. The dark blue colour at the top shows the presence of liquid phase. There is also a relatively thin green areas which in the interface between solid and liquid zone. This also known as the moving cuttings bed which helps in moving the stationary solid cuttings.

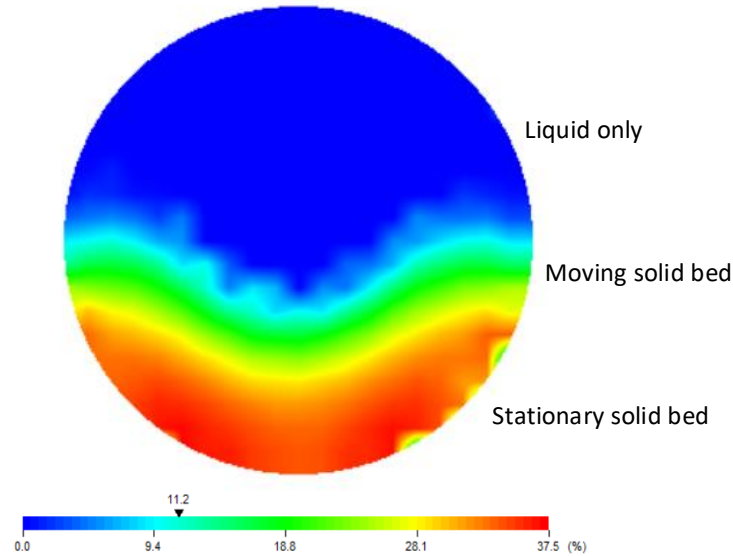


Figure 5-10: ERT concentration tomogram of solid and liquid phases

5.2.2 High-Speed Visualization

FASTCAM SA3 model 120K-M3 high-speed camera was used to capture solid movement patterns from the visualization section. The effect of fluid velocity, fluid rheology and drill pipe rotation were considered in high-speed visualization. The shutter speed was set as $\frac{1}{2000}$ sec. Several videos of 3.03 seconds durations were captured corresponding to 5427 frames of image for each experimental run. Each video was captured at a resolution of 1024 X 1024 pixels. Experimental study showed that this resolution was sufficient to capture individual solid movement patterns. Photron FASTCAM Viewer software were used for image processing. This allows a precise analysing of slow-motion video by further adjusting the frame rate (frame per second, fps) for the

video playback. A typical image processing interface is shown in **Figure 5-11**. Two studio-grade flashlights were also used to adjust the lighting of the visualization section. Besides the high-speed visualization, a DSLR camera was also used in this study to monitor the solid dune height.

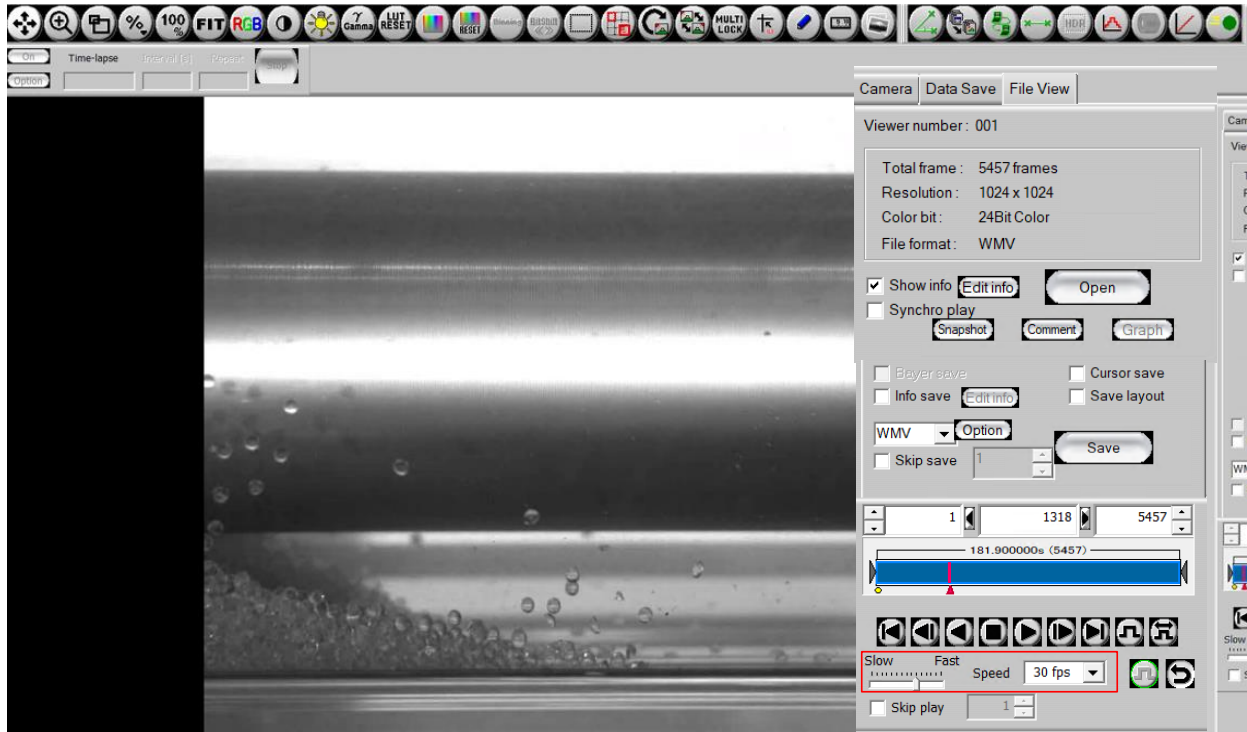


Figure 5-11: High speed image processing interface

5.2.3 Fluid Rheology

In this experimental study, a commercial grade biopolymer (Xanthan gum) was used as drilling mud due to the transparent nature while maintaining the sufficient fluid viscosity for cuttings transport. This transparent behavior helps in observing the cuttings movement pattern with a high-speed camera. Three different fluids (LV, MV and HV) were prepared in the lab by mixing water with biopolymer at different concentrations where fluid LV contains the least amount, and fluid HV contains the highest amount of polymer. Fluid rheology was tested in the lab with Grace M3600 rotational viscosity meter. This viscosity meter can support rotational speed as high as 600

RPM and as low as 0.1RPM which allows a precise estimation of fluid rheology at low shear rate.

The shear stress vs. shear rate curve for all three fluids are plotted in **Figure 5-12**.

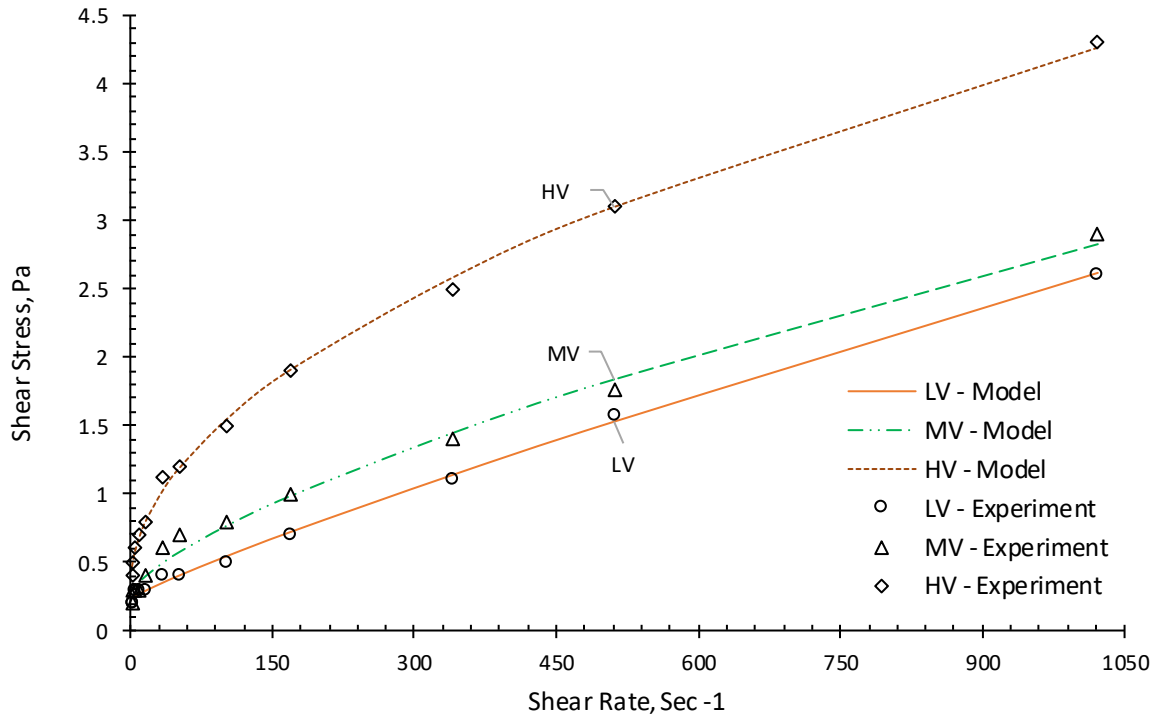


Figure 5-12: Fluid rheology analysis

A non-linear curve fittings model with spreadsheet solver is used to estimate the unknown parameters of the fluid from the experimental data. The respective models are plotted by a continuous line in **Figure 5-12**. The fluid rheology test showed a power law fluid behavior for all three fluids, with a small intercept in the shear stress axis. For this reason, it can be assumed that all three fluids exhibit a Herschel-Bulkley fluid behavior with a yield stress T_0 . The details of fluid rheology are shown in **Table 5-1**. Data showed that an increase in polymer concentration indicates more viscous and non-Newtonian behavior.

Table 5-1: Fluid rheology test summary

Fluid Properties	Fluid Name		
	LV	MV	HV
Polymer Concentration (wt %)	0.05	0.075	0.125
Yield Stress, T_o (pa)	0.229	0.234	0.308
Consistency Index, k (Pa·s ⁿ)	0.005	0.020	0.116
Flow Behavior Index, n	0.878	0.702	0.510
R-squared, R ²	0.997	0.998	0.999
Apparent Viscosity, mPas	2.15	2.54	3.89
Hedstrom Number, He	127,845	93,600	52,526

Hedstrom number can be defined as

$$He = \frac{(\rho \cdot D^2) \cdot \tau_o}{\mu^2} \quad (5-3)$$

Where, He is Hedstrom number (dimensionless), ρ is the mass density of fluid (kg/m³), D is the diameter (m), τ_o is the yield stress of fluid (N/m²) and μ is the dynamic viscosity of the fluid (kg/m·s)

5.2.4 Experimental Matrix

The experimental test matrix for this study is shown in **Table 5-2**. Mud pump can deliver the fluid at a velocity ranging from 0.482 m/s to 0.818 m/s in the annular section. Four different drill pipe rotational conditions (0, 40, 80 and 120 RPM) were used for each flow rate. Eccentricity was set at zero, and the solid input fraction was kept at 4% (w/w) for all test cases. Two different inclination (5° and 10°) were considered in this study. Most of the operating condition for fluid LV and MV showed that a turbulent flow regime exists in the system whereas fluid HV shows a transitional behavior. An increase in the fluid viscosity significantly decreases the Reynolds number, as shown by the last column of **Table 5-2**.

The generalized expression of Reynolds number for Herschel-Bulkley can be defined by Madlener et al. (2009) as

$$Re_{genHB} = \frac{\rho \bar{u}^{2-n} D^n}{\left(\frac{\tau_o}{8}\right) \left(\frac{D}{\bar{u}}\right)^n + K \left(\frac{3m+1}{4m}\right)^n 8^{n-1}} \quad (5-4)$$

$$with \quad m = \frac{nK \left(\frac{8\bar{u}}{D}\right)^n}{\tau_o + K \left(\frac{8\bar{u}}{D}\right)^n} \quad (5-5)$$

where ρ and \bar{u} introduce the density and velocity of the fluid, and R_h stands for the hydraulic radius of the test section. The remaining parameters are related to the Herschel-Bulkley fluid properties. Tang et al. (2019, 2016) proposed the modification of the expression of Reynolds number for the annular flow as

$$Re_{Ann-HB} = \frac{\rho \bar{u}^{2-n} D^n}{\left(\frac{\tau_o}{8}\right) \left(\frac{D}{\bar{u}}\right)^n + K \left(\frac{a_f + b_f m}{m}\right)^n 8^{n-1}} \quad (5-6)$$

Where annular parameters (a_f and b_f) can be approximated as: $a_f \approx 0.5$ and $b_f \approx 1$ for the annular diameter ratio greater than 0.3. Tang et al. (2019) reported the maximum errors of 3% will be caused by using the approximated values for a_f and b_f .

Table 5-2: Experimental test matrix

Matrix No	Fluid	Inner Pipe Rotation (RPM)	Flowrate, (m/s)	Inclination (θ)	Total Test	Re (min-max)
1	LV	0, 40, 80, 120	0.482, 0.571, 0.651, 0.717	0, 5°, 10°	48	2784-5097
2	MV	0, 40, 80, 120	0.571, 0.651, 0.717, 0.818	0, 5°, 10°	48	2564-4406
3	HV	0, 40, 80, 120	0.717, 0.818	0, 5°, 10°	24	1831-2255

Solid glass beads were chosen to replicate cuttings for this experimental study since glass beads shows a representative density of sandstone cuttings. Solid glass bed with spherical shape minimizes the equipment from internal scratch. Cuttings size lower than 1 mm tends to clog the pump and flow meters. A higher cuttings size (5 mm and above) may cause a high impact force

on the equipment and the visualization section. So, 2.5-3.0 mm spherical solid particles were used as cuttings in this experiment. The experimental setup and cuttings details are listed in **Table 5-3**.

Table 5-3: Experimental set up and cuttings properties

Name	Value
Test section length, m	6.16
Inner pipe diameter (D_i), mm	63.5
Inner pipe material	Aluminum
Outer pipe diameter (D_o), mm	114.3
Outer pipe material	Acrylic
Hydraulic diameter ($D_o - D_i$), mm	63.5
Diameter ratio, D_i/D_o	0.56
Cuttings size, mm	2.5-3.0
Cuttings shape	Spherical
Cuttings density, kgm^{-3}	2650
Mud density, kgm^{-3}	1000
Mud conductivity, mS/m	0.1
Cutting conductivity, mS/m	0

5.3 Results and Discussion

This section summarizes the result from the experiment. Experimental results are presented in three groups. i) High-speed camera visualization of cuttings movement ii) Solid bed height estimation from video camera and time estimation from ERT, and iii) Comparison of annular solid cuttings volume fraction data from ERT system.

5.3.1 Visualization Study

High speed camera was used to visualize the impact of fluid velocity and fluid rheology on solid transport in inclined well.

5.3.1.1 Visualization of the Effect of Fluid Velocity

Figure 5-13 shows the effect of mud velocity in cuttings transport with fluid ‘MV’ in a 10° inclined well configuration. The drill pipe was kept in a stationary position to minimize the effect of drill pipe rotation. Four different fluid velocities, 0.571 m/s, 0.651 m/s, 0.717 m/s and 0.818 m/s were tested for this case. The corresponding schematic diagram is shown in **Figure 5-14**.

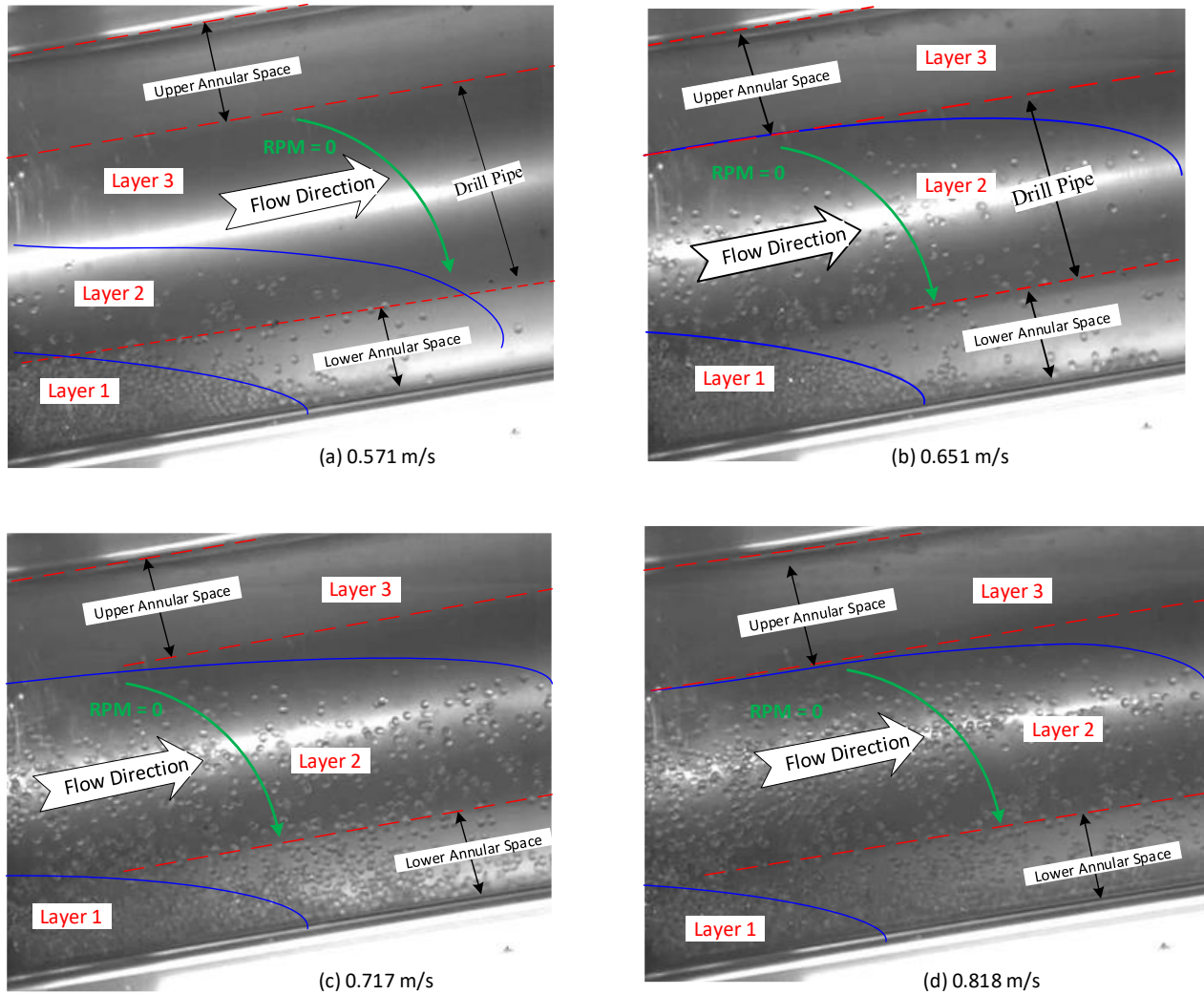


Figure 5-13: Effect of fluid velocity on cuttings transport in 10° inclined well.

At low mud velocity (0.571 m/s), visualization images showed that there is a stationary solid bed at the lower annular section. At this point, the cuttings transport mechanism is mostly by the rolling mechanism. Some rolling particles, a stationary bed and a cuttings free region were observed at this velocity as shown in **Figure 5-13** (a). This can be represented as mechanistic three-layer model behavior. Three layers are i) a stationary cuttings bed, ii) a rolling cuttings region, and iii) a cuttings free region. In this case, fluid drag force was higher than particle resistance force due to gravity.

Particles located at the outer surface of the sand dune was start moving and sliding over the dune outer surface. Since cuttings surface were not smooth enough for sliding, with an increase in fluid drag force converted the sliding behavior into rolling motion. Few solid from top of the stationary bed roll over and move forward in the direction of fluid flow. Therefore, the solid dune is moving forward slowly. The thickness of the 'rolling cuttings region' indicates the strength of cuttings transport as shown in **Figure 5-14** by Layer 2.

A thick rolling cuttings region in Layer 2 demonstrates that many cuttings are moving together and better hole cleaning. A thin rolling cuttings region is often associated with low mud velocity. An increase in mud velocity initiates increase in the thickness of the region of the rolling cuttings in Layer 2 and decreasing stationary solid bed thickness in Layer 1. Further increase in mud velocity, it showed that more solid particles were suspended into the drilling mud and gradually the stationary bed had been diminishing as shown in **Figure 5-14** (d). Suspension is an excellent form of cuttings transport mechanism. Cutting suspension capability largely depends on the cuttings size, fluid drag and fluid viscosity. Suspension mechanism is a balance between fluid drag and gravity force. If the gravity force is less or negligible compared to the fluid drag, cuttings can be suspended into the drilling mud. Also, a viscous mud with sufficient gel strength aids in cuttings suspension. The comparison of these four images in **Figure 5-13** shows the effectiveness of mud velocity in cuttings transport in inclined well.

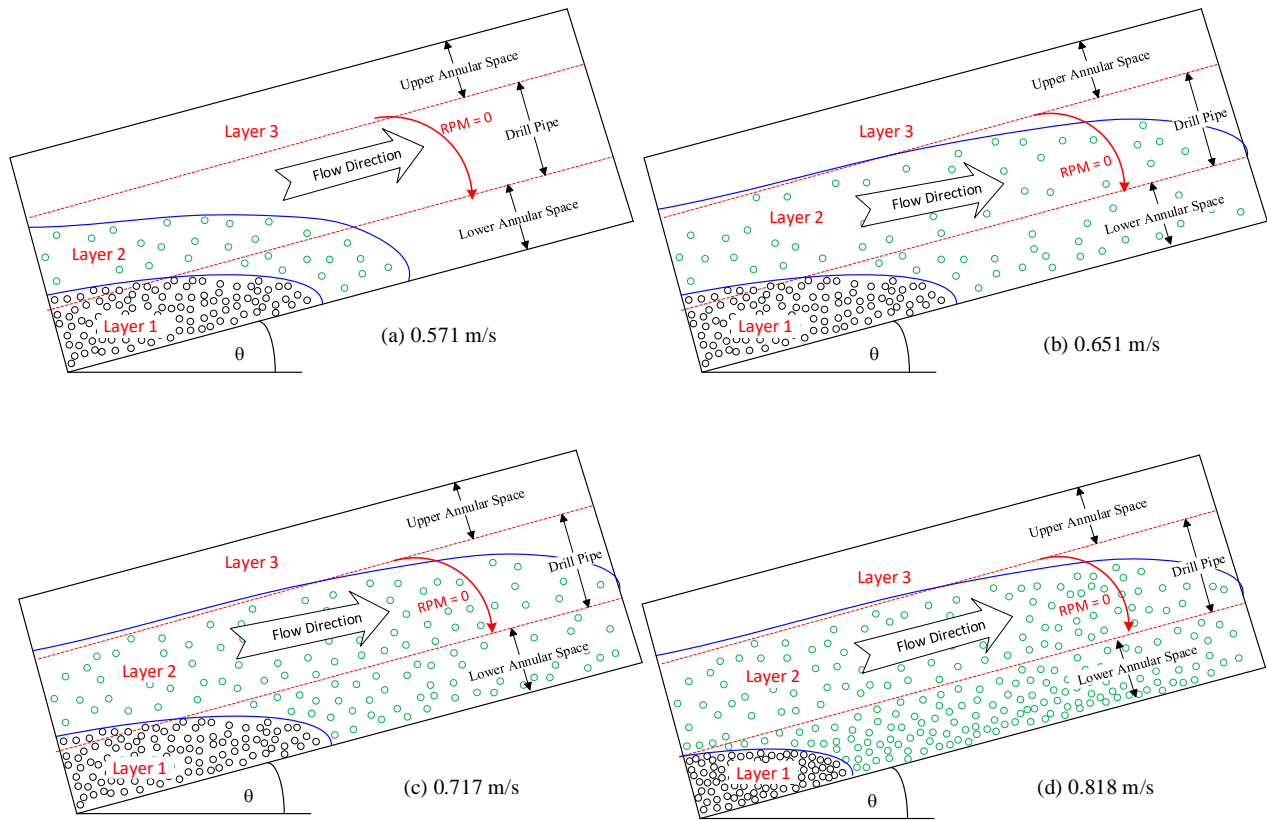


Figure 5-14: Schematic of solid transport in inclined well with change in mud velocity.

5.3.1.2 Visualization of the Effect of Drill Pipe Rotation

To observe the effect of inner pipe rotation on solid transport mechanism, we first investigated the solid transport mechanism for a stationary inner pipe condition and then compared the flow pattern with a rotating inner pipe. High-speed camera visualization for solid particle movement patterns for a stationary inner pipe condition with a 5° inclination is shown in **Figure 5-15**. In this case, solid particles are moving by drag force due to the fluid velocity. Four distinct solid movement patterns were observed from the visualization: i) A stationary bed, ii) rolling particles over the stationary bed, iii) particles sliding backward, and iv) suspended particles.

One remarkable characteristic of cuttings transport in inclined well is that there is a backward movement of some cuttings at the dune front and these cuttings are accumulated with the stationary

cuttings bed. High-speed camera visualization shows that the intensity of backward particle movement largely depends on the fluid velocity, fluid viscosity and inclination. Backward movement largely observed with a least viscous fluid and higher inclination. A less viscous fluid shows the poor suspension capability of solid cuttings and some of the solid cuttings tends to settle down in the lower section at the dune front. Finally, solid cuttings at dune front tends to roll back due to the gravity effect. Also, solid cuttings show a higher tendency in moving backward for an increase in inclination from the horizontal position.

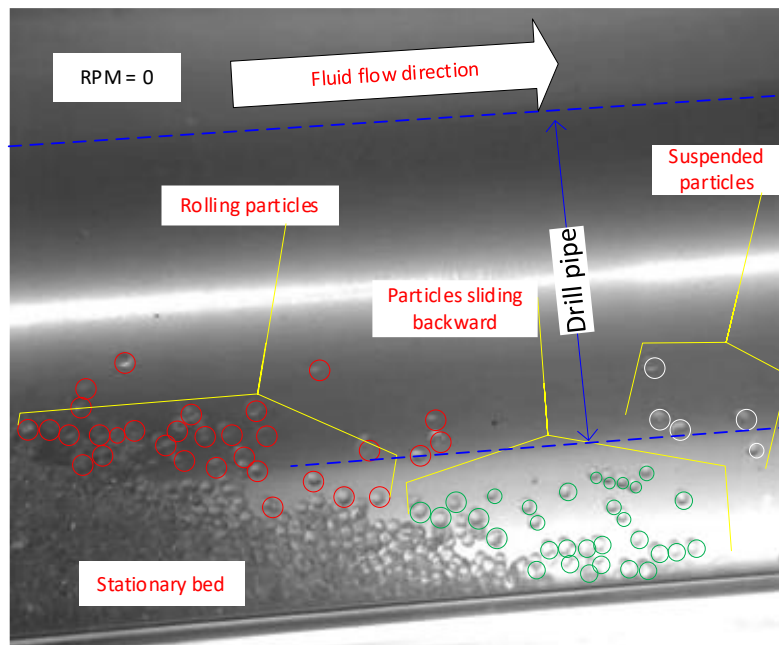


Figure 5-15: High-speed camera visualization of solid particles movement (RPM = 0)

However, increasing the fluid velocity, backward movement trend is less due to the high drag force on the particles by fluid motion. Also, an increase in fluid viscosity reduces the backward movement characteristics since a high viscous fluid can carry more solid in the suspended form, and there is less slip between solid and drilling fluid. A schematic of cuttings movement patterns in inclined well with no drill pipe rotation is shown in **Figure 5-16**.

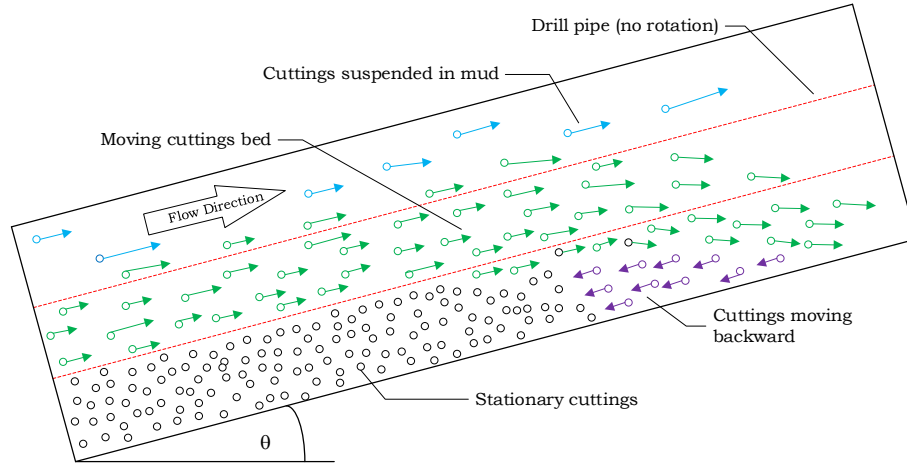


Figure 5-16: Cuttings moving in inclined well with no inner pipe rotation.

Figure 5-17 shows a high-speed camera image of 5° inclined well with an inner pipe rotation, and **Figure 5-18** shows a schematic of the cuttings movement pattern with drill pipe rotation. Like the static inner pipe condition, a stationary bed, rolling particles and backward particles flow were also observed. However, imposing the inner rotation made a distinct change in the movement pattern.

A helical movement of cuttings was observed with imposing inner pipe rotation. This helical motion was developed as a resultant behavior of the axial drag force of the fluid and rotational movement of the drill pipe. Few solid particles were rolling around the drill pipe as upward helical motion. Garcia-Hernandez et al. (2007) also reported this behavior in their study. Solid particles (top layer of the stationary sand dune) in contact with drill pipe get momentum to flow when the drill pipe is in motion. For this reason, a rotating drill pipe shows less solid bed height and aids in cuttings transport.

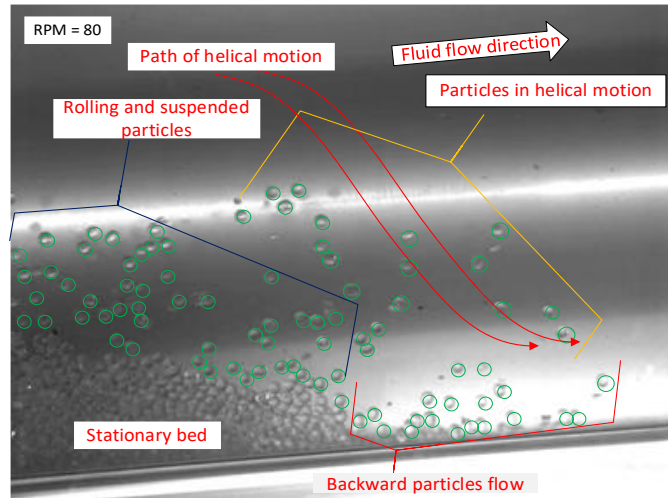


Figure 5-17: Inclined well with inner pipe rotation.

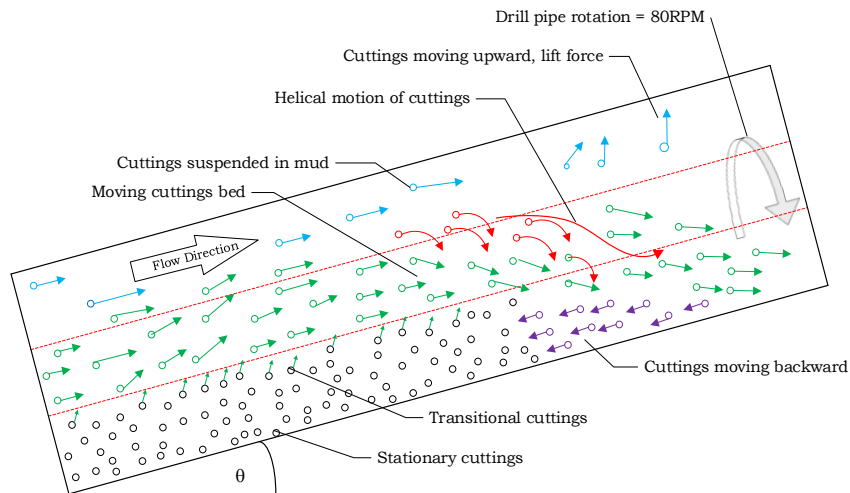
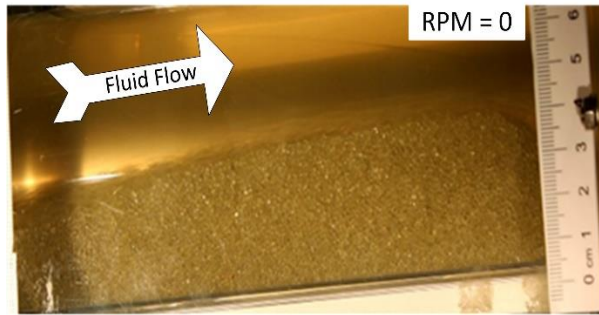
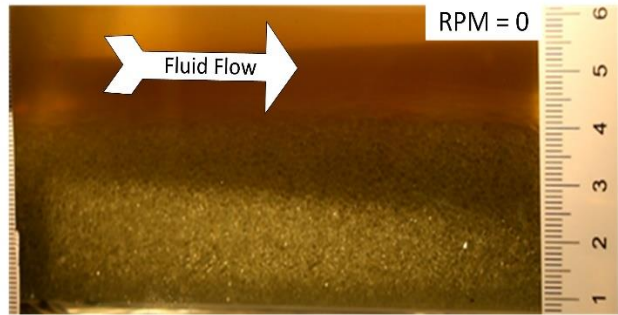


Figure 5-18: Schematic of cuttings transport in inclined well with inner pipe rotation

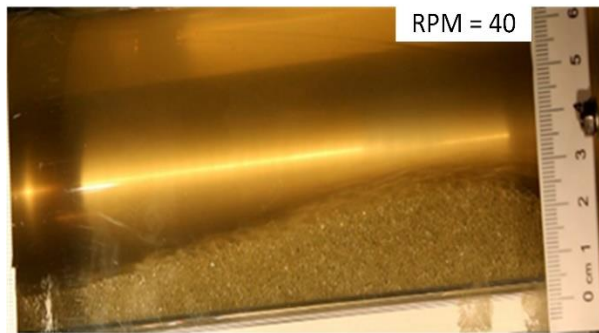
Figure 5-19 shows the effect of drill pipe rotation on solid dune height with fluid ‘LV’ at 5° inclination and horizontal position. These images were captured from the DSLR camera to measure the bed height. Since fluid velocity has a significant impact on solid bed movement, the effect of drill pipe rotation was tested at a comparatively low mud flow rate of 0.482 m/s to minimize the impact of fluid velocity. For 5° inclination, the highest solid bed height was estimated as 4 cm at stationary inner pipe condition.



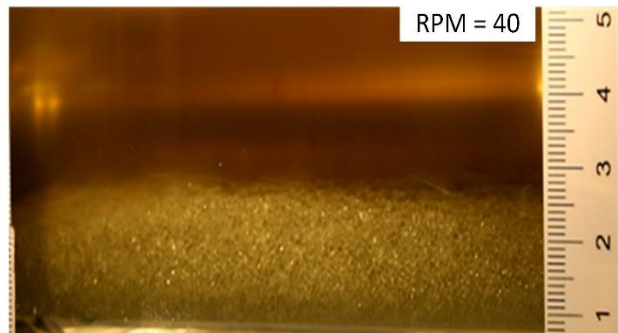
5 Inclination, 0.482 m/s, Fluid LV



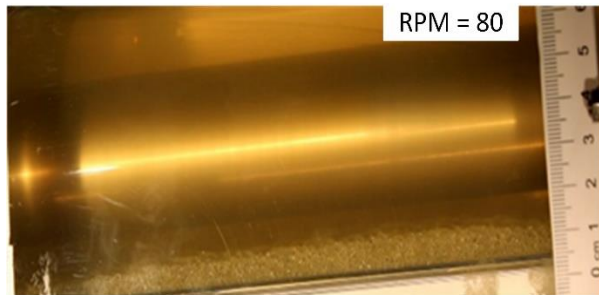
Horizontal, 0.482 m/s, Fluid LV



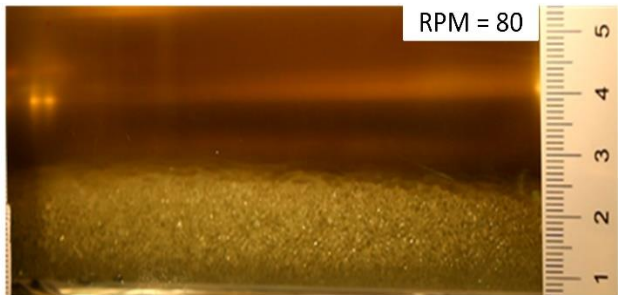
5 Inclination, 0.482 m/s, Fluid LV



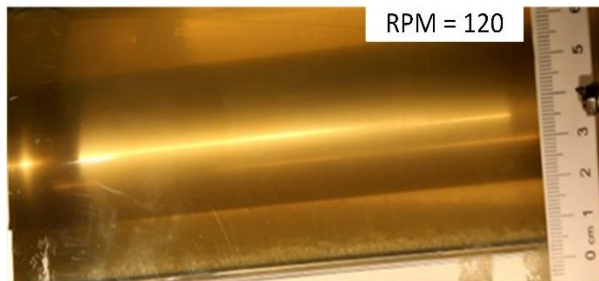
Horizontal, 0.482 m/s, Fluid LV



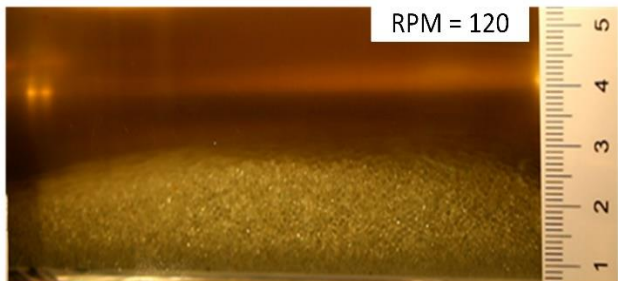
5 Inclination, 0.482 m/s, Fluid LV



Horizontal, 0.482 m/s, Fluid LV



5 Inclination, 0.482 m/s, Fluid LV



Horizontal, 0.482 m/s, Fluid LV

Figure 5-19: Change in solid bed height with drill pipe rotation for fluid LV
(Mud velocity of 0.482 m/s at 5° inclination and horizontal well configuration)

Solid dune height started decreasing with initiating drill pipe rotation. It shows the maximum bed height is about 2.7 cm for drill pipe rotation of 40 RPM, around 1 cm for 80 RPM, and less than 1 cm for 120 RPM. Imposing drill pipe rotation breaks the solid dune and move solid particles into the fluid flow stream. However, due to the inclination, some of the solid particles rolls back at low mud velocity. For horizontal well configuration, there was similar improvement in bed height from stationary position to 40 RPM, but no further improvement was observed above 40 RPM. Moreover, there is no roll back trends of solid cuttings similar to inclined position.

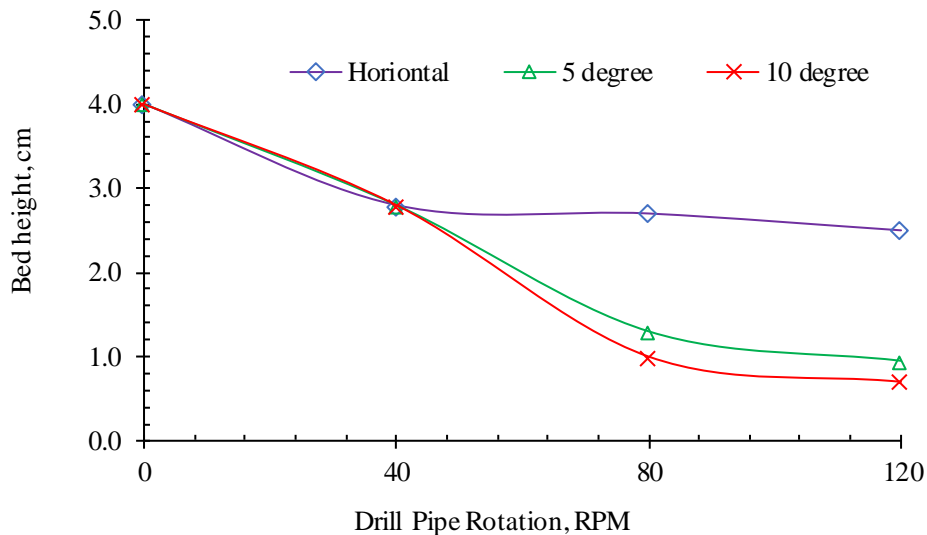


Figure 5-20: Solid bed height at different inclination angles with fluid LV

A comparison of solid bed height with drill pipe rotation at a different inclination (horizontal, 5° and 10°) is shown in **Figure 5-20**. It shows that solid bed height is approximately 4 cm at stationary inner pipe condition for all inclinations. At 40 RPM of inner pipe rotation, solid bed height is about 2.8 cm for all three-drill pipe orientation. This indicates almost 30% reduction in solid bed height from the stationary drill pipe. Further increase in drill pipe rotation showed that almost steady bed height for the horizontal annular section. However, for both inclined well configurations, solid bed

height dropped significantly with the drill pipe rotation. From visualization images and ERT data showed that a long bed with low height was formed in the lower annular section for the inclined well.

Figure 5-21 shows the time spent by a solid dune across the ERT system for two different inclinations using fluid LV. The time difference is significant at low mud velocity. Horizontal well always shows a less time compared to a near horizontal position. An increase in inclination from 5° to 10° showed a slight increase in time to move the dune in the test section for all fluid velocities. It can be concluded that drill pipe rotation has a significant positive impact on minimizing the cuttings bed height in the inclined well compared to a horizontal well. However, inclined section cleaning takes a longer time to clean with low viscous fluid.

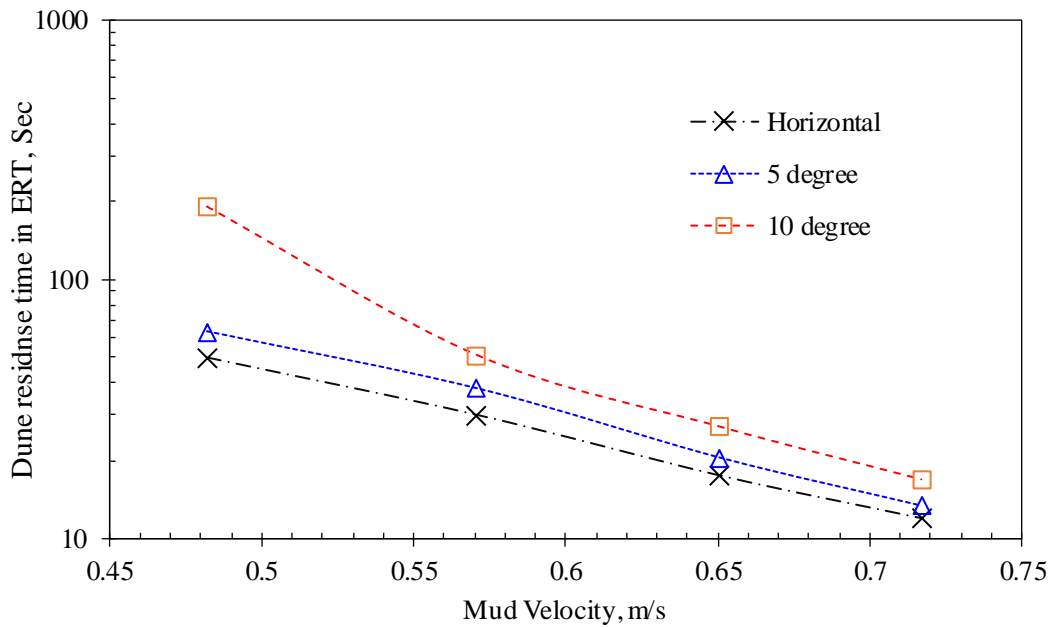


Figure 5-21: Dune moving time recorded by ERT system for fluid LV.

5.3.2 Analysis of ERT Data

Data obtained from the ERT system are presented in this section. ERT data shows in-situ cuttings volume fraction with respect to the drilling mud in the annular section. Annular cuttings volume fraction from the different operating condition are compared in this study. Several repeatability tests were performed for different drill pipe rotation and inclination to check the consistency of the result from the ERT analysis. For each set of drill pipe rotation and inclination, three separate experimental runs were performed with fluid MV and flow rate was kept approximately 0.72 m/s. Data obtained from the ERT systems are compared for each operating condition. The analysis shows that three experimental runs produced excellent repeatability in terms of annular solid volume fraction with a maximum standard deviation of 0.13 for 5°/80 RPM and a minimum of 0.05 for 10°/0 RPM condition as shown in **Figure 5-22**.

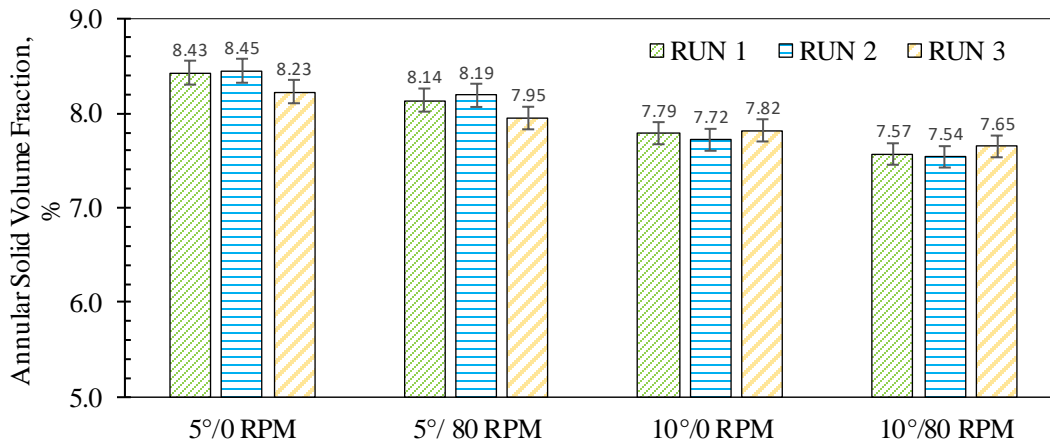


Figure 5-22: Repeatability test for different operating conditions with fluid MV at 0.7 m/s

5.3.2.1 ERT Analysis: Effect of Mud Velocity

A change in annular solid volume fraction with change in fluid velocity for fluid LV and HV are shown in **Figure 5-23**. The solid line represents the annular solid percentage with fluid LV, and

the dotted line represents fluid HV. It shows that an increase in the fluid velocity decreases the overall solid concentration in the horizontal annular section for fluid LV.

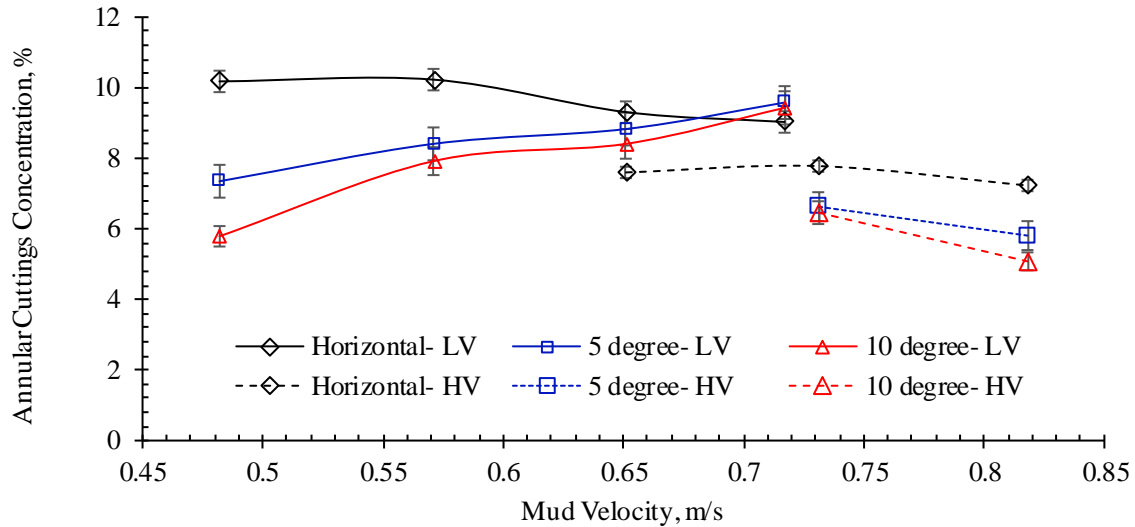


Figure 5-23: Effect of mud velocity at different inclination angles

A low-viscous fluid mainly transports solid by the rolling mechanism. The rolling particles always have a collision with stationary particles and gradually deplete its kinetic energy and finally lose its momentum to flow. A strong hydrodynamics force is required to keep solid particles in motion. Therefore, a higher fluid velocity is required to maintain the particles momentum and continue solid transport by rolling mechanism. In horizontal well, it shows that solid cutting concentration slightly decreases with increase in fluid velocity. This indicated that higher fluid velocity adds significant amount of kinetic energy that keep solid in motion. Whereas for the inclined well, at same mud velocity, a large portion of fluid momentum force devoted to overcoming the gravitational effect. The remaining momentum forces is not sufficient to clean the hole in inclined section. For this reason, there is an increasing trend of solid volume fraction with inclination when a low viscous fluid is used. However, with high viscous fluid, solid cuttings are transported via

suspension. Higher the fluid velocity indicates a higher solid are being transported and less amount of solid are entrapped in the annular section.

Experimental study showed that fluid HV required a higher pumping power and solid dune were not moving until mud velocity reached 0.65 m/s for the horizontal position. For the inclined position, it took at least 0.72 m/s mud velocity to move the dune in the annular section. Therefore, there is no experimental data point prior to this mud velocity. However, due to experimental set up restriction, it was not possible to achieve mud velocity higher than 0.82 m/s. Fluid HV showed the opposite trend in solid concentration with an increase in fluid velocity compared to fluid LV. It can be concluded that an increase in mud velocity decreases solid dune volume fraction for fluid HV in ERT system since fluid HV carries more solid as suspended form.

Also, high-speed visualization for low viscous fluid showed that rolling mechanism is dominant. Solid particles roll over stationary sand dune and increased the dune height. This shows a higher solid volume fraction estimated by ERT system. However, at high viscous fluid, suspension mechanism dominant over rolling mechanism. So, higher amount of solid were suspended into the mud. In this case, a low solid bed height was observed compared with a low viscous fluid, though fluid was carrying substantial amount of solid. A low solid bed height cause less solid volume fraction in the sand dune estimated by ERT system.

5.3.2.2 ERT Analysis: Effect of Fluid Rheology on Inclination

The effect of fluid rheology on cuttings transport in the inclined well was tested for the fluid velocity of 0.717 m/s with fluid LV and HV. Fluid rheology effect was tested for three different inclinations, horizontal, 5° and 10° deviation from the horizontal well as shown in **Figure 5-24**. These two fluids show the opposite trend in annular cuttings volume fraction with a change in

inclination. Fluid LV (less viscous) shows that any increase in inclination causes an increase in the annular solid fraction for all condition of drill pipe rotation.

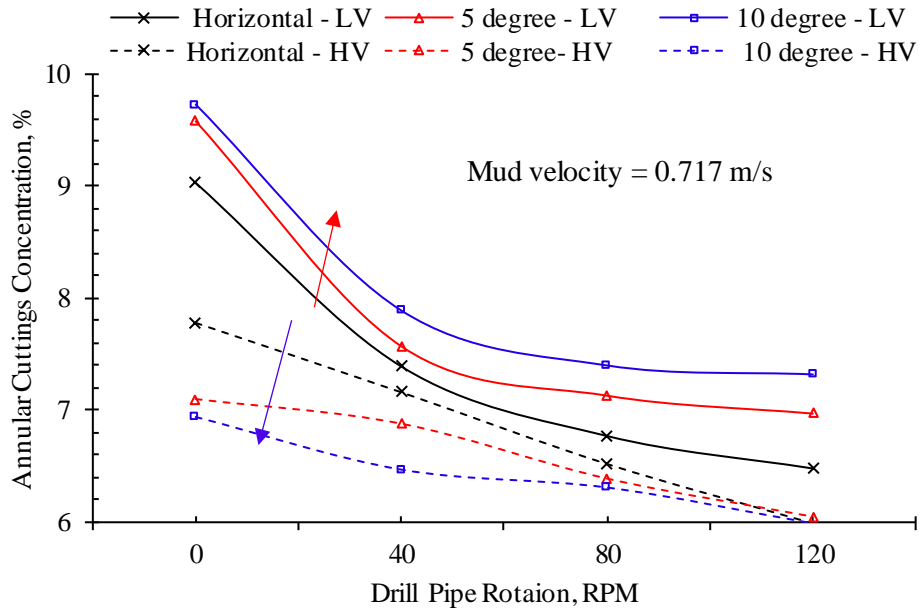


Figure 5-24: Effect of inclination on fluid rheology

Similar behavior was observed for fluid LV in **Figure 5-23** for other fluid velocities. However, fluid HV shows a decrease in solid volume fraction with an increase in the inclination. From these observations, it can be concluded that a higher viscous fluid is beneficial for the inclined well. A comparison of fluid LV and HV shows that there is a negative interaction effect (Huque et al., 2020) in cuttings transport between low viscous fluid and inclination. However, high viscous fluid shows a positive interaction effect between viscosity and inclination.

Also, fluid LV showed a significant improvement in minimizing the annular solid percentage when drill pipe rotating at 40 RPM from the stationary condition for all inclination. A slight improvement in solid fraction was observed upto 80 RPM. However, no remarkable improvement

is observed above 80 RPM. Drill pipe rotation shows less impact on cuttings transport for the viscous fluid HV.

5.4 Conclusions

A concept of in-line data acquisition of solid cuttings transport is introduced in this study using Electrical Resistance Tomography (ERT) method. This non-intrusive acquisition system can provide better understanding about solid transport behavior in a drilling operation where visual inspection is not possible. Application of sophisticated ERT system can provide an early indication of solid deposition behavior in the annular section and helps in detecting the hole cleaning problem in advance. The use of inline solid transport data acquisition system while drilling widens the scope of better control on hole cleaning strategy.

In this study, cuttings transport behavior in near-horizontal well (5° and 10° inclination from horizontal) was investigated with a high-speed camera and ERT system with three different drilling muds. Inclined well results were compared with a horizontal well. The visualization study showed different solid flow patterns in the annular section such as rolling particles, transitional particles, stationary bed, particles rolling backward, suspended particles and particles in helical motions. The analysis shows that fluid viscosity has a high impact on solid transport capability in inclined wells. Besides the visualization study, the following conclusion can be drawn from ERT data analysis.

- i. An increase in inclination ($\theta > 0$) from the horizontal position ($\theta = 0$) shows an increasing trend of annular solid volume fraction for low viscous fluid ($\mu_a = 2.15$ cP; $k = 0.005$ Pa-sⁿ), and a decreasing trend in solid volume fraction for high viscous fluid ($\mu_a = 3.89$ cP; $k = 0.116$ Pa-sⁿ). For a given mud velocity, low viscous fluid exhibits less solid suspension

capability that causes a decrease in transport efficiency against the gravitational force. The annular solid volume fraction trend shows that a higher viscous fluid performs better in cuttings transport for inclined well.

- ii. Analysis with low viscous fluid (LV, $k = 0.005 \text{ Pa}\cdot\text{s}^n$) shows that an increase in fluid velocity from 0.482 m/s to 0.717 m/s showed an increase in annular solid volume fraction from 7.35% to 9.43% for 5° inclination, and 5.8% to 9.4% for 10° inclination. Fluid velocity in the low viscous fluid has an inverse impact on hole cleaning in inclined well, and that impact increases with the inclination. (i.e. 10° inclination shows the greatest loss in cuttings transport capability with increased flow velocity).
- iii. Drill pipe rotation above 80 RPM shows approximately 70% decrease in solid bed height for the inclined well compared to a horizontal well. Drill pipe rotation breaks the solid dune and adds a momentum force to the stationary cuttings so that cuttings can move into the flowing stream. A drill pipe rotation is beneficial for the inclined well even at low mud velocity.

Acknowledgements

The researchers gratefully acknowledge and thank Equinor Canada, Memorial University, InnovateNL, and the Natural Sciences and Engineering Research Council of Canada (NSERC) to support this research work. This publication was also made possible by the grant NPRP10-0101-170091 from Qatar National Research Fund (a member of the Qatar Foundation).

Nomenclature

DSLR	Digital Single-lens Reflex Camera
ERT	Electrical Resistance Tomography
He	Hedstrom Number
HV	High Viscous Mud
LV	Low Viscous Mud
MTV	Minimum Transport Velocity
MV	Medium Viscous Mud
Re	Reynolds Number
RPM	Revolution Per Minutes

References

- Akhshik, S., Behzad, M., Rajabi, M., 2015. CFD-DEM approach to investigate the effect of drill pipe rotation on cuttings transport behavior. *J. Pet. Sci. Eng.* 127, 229–244.
<https://doi.org/10.1016/j.petrol.2015.01.017>
- Azar, J., Sanchez, R.A., 1997. Important Issues in Cuttings Transport for Drilling Directional Wells, in: *Fifth Latin American and Caribbean Petroleum Engineering Conference and Exhibition*. Rio de Janeiro, Brazil 30 August -3 September. <https://doi.org/10.2118/39020-MS>
- Barbosa, M. V., De Lai, F.C., Junqueira, S.L.M., 2019. Numerical Evaluation of CFD-DEM Coupling Applied to Lost Circulation Control: Effects of Particle and Flow Inertia. *Math. Probl. Eng.* 2019. <https://doi.org/10.1155/2019/6742371>

- Beck, M.S., Williams, 1995. Process Tomography: Principles, Techniques and Applications, 1st ed. Butterworth-Heinemann. <https://doi.org/10.1016/C2009-0-24202-4>
- Boyou, N.V., Ismail, I., Wan Sulaiman, W.R., Sharifi Haddad, A., Husein, N., Hui, H.T., Nadaraja, K., 2019. Experimental investigation of hole cleaning in directional drilling by using nano-enhanced water-based drilling fluids. *J. Pet. Sci. Eng.* 176, 220–231. <https://doi.org/10.1016/j.petrol.2019.01.063>
- Busch, A., Johansen, S.T., 2020. Cuttings transport: On the effect of drill pipe rotation and lateral motion on the cuttings bed. *J. Pet. Sci. Eng.* 191, 107136. <https://doi.org/10.1016/j.petrol.2020.107136>
- Clark, R.K., Bickham, K.L., 1994. A Mechanistic Model for Cuttings Transport, in: SPE 69th Annual Technical Conference and Exhibition. New Orleans, La, U.S.A., 25–28 September, pp. 139–154. <https://doi.org/10.2118/28306-MS>
- Epelle, E.I., Gerogiorgis, D.I., 2019. Drill cuttings transport and deposition in complex annular geometries of deviated oil and gas wells: A multiphase flow analysis of positional variability. *Chem. Eng. Res. Des.* 151, 214–230. <https://doi.org/10.1016/j.cherd.2019.09.013>
- Erge, O., van Oort, E., 2020. Modeling the effects of drillstring eccentricity, pipe rotation and annular blockage on cuttings transport in deviated wells. *J. Nat. Gas Sci. Eng.* 79, 103221. <https://doi.org/10.1016/j.jngse.2020.103221>
- Ford, J.T., Peden, J.M., Oyenyin, M.B., Gao, E., Zarrouh, R., 1990. Experimental Investigation of Drilled Cuttings Transport in Inclined Boreholes, in: SPE Annual Technical Conference and Exhibition. pp. 197–206. <https://doi.org/10.2118/20421-MS>

- Garcia-Hernandez, A.J., Miska, S.Z., Yu, M., Takach, N.E., Zettner, C.M., 2007. Determination of Cuttings Lag in Horizontal and Deviated Wells, in: SPE Annual Technical Conference and Exhibition. Anaheim, California, U.S.A., 11–14 November.
<https://doi.org/10.2118/109630-MS>
- GhasemiKafrudi, E., Hashemabadi, S.H., 2016. Numerical study on cuttings transport in vertical wells with eccentric drillpipe. *J. Pet. Sci. Eng.* 140, 85–96.
<https://doi.org/10.1016/j.petrol.2015.12.026>
- Gul, S., Kuru, E., Parlaktuna, M., 2017. Experimental investigation of cuttings transport in horizontal wells using aerated drilling fluids, in: SPE Abu Dhabi International Petroleum Exhibition and Conference. <https://doi.org/10.2118/188901-ms>
- Hakim, H., Katende, A., Sagala, F., Ismail, I., Nsamba, H., 2018. Performance of polyethylene and polypropylene beads towards drill cuttings transportation in horizontal wellbore. *J. Pet. Sci. Eng.* 165, 962–969. <https://doi.org/10.1016/j.petrol.2018.01.075>
- Heshamudin, N.S., Katende, A., Rashid, H.A., Ismail, I., Sagala, F., Samsuri, A., 2019. Experimental investigation of the effect of drill pipe rotation on improving hole cleaning using water-based mud enriched with polypropylene beads in vertical and horizontal wellbores. *J. Pet. Sci. Eng.* 179, 1173–1185. <https://doi.org/10.1016/j.petrol.2019.04.086>
- Heydari, O., Sahraei, E., Skalle, P., 2017. Investigating the Impact of Drillpipe's Rotation and Eccentricity on Cuttings Transport Phenomenon in Various Horizontal Annuluses using Computational Fluid Dynamics (CFD). *J. Pet. Sci. Eng.* 156, 801–813.
<https://doi.org/10.1016/j.petrol.2017.06.059>

- Hirpa, M.M., Kuru, E., 2020. Hole cleaning in horizontal wells using viscoelastic fluids -an experimental study of drilling fluid properties on the bed erosion dynamics, in: SPE/IADC Drilling Conference. Galveston, Texas. <https://doi.org/10.2118/199636-pa>
- Huque, M.M., Butt, S., Zendehboudi, S., Imtiaz, S., 2020. Systematic Sensitivity Analysis of Cuttings Transport in Drilling Operation Using Computational Fluid Dynamics Approach. *J. Nat. Gas Sci. Eng.* 81, 103386. <https://doi.org/10.1016/j.jngse.2020.103386>
- Kelessidis, V.C., Bandelis, G.E., 2004. Flow Patterns and Minimum Suspension Velocity for Efficient Cuttings Transport in Horizontal and Deviated Wells in Coiled-Tubing Drilling. *SPE Drill. Complet.* <https://doi.org/10.2118/81746-PA>
- Kelessidis, V.C., Bandelis, G.E., Li, J., 2007. Flow of Dilute Solid-liquid Mixtures in Horizontal Concentric and Eccentric Annuli. *J. Can. Pet. Technol.* 46, 56–61. <https://doi.org/10.2118/07-05-06>
- Kim, Y.J., Woo, N.S., Hwang, Y.K., Kim, J.H., Han, S.M., 2014. Transport of small cuttings in solid-liquid flow with inclined slim hole annulus. *J. Mech. Sci. Technol.* 28, 115–126. <https://doi.org/10.1007/s12206-013-0952-7>
- Madlener, K., Frey, B., Ciezki, H.K., 2009. Generalized reynolds number for non-newtonian fluids 1, 237–250. <https://doi.org/10.1051/eucass/200901237>
- Martin, M., Georges, C., Bisson, P., Konirsch, O., 1987. Transport of Cuttings in Directional Wells, in: SPE/IADC Drilling Conference. New Orleans, Louisiana, USA, 15-18 March. <https://doi.org/10.2118/16083-MS>

- Masuda, Y., Doan, Q., Oguztoreli, M., Naganawa, S., Yonezawa, T., Kbayashi, A., Kamp, A., 2000. Critical Cuttings Transport Velocity in Inclined Annulus: Experimental Studies and Numerical Simulation, in: SPE/CIM International Conference on Horizontal Well Technology. Calgary, Alberta, Canada, 6-8 November. <https://doi.org/10.2118/65502-MS>
- Naganawa, S., Sato, R., Ishikawa, M., 2017. Cuttings-transport simulation combined with large-scale-flow-loop experimental results and logging-while-drilling data for hole-cleaning evaluation in directional drilling. SPE Drill. Complet. 32, 194–207. <https://doi.org/10.2118/171740-PA>
- Ozbayoglu, E.M., Etehad Osgouei, R., Ozbayoglu, M.A., Yuksel, E.H., 2012. Hole-Cleaning Performance of Gasified Drilling Fluids in Horizontal Well Sections. SPE J. 17, 912–923. <https://doi.org/10.2118/131378-PA>
- Ozbayoglu, E.M., Miska, S.Z., Reed, T., Takach, N., 2003. Cuttings Transport with Foam in Horizontal & Highly-Inclined Wellbores, in: SPE/IADC Drilling Conference. <https://doi.org/10.2118/79856-MS>
- Ozbayoglu, E.M., Osgouei, R.E. et al., 2012. Hole-Cleaning Performance of Gasified Drilling Fluids in Horizontal Well Sections. SPE J. <https://doi.org/10.2118/131378-PA>
- Ozbayoglu, M.E., Saasen, A., Sorgun, M., Svanes, K., 2008. Effect of Pipe Rotation on Hole Cleaning for Water-Based Drilling Fluids in Horizontal and Deviated Wells, in: IADC/SPE Asia Pacific Drilling Technology Conference and Exhibition. Jakarta, Indonesia. 25–27 August. <https://doi.org/10.2118/114965-MS>

- Pang, B., Wang, S., Jiang, X., Lu, H., 2019. Effect of orbital motion of drill pipe on the transport of non-Newtonian fluid-cuttings mixture in horizontal drilling annulus. *J. Pet. Sci. Eng.* 174, 201–215. <https://doi.org/10.1016/j.petrol.2018.11.009>
- Pang, B., Wang, S., Wang, Q., Yang, K., Lu, H., Hassan, M., Jiang, X., 2018a. Numerical prediction of cuttings transport behavior in well drilling using kinetic theory of granular flow. *J. Pet. Sci. Eng.* 161, 190–203. <https://doi.org/10.1016/j.petrol.2017.11.028>
- Pang, B., Wang, S., Wang, Q., Yang, K., Lu, H., Hassan, M., Jiang, X., 2018b. Numerical Prediction of Cuttings Transport Behavior in Well Drilling Using Kinetic Theory of Granular Flow. *J. Pet. Sci. Eng.* 161, 190–203. <https://doi.org/10.1016/j.petrol.2017.11.028>
- Piroozian, A., Ismail, I., Yaacob, Z., Babakhani, P., Ismail, A.S.I., 2012. Impact of drilling fluid viscosity, velocity and hole inclination on cuttings transport in horizontal and highly deviated wells. *J. Pet. Explor. Prod. Technol.* 2, 149–156. <https://doi.org/10.1007/s13202-012-0031-0>
- Qureshi, M.F., Ali, M., Rahman, M.A., Hassan, I., Rasul, G., Hassan, R., 2019. Experimental investigation of multi-phase flow in an annulus using electric resistance tomography, in: *SPE Kuwait Oil and Gas Show and Conference 2019, KOGS 2019*. Mishref, Kuwait. <https://doi.org/10.2118/198011-ms>
- Qureshi, M.F., Ali, M.H., Ferroudji, H., Rasul, G., Khan, M.S., Azizur, M., Hasan, R., Hassan, I., 2021. Measuring solid cuttings transport in Newtonian fluid across horizontal annulus using electrical resistance tomography (ERT). *Flow Meas. Instrum.* 77, 101841. <https://doi.org/10.1016/j.flowmeasinst.2020.101841>

- Rasul, G., Qureshi, M.F., Ferroudji, H., Butt, S., Hasan, R., Hassan, I., Rahman, M.A., 2020. Analysis of cuttings transport and flow pattern in nearly horizontal extended reach well. *J. Adv. Res. Fluid Mech. Therm. Sci.* 71, 69–86. <https://doi.org/10.37934/arfmts.71.2.6986>
- Raza, S., Zahid, A.A., Hasan, A., Hassan, I., 2019. Experimental Investigation of Volume Fraction in an Annulus Using Electrical Resistance Tomography. *SPE J.* 1–10. <https://doi.org/10.2118/194211-PA>
- Rodriguez Corredor, F., Bizhani, M., Kuru, E., 2016. Experimental investigation of cuttings bed erosion in horizontal wells using water and drag reducing fluids. *J. Pet. Sci. Eng.* 147, 129–142. <https://doi.org/10.1016/j.petrol.2016.05.013>
- Sanchez, R.A., Azar, J.J., Bassal, A.A., Martins, A.L., 1997. The Effect of Drillpipe Rotation on Hole Cleaning During Directional Well Drilling, in: *SPE/IADC Drilling Conference*. Amsterdam, The Netherlands, 4-6 March. <https://doi.org/10.2118/37626-MS>
- Sayindla, S., Lund, B., Taghipour, A., Werner, B., Ytrehus, J.D., 2016. Experimental investigation of cuttings transport with oil based drilling fluids, in: *35th International Conference on Ocean, Offshore and Arctic Engineering*. pp. 1–9. <https://doi.org/10.1115/OMAE2016-54047>
- Sayindla, S., Lund, B., Ytrehus, J.D., Saasen, A., 2019. CFD modeling of hydraulic behavior of oil- and water-based drilling fluids in laminar flow. *SPE Drill. Complet.* 34, 207–215. <https://doi.org/10.2118/184660-PA>
- Shadizadeh, S.R., Zoveidavianpoor, M., 2012. An experimental modeling of cuttings transport for an Iranian directional and horizontal well drilling. *Pet. Sci. Technol.* 30, 786–799. <https://doi.org/10.1080/10916466.2010.490816>

- Shao, B., Yan, Y., Yan, X., Xu, Z., 2019. A study on non-spherical cuttings transport in CBM well drilling by coupled CFD-DEM. *Eng. Appl. Comput. Fluid Mech.* 13, 579–590. <https://doi.org/10.1080/19942060.2019.1615553>
- Sifferman, T.R., Becker, T.E., 1992. Hole Cleaning in Full-Scale Inclined Wellbores. *SPE Drill. Eng.* 7, 115–120. <https://doi.org/10.2118/20422-PA>
- Sun, X., Wang, K., Yan, T., Shao, S., Jiao, J., 2014. Effect of drillpipe rotation on cuttings transport using computational fluid dynamics (CFD) in complex structure wells. *J. Pet. Explor. Prod. Technol.* 4, 255–261. <https://doi.org/10.1007/s13202-014-0118-x>
- Tang, M., Ahmed, R., Srivastav, R., He, S., 2016. Simplified surge pressure model for yield power law fluid in eccentric annuli. *J. Pet. Sci. Eng.* 145, 346–356. <https://doi.org/10.1016/j.petrol.2016.05.038>
- Tang, M., He, L., Kong, L., He, S., Zhang, T., 2019. Simplified modeling of laminar helical flow in eccentric annulus with YPL fluid. *Energy Sources, Part A Recover. Util. Environ. Eff.* 0, 1–14. <https://doi.org/10.1080/15567036.2019.1649322>
- Tomren, P.H., Iyoho, A.W., Azar, J.J., 1986. Experimental Study of Cuttings Transport in Directional Wells. *SPE Drill. Eng.* 43–56. <https://doi.org/10.2118/12123-PA>
- Vaziri, E., Simjoo, M., Chahardowli, M., 2020. Application of foam as drilling fluid for cuttings transport in horizontal and inclined wells: A numerical study using computational fluid dynamics. *J. Pet. Sci. Eng.* 194, 107325. <https://doi.org/10.1016/j.petrol.2020.107325>

- Wei, N., Meng, Y., Li, G., Wan, L., Xu, Z., Xu, X., Zhang, Y., 2013. Cuttings transport models and experimental visualization of underbalanced horizontal drilling. *Math. Probl. Eng.* 2013. <https://doi.org/10.1155/2013/764782>
- Yeu, W.J., Katende, A., Sagala, F., Ismail, I., 2019. Improving hole cleaning using low density polyethylene beads at different mud circulation rates in different hole angles. *J. Nat. Gas Sci. Eng.* 61, 333–343. <https://doi.org/10.1016/j.jngse.2018.11.012>
- Zahid, A.A., ur Rehman, S.R., Rushd, S., Hasan, A., Rahman, M.A., 2018. Experimental investigation of multiphase flow behavior in drilling annuli using high speed visualization technique. *Front. Energy* 13–17. <https://doi.org/10.1007/s11708-018-0582-y>
- Zhang, C., Tang, J., Wang, L., Zhang, G., 2018. Flow pattern maps for particle-fluid mixture transport in a horizontal pipe - application of a three-layer model. *J. Dispers. Sci. Technol.* 39, 1664–1674. <https://doi.org/10.1080/01932691.2018.1461640>
- Zhang, F., Miska, S., Yu, M., Ozbayoglu, E., 2018. A unified transient solid-liquid two-phase flow model for cuttings transport- modelling part. *J. Pet. Sci. Eng.* 166, 146–156. <https://doi.org/10.1016/j.petrol.2018.03.027>

Chapter 6 : Experimental and Numerical Study of Cuttings Transport in the Inclined Drilling Operation

Mohammad Mojammel Huque¹, Aziz Rahman², Sohrab Zendehboudi¹, Stephen Butt¹,
Syed Imtiaz¹

¹Memorial University of Newfoundland.

²Texas A & M University at Qatar.

Abstract:

Directional drilling has become popular in recent decades in both onshore and offshore operations due to reduced drilling costs and improved recovery. In a directional well, drill cuttings tend to settle down at the lower side of the inclined annular section. If the generated cuttings are not removed from the hole section properly, it causes a cuttings bed formation in the annular section. Different drilling related problem such as poor rate of penetration, excessive torque and drag, increase differential sticking often associated with a poor hole cleaning which eventually lead to increase in non-productive time (NPT). Therefore, the success of inclined well drilling operation largely depends on effective cleaning of drill cuttings from the annular section. A variety of parameters, including the fluid rheology, mud velocity, cuttings size, drill pipe rotation and drill pipe inclination generally influence the cuttings transport performance. Optimization of these drilling parameters is crucial to ensure proper hole cleaning. In this study, a Computational Fluid Dynamics (CFD) model for the inclined well section is used to investigate the cuttings transport efficiency (CTE). An Eulerian-Eulerian multiphase flow model is proposed and validated with lab scale experimental data. The experiments were performed in a 6.16-meter-long annular test section having an outer pipe diameter of 4.5-inch and an inner pipe diameter of 2.5-inch. The setup is equipped with Electrical Resistance Tomography (ERT) system to measure the instantaneous solid

volume fraction and a visualization section. A non-Newtonian Heschel-Bulkley (HB) fluid was used as drilling mud and solid glass beads of 2.50 mm - 3.00 mm were used as cuttings in the experiment. This study shows a good agreement in visualization of mechanistic three-layer model of cuttings transport in terms of ERT data from experiment and CFD simulation. The validated CFD model is used to perform 5- Factors factorial design and analysis of variance (ANOVA) study. ANOVA shows that the interaction effects of mud velocity-cuttings size, mud velocity-inclination are statistically significant. Finally, this study proposed a statistical model to estimate the CTE of an inclined well considering the two factor and three factor interactions among the variables. Also, the model shows that drill pipe rotation has negligible effect in improving cuttings transport efficiency in the inclined well. The proposed model also reveals that cuttings size and fluid velocity account for 78% contribution in the transport efficiency for an inclined well. Furthermore, an Artificial Neural Network (ANN) method is used to verify the contribution of lower order interaction in the statistical model. Though empirical model shows few lower order two factor interactions (fluid rheology -cuttings size, fluid rheology-inclination), and three factor interactions (velocity-cuttings size-inclination, fluid rheology-cuttings size-inclination); ANN model shows that lower order interaction are significant in model prediction and should not be ignored. The findings of this study can help in better understanding the interaction behaviour among drilling parameters and optimized cuttings transport efficiency in the inclined drilling operation for a wide variety drilling parameter.

Keyword: Inclined well, Cuttings transport, CFD, ANOVA, DOE, ANN

6.1 Introduction:

Poor hole cleaning in a drilling operation is often associated with a variety of problems such as stuck pipe, excessive bit wear, low rate of penetration, excessive torque and drag. All these problems eventually lead to increase the non-productive time (NPT), expensive remedial action, and high drilling costs (Li and Walker, 1999; Pilehvari et al., 2007; Xiaofeng et al., 2013). The hole cleaning problem becomes more complicated in the horizontal and directional wells where drill cuttings are accumulated in the lower side of the annular section. With the advancement of drilling expertise, the number of directional drilling projects have been increased in recent years. The increased deliverability and performance of a directional well often have its downside of poor hole cleaning during the drilling operation. Therefore, optimization of drilling parameters is required to prevent complications in hole cleaning for an inclined well.

Cuttings transport in the inclined well were investigate experimentally by a number of researchers since the 1980s. Tomren et al. (1986) were one of the first group of researchers who investigated the cuttings transport in inclined well. Their study revealed that angles between 35° to 55° from vertical are critical in hole cleaning; not only for cuttings bed formation but also cuttings bed tend to slide down at this inclination. They also found that mud velocity, hole inclination, and fluid rheology play main role in cuttings transport in the inclined well. A schematic of cuttings transport mechanism in inclined well is shown in **Figure 6-1**.

Other experimental studies mentioned various inclination ranges that impact hole cleaning performance. Okrajni and Azar (1986) claimed that this angle range is 40° to 45° ; Peden et al. (1990) reported 40° to 60° ; Sifferman and Becker (1992) mentioned the range of 45° to 60° ; Capo et al. (2004) examined the angle range of 45° to 65° ; and Katende et al. (2019) reported a range of 40° to 60° . According to Sifferman and Becker (1992), the cuttings beds are dormant with barely

sliding or tumbling tendency for the angle between 60° to 90° with respect to the vertical axis. The experimental work conducted by Shadzadeh and Zoveidavianpoor (2012) shows that the worst hole cleaning can occur at an inclination angle greater than 70° from the vertical axis, which is slightly different from the past studies. According to the literature, a wide range of critical angle in hole cleaning, ranging from 35° to the 70° or even higher inclination angles has been reported. In fact, the specific inclination critical to hole cleaning is a function of a wide range of parameters such as fluid rheology, well geometry, cuttings size, and drill pipe rotation.

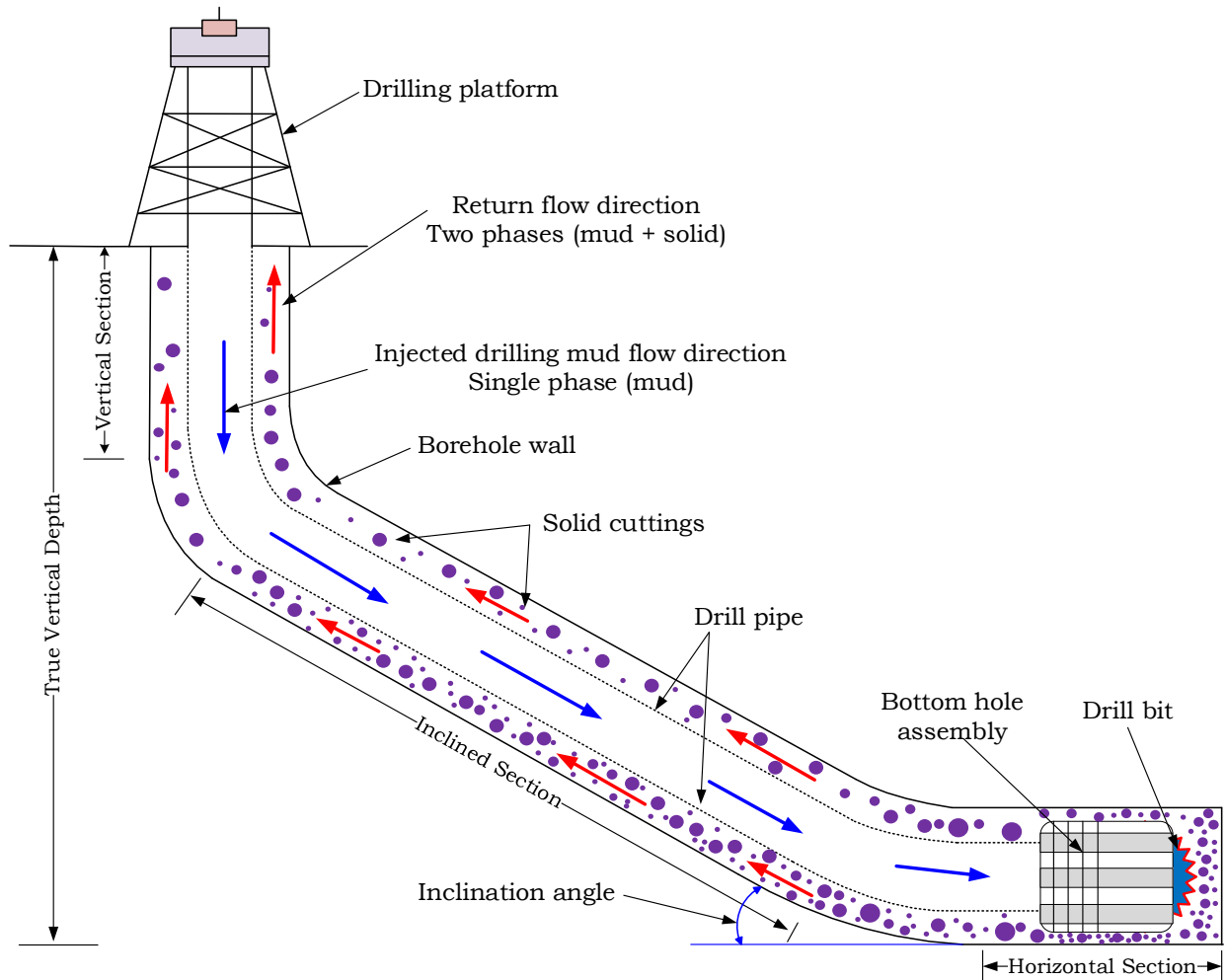


Figure 6-1: Schematic of cuttings transport in inclined drilling operation

The effect of fluid rheology and Minimum Transport Velocity (MTV) on cuttings transport in the inclined well was investigated in the previous works. Ford et al. (1990) concluded that an MTV is required to transport cuttings in the inclined section, and the MTV varies with change in inclination. Although it was claimed that fluid velocity lowers the annular cuttings concentration; Chen et al. (2007) found that cuttings accumulated in the horizontal well do not transport cuttings until a critical fluid velocity or MTV is reached. Conducting an experimental work, Katende et al. (2019) showed that the hole angle 40° to 60° is crucial for cuttings transport since MTV is the highest at this interval. Their study also revealed that the cuttings with small size (0.5 mm to 1.00 mm) exhibit a better hole cleaning performance in the inclined section, compared to 4 mm cuttings.

A number of experimental studies focused on the impact of drill pipe rotation in the inclined section. Avila et al. (2004) noticed that increasing drill pipe rotation above 80 RPM increases the annular cuttings concentration at 45° inclination due to the combined effects of centrifugal and gravitational forces. Ozbayoglu et al. (2008) investigation showed that the effect of mud viscosity on cuttings transport decreases upon an increase in drill pipe rotation. Similar observations were reported by other researchers (Katende et al., 2020; Keshavarz Moraveji et al., 2017; Woo et al., 2011). Although the effect of drill pipe rotation at different inclinations on cuttings transport have been investigated in the literature, researchers have not developed any interaction effect of drill pipe rotation and inclination on cuttings transport.

Ramadan et al. (2001) described the cuttings transport behavior in the inclined well using a mechanistic model. They reported that there is an optimum cuttings size that exhibits improved hole cleaning in relation to optimal fluid velocity, fluid rheology, and inclination. This dependency can be interpreted as the interaction between drilling parameters (fluid velocity, fluid rheology and inclination); however, they did not report any interaction effect or relative dependency between

parameters on cuttings transport (Huque et al., 2020). According to an experimental work by Allahvirdizadeh et al. (2016) with varying partially hydrolyzed polyacrylamide (PHPA), increasing the mud viscosity is not always an efficient solution for hole cleaning problem with high fluid velocities. Also previous studies (Allahvirdizadeh et al., 2016; Pang et al., 2018; Piroozian et al., 2012) did not report the “fluid velocity - fluid viscosity” interaction effect on cuttings transport. In recent years, researchers have focused more on improving the cuttings transport behavior by using enhanced fluid rheology (Boyou et al., 2019; Gul et al., 2017; Hakim et al., 2018; Heshamudin et al., 2019; Hirpa and Kuru, 2020; Rodriguez Corredor et al., 2016; Yeu et al., 2019) and transport mechanism (Kim et al., 2014; Naganawa et al., 2017; Rasul et al., 2020). Boyou et al. (2019) investigation showed that nano silica based aqueous solution provide an improved cuttings transport efficiency for any inclination. It was found that addition of nano silica can be an alternative solution to the oil-based drilling mud. Several other research studies (Hakim et al., 2018; Heshamudin et al., 2019; Yeu et al., 2019) used improved water based mud with polyethylene and polypropylene. It was concluded that addition of polyethylene beads can improve the transport ratio by approximately 16%.

The flow behaviour and solid dune movement pattern also investigated by several studies (Czuprat et al., 2020; Fajemidupe et al., 2019; Huque et al., 2021b; Kamyab and Rasouli, 2016; Kelessidis et al., 2007; Kelessidis and Bandelis, 2004; Li and Luft, 2014; Pandya et al., 2020). These study shows visualization of solid cuttings transport behaviour in the horizontal and inclined annular section at different operating condition. Beside experimental studies, a number of CFD studies investigated the drill cuttings transport behavior in horizontal and inclined wells. Although most of the CFD research studies focused on solid cuttings transport in the horizontal well, a few studies (Epelle and Gerogiorgis, 2017; Keshavarz Moraveji et al., 2017; Rooki et al., 2014; Siamak et al.,

2015; Sun et al., 2017; Vaziri et al., 2020) included the effect of inclination in the simulation. For instance, Epelle and Gerogiorgis (2017) concluded that annular solid concentration could increase by 51% when the orientation changes from the vertical to a 60° inclination. A few more studies (Capo et al., 2004; Kim et al., 2014; Osunde and Kuru, 2008; Sun et al., 2017; Vaziri et al., 2020) also reported a similar observation but at different solid concentrations and inclination angles. Rooki et al. (2014) showed that a power law fluid exhibits better cuttings transport capability in the inclined annulus; however, both power law fluid and Herschel Bulkley fluid shows similar performance for the vertical well. Pang et al. (2018) conducted a CFD study and reported that cuttings transport ratio is at the minimum level and pressure drop is at the maximum level for the inclination range 35° to 65°. It was also found that an increase in cuttings size decreases the cutting transport ratio but increases the pressure drop.

Most of the experimental studies, mechanistic model, and CFD simulation on the inclined well investigated the impact of individual parameters on cuttings transport. According to the literature, fluid viscosity, inclination, and fluid velocity have a significant influence on cuttings transport. Moreover, almost all of the experiential studies were conducted with different experimental set up and conditions in terms of dimension, flow rate, cuttings size, and fluid rheology, which impact the experimental results. The traditional ‘One Factor at a Time’ (OFAT) method is not beneficial when there are interactions among the parameters. Also, the ranges of input parameters have not been wide enough to capture all important behaviors in cuttings transport. In real-time drilling, many parameters directly interact with each other, which considerably affect the performance of cuttings transport. Due to the experimental limitations, all parameters might not be investigated simultaneously. Hence, the interaction between influential parameters, which is another vital aspect; has been ignored in most of the past studies. These drawbacks motivate the authors to

further investigate the interactions between drilling parameters in inclined well using a systematic Design of Experiment (DOE) method. This study investigates the impact of individual parameters in drilling operations, the positive and negative interaction among the parameters, and interaction impact on hole cleaning operation.

There are several parameters involved in drill cuttings transport such as fluid rheology, inclination, volumetric flowrate, drill pipe rotation, and cuttings size. Thus, it is important to determine the vital parameters that have significant influences on target objectives such as the cuttings transport efficiency (CTE). It is not an easy task to estimate the CTE by a single mathematical expression when several variables are involved. The following expression shows that CTE is a function of a number of factors A, B, C, and D and their interactions; where A, B, C, D can be fluid rheology, mud velocity, cuttings size, and drill pipe rotation.

$$CTE = f(A, B, C, D, \dots, AB, AC, AD, BC, \dots, ABC, \dots, ACD, \dots, ABCD, \dots, etc.) \dots\dots\dots (6-1)$$

where AB indicates the interaction between variables A and B, and AC indicates the interaction between variables A and C. Similarly, CTE can be a function of higher-order interaction among the variables such as ABC and ACD. Therefore, it is a challenging task to determine which independent variable and interactions have more impact on CTE.

In this study, CTE was investigated using experimental analysis for the slightly inclined well. A multiphase flow model was developed to simulate the cuttings transport behavior in the inclined well. The multiphase flow model was validated with experimental data. The five factors full factorial experimental design method was then used to evaluate cuttings transport efficiency in the inclined section. The factors are fluid viscosity (A), mud velocity (B), cuttings size (C), drill pipe

rotation (D), and inclination (E). The selection of these five factors is based on the literature review.

This manuscript is organized as follows. **Section 6.2** covers the ‘Materials and Methods’ section, which includes an overall methodology flow chart, CFD model development, grid independence study, experimental procedure, fluid rheology analysis, Design of Experiment, and performance measurement indicator. **Section 6.3** described the results and discussion of this study. This section includes experimental result from ERT and visualization section, validation of CFD model, sensitivity analysis of transient solid dune movement, factorial design, interaction study, parametric study, and analysis of variance (ANOVA). ANOVA suggested an empirical model to describe the most critical parameters in cuttings transport study. **Section 6.3** also covers comparison of the developed ANOVA model with Artificial Neural Network (ANN) model. Finally, **Section 6.4** includes a summary and conclusion drawn from this investigation.

6.2 Materials and Methods:

6.2.1 Methodology

An overview of the methodology used in this study is shown in **Figure 6-2**. The complete workflow is grouped into 5 tasks. Task 1 covers the fluid rheology analysis and experimental phase. Task 2 describes the development of a multiphase flow model using CFD for the inclined well section. Task 3 covers CFD model validation with experimental work in the inclined well. Once CFD model is validated, an extended simulation runs were performed with different fluids and different inclinations ranging from horizontal to vertical at the interval of 15° . The summary of the extended simulation run gives an overall impression of critical angle prone to hole cleaning.

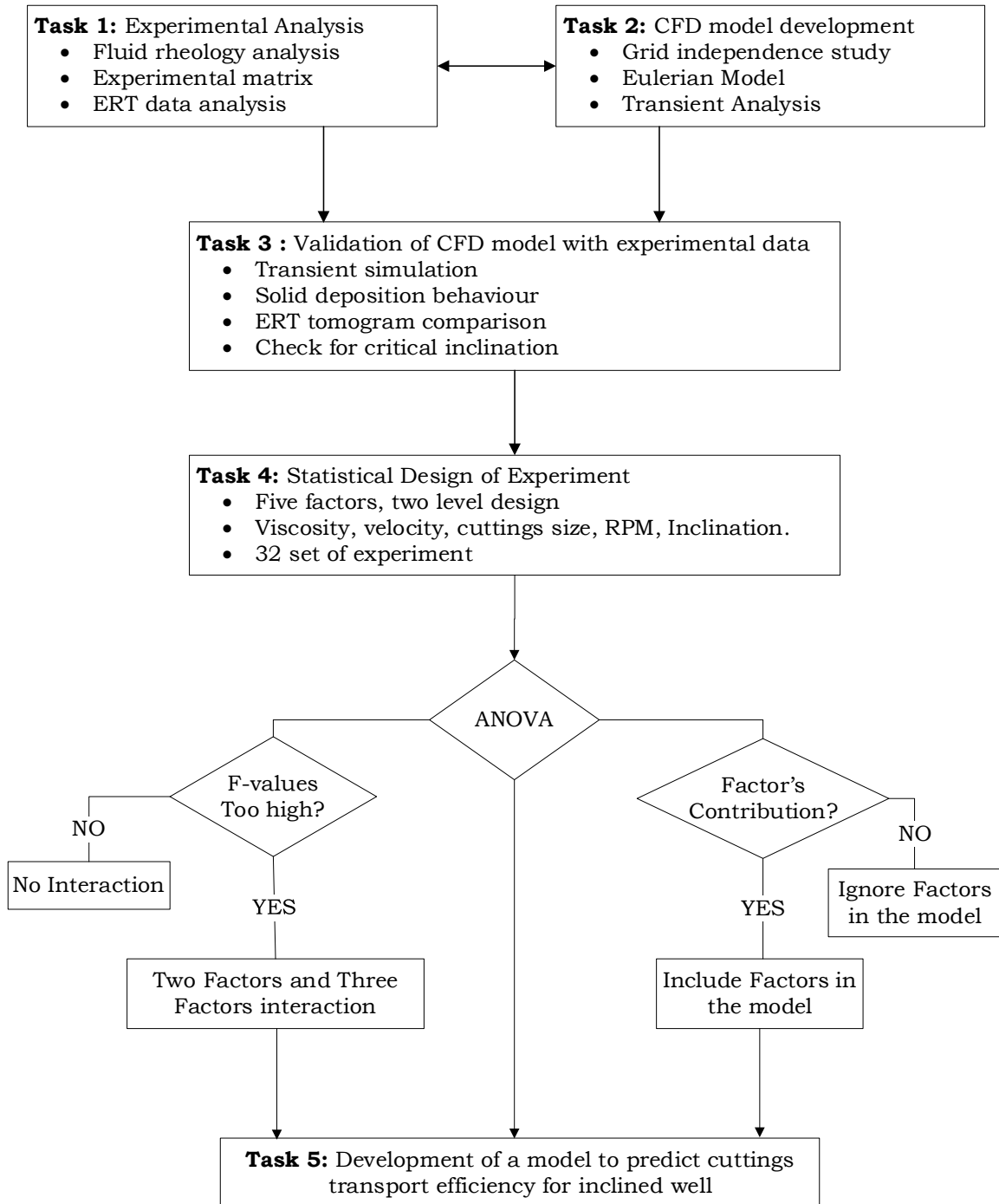


Figure 6-2: Overall methodology to study effect of drilling parameters on cutting transport.

Task 4 focuses on five factors - two level design of experiment (DOE) and ANOVA. Task 5 includes the statistical CTE model development and validation using artificial neural network (ANN).

Once the range of critical angle is identified, a two-level factorial DOE was planned with 5 factors Rheology (A), Velocity (B), Cuttings Size (C), Drill Pipe Rotation (D), and Inclination (E). A total of 32 ($2^5 = 32$) experimental trials were designed for this factorial experiment. The outcomes are CTE, annular solid volume fraction and annular pressure drop.

Statistical test ANOVA (Kim, 2014; Tabachnick, 2007) was performed on the outcomes, and examined the F-values, and p-values were calculated to examine the interaction among the parameters and factor's contribution in the statistical analysis. Two-factor and three-factor interactions were also investigated. Finally, this study proposes a model to predict and optimize the cuttings transport efficiency in the inclined well.

6.2.2 CFD model development

In a recent study by the authors (Huque et al., 2020), a CFD model for cuttings transport in the horizontal well was proposed. In this study, model geometry is updated for the different inclinations ranging from 0° - 90° where 0° represents the horizontal well and 90° represents a vertical well. Cuttings transport in the annular section simulates a two-phase flow behavior where drilling mud can be treated as a primary phase and solid cuttings as a secondary phase. Multiphase Eulerian - Eulerian model was adopted in this study where cuttings are treated as a continuum. The drilling mud was considered as an incompressible fluid, and drill cuttings size and density were considered constant in this model. Also, there is no interphase mass transfer between the phases, and the system was isothermal.

Mass conservation. The continuity equation for the drilling mud (liquid) is given below (Fluent, 2015):

$$\frac{\partial}{\partial t}(\alpha_l \rho_l) + \nabla \cdot (\alpha_l \rho_l \vec{v}_l) = \Sigma(\dot{m}_{ls} - \dot{m}_{sl}) = 0 \quad (6-2)$$

In which, v_l is the velocity of the liquid phase; ρ_l denotes the density of the liquid phase, \dot{m}_{ls} refers to the mass transfer from the liquid phase to the solid phase; and \dot{m}_{sl} resembles the mass transfer from the solid phase to the liquid phase. The volume fraction is defined as α_l for the mud phase and α_s for the cuttings, where $\alpha_l + \alpha_s = 1$. The subscripts l and s are used for the mud (liquid) and cuttings (solid) phases, respectively.

Similarly, the continuity equation for the solid phase is represented by the following relationship (Fluent, 2015):

$$\frac{\partial}{\partial t}(\alpha_s \rho_s) + \nabla \cdot (\alpha_s \rho_s \vec{v}_s) = \Sigma(\dot{m}_{sl} - \dot{m}_{ls}) = 0 \quad (6-3)$$

In which, v_s is the velocity of the solid phase, and ρ_s stands for the density of the solid phase.

Momentum conservation. The momentum balance for the liquid phase is given by the following equation (Fluent, 2015):

$$\frac{\partial}{\partial t}(\alpha_l \rho_l \vec{v}_l) + \nabla \cdot (\alpha_l \rho_l \vec{v}_l \vec{v}_l) = -\alpha_l \nabla p + \nabla \cdot \bar{\bar{\tau}}_l + \alpha_l \rho_l \vec{g} + \Sigma(\vec{R}_{sl} + \dot{m}_{sl} \vec{v}_{sl} - \dot{m}_{ls} \vec{v}_{ls}) + (\vec{F}_l + \vec{F}_{lift,l} + \vec{F}_{wl,l} + \vec{F}_{vm,l} + \vec{F}_{td,l}) \quad (6-4)$$

in which, F_l is an external body force; $\vec{F}_{lift,l}$ represents a lift force; $\vec{F}_{wl,l}$ symbolizes the wall lubrication force; $\vec{F}_{vm,l}$ is the virtual mass force; $\vec{F}_{td,l}$ stands for a turbulent dispersion force; p introduces the pressure shared by both solid and liquid phases; and \vec{v}_{sl} is the interphase velocity defined as: $\vec{v}_{sl} = \vec{v}_s$ if $\dot{m}_{sl} < 0$.

$\bar{\bar{\tau}}_l$ also introduces the stress-strain tensor for the liquid phase, as defined below (Fluent, 2015):

$$\bar{\bar{\tau}}_l = \alpha_l \mu_l (\nabla \vec{v}_l + \nabla \vec{v}_l^T) + \alpha_l (\lambda_l - \frac{2}{3} \mu_l) \nabla \cdot \vec{v}_l \vec{I} \quad (6-5)$$

In Equation (6-5), μ_l and λ_l denote the shear and bulk viscosity of liquid phase, respectively.

The conservation of momentum for the solid phase is expressed as follows (Fluent, 2015):

$$\frac{\partial}{\partial t}(\alpha_s \rho_s \vec{v}_s) + \nabla \cdot (\alpha_s \rho_s \vec{v}_s \vec{v}_s) = -\alpha_s \nabla p - \nabla p_s + \nabla \cdot \vec{\tau}_s + \alpha_s \rho_s \vec{g} + \sum (K_{ls}(\vec{v}_l - \vec{v}_s) + \dot{m}_{ls} \vec{v}_{ls} - \dot{m}_{sl} \vec{v}_{sl}) + (\vec{F}_s + \vec{F}_{lift,s} + \vec{F}_{wl,s} + \vec{F}_{vm,s} + \vec{F}_{td,s}) \quad (6-6)$$

where p introduces the pressure shared by both solid and liquid phases; p_s stands for the solid phase pressure. \vec{v}_{sl} is the interphase velocity defined as: $\vec{v}_{sl} = \vec{v}_s$ if $\dot{m}_{sl} < 0$. F_s is an external body force; $\vec{F}_{lift,s}$ represents a lift force; $\vec{F}_{wl,s}$ symbolizes the wall lubrication force; $\vec{F}_{vm,s}$ is the virtual mass force; $\vec{F}_{td,s}$ stands for a turbulent dispersion force. \vec{R}_{sl} is the interaction force between the solid and liquid phases. This force mainly depends on the friction and pressure cohesion and is subject to the condition that $\vec{R}_{sl} = -\vec{R}_{ls}$ and $\vec{R}_{ll} = 0$ (Fluent, 2015), as given below:

$$\sum \vec{R}_{sl} = \sum K_{sl}(\vec{v}_s - \vec{v}_l) = 0 \quad (6-7)$$

Here, K_{sl} ($= K_{ls}$) introduces the interphase momentum exchange coefficient; and \vec{v}_s and \vec{v}_l are the solid and liquid phase velocities, respectively. The details model assumption is described in previous studies (Huque et al., 2020).

6.2.3 Mesh Size and Grid Study:

A grid independence study was performed to choose the optimum number of mesh size that can produce an acceptable simulation result with a reasonable accuracy. Water with flow rate 1 m/s was used to check the pressure drop for different elements sizes as shown in **Figure 6-3**. The grid independency test shows that approximately 1.5 million elements can produce almost an error free result for a concentric annular section. The minimum orthogonality was 0.995 and the average orthogonality was 0.997, implying a good mesh quality of the selected mesh size. The average skewness was 0.049 (minimum 0.0349 and maximum 0.06514); this represents that there is a very good consistency among each cell.

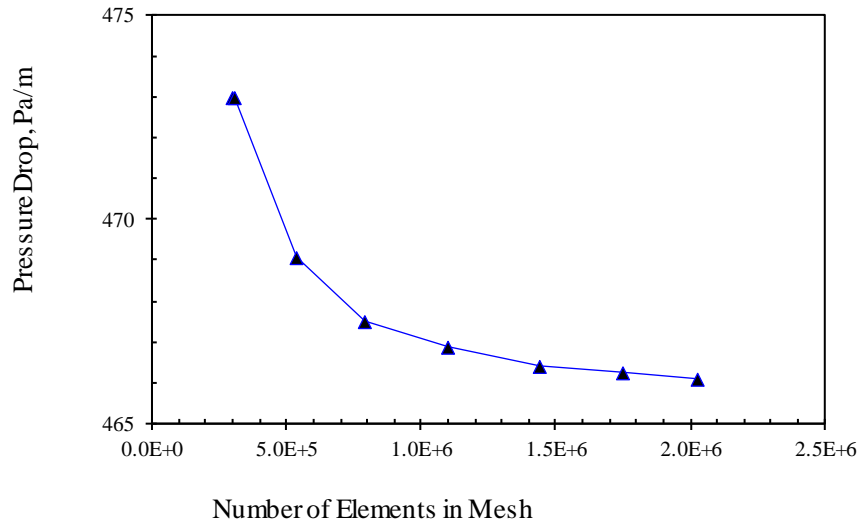


Figure 6-3: Grid study for concentric annular section

Transient simulations were performed with “Compute Canada” supercomputer servers ‘Graham’ and ‘Cedar’. For the validation phase, time step was set for 0.005 sec and 20 iteration per time steps was used. Simulation time for each run depends on the available resources such as number of available CPU in Intel(R) Xeon(R) E5-2683 v4 processor (ranging from 96 cores to 148 cores), RAM, grid size and calculation methods. The simulation run time varies between 48 hrs to 96 hrs for 3 minutes of real time transient transport.

6.2.4 Experimental Procedure:

The experimental studies were conducted at the multiphase flow loop lab at Texas A & M University at Qatar (TAMUQ). **Figure 6-4** shows a simplified schematic view of the 6.16-meter-long experimental test section with a 4.5-inch outer pipe and a 2.5-inch inner pipe. The inner pipe can be rotated up to 120 RPM. The solid cuttings and drilling mud are pumped from the mud tank to the test section, where the ERT sensor (Huque et al., 2021b) measures/captures the instantaneous solid volume fraction and 2-D tomogram of solid distribution in the annular section. Finally, solids and drilling mud are returned to the mud tank via a drain line. There is also a visualization section

at the downstream of the inclined section to capture solid movement pattern using a high-speed camera and digital single-lens reflex camera (DSLR) camera. In this experiment, high speed camera is used to track particles movement at 2000 frames per second (fps). The actual lab image is shown in **Figure 6-5** with a 5° inclination.

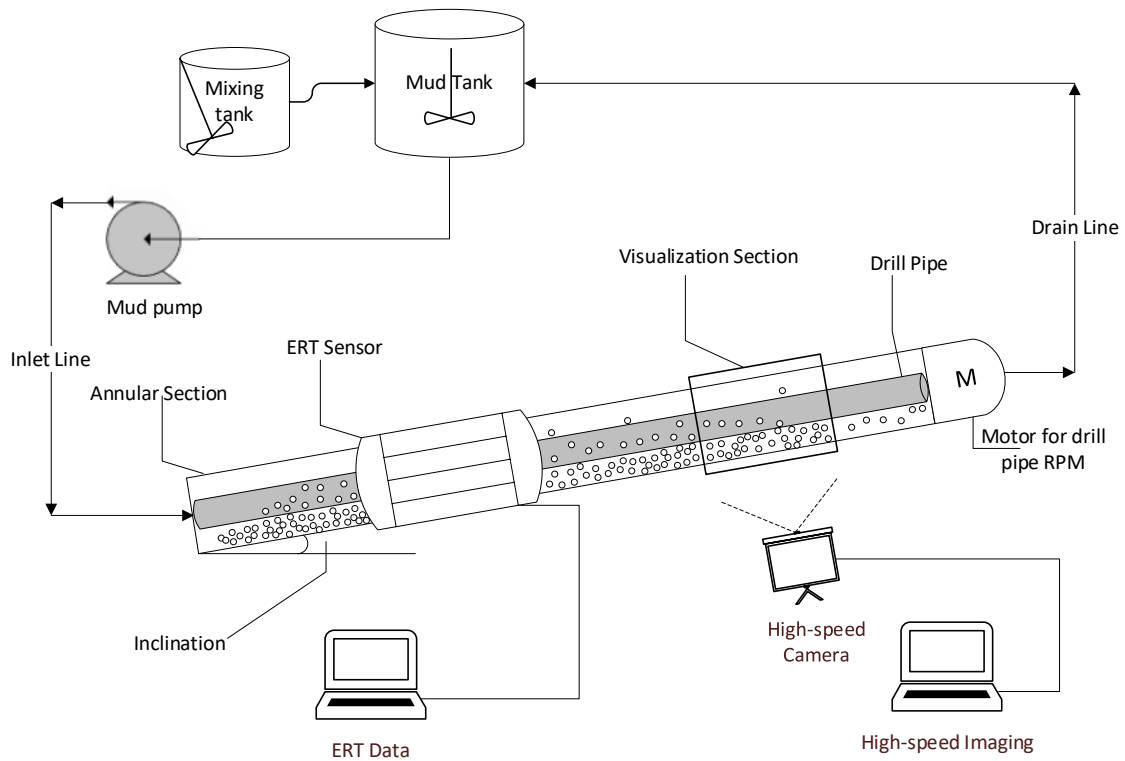


Figure 6-4: Experimental section schematic

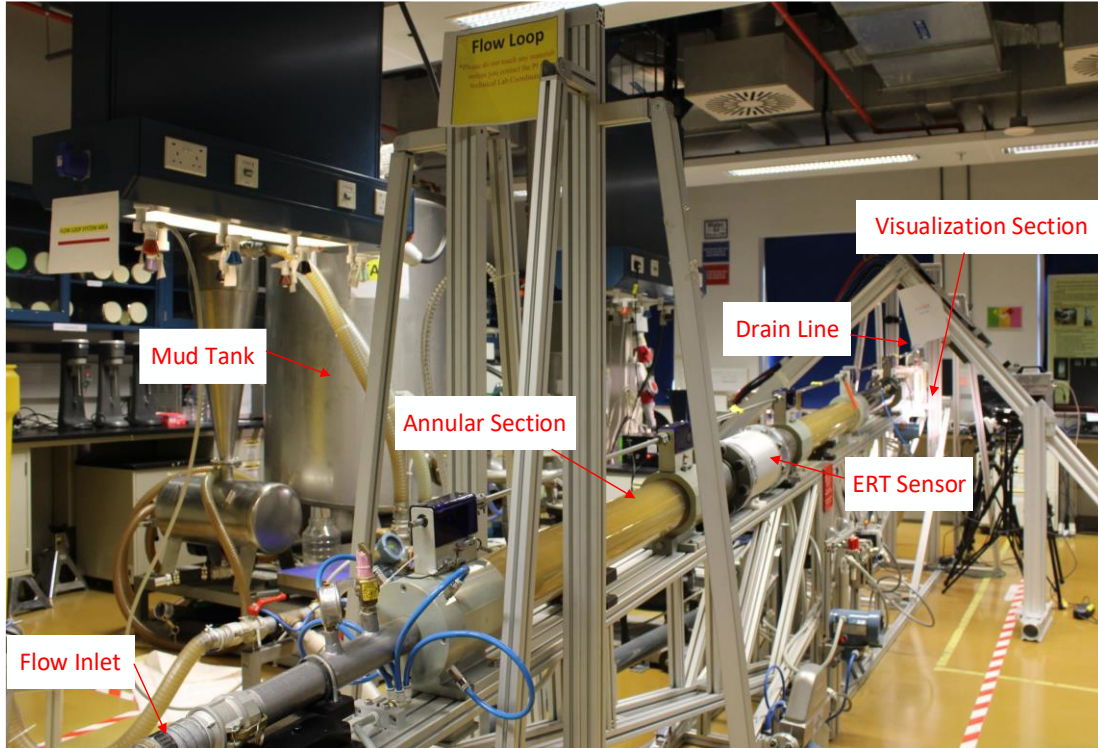


Figure 6-5: Experimental set up image at 5° inclination

The experiment begins with preparing 75 to 80-liter drilling fluid in a mud mixing tank by adding a commercial biopolymer with water. An agitator is used for the mud preparation in the mixing tank. Once prepared, the drilling mud is then pumped into the main mud tank. This process continues until at least 300 liters of mud is prepared to run the experiment. Once the mud is prepared, 12 kg of 2.5 to 3 mm spherical glass beads are placed into the mud tank to simulate the solid drill cuttings. An agitator is used to mix the solid cuttings with drilling mud. Once a homogenous mixture is prepared, the two-phase slurry is pumped into the test section inlet by a mud slurry pump. The pump flow rate can be controlled electronically from 160 to 350 liter per minute (LPM). The test section can be set at 0°, 5° and 10° inclined position where 0° represents the horizontal orientation and other deviation angles are measured from the horizontal position. A simplified flowchart of the complete experimental procedure is shown in **Figure 6-6**.

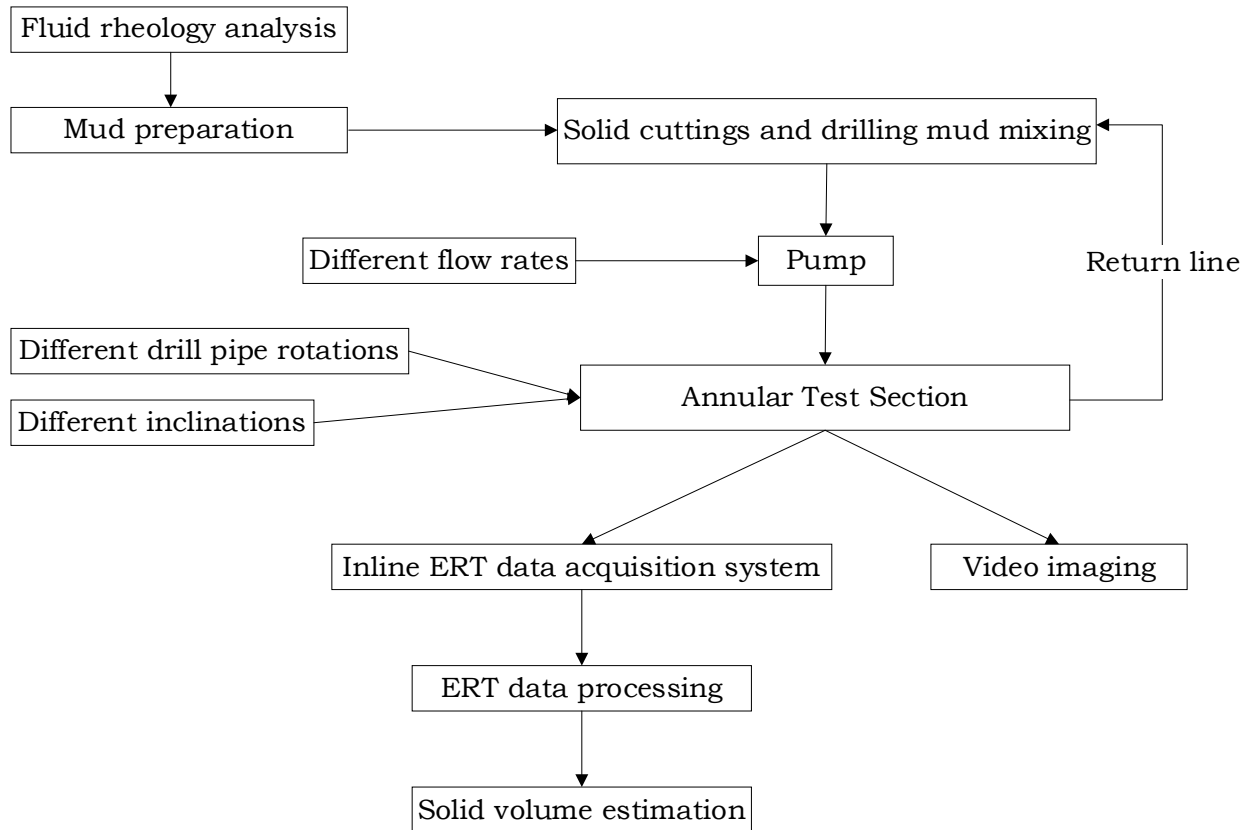


Figure 6-6: Simplified experimental procedure flowchart.

Depending on the operating conditions (pump flow rate, drill pipe rotation, inclination, fluid rheology) drilling fluid may not be able to transport all of the solid particles pumped to the test section, and a gradual solid cuttings bed is formed in the annular section. The electrical resistance tomography (ERT) section is placed at 2.5 meters from the inlet section. ERT section consist of two parallel circular sensing electrode section with 16 electrodes per sensor as shown in **Figure 6-7**.

These circular cross sections are used to measure instantaneous real-time conductivity of the medium (air, liquid, solid etc.) flowing inside the ERT section. ERT system initially creates an localized electrical field with primary medium such as drilling mud. Any presence of non-

conducting secondary phases (in this study - solid glass beads) causes a change in electrical field behaviour inside the ERT system. Finally, ERT system used a conductivity-concentration transformation algorithm to estimate the change in conductivity into a concentration profile. In this study, ERT system measures the instantaneous solid volume fraction of a two-phase flow over the experiment. Also, ERT system generates a 2-D tomogram of a solid volume fraction to show a real-time visualization of solid content inside the annular section. The results obtained from the ERT tomography are presented in ‘Results and Discussions’ section.

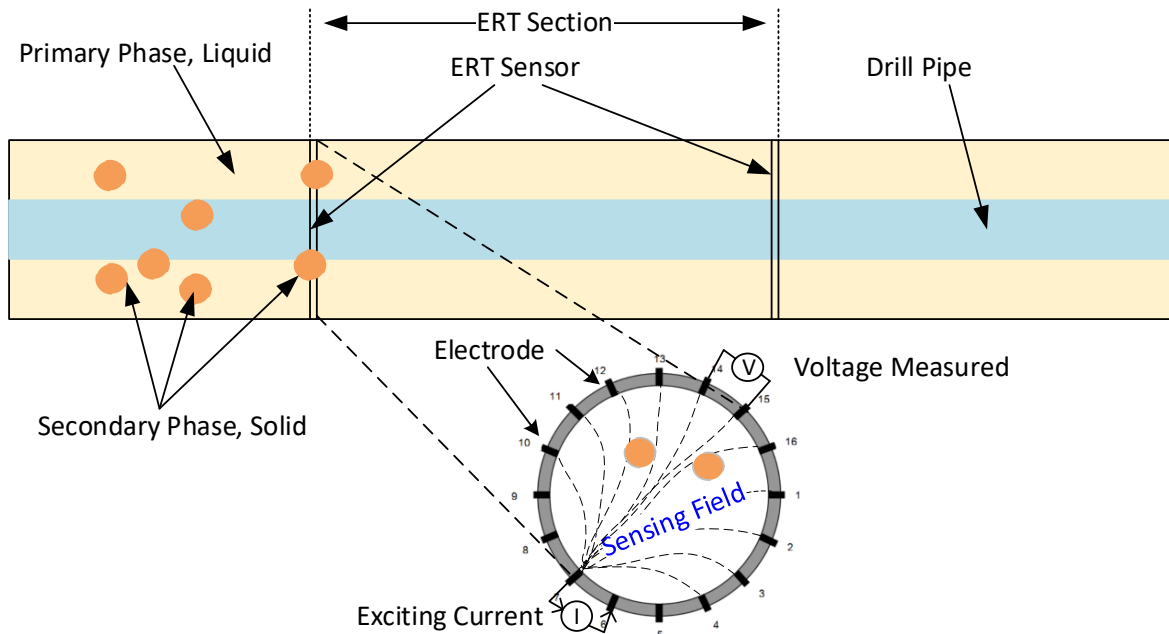


Figure 6-7: Schematic of ERT sensor (Huque et al., 2021b)

6.2.5 Fluid Rheology Estimation:

Four different non-Newtonian fluids (FZ 1, FZ 2, FZ 3 and FZ 4) are prepared by mixing the Xanthan gum-based biopolymer at different concentrations ranging from 0.05 -0.125 (wt./wt.) %. The fluid rheology is estimated using a rotational viscosity meter. The fluid rheology test shows that all four fluids follow a power law trend with yield stress value, commonly known as the

Herschel-Bulkley fluid as shown in **Figure 6-8**. The discrete points illustrate the experimental results and continuous lines represent the model behaviours. A nonlinear curve fittings model is used to verify the experimental result with Herschel-Bulkley fluid ($\tau = \tau_o + k\dot{\gamma}^n$) parameters. The details of flow behaviour are presented in **Table 6-1**. R^2 values indicates the goodness-of-fit measure for curve fittings model where $R^2=1$ indicates a best fit.

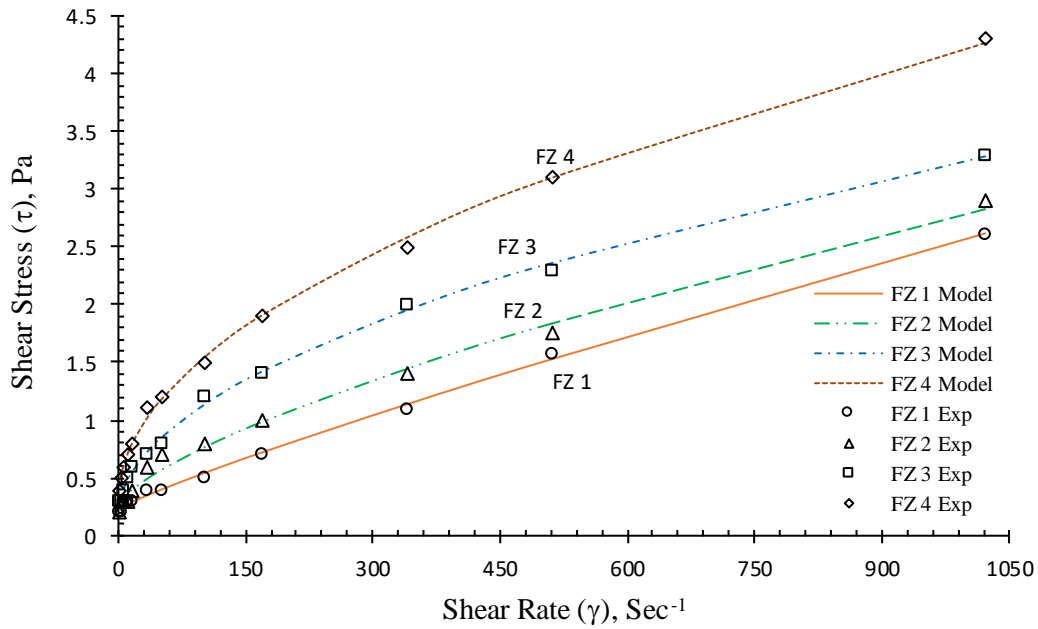


Figure 6-8 : Shear stress vs. shear rate behavior for fluids FZ 1, FZ 2, FZ 3 and FZ 4

Table 6-1: Summary of fluid rheology tests (Huque et al., 2021a).

Fluid Properties	FZ 1	FZ 2	FZ 3	FZ 4
Polymer Concentration (wt./wt.), %	0.050	0.075	0.100	0.125
Yield Stress, τ_o (pa)	0.229	0.234	0.269	0.308
Consistency Index, k (Pa-s ⁿ)	0.005	0.020	0.064	0.116
Flow Behaviour Index, n	0.878	0.702	0.557	0.510
R^2	0.997	0.998	0.999	0.999

6.2.6 Design of Experiment:

In this study, a two-level five factorial design of the experiment (DOE) (Pierlot et al., 2008; Rolf Carlson, 1992) was used by considering the most significant parameters, including the inclination, as shown in **Table 6-2** with range of investigation. The main goal of this DoE is to investigate the cuttings transport behaviour of Herschel Bulkley fluid in the inclined well and check for the interaction behaviour.

Table 6-2: Factors used in the simulation with their ranges.

Factor	Name	Units	Type	Minimum	Maximum	Coded Low	Coded High
A	Mud viscosity, k	Pa-s	Numeric	0.005	0.116	-1 ↔ 0.005	+1 ↔ 0.112
B	Mud velocity	m/s	Numeric	0.5	2	-1 ↔ 0.50	+1 ↔ 2.0
C	Cuttings size	mm	Numeric	1	4	-1 ↔ 1	+1 ↔ 4
D	Drill pipe rotation	RPM	Numeric	10	80	-1 ↔ 10	+1 ↔ 80
E	Inclination	degree	Numeric	15°	60°	-1 ↔ 15	+1 ↔ 60

6.2.7 Performance measurement:

Cuttings Transport Efficiency (CTE) is defined as follows (Sifferman et al., 1973):

$$CTE = \frac{v_c}{v_m} \times 100\% \quad (6-8)$$

where v_c refers to the cuttings velocity and v_m represents the drilling mud velocity in the annular section. Annular Cuttings Volume Fraction (ACVF) (Cl Kleinstreuer, 2003) is defined as the ratio of cuttings volume in the annular section to the total volume of the annular section as given below.

$$ACVF = \frac{\text{Volume occupied by solids}}{\text{Volume occupied by mixture}} \quad (6-9)$$

A higher CTE always corresponds to a low an ACVF since most of the cuttings are transported with drilling mud and less cuttings are accumulated in the annular space.

6.2.8 Novelty and Limitations:

This section includes the advantage and novelty of this study:

- ❖ This study incorporates the use of the state of art electronic resistance tomography (ERT) system to measure in-line solid volume fraction in the experimental phase. This is a quick and reliable secondary phase volume fraction estimation method while conducting an experiment. ERT enables a real-time distribution of solid in the annular section by 2-D tomographic video and images.
- ❖ A cuttings transport efficiency (CTE) prediction model is proposed in this study. This model considers two factors and three factors incarnation among the variables which have been ignored in past studies.
- ❖ This CTE prediction model is capable to predict cuttings transport efficiency for a wide range of fluid rheology, fluid velocity, cuttings size, and inclination.

The followings are the limitation of this study and can be improved in future investigation.

- ❖ The experimental work and simulation study assumed solid cuttings are spherical, however in actual drilling operation, different solid cuttings size and shape can be found simultaneously.
- ❖ Due to pumping capacity restrictions, annular mud flow rate is limited to 350 liters per minute which corresponds to the maximum an annular mud velocity of 0.818 m/s.
- ❖ The experimental facility is limited to slightly inclined well.
- ❖ The proposed cuttings transport efficiency model is based on water-based drilling mud. The effectiveness of this model is not tested for the oil-based mud.
- ❖ This model did not consider the effect of drill pipe eccentricity in the inclined section.

6.3 Result:

6.3.1 ERT analysis and visualization:

ERT system measures the instantaneous secondary phase (solid) volume fraction with respect to the primary phase (liquid) in the annular test section. Solid volume fraction data obtained from the ERT analysis for different experimental run are compared in this study. **Figure 6-9** shows the solid volume fraction with different mud velocities for fluid FZ 1, FZ 2, FZ 3 and FZ 4 with inclination of 5 degree and 10 degrees. The solid lines represent the 5-degree inclination and dotted line shows the result for 10-degree inclination. Due to a high ‘minimum transport velocity (MTV)’ requirement for fluid FZ 4 (the most viscous fluid), some data points are not available at lower mud velocities.

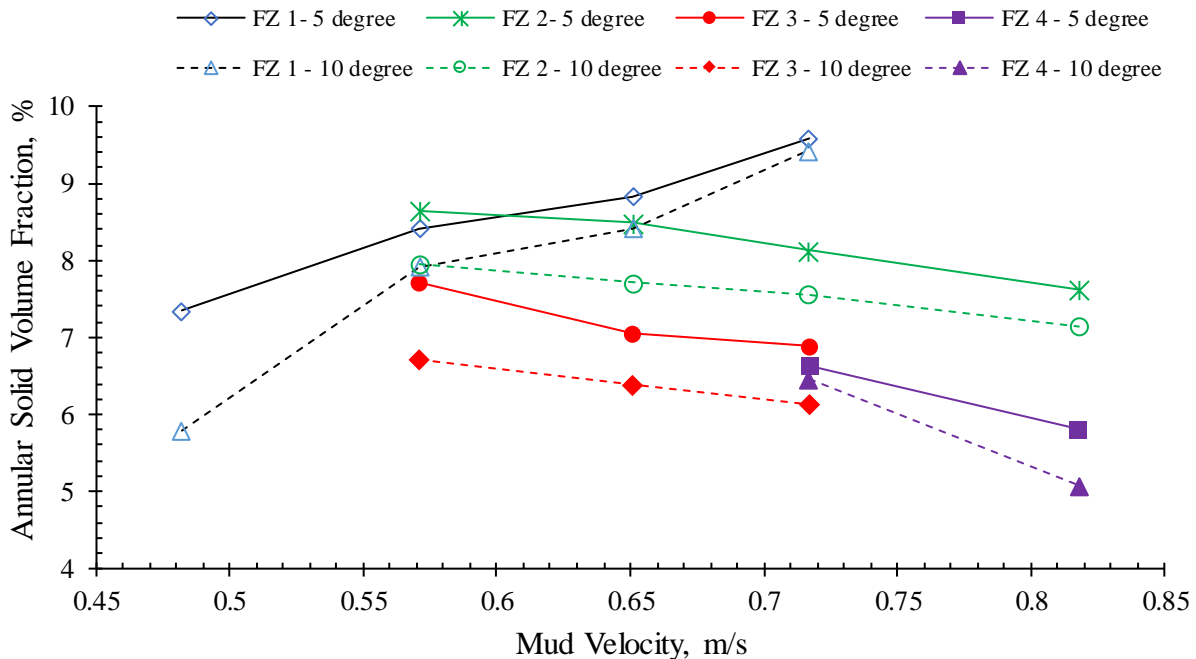
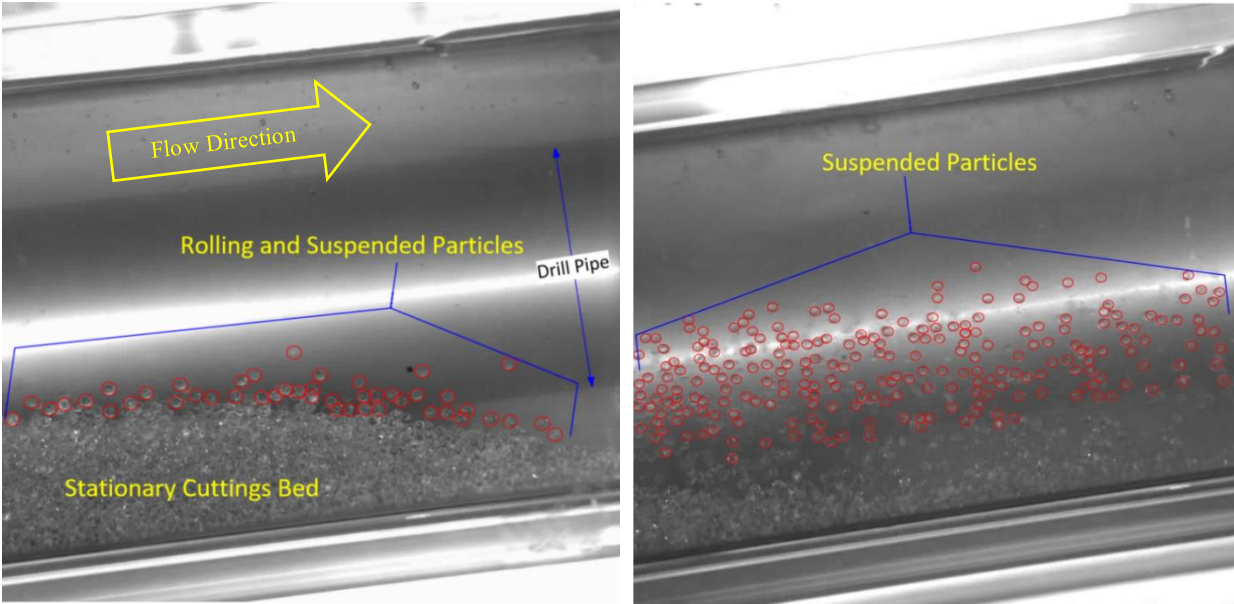


Figure 6-9 : Effect of inclination and fluid rheology on annular solid volume fraction

It is observed that for all four fluids except FZ 1, an increase in mud velocity shows a gradual decreasing trend in annular solid volume fraction. According to **Figure 6-9**, an increase in inclination from 5° to 10° shows a decrease in annular solid volume fraction for FZ 2, FZ 3 and FZ 4. A lower annular solid volume fraction represents an improved hole cleaning. This indicates that an improved cuttings transport efficiency is observed with increasing in inclination. Moreover, an increase in fluid viscosity ($\mu_{FZ1} < \mu_{FZ2} < \mu_{FZ3} < \mu_{FZ4}$) shows a decrease in annular solid volume fraction. Thus, it can be concluded that an increase in fluid velocity, inclination (from horizontal position), and fluid viscosity shows an improved hole cleaning performance in inclined well.

However, fluid FZ 1 shows the opposite trend. Fluid FZ 1 is the least viscous fluid as shown in **Table 6-1**. Experimental study and visualization pattern shows that fluid FZ 1 exhibit low suspension capability, therefore fluid FZ 1 shows poor solid cuttings transport performance against gravity in the inclined well. High-speed image captured at 2000 frames per second(fps) shows that a less viscous fluid primarily transports solid cuttings by rolling mechanism with few suspended particles as shown in **Figure 6-10** panel (a). On the other hand, **Figure 6-10** panel (b) shows the high-speed camera image for fluid FZ 3. It shows that a numerous amount suspended solid flowing in the annular section. Therefore, ERT shows a less amount of annular solid volume fraction from the stationary bed for FZ 3 compared to FZ 1.



(a) Fluid FZ 1

(b) Fluid FZ 3

Figure 6-10: High-speed image (2000 fps) visualization of solid particle movement

[10°-inclined well configuration with fluid FZ 1 and FZ 3]

6.3.2 Validation of CFD Model:

Cuttings volume fraction data obtained from the ERT system was compared with the transient simulation data for the time duration of 45 seconds (experimental run time). There is a very good match between simulation and experimental data for fluid FZ 3, as shown in **Figure 6-11**. The relative error based on the comparison of the experimental and simulated data is less than 9 %. The minimum error for stationary drill pipe condition (RPM = 0) is 1.72%, whereas it is 8.56 % for the drill pipe rotation of 80 RPM. This CFD model was also validated for the horizontal and vertical orientation where different fluids rheology and flowrates were tested (Huque et al., 2020).

Figure 6-12 (a) represents the solid cuttings distribution in the annular section from the simulation, and **Figure 6-12 (b)** represents the corresponding experimental solid distribution from the ERT tomogram. The image from ERT shows a cross-section view of solid cuttings in the annular section

representing the mechanistic three layers model of cuttings transport. In a three-layer model, there is a stationary solid bed at the bottom that is represented by the red colour in **Figure 6-12 (a), (b)** and a moving cuttings region above the solid stationary bed. There is also a cuttings free region shown by the blue colour in the contour map.

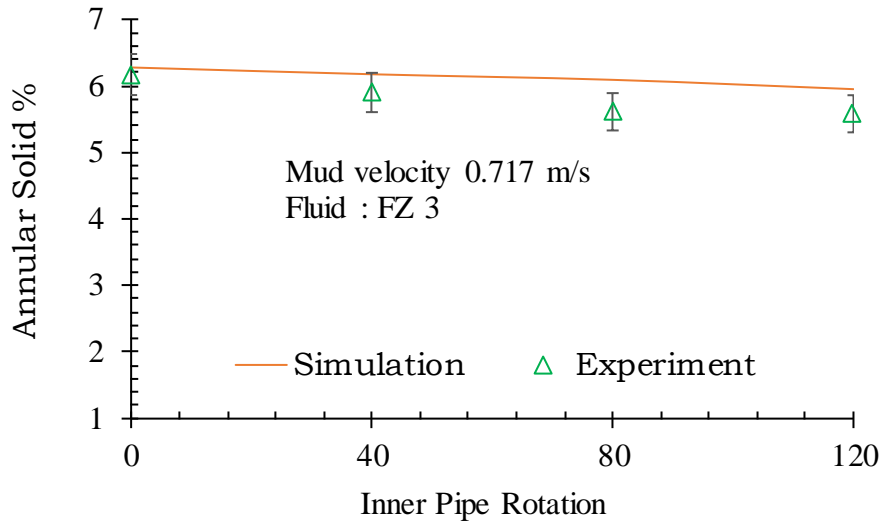


Figure 6-11: CFD model validation. Experimental data vs. Simulation result

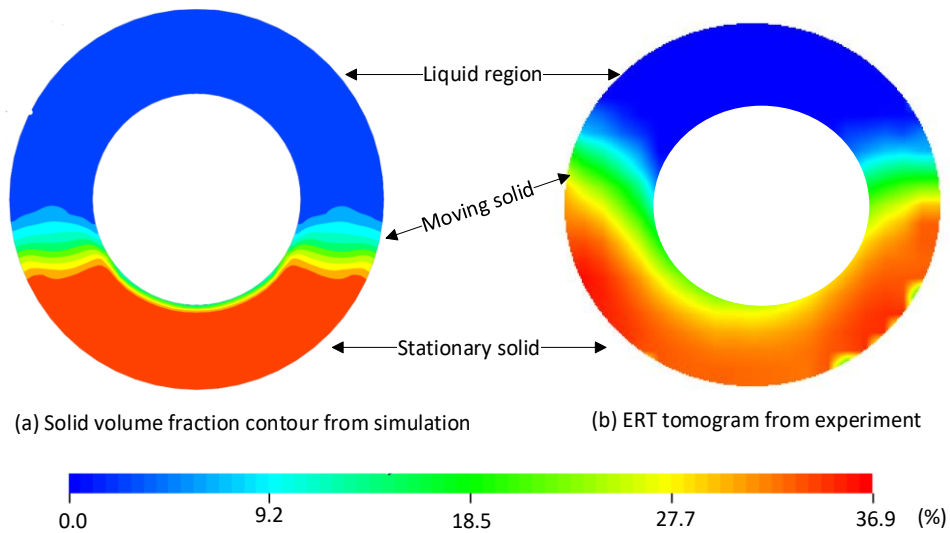


Figure 6-12: CFD Simulation contour vs. ERT Tomogram

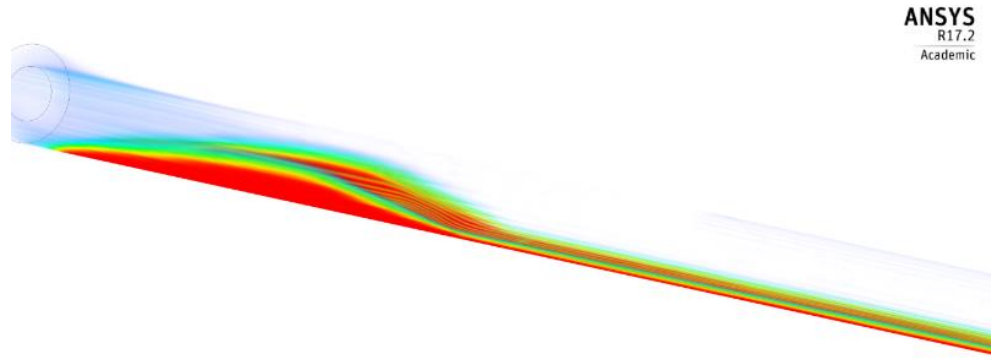
[$V_m = 0.717$ m/s, FZ 3, Input solid 1.51%]

Six different mud velocities ranging from 0.397 m/s to 0.818 m/s were tested in the experimental work at different orientation angle including horizontal. Based on the fluid velocity, solid dune begins to form at different length from the inlet section. At relatively low mud velocity (0.397 m/s), solid dune form at very early stages in the test section and shows stagnant behaviour with time. For a moderate mud velocity (0.571 m/s), solid dune formed, moving forward, and leaving a stationary solid bed behind the moving dune. However, at relatively high mud velocity such as 0.717 m/s, solid dune is formed but not showing any dormant behaviour. The complete dune is gradually moving forward as dune body with no stationary bed left behind the dune.

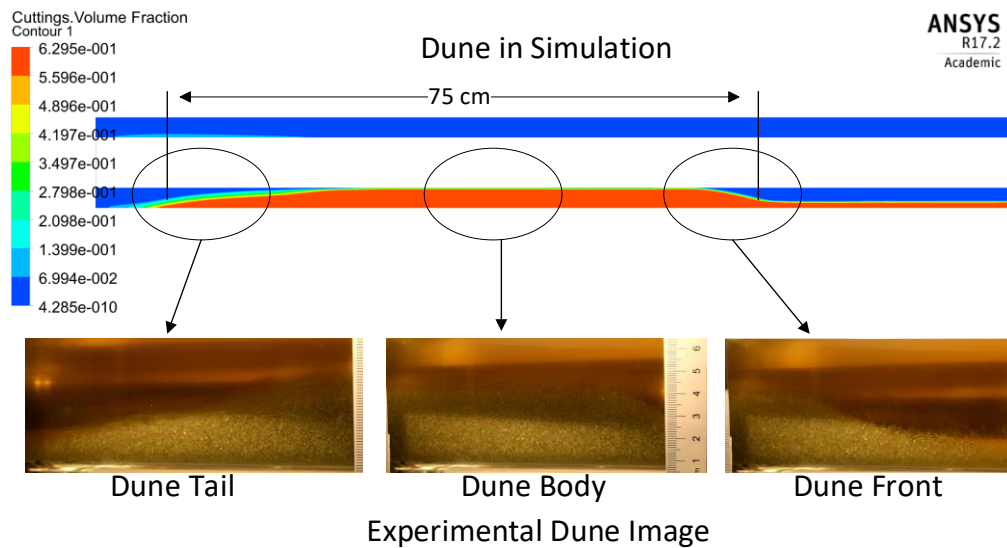
According to the visualization study, the solid cuttings are being transported with different mechanisms, especially rolling and suspended mechanisms. At a low mud velocity, the solid cuttings tend to settle down at the low side of the annular section. The upper layer of solid dune is rolled by fluid drag forces. At a high mud velocity, a moving cuttings layer was observed above the stationary solid dune. A solid dune was characterized by a downslope ramp as the dune front, the main dune body, and a dune tail with an upward slope, as shown in **Figure 6-13**.

A 3-dimensional view of solid dune is shown in **Figure 6-13 (a)**. It clearly shows a solid dune in the lower side of the annular section with a dune front and dune tail. Also, the red colour indicates a stationary solid dune, and the green colour indicates moving cuttings region above the dune body. The solid dune movement pattern for fluid FZ 3 with a mud velocity of 0.717 m/s is compared with the simulation. An almost similar dune pattern is noticed for the experimental and simulation phases. The experimental dune length was 69 cm, where the simulated dune shape was 75 cm, as shown in **Figure 6-13 (b)**. The relative error on the basis of experimental and simulated dune length was 8.7 %, thus, the simulation can offer a good estimate of dune length from the simulation. This relative error is mainly due to the variation of solid cuttings supply by the agitator during the

experimental run. It should be noted that both experiments and simulations were run for the same time interval of 45 seconds.



(a) Three-dimensional view



(b) Two-dimensional view

Figure 6-13: Solid dune movement along the annular section

(a) 3-D view of a solid of a solid dune, (b) 2 -D view of solid dune movement comparison of simulation and experimental dune, image taken by DSLR camera.

6.3.3 Sensitivity Analysis: Transient solid dune movement

The solid dune distributions in a 10° inclined well section are shown in **Figure 6-14** at 15 sec, 30 sec, 45 sec and 60 sec time intervals. The mud velocity was set at 0.651 m/s for the case of fluid FZ 1 with no drill pipe rotation. The colour legend shows the annular solid volume fraction (top legend), black and white legend (bottom legend) shows the length for all 4 cases.

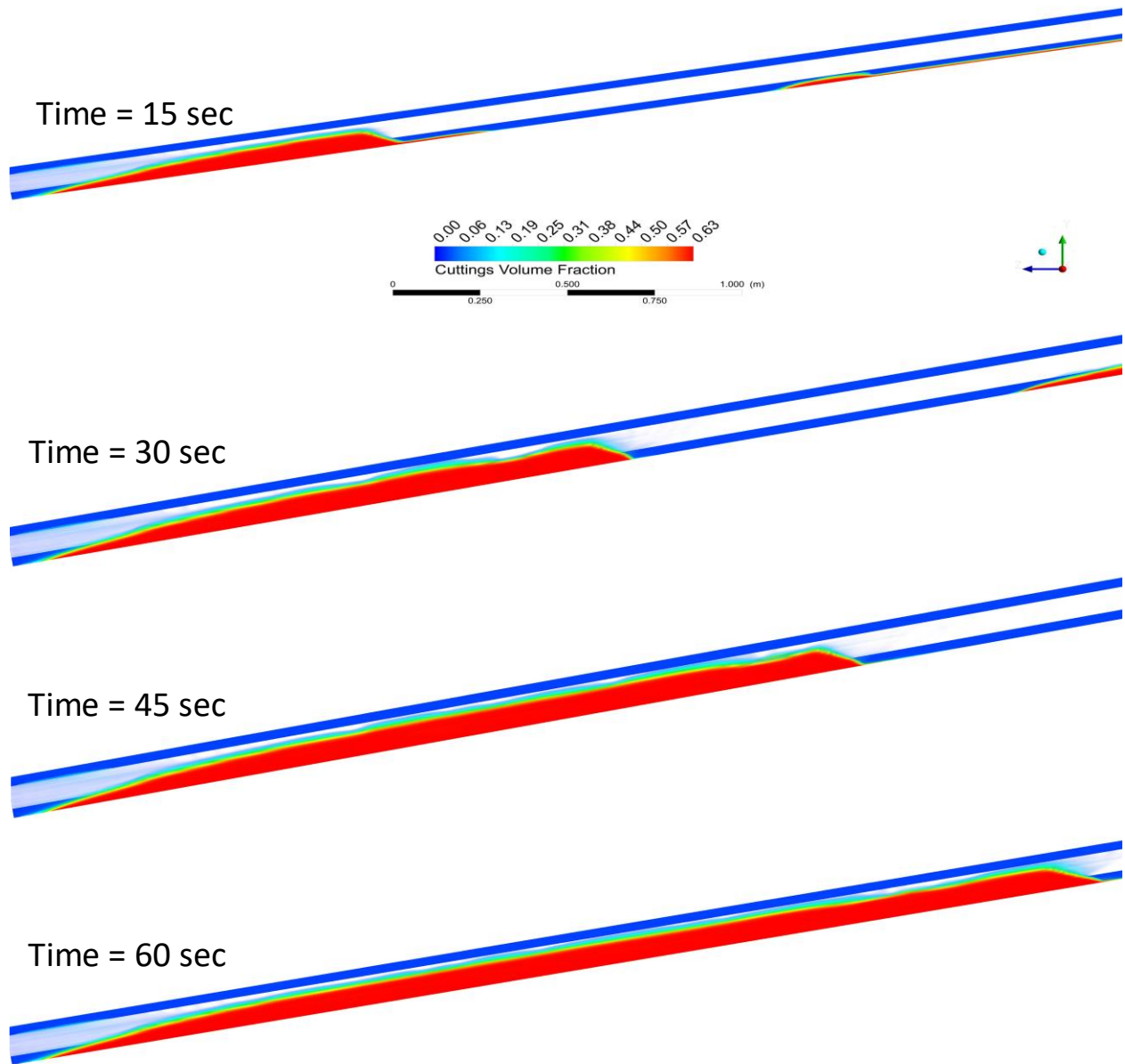


Figure 6-14: Solid dune profile at different time interval

Based on the transient behaviour over time, the length of the solid dune gradually increases, and the solid cuttings are deposited in the lower annular section. The accumulation of solid cuttings at a large portion of the annular section implies a poor hole cleaning with fluid FZ 1 at a velocity of 0.651 m/s.

Due to the experimental limitations, no experiment was performed above 10° inclination from the horizontal orientation. Hence, numerical simulations were performed for an extended period of time (3 minutes simulation) at a time step of 0.005 seconds. Two different fluids were used in the simulation at a different orientation from horizontal to a vertical position at a 15° interval with two different fluid (FZ 1 and FZ 4) two different velocities (0.65 m/s and 1.15 m/s).

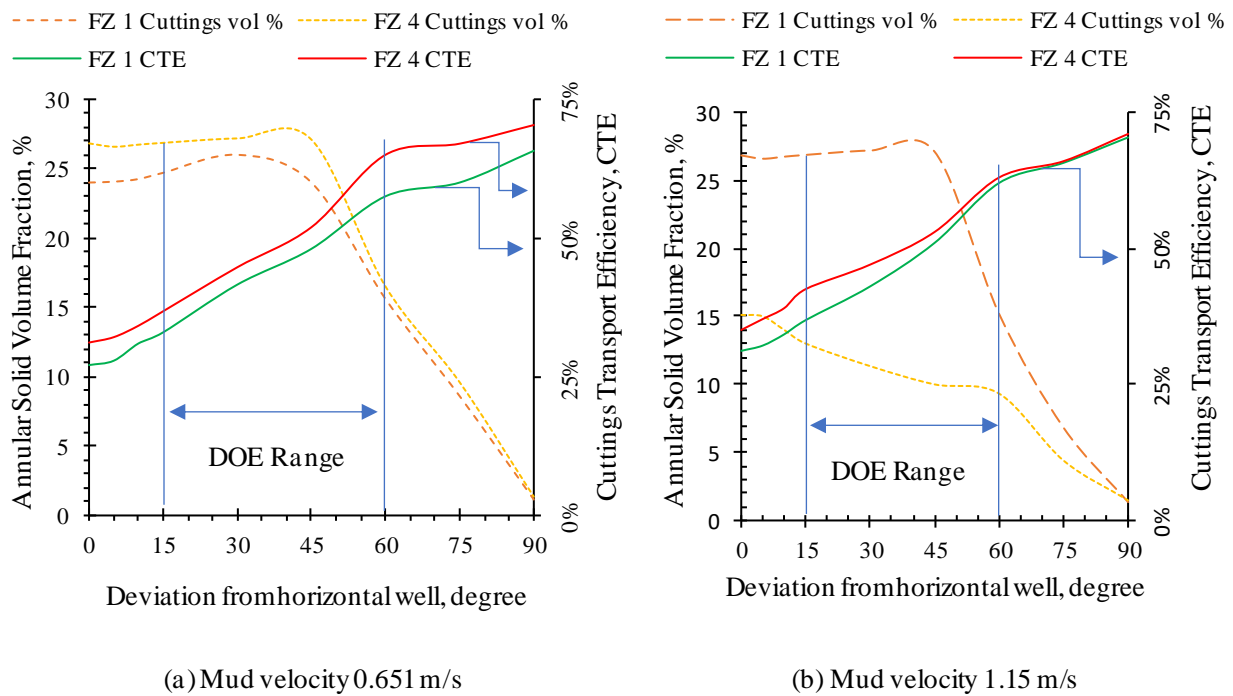


Figure 6-15: CTE response against inclination for fluid FZ 1 and FZ 4

The simulation results for CTE response in terms of inclination are provided in **Figure 6-15** (a) and (b). The annular solid volume fraction and CTE are compared for fluid FZ 1 and FZ 4 at mud velocity 0.65 m/s and 1.15 m/s. For both cases, CTE gradually increases from a horizontal position

to a vertical position regardless of mud velocity and mud viscosity. At both high and low mud velocities, fluid FZ 1 shows a substantial amount of annular accumulated solid volume fraction up to inclination 45° but it is significantly decreased when the inclination is 60° from the horizontal axis. A significant amount of accumulated solid is noticed up to 60° for fluid FZ 4. Since horizontal and near horizontal (15° inclination) well shows an almost similar amount of annular solid volume fraction with fluid FZ 1 and FZ 4, we choose the interval between 15° inclination and 60° inclination to observe the effect of inclination in a two-factor interaction study.

6.3.4 Factorial Design – Response Table:

To perform a complete two level full factorial design with 5 factors, a total $2^5 = 32$ experimental runs are required. Three responses were reported from the simulation. ‘+’ and ‘-’ signs indicate the maximum and minimum levels of the factors. The complete results are listed in **Table 6-3**.

Figure 6-16 shows the Half – normal plot (Taam, 2014) and normal plot (Boylan and Cho, 2012) of CTE for all five parameters and interaction effect. Based on the normal plot, cuttings size (C), mud velocity- inclination interaction (BE), and viscosity- inclination interaction (AE) have a negative impact on the cuttings transport efficiency. On the other hand, mud velocity (B), inclination (E), mud viscosity (A), velocity- cuttings size interaction (BC), viscosity- cuttings size interaction (AC), viscosity-cuttings size-inclination interaction (ACE), velocity-cuttings size-inclination (BCE) exhibit positive impact on the cuttings transport capability.

Figure 6-17 shows the relative effect of each factor on cuttings transport efficiency (CTE). A high transport efficiency indicates that solid dune moving in the annular inclined section with a low annular solid concentration. The plots of mud viscosity, mud velocity and inclination show upward slope, implying that an increase in factor value generally improves the CTE. This replicates the

trend from the experimental result with improved performance for increase in mud velocity, fluid viscosity and inclination as described in **Figure 6-9**.

Table 6-3: Factorial design for 5 factors interaction study

Run No	Factor					Response		
	A Mud Type	B Mud Velocity, m/s	C Cuttings Size, mm	D Drill Pipe Rotation, RPM	E Inclination, Degree	1 CTE, %	2 Cuttings Volume Fraction, %	3 Pressure Drop, Pa/m
1	-	-	-	-	-	41.18	4.8	2898
2	+	-	-	-	-	48.11	4.5	3020
3	-	+	-	-	-	64.53	4.01	4695
4	+	+	-	-	-	71.01	3.92	4873
5	-	-	+	-	-	6.37	5.02	2943
6	+	-	+	-	-	9.49	4.97	3104
7	-	+	+	-	-	37.82	3.55	5846
8	+	+	+	-	-	44.16	3.22	6221
9	-	-	-	+	-	43.22	4.79	2907
10	+	-	-	+	-	50.2	4.62	3034
11	-	+	-	+	-	65.67	4.37	4666
12	+	+	-	+	-	72.50	4.33	4853
13	-	-	+	+	-	6.51	5.01	2912
14	+	-	+	+	-	8.68	4.98	3082
15	-	+	+	+	-	37.62	3.17	5782
16	+	+	+	+	-	44.37	2.9	6134
17	-	-	-	-	+	75.64	4.5	9253
18	+	-	-	-	+	76.36	4.5	9255
19	-	+	-	-	+	71.14	3.02	10606
20	+	+	-	-	+	71.14	3.02	10606
21	-	-	+	-	+	17.65	5.03	9238
22	+	-	+	-	+	21.68	4.96	9349
23	-	+	+	-	+	44.31	2.82	12182
24	+	+	+	-	+	52.39	2.27	12565
25	-	-	-	+	+	76.36	4.6	9257
26	+	-	-	+	+	73.50	4.57	9258
27	-	+	-	+	+	72.88	3.63	10759
28	+	+	-	+	+	73.03	3.74	10777
29	-	-	+	+	+	17.84	5.04	9271
30	+	-	+	+	+	20.14	5.01	9353
31	-	+	+	+	+	45.89	2.43	12193
32	+	+	+	+	+	54.03	2.21	12537

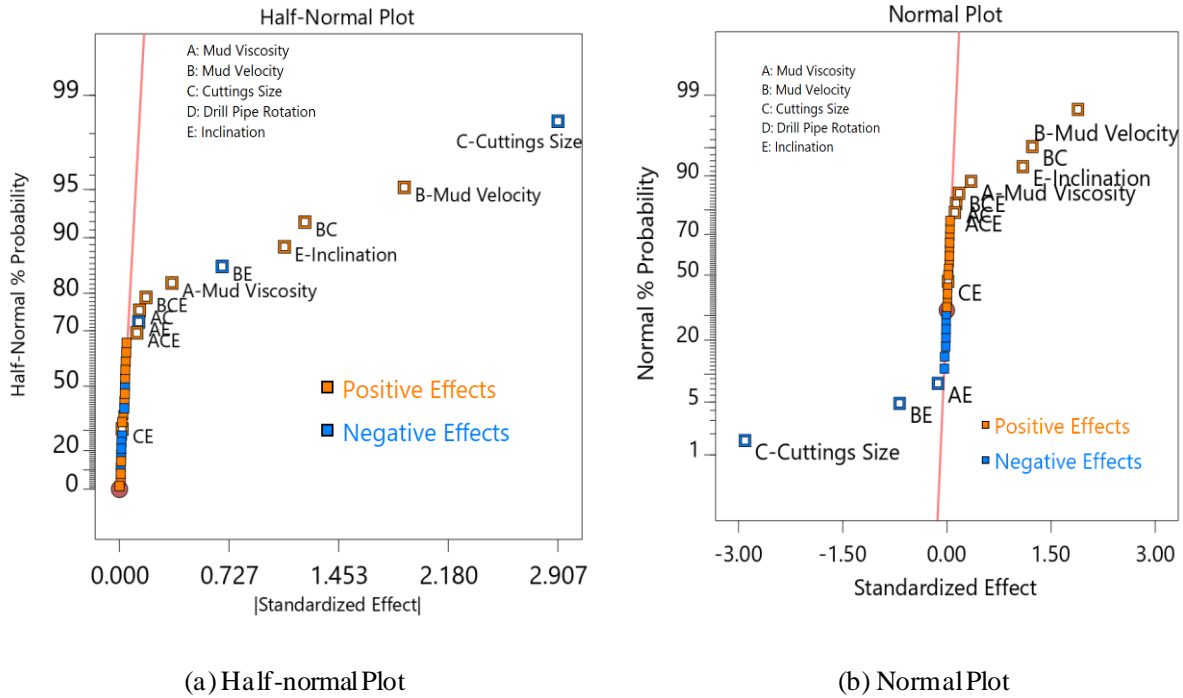


Figure 6-16: Half - Normal and Normal Plot

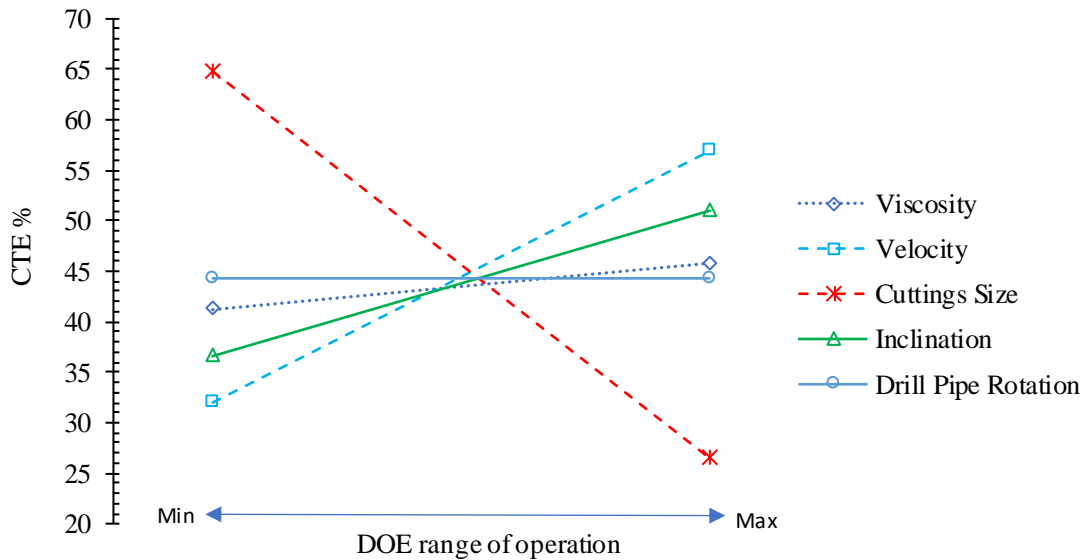


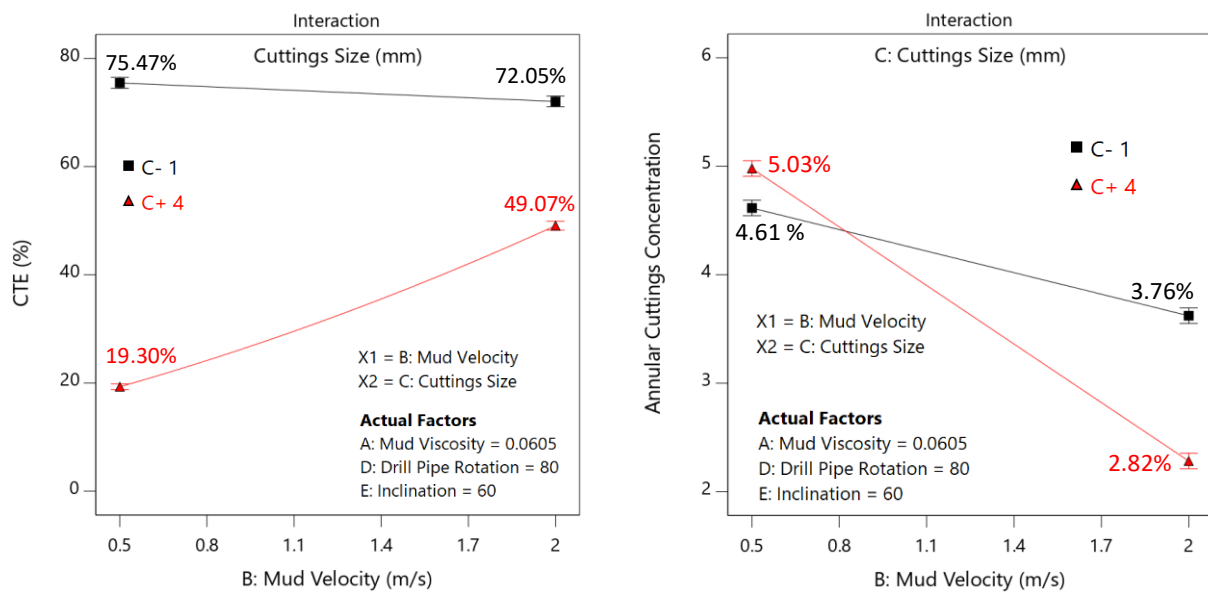
Figure 6-17: Mean dependency of CTE on other parameters

In contrary, cuttings size plot shows a negative slope, indicating that increase in cuttings size decreases the CTE. Although drill pipe rotation leads to a very slight improvement in CTE in as

shown in **Table 6-3**, its impact is minor compared to the other parameters. Hence, the effect of drill pipe rotation is not included in the selected ANOVA model.

6.3.5 Interaction Effects:

This section describes the interactions among the parameters. In this study, AC (viscosity-cuttings size), AE (viscosity-inclination), BC (velocity-cuttings size) and BE (velocity- inclination) shows significant interaction effects.



(a) Velocity and cuttings size (BC) interaction effect on transport efficiency (b) Velocity and cuttings size (BC) interaction effect on annular cuttings concentration

Figure 6-18: Interaction between mud velocity and cuttings size

Figure 6-18 (a) and (b) show the interaction behaviour between mud velocity and solid cuttings size in terms of CTE and annular cuttings concentration, respectively. In both figures, the black line represents the response of 1 mm cuttings size, and the red line represents 4 mm cuttings. **Figure 6-18** (a) shows that CTE for 1 mm cuttings slightly decreases by 3% upon an increase in mud velocity. However, for 4 mm cuttings, CTE is significantly increased by 30%. It is concluded

that an increase in mud velocity is more beneficial for larger cuttings size. This indicated indicates a positive interaction between mud velocity and cuttings size.

According to **Figure 6-18** (b), increasing the mud velocity, decreases the annular solid concentration for both cuttings sizes. This indicates a negative interaction between mud velocity and cuttings size in terms of annular cuttings concentration. However, 4 mm cuttings size shows significantly less annular solid concentration compared to the 1 mm cutting.

6.3.6 Parametric Analysis:

Figure 6-19 (a) describes CTE for a range of cuttings sizes and inclinations at mud velocity 0.5 m/s, whereas **Figure 6-19** (b) shows the same for the mud velocity 2.0 m/s. Based on **Figure 6-19** (a), the lowest CTE is about 8.6 % at 15° inclination with 4 mm cuttings. For the same cuttings size and inclination, a mud velocity of 2.0 m/s increases the transport efficiency to 42%. It implies that a greater mud velocity is required for larger cuttings size.

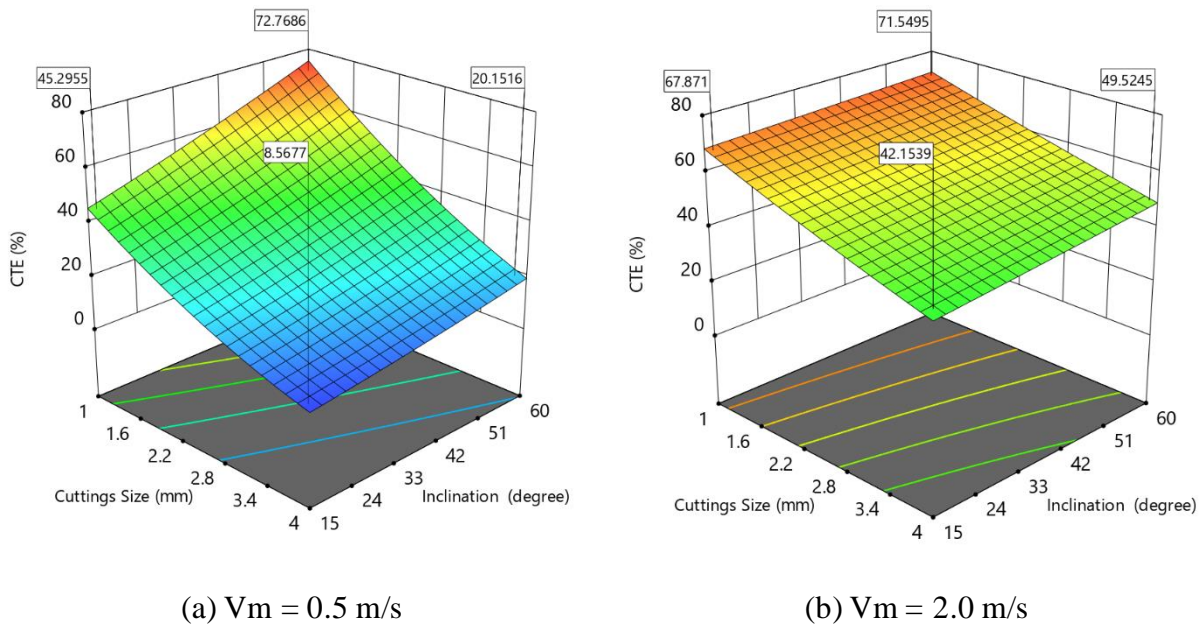
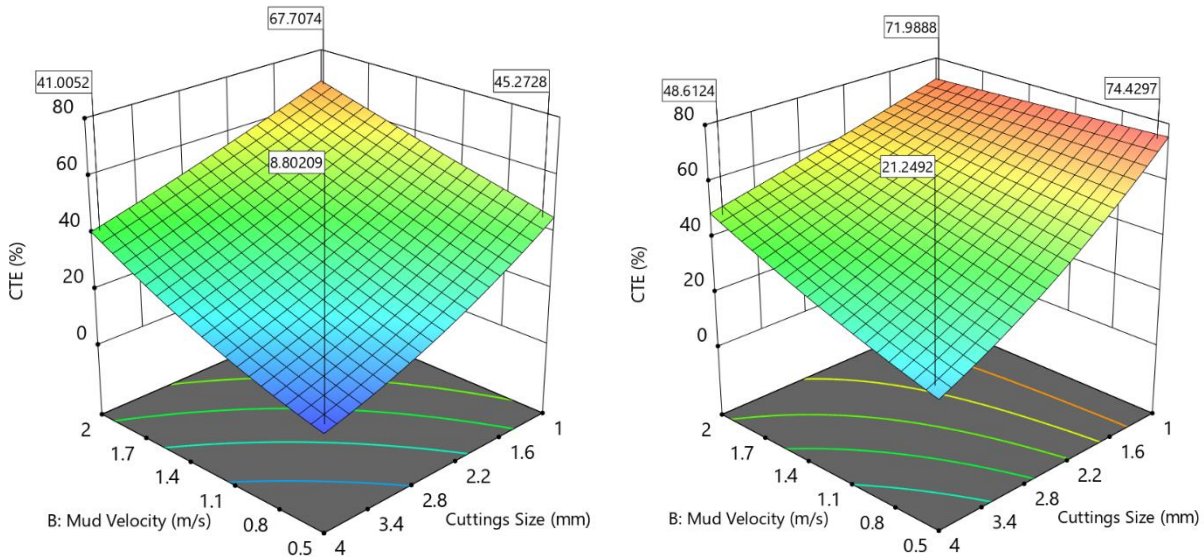


Figure 6-19: Effect of fluid velocity on cutting transport efficiency.

Increasing in mud velocity from 0.5 m/s to 2.0 m/s, CTE increases by about 33% for 4 mm cuttings, while it increases by 23% for 1 mm cuttings. However, no improvement in CTE was observed for the cuttings size 1 mm at 60° inclination. For a low cuttings size (≈ 1 mm), increasing the inclination improved the CTE by 27% for a mud velocity 0.5 m/s, whereas it is only 3.6% at the mud velocity 2.0 m/s.

Figure 6-20 shows the effect of inclination on CTE for a range of mud velocities and cuttings sizes. At 15° inclination, for cutting the size of 1 mm, increasing the mud velocity from 0.5 m/s to 2.0 m/s increases the transport efficiency by 22%. However, at 60° inclination, CTE remains almost constant for the cuttings size less than 1 mm.



(a) 15° inclination

(b) 60° inclination

Figure 6-20: Effect of inclination on cutting transport efficiency.

Figure 6-21 (a) shows for smaller cuttings size (1 mm), CTE is almost similar except a slightly downward trend at 15° inclination and low mud velocity. According to **Figure 6-21** (b), CTE varies almost linearly with increasing the mud velocity for 4 mm cuttings size. Increasing the inclination has a positive impact on the CTE for both cuttings sizes.

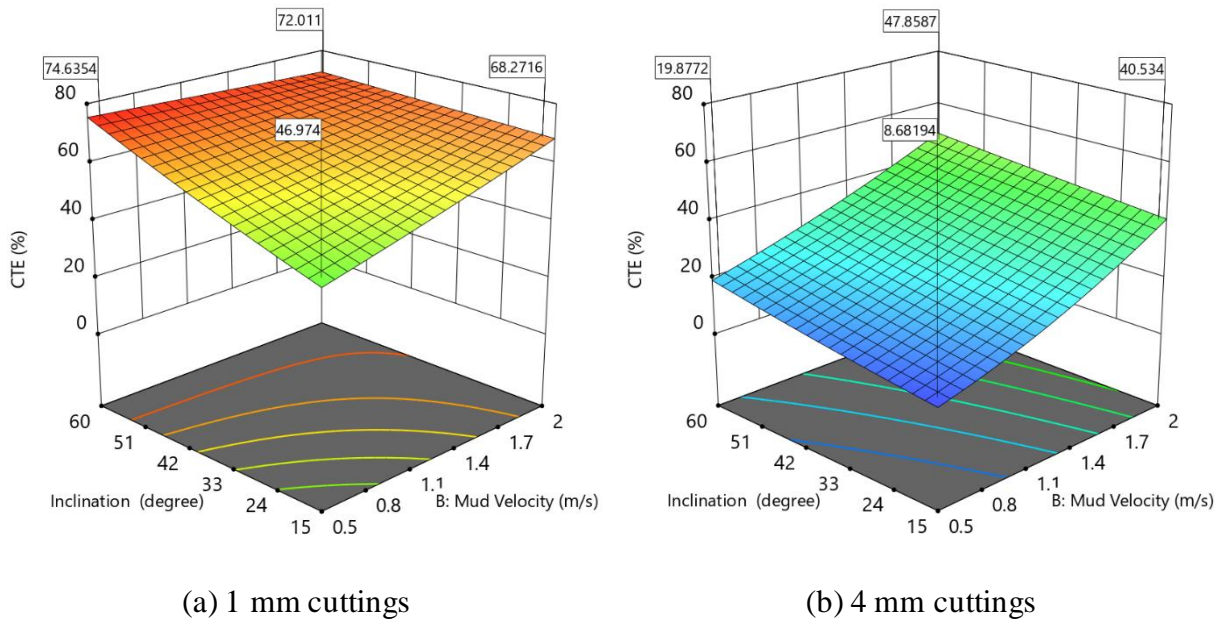


Figure 6-21: Effect of cuttings size

6.3.7 Analysis of Variance - ANOVA:

Table 6-4 presents the analysis of variance (ANOVA) table of the selected model that includes the sum of squares (SS), degree of freedom (DF), F-value, p-value, and percentage of contribution of each parameter in the predicted model.

A higher magnitude of F for a factor indicates that the corresponding parameter has a high impact of factors on the response, i.e., CTE. The F-value of 1771.28 implies that the model is significant. There is only a 0.01% chance that an F-value larger than 1771.28 could occur due to noise. The

relative contribution of each factor, two factors interactions, and three factors interactions are reported in **Figure 6-22**.

Table 6-4: ANOVA for the selected model

Source	Sum of Squares	df	Mean Square	F-value	p-value
Model	123.09	11	11.19	1771.28	< 0.0001
A-Mud Viscosity	0.9698	1	0.9698	153.51	< 0.0001
B-Mud Velocity	28.52	1	28.52	4513.84	< 0.0001
C-Cuttings Size	67.6	1	67.6	10700.06	< 0.0001
E-Inclination	9.58	1	9.58	1515.63	< 0.0001
AC	0.142	1	0.142	22.48	0.0001
AE	0.131	1	0.131	20.74	0.0002
BC	12.09	1	12.09	1913.49	< 0.0001
BE	3.71	1	3.71	587.49	< 0.0001
<i>CE*</i>	<i>0.0026</i>	<i>1</i>	<i>0.0026</i>	<i>0.4117</i>	<i>0.5284</i>
ACE	0.1072	1	0.1072	16.97	0.0005
BCE	0.2492	1	0.2492	39.45	< 0.0001
Residual	0.1264	20	0.0063		
Cor Total	123.22	31			

* Term added to maintain model hierarchy.

Moreover, ANOVA is also combined with Fisher’s statistical test ($p < 0.05$) named as p-value. A p-value of less than 0.05 indicates that selected parameters have a significant impact on the model outcome. In this case, A, B, C, E, AC, AE, BC, BE, ACE, and BCE are the important terms in the model. Values greater than 0.1000 indicate that the model terms are not significant. In this model, the term CE is added only to maintain the model hierarchy.

The statistical parameters of the model are listed in **Table 6-5**. The Predicted R^2 of 0.9974 is in reasonable agreement with the Adjusted R^2 of 0.9984, i.e., the difference is less than 0.2. ‘Adeq Precision’ measures the signal to noise ratio. A ratio greater than 4 is desirable. In this model, the ratio is 126.964, which indicates adequate signal and good reliability. Thus, this model can be used to navigate the design space.

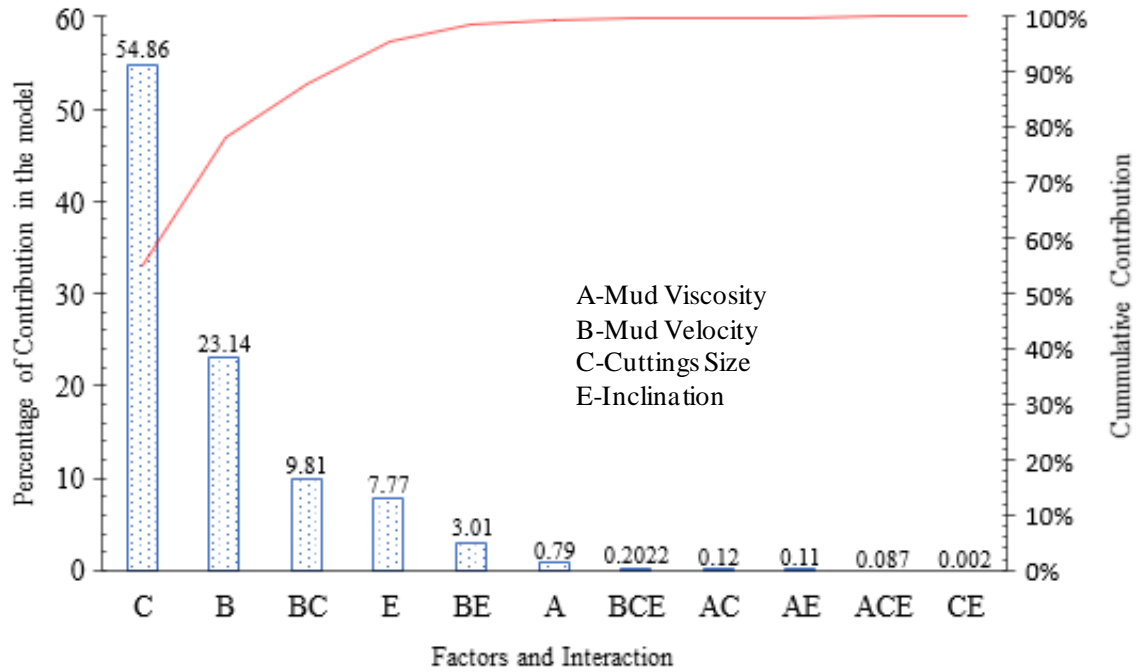


Figure 6-22: Factors and interactions contributions in the model

Table 6-5: The model fit statistics

Std. Dev.	0.0794	R ²	0.999
Mean	6.6	Adjusted R ²	0.9984
C.V. %	1.2	Predicted R ²	0.9974
		Adeq Precision	126.964

ANOVA suggested the following generalized expression for the cuttings transport efficiency (CTE). This includes contribution of all individual parameters, two factors and three factors interactions among the parameters with positive impact and negative impact.

$$\sqrt{CTE} = 6.551 + 5.954 * A + 0.977 * B - 1.477 * C + 0.0675 * E - 0.359 * A * C - 0.128 * A * E + 0.416 * B * C - 0.03 * B * E - 0.006 * C * E + 0.031 * A * C * E + 0.0035 * B * C * E$$

----- (6-10)

where,

A = Mud viscosity (consistency index, k), Pa-s

B = Mud velocity, m/s

C = Cuttings size, mm

E = Inclination, degree

The coefficients in **Equation (6-10)** indicate the relative weight of the corresponding variables. Also, a negative sign for a parameter coefficient denotes the negative impact of the parameter on CTE, and a positive sign shows a positive effect. It should be noted that AE, BC, BE, and CE show the two-factor interactions and ACE, and BCE are the three-factor interactions in the model.

The CTE simulation results and model predictions are provided in **Figure 6-23**. It shows that cuttings transport efficiency comparison of DOE data (actual value) and ANOVA model (predicted value). Since all points follow almost same line, this indicates that the model predicted value are just as close as actual value.

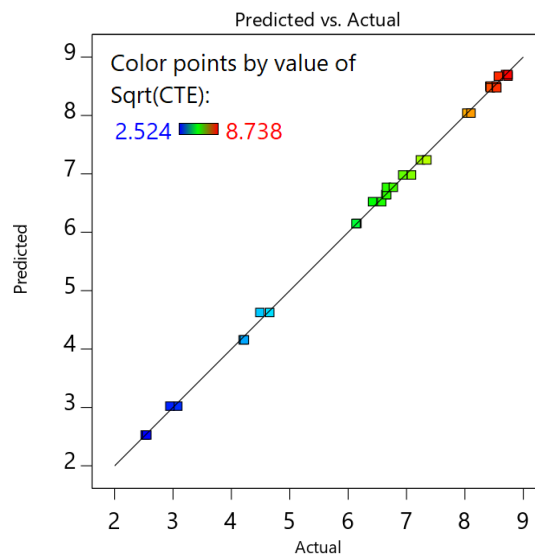


Figure 6-23: Actual vs. Predicted value of CTE for the selected model

This study also developed a generalized model to estimate annular cuttings concentration estimation and annular pressure drop based on the design of experiment and interaction effect analysis. A summary of annular solid volume fraction model is presented in the **Appendix 6-1** and more information on the pressure drop model is found in **Appendix 6-2**.

6.3.8 Artificial Neural Network (ANN) for model validation

To evaluate the CTE prediction model (Equation 6-10) performance, artificial neural network (ANN) method was used in this study. The ANN approach includes 4 inputs (e.g. viscosity, velocity, cuttings size, and inclination) and one output (CTE). In two-layer ANN model, there consist of two layers between input and output; known as ‘Hidden Layer’ and ‘Output Layer’ as shown **Figure 6-24**. The hidden layer consists of several neurons, which control the relationship between inputs and output.

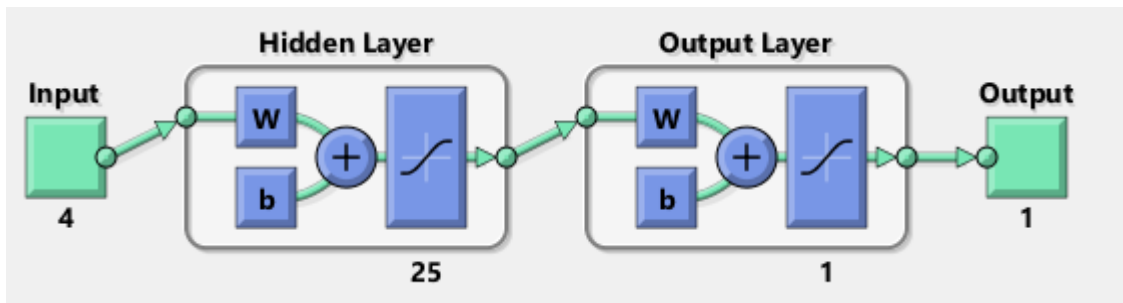


Figure 6-24: ANN architecture for 25 neurons in hidden layer

More than 5000 data points were generated by using **Equation 6-10**. The data was divided into 70% training and 30% for validation and testing purposes. The ANN model performance was checked for different number of neurons in terms of R-squared (R^2) and mean squared error (MSE). The number of neurons in the hidden layers was changed manually, and the outcomes for different neurons configuration were tabulated in **Table 6-6**.

Table 6-6: MSE and R² values based on different numbers of neurons used for CTE model.

Number of Neurons	R ²				MSE
	Training	Validation	Test	ALL	
4	0.99864	0.99874	0.99854	0.99864	1.6393
5	0.99924	0.99925	0.99919	0.99923	0.802104
10	0.99992	0.99991	0.99991	0.99992	0.10248
15	0.99998	0.99998	0.99998	0.99998	0.032145
20	1	0.99999	0.99999	1	0.005762
25	1	1	1	1	0.005204

Using 25 neurons in the hidden layer, CTE model can be predicted by the ANN approach with a high precision (R² =1) attained for all training, validation, and testing phases. MSE also holds the lowest value at this condition.

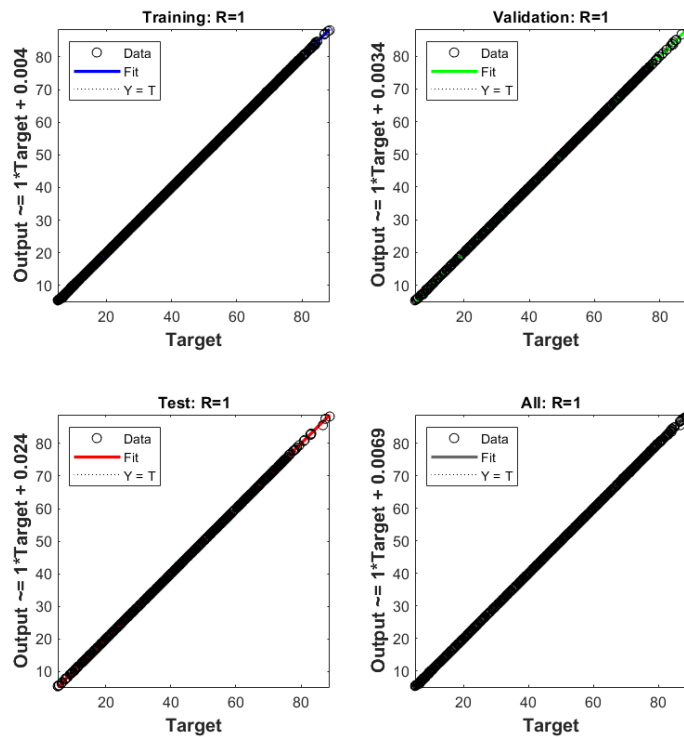


Figure 6-25: Regression analysis for N =25

Figure 6-25 shows the parity plot for all ANN modeling stages for the CTR model with $N = 25$. **Figure 6-26** illustrates the training and testing data for ANN model using 400 Test data points. As it is clear, there is a good match between the predictions and real data for both ANN training and testing phases. The corresponding errors resulted from the ANN model are given in **Figure 6-27**.

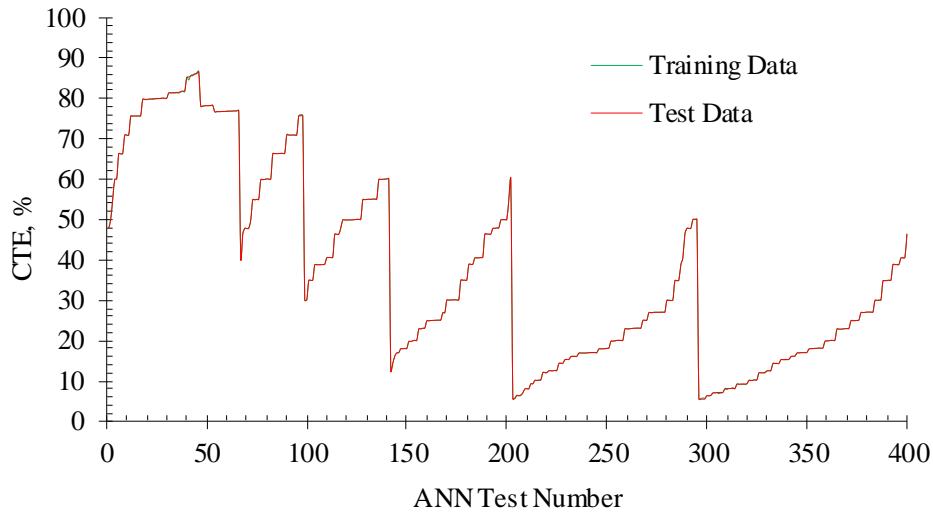


Figure 6-26: CTE versus data index for $N=25$

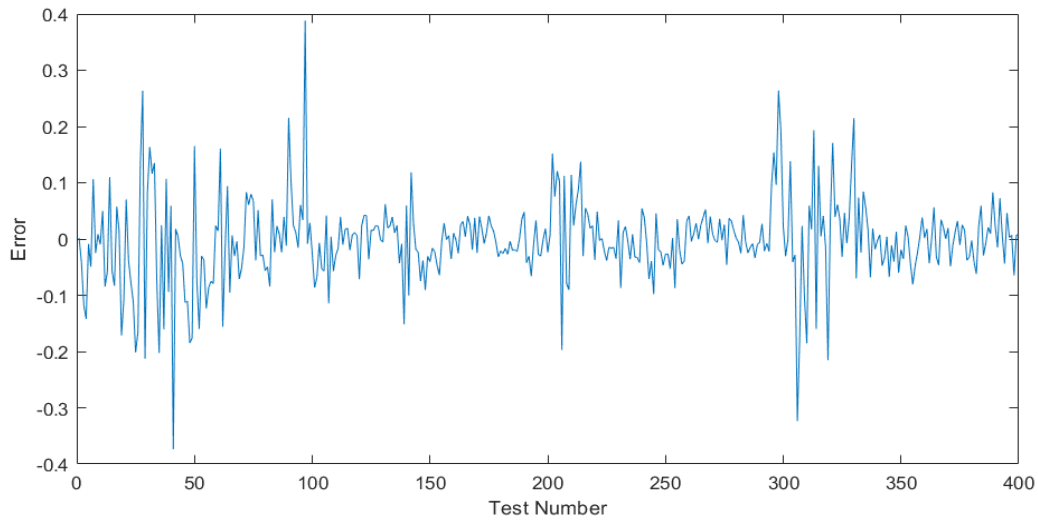


Figure 6-27: Error in trained ANN model for $N = 25$

Once the ANN model is established, the ANN predictions are compared with initial DOE outcomes (from **Table 6-3**) based on the simulation outputs as shown in **Figure 6-28**. It is observed that the ANN model (solid line) predicts the DOE outcomes with a MSE of 0.575. Thus, it can be concluded that the proposed CTE model (Equation 6-10) can reproduce the cuttings transport efficiency with a high accuracy and reliability.

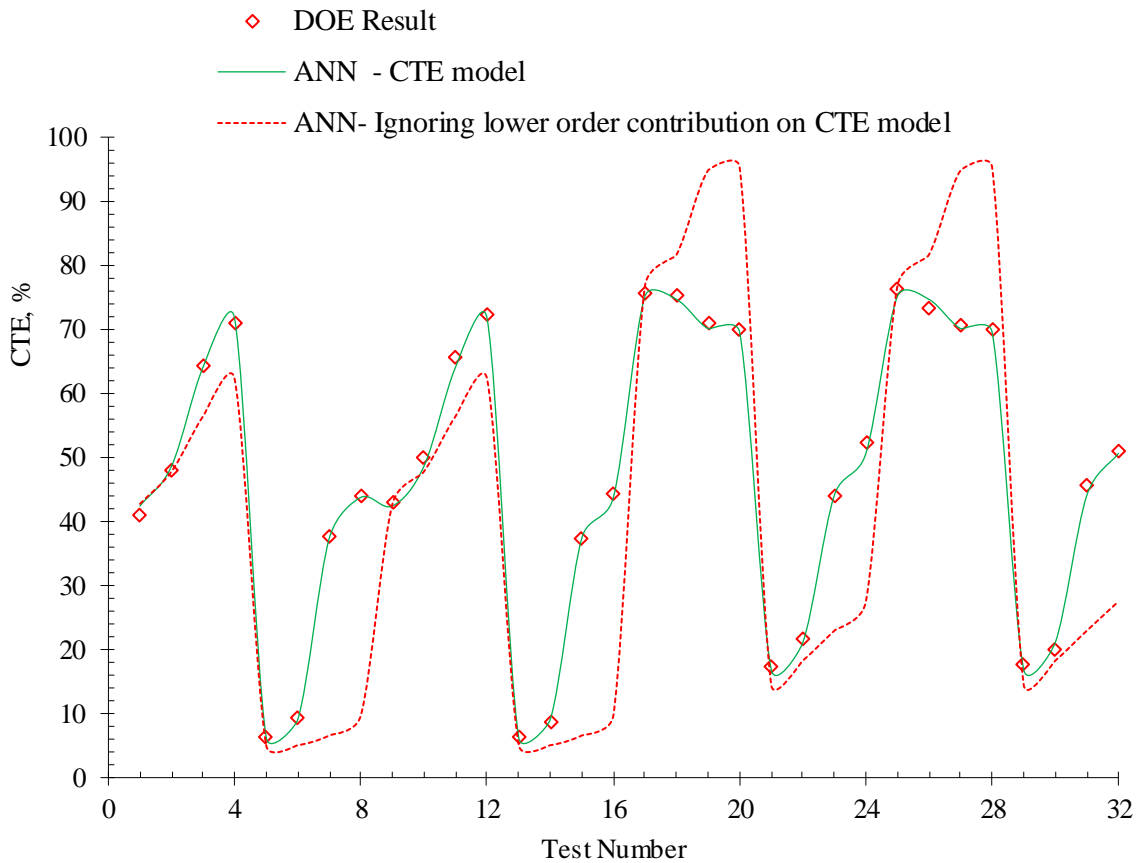


Figure 6-28: Comparison of ANN model with DOE outcome

An attempt was made to check the dependency of lower order interaction in the CTE model [(refer to Equation (6-10)]. Based on **Figure 6-22**, factors BCE, AC, AE, ACE, and CE has less contribution compared to the parameters C, B, BC, E and EA. Therefore, a new ANN model was

tested with ignoring the parameters having low contribution on CTE model (see the dotted line in **Figure 6-28**).

As it is clearly seen in **Figure 6-28**, the revised ANN model (dotted line) follows a trend similar to the initial DOE data. However, it substantially overpredicts for the test numbers of 17,18, 19, 25, 26, and 27 while underpredicts for the test numbers of 6,7, 15, 31, and 32. Upon ignoring the lower order contributing terms, the revised ANN model can predict approximately 35% of the tested data. Therefore, it can be concluded that the model terms with low contribution can still play a considerable role in predicting the CTE.

For the comparison of the ANN model; DOE outcome (from **Table 6-3**) is also used to build another ANN model. Although there is a limited number of data points (32 points) due to transient simulation, 24 data points for training ANN model and 8 data points for the testing phase of the ANN model. A trial-and-error method is used to select the appropriate number of hidden neurons in ANN model. It is found that MSE has the lowest value when $N = 6$ as seen in **Table 6-7**

Table 6-7: MSE and R^2 correlations for different neurons used for DOE data.

Number of hidden neurons	R^2				MSE
	Training	Validation	Test	All	
3	0.9997	0.98248	0.9927	0.99449	126.78
4	0.99952	0.9996	0.9786	0.99738	7.65
6	0.99383	0.99914	0.99568	0.99484	2.11
8	0.99964	0.99965	0.98085	0.93692	55.34
10	0.9996	0.9933	0.94127	0.96654	319.67

Figure 6-29 presents a comparison between DOE test data (see **Table 6-3**), ANN model (see **Table 6-7**) with 6 hidden neurons and CTE model obtained from ANOVA analysis. A good agreement is noticed between the models.

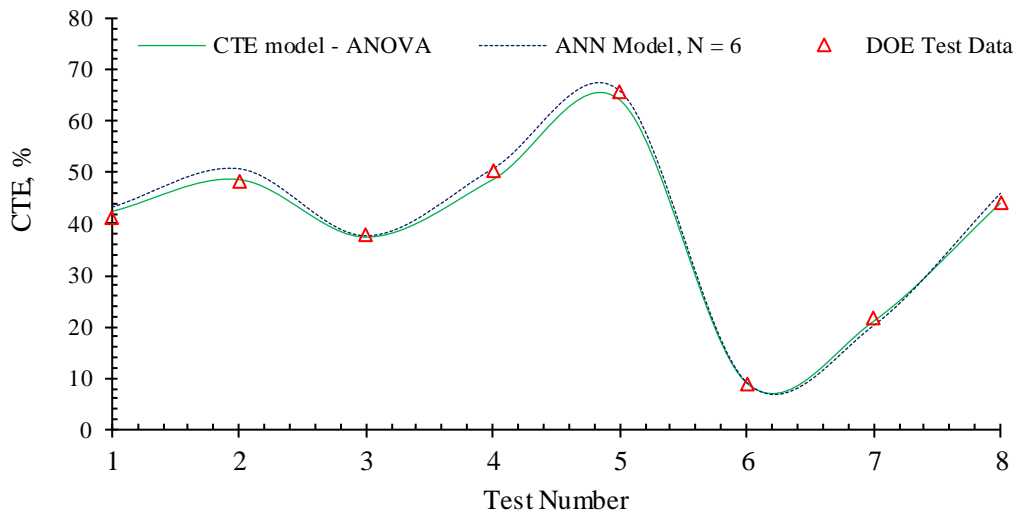


Figure 6-29: Comparison of DOE test data, CTE model based on ANOVA and ANN model

6.4 Summary and Conclusions:

In this study, cuttings transport efficiency in the inclined well with non-Newtonian Herschel-Bulkley fluid was investigated using computational fluid dynamics and experimental investigation. A 5-factor design of the experiment was presented, and interaction effects of different drilling parameters were analysed. The factors are the fluid viscosity, mud velocity, cuttings size, drill pipe rotation and inclination. Out of 5 factors, mud viscosity and inclination show a slightly positive impact; mud velocity exhibits a significantly positive impact; and cuttings size shows a significant negative effect on CTE. Drill pipe rotation has a negligible impact on the magnitude of CTE for the inclined sections. Finally, a generalized expression for CTE is presented, which includes all influential parameters and interactions. The following conclusion can be drawn from this study.

- Significant two factor interactions are identified in cuttings transport within the inclined well. They include the mud viscosity-cuttings size, mud viscosity-inclination, mud velocity-cuttings size, mud velocity- inclination, and cuttings size-inclination. Also, three-

factor interaction such as viscosity-cuttings size-inclination and velocity-cuttings size-inclination are included in the statistical model. The higher-order interactions are ignored due to the negligible impact on the model.

- Cuttings size has the highest contribution of 55% in the CTE model, while the velocity has a 23 % contribution, and the inclination has a contribution of 8%. Velocity -cuttings size interaction has an almost 10% impact on the CTE model. Also, velocity-inclination interaction exhibits a 3 % contribution in the proposed model.
- An inclination up to 60° from the horizontal orientation is more prone to cuttings accumulation regardless of fluid viscosity.
- Based on the statistical analysis, drill pipe rotation has no significant impact on the cuttings transport efficiency (CTE) when compared with the effects of mud velocity, mud viscosity, and inclination.
- The artificial neural network (ANN) model shows that the parameters with even low contribution still considerably affect the CTE predictions.

Acknowledgement:

The researchers gratefully acknowledge and thank Equinor Canada, Memorial University, InnovateNL, and the Natural Sciences and Engineering Research Council of Canada (NSERC) to support this research work. This publication was also made possible by the grant NPRP10-0101-170091 from Qatar National Research Fund (a member of the Qatar Foundation).

Acronyms

- ANOVA - Analysis of Variance
- ANN - Artificial Neural Network

CFD	-	Computational Fluid Dynamics
CPU	-	Central Processing Unit
CTE	-	Cuttings Transport Efficiency
C.V	-	Coefficient of Variance
DF	-	Degree of Freedom
DOE	-	Design of Experiment
DSLR	-	Digital Single Lens Reflex
ERT	-	Electrical Resistance Tomography
fps	-	Frames per second
HB	-	Herschel Bulkley
FZ	-	Flowzan Biopolymer
LPM	-	Liter Per Minutes
MTV	-	Minimum Transport Velocity
NPT	-	Non-Productive Time
RAM	-	Random Access Memory
RPM	-	Revolution Per Minutes
Std. Dev.	-	Standard Deviation
TAMUQ	-	Texas A & M University at Qatar

Variables/Symbols

I_{2D}	-	second variant of deviatoric stress tensor	(-)
e_{ss}	-	coefficient of restitution	(-)
F	-	external body force	(N, lb _f)
F_{lift}	-	lift force	(N, lb _f)
F_{wl}	-	wall lubrication force	(N, lb _f)
F_{vm}	-	virtual mass force	(N, lb _f)
F_{td}	-	turbulent dispersion force	(N, lb _f)
C_D	-	drag coefficient	(-)
$g_{0,ss}$	-	distribution function	(-)
v	-	velocity	(ms ⁻¹)
p	-	pressure	(Pa)
g	-	gravitational acceleration	(m/s ² , ft/s ²)
\dot{m}	-	mass flow rate	(kg/s, lb _m /s)
C_l	-	lift coefficient	(-)

R	-	interaction force between phases	(-)
R^2	-	Coefficient of determination	(-)
K	-	interphase momentum exchange coefficient	(-)
K	-	consistency index	(Pa.s ⁿ)
v_c	-	average velocity of the cuttings	(ms ⁻¹)
v_m	-	average velocity of the drilling mud	(ms ⁻¹)
n	-	flow behaviour index	(-)

Greek Letters

α	-	volume fraction	(-)
π	-	mathematical constant	3.1417
τ_o	-	yield stress	(Pa)
τ	-	shear stress	(Pa)
$\dot{\gamma}$	-	shear rate	(s ⁻¹)
δ	-	offset from the centre	(mm, inch)
∇	-	derivative	(-)
β	-	ratio of vorticity Reynolds number to particle	(-)
$\bar{\bar{\epsilon}}$	-	stress strain tensor	(-)
ρ	-	density	(kg.m ⁻³)
μ	-	shear viscosity	(ms ⁻¹)
λ	-	bulk viscosity	(ms ⁻¹)
Θ	-	granular temperature	(m ² /s ²)
\emptyset	-	angel of internal friction	(rad)

Subscripts

c	-	cuttings
m	-	mud
l	-	liquid phase
s	-	solid phase
kin	-	kinetic component
col	-	collisional component
fr	-	frictional component
ls	-	liquid to solid
sl	-	solid to liquid

References:

- Allahvirdizadeh, P., Kuru, E., Parlaktuna, M., 2016. Experimental investigation of solids transport in horizontal concentric annuli using water and drag reducing polymer-based fluids. *J. Nat. Gas Sci. Eng.* 35, 1070–1078. <https://doi.org/10.1016/j.jngse.2016.09.052>
- Avila, R., Pereira, E., Miska, S., Takach, N., 2004. Correlations and Analysis of Cuttings Transport with Aerated Fluids in Deviated Wells, in: IADC/SPE Drilling Conference. Dallas, Texas, U.S.A., 2 – 4 March. <https://doi.org/10.2118/87180-MS>
- Boylan, G.L., Cho, B.R., 2012. The Normal Probability Plot as a Tool for Understanding Data: A Shape Analysis from the Perspective of Skewness, Kurtosis, and Variability. *Qual. Reliab. Eng. Int.* 28, 249–264. <https://doi.org/10.1002/qre.1241>
- Boyou, N.V., Ismail, I., Wan Sulaiman, W.R., Sharifi Haddad, A., Husein, N., Hui, H.T., Nadaraja, K., 2019. Experimental investigation of hole cleaning in directional drilling by using nano-enhanced water-based drilling fluids. *J. Pet. Sci. Eng.* 176, 220–231. <https://doi.org/10.1016/j.petrol.2019.01.063>
- Capo, J., Yu, M., Miska, S.Z., Takach, N., Ahmed, R., 2004. Cuttings Transport with Aqueous Foam at Intermediate Inclined Wells, in: SPE/ICoTA Coiled Tubing Conference and Exhibition. Houston, Texas, U.S.A. <https://doi.org/10.2118/89534-MS>
- Chen, Z., Ahmed, R.M., Miska, S.Z., Takach, N.E., Yu, M., Pickell, M.B., Hallman, J.H., 2007. Experimental Study on Cuttings Transport With Foam Under Simulated Horizontal Downhole Conditions. *SPE Drill. Complet.* 22, 304–312. <https://doi.org/10.2118/99201-PA>
- Cl Kleinstreuer, 2003. *Two-Phase Flow Theory and Applications*. Routledge, New York. <https://doi.org/https://doi.org/10.1201/9780203734865>

- Czuprat, O., Faugstad, A.M., Byrski, P., Schulze, K., 2020. Hole cleaning efficiency of sweeping pills in horizontal wells - Facts or philosophy?, in: SPE Annual Technical Conference and Exhibition. Denver, Colorado, USA. <https://doi.org/10.2118/201634-ms>
- Epelle, E.I., Gerogiorgis, D.I., 2017. A Multiparametric CFD Analysis of Multiphase Annular Flows for Oil and Gas Drilling Applications. *Comput. Chem. Eng.* 106, 645–661. <https://doi.org/10.1016/j.compchemeng.2017.08.011>
- Fajemidupe, O.T., Aliyu, A.M., Baba, Y.D., Archibong, A.E., Okeke, N.E., Ehinmowo, A.B., Yeung, H., 2019. Minimum sand transport conditions in gas-solid-liquid three-phase stratified flow in horizontal pipelines. *Soc. Pet. Eng. - SPE Niger. Annu. Int. Conf. Exhib. 2019, NAIC 2019.* <https://doi.org/10.2118/198726-MS>
- Fluent, 2015. ANSYS FLUENT User 's Guide 15317, 2794.
- Ford, J.T., Peden, J.M., Oyenehin, M.B., Gao, E., Zarrouh, R., 1990. Experimental investigation of drilled cuttings transport in inclined boreholes, in: SPE Annual Technical Conference and Exhibition. New Orleans, LA, U.S.A., 23-26 September, pp. 197–206. <https://doi.org/10.2523/20421-ms>
- Gul, S., Kuru, E., Parlaktuna, M., 2017. Experimental investigation of cuttings transport in horizontal wells using aerated drilling fluids, in: SPE Abu Dhabi International Petroleum Exhibition and Conference. <https://doi.org/10.2118/188901-ms>
- Hakim, H., Katende, A., Sagala, F., Ismail, I., Nsamba, H., 2018. Performance of polyethylene and polypropylene beads towards drill cuttings transportation in horizontal wellbore. *J. Pet. Sci. Eng.* 165, 962–969. <https://doi.org/10.1016/j.petrol.2018.01.075>

- Heshamudin, N.S., Katende, A., Rashid, H.A., Ismail, I., Sagala, F., Samsuri, A., 2019. Experimental investigation of the effect of drill pipe rotation on improving hole cleaning using water-based mud enriched with polypropylene beads in vertical and horizontal wellbores. *J. Pet. Sci. Eng.* 179, 1173–1185. <https://doi.org/10.1016/j.petrol.2019.04.086>
- Hirpa, M.M., Kuru, E., 2020. Hole cleaning in horizontal wells using viscoelastic fluids-an experimental study of drilling fluid properties on the bed erosion dynamics, in: *SPE/IADC Drilling Conference*. Galveston, Texas. <https://doi.org/10.2118/199636-pa>
- Huque, M.M., Azizur, M., Zendeboudi, S., 2021a. Investigation of cuttings transport in a horizontal well with high-speed visualization and electrical resistance tomography technique. *J. Nat. Gas Sci. Eng.* 92, 103968. <https://doi.org/10.1016/j.jngse.2021.103968>
- Huque, M.M., Butt, S., Zendeboudi, S., Imtiaz, S., 2020. Systematic Sensitivity Analysis of Cuttings Transport in Drilling Operation Using Computational Fluid Dynamics Approach. *J. Nat. Gas Sci. Eng.* 81, 103386. <https://doi.org/10.1016/j.jngse.2020.103386>
- Huque, M.M., Imtiaz, S., Zendeboudi, S., Butt, S., Rahman, M.A., Maheshwari, P., 2021b. Experimental study of cuttings transport with non-Newtonian fluid in an inclined well using visualization and ERT techniques. *SPE Drill. Complet.* SPE-201709-PA. <https://doi.org/10.2118/201709-ms>
- Kamyab, M., Rasouli, V., 2016. Experimental and numerical simulation of cuttings transportation in coiled tubing drilling. *J. Nat. Gas Sci. Eng.* 29, 284–302. <https://doi.org/10.1016/j.jngse.2015.11.022>
- Katende, A., Segar, B., Ismail, I., Sagala, F., Saadiah, H.H.A.R., Samsuri, A., 2020. The effect of drill-pipe rotation on improving hole cleaning using polypropylene beads in water-based mud

at different hole angles. *J. Pet. Explor. Prod. Technol.* 10, 1253–1262.
<https://doi.org/10.1007/s13202-019-00815-1>

Katende, A., Segar, B., Ismail, I., Sagala, F., Saadiah, H.H.A.R., Samsuri, A., 2019. The effect of drill–pipe rotation on improving hole cleaning using polypropylene beads in water-based mud at different hole angles. *J. Pet. Explor. Prod. Technol.* <https://doi.org/10.1007/s13202-019-00815-1>

Kelessidis, V.C., Bandelis, G.E., 2004. Flow Patterns and Minimum Suspension Velocity for Efficient Cuttings Transport in Horizontal and Deviated Wells in Coiled-Tubing Drilling. *SPE Drill. Complet.* <https://doi.org/10.2118/81746-PA>

Kelessidis, V.C., Bandelis, G.E., Li, J., 2007. Flow of dilute solid-liquid mixtures in horizontal concentric and eccentric annuli. *J. Can. Pet. Technol.* 46, 56–61. <https://doi.org/10.2118/07-05-06>

Keshavarz Moraveji, M., Sabah, M., Shahryari, A., Ghaffarkhah, A., 2017. Investigation of drill pipe rotation effect on cutting transport with aerated mud using CFD approach. *Adv. Powder Technol.* 28, 1141–1153. <https://doi.org/10.1016/j.appt.2017.01.020>

Kim, H.-Y., 2014. Analysis of variance (ANOVA) comparing means of more than two groups. *Restor. Dent. Endod.* 39, 74–77. <https://doi.org/10.5395/rde.2014.39.1.74>

Kim, Y.J., Woo, N.S., Hwang, Y.K., Kim, J.H., Han, S.M., 2014. Transport of small cuttings in solid-liquid flow with inclined slim hole annulus. *J. Mech. Sci. Technol.* 28, 115–126. <https://doi.org/10.1007/s12206-013-0952-7>

Li, J., Luft, B., 2014. Overview of solids transport studies and applications in oil and gas industry

- Experimental work. Soc. Pet. Eng. - SPE Russ. Oil Gas Explor. Prod. Tech. Conf. Exhib. 2014, RO G 2014 - Sustain. Optimising Prod. Challenging Limits with Technol. 2, 1365–1401. <https://doi.org/10.2118/171285-ms>
- Li, J., Walker, S., 2007. Sensitivity Analysis of Hole Cleaning Parameters in Directional Wells Wells, in: SPE/ICoTA Coiled Tubing Roundtable. pp. 976–980. <https://doi.org/10.2118/74710-PA>
- Naganawa, S., Sato, R., Ishikawa, M., 2017. Cuttings-transport simulation combined with large-scale-flow-loop experimental results and logging-while-drilling data for hole-cleaning evaluation in directional drilling. SPE Drill. Complet. 32, 194–207. <https://doi.org/10.2118/171740-PA>
- Okrajni, S., Azar, J.J., 1986. The Effects of Mud Rheology on Annular Hole Cleaning in Directional Wells. SPE Drill. Eng. 1, 297–308. <https://doi.org/10.2118/14178-PA>
- Osunde, O., Kuru, E., 2008. Numerical Modelling of Cuttings Transport with Foam in Inclined Wells. Open Fuels Energy Sci. J. 1, 19–33. <https://doi.org/10.2118/2006-071>
- Ozbayoglu, M.E., Saasen, A., Sorgun, M., Svanes, K., 2008. Effect of Pipe Rotation on Hole Cleaning for Water-Based Drilling Fluids in Horizontal and Deviated Wells, in: IADC/SPE Asia Pacific Drilling Technology Conference and Exhibition. Jakarta, Indonesia. 25–27 August. <https://doi.org/10.2118/114965-MS>
- Pandya, S., Ahmed, R., Shah, S., 2020. Wellbore cleanout in inclined and horizontal wellbores: The effects of flow rate, fluid rheology, and solids density. SPE Drill. Complet. 35, 48–68. <https://doi.org/10.2118/194240-PA>

- Pang, B., Wang, S., Wang, Q., Yang, K., Lu, H., Hassan, M., Jiang, X., 2018. Numerical Prediction of Cuttings Transport Behavior in Well Drilling Using Kinetic Theory of Granular Flow. *J. Pet. Sci. Eng.* 161, 190–203. <https://doi.org/10.1016/j.petrol.2017.11.028>
- Peden, J.M., Ford, J.T., Oyenehin, M.B., 1990. Comprehensive Experimental Investigation of Drilled Cuttings Transport in Inclined Wells Including the Effects of Rotation and Eccentricity, in: *European Petroleum Conference*. The Hague, The Netherlands, 22-24 October. <https://doi.org/10.2118/20925-MS>
- Pierlot, C., Pawlowski, L., Bigan, M., Chagnon, P., 2008. Design of experiments in thermal spraying: A review. *Surf. Coatings Technol.* 202, 4483–4490. <https://doi.org/https://doi.org/10.1016/j.surfcoat.2008.04.031>
- Pilehvari, A.A., Azar, J.J., Shirazi, S.A., 2007. State-of-the-Art Cuttings Transport in Horizontal Wellbores. *SPE Drill. Complet.* 14, 196–200. <https://doi.org/10.2118/57716-pa>
- Piroozian, A., Ismail, I., Yaacob, Z., Babakhani, P., Ismail, A.S.I., 2012. Impact of Drilling Fluid Viscosity, Velocity And Hole Inclination On Cuttings Transport In Horizontal And Highly Deviated Wells. *J. Pet. Explor. Prod. Technol.* 2, 149–156. <https://doi.org/10.1007/s13202-012-0031-0>
- Ramadan, A., Skalle, P., Johansen, S.T., Svein, J., Saasen, A., 2001. Mechanistic Model for Cuttings Removal From Solid Bed in Inclined Channels. *J. Pet. Sci. Eng.* 30, 129–141. [https://doi.org/10.1016/S0920-4105\(01\)00108-5](https://doi.org/10.1016/S0920-4105(01)00108-5)
- Rasul, G., Qureshi, M.F., Ferroudji, H., Butt, S., Hasan, R., Hassan, I., Rahman, M.A., 2020. Analysis of cuttings transport and flow pattern in nearly horizontal extended reach well. *J. Adv. Res. Fluid Mech. Therm. Sci.* 71, 69–86. <https://doi.org/10.37934/arfmts.71.2.6986>

- Rodriguez Corredor, F., Bizhani, M., Kuru, E., 2016. Experimental investigation of cuttings bed erosion in horizontal wells using water and drag reducing fluids. *J. Pet. Sci. Eng.* 147, 129–142. <https://doi.org/10.1016/j.petrol.2016.05.013>
- Rolf Carlson, 1992. Two-level factorial designs, in: Carlson, R.B.T.-D.H. in S. and T. (Ed.), *Design and Optimization in Organic Synthesis*. Elsevier, pp. 89–122. [https://doi.org/https://doi.org/10.1016/S0922-3487\(08\)70252-1](https://doi.org/https://doi.org/10.1016/S0922-3487(08)70252-1)
- Rooki, R., Doulati Ardejani, F., Moradzadeh, A., Norouzi, M., 2014. Simulation of Cuttings Transport with Foam in Deviated Wellbores Using Computational Fluid Dynamics. *J. Pet. Explor. Prod. Technol.* 4, 263–273. <https://doi.org/10.1007/s13202-013-0077-7>
- Shadizadeh, S.R., Zoveidavianpoor, M., 2012. An experimental modeling of cuttings transport for an Iranian directional and horizontal well drilling. *Pet. Sci. Technol.* 30, 786–799. <https://doi.org/10.1080/10916466.2010.490816>
- Siamak, A., Mehdi, B., Majid, R., 2015. CFD-DEM approach to investigate the effect of drill pipe rotation on cuttings transport behavior. *J. Pet. Sci. Eng.* 127, 229–244. <https://doi.org/10.1016/j.petrol.2015.01.017>
- Sifferman, T.R., Becker, T.E., 1992. Hole Cleaning in Full-Scale Inclined Wellbores. *SPE Drill. Eng.* 7, 115–120. <https://doi.org/10.2118/20422-PA>
- Sifferman, T.R., Myers, G.M., Haden, E.L., Wahl, H.A., 1973. Drill Cutting Transport in Full Scale Vertical Annuli, in: *Society of Petroleum Engineers of AIME*. Las Vegas, p. 5.
- Sun, B., Xiang, H., Li, H., Li, X., 2017. Modeling of the Critical Deposition Velocity of Cuttings in an Inclined-Slimhole Annulus. *SPE J.* 22, 1213–1224. <https://doi.org/10.2118/185168-PA>

- Taam, W., 2014. Half-normal plot - Some examples. Wiley StatsRef Stat. Ref. Online, Major Reference Works. <https://doi.org/doi:10.1002/9781118445112.stat04081>
- Tabachnick, B., 2007. Experimental Designs Using ANOVA.
- Tomren, P.H., Iyoho, A.W., Azar, J.J., 1986. Experimental Study of Cuttings Transport in Directional Wells. SPE Drill. Eng. 43–56. <https://doi.org/10.2118/12123-PA>
- Vaziri, E., Simjoo, M., Chahardowli, M., 2020. Application of foam as drilling fluid for cuttings transport in horizontal and inclined wells: A numerical study using computational fluid dynamics. J. Pet. Sci. Eng. 194, 107325. <https://doi.org/10.1016/j.petrol.2020.107325>
- Woo, N., Kim, Y., Kwon, J., Chung, S., Park, E., 2011. A Study on the Solid-liquid Rotating Flow for Cuttings Transportation in Inclined Annulus. Isope 8, 771–776.
- Xiaofeng, S., Kelin, W., Tie, Y., Yang, Z., Shuai, S., Shizhu, L., 2013. Review of Hole Cleaning in Complex Structural Wells. Open Pet. Eng. J. 6, 25–32. <https://doi.org/10.2174/1874834101306010025>
- Yeu, W.J., Katende, A., Sagala, F., Ismail, I., 2019. Improving hole cleaning using low density polyethylene beads at different mud circulation rates in different hole angles. J. Nat. Gas Sci. Eng. 61, 333–343. <https://doi.org/10.1016/j.jngse.2018.11.012>

Appendix 6-1

Table 6-8: ANOVA for annular cuttings concentration

Source	Sum of Squares	df	Mean Square	F-value	p-value
Model	26.06	13	2	252.38	< 0.0001
A-Mud Viscosity	0.1339	1	0.1339	16.86	0.0007
B-Mud Velocity	18.44	1	18.44	2321.53	< 0.0001
C-Cuttings Size	0.5859	1	0.5859	73.77	< 0.0001
D-Drill Pipe Rotation	0.052	1	0.052	6.55	0.0197
E-Inclination	1.45	1	1.45	182.48	< 0.0001
AB	0.0158	1	0.0158	1.98	0.1761
AC	0.0332	1	0.0332	4.17	0.056
BC	3.52	1	3.52	442.95	< 0.0001
BD	0.0116	1	0.0116	1.46	0.2419
BE	1.07	1	1.07	134.66	< 0.0001
CD	0.3763	1	0.3763	47.38	< 0.0001
ABC	0.0872	1	0.0872	10.97	0.0039
BCD	0.2869	1	0.2869	36.12	< 0.0001
Residual	0.143	18	0.0079		
Cor Total	26.2	31			

Generalized expression for annular cuttings concentration.

Annular Solid Volume Fraction, (%)

$$\begin{aligned}
 &= 4.6883 - 2.1446 * A - 0.2664 * B + 0.1961 * C - 0.0021 * D + 0.0041 \\
 &* E + 1.5566 * A * B + 0.6582 * A * C - 0.1359 * B * C + 0.0067 * B * D \\
 &- 0.01083 * B * E + 0.00094 * C * D - 0.835836 * A * B * C - 0.0024 * B * C \\
 &* D
 \end{aligned}$$

Where, A = Mud viscosity (consistency index, k), Pa-s

B = Mud velocity, m/s

C = Cuttings size, mm

D = Drill pipe rotation, rpm

E = Inclination, degree

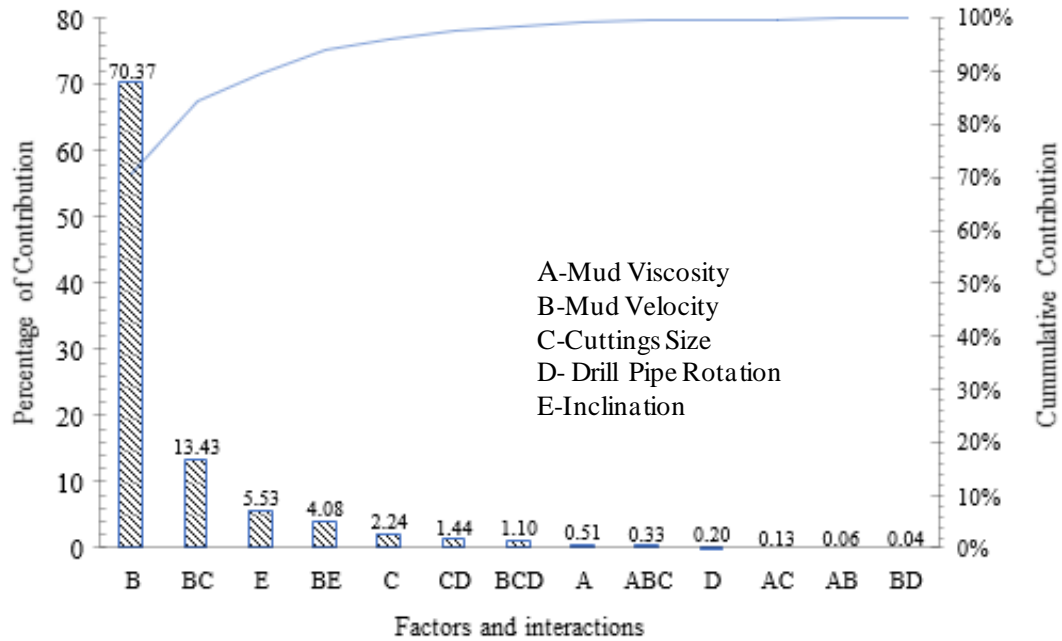


Figure 6-30: Factors and interaction contribution in annular solid concentration.

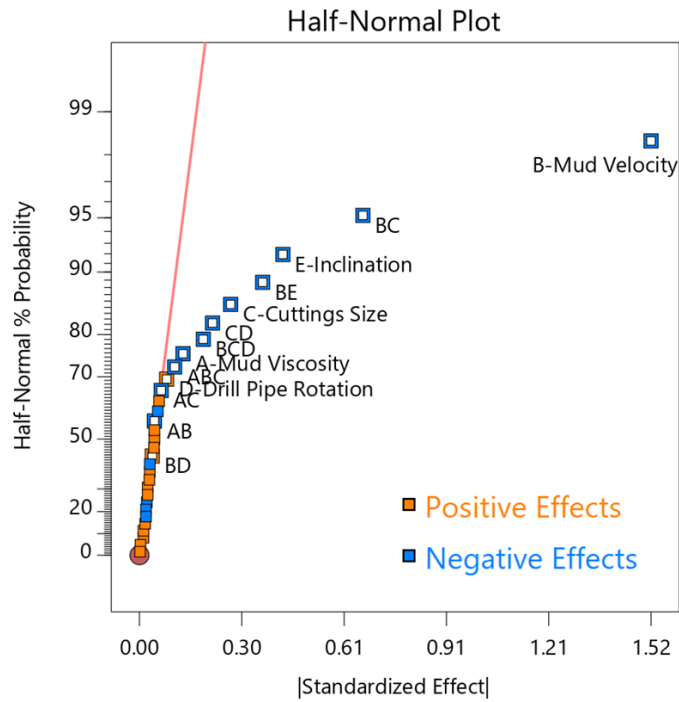


Figure 6-31: Half normal plot for annular cuttings concentration.

A negative effect indicates that increase an input parameter value decrease the response value (annular cutting concentration). In this case, a negative effect is desirable since it decrease annular solid concentration.

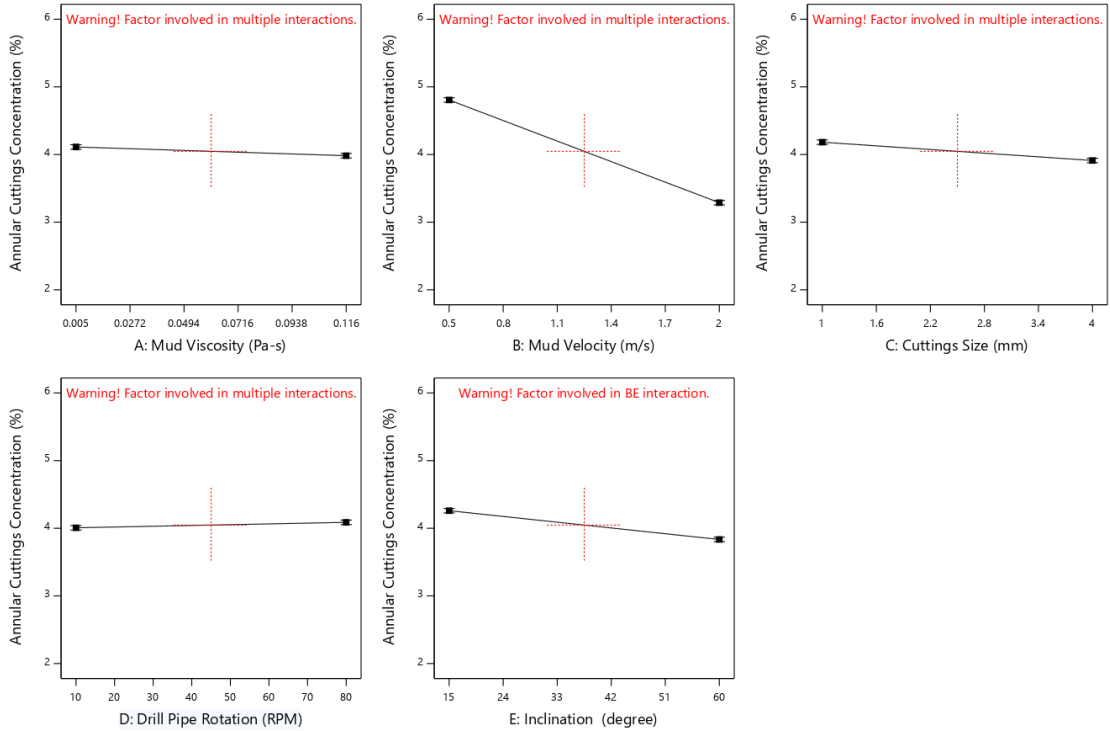
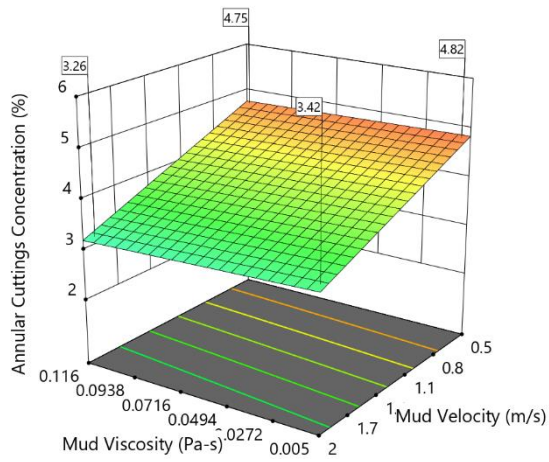
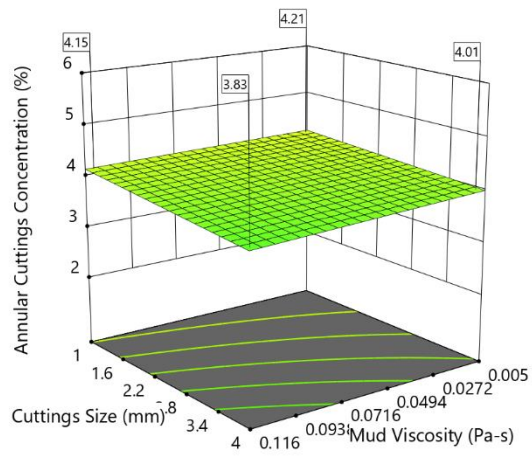


Figure 6-32: Mean dependency of annular concentration on other parameters

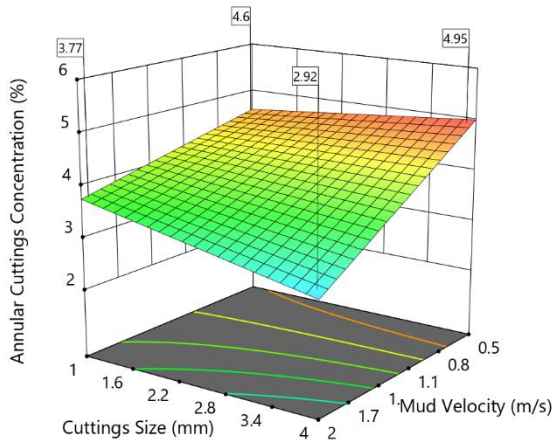
Interaction Behaviour with respect to annular cuttings concentration



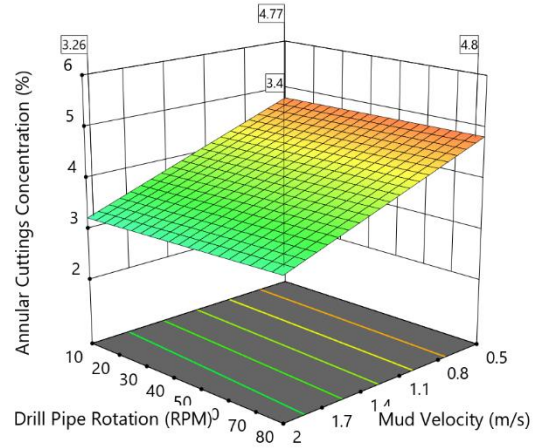
(a) Viscosity-velocity interaction



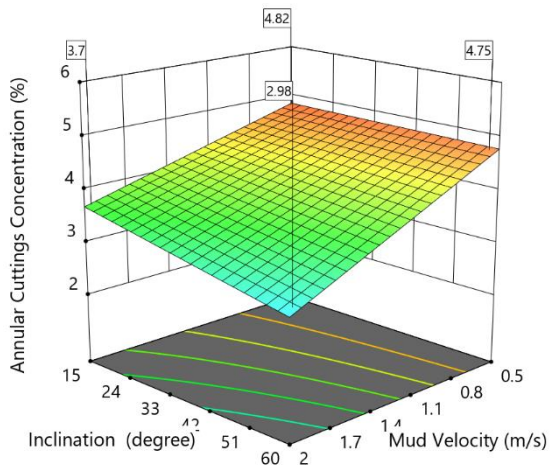
(b) Viscosity- cuttings size interaction



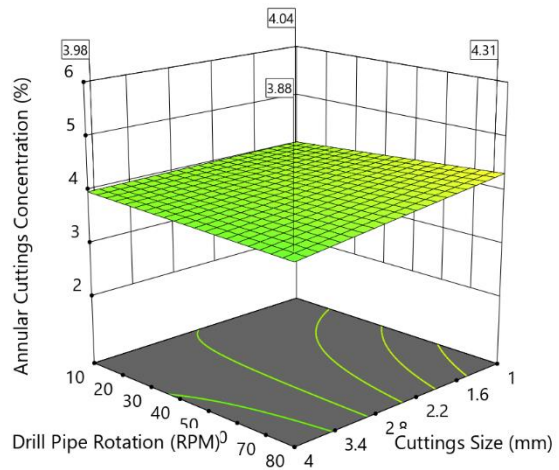
(c) Cuttings size- velocity interaction



(d) Drill pipe rotation- velocity interaction



(e) Inclination- velocity interaction



(f) Drill pipe rotation-cuttings size interaction

Figure 6-33: Two factor interaction in annular cuttings concentration

Appendix 6-2

Table 6-9: ANOVA for pressure drop.

Source	Sum of Squares	df	Mean Square	F-value	p-value
Model	3.61E+08	5	7.22E+07	4422.99	< 0.0001
A-Mud Viscosity	2.13E+05	1	2.13E+05	13.07	0.0013
B-Mud Velocity	4.32E+07	1	4.32E+07	2642.65	< 0.0001
C-Cuttings Size	4.50E+06	1	4.50E+06	275.34	< 0.0001
E-Inclination	3.09E+08	1	3.09E+08	18941.5	< 0.0001
BC	3.96E+06	1	3.96E+06	242.41	< 0.0001
Residual	4.25E+05	26	16329.98		
Cor Total	3.62E+08	31			

The Model F-value of 4422.99 implies the model is significant. There is only a 0.01% chance that an F-value this large could occur due to noise.

P-values less than 0.0500 indicate model terms are significant. In this case A, B, C, E, BC are significant model terms. Values greater than 0.1000 indicate the model terms are not significant.

$$\text{Annular pressure drop, } \frac{\text{Pa}}{\text{m}} = 440.7 + 1471.3 * A + 776.8 * B - 140.9 * C + 137.2 * E + 312.6 * B * C$$

Where, A = Mud viscosity (consistency index, k), Pa-s

B = Mud velocity, m/s

C = Cuttings size, mm

E = Inclination, degree

*The impact of drill pipe rotation on the inclined section is negligible and hence it is ignored in the model.

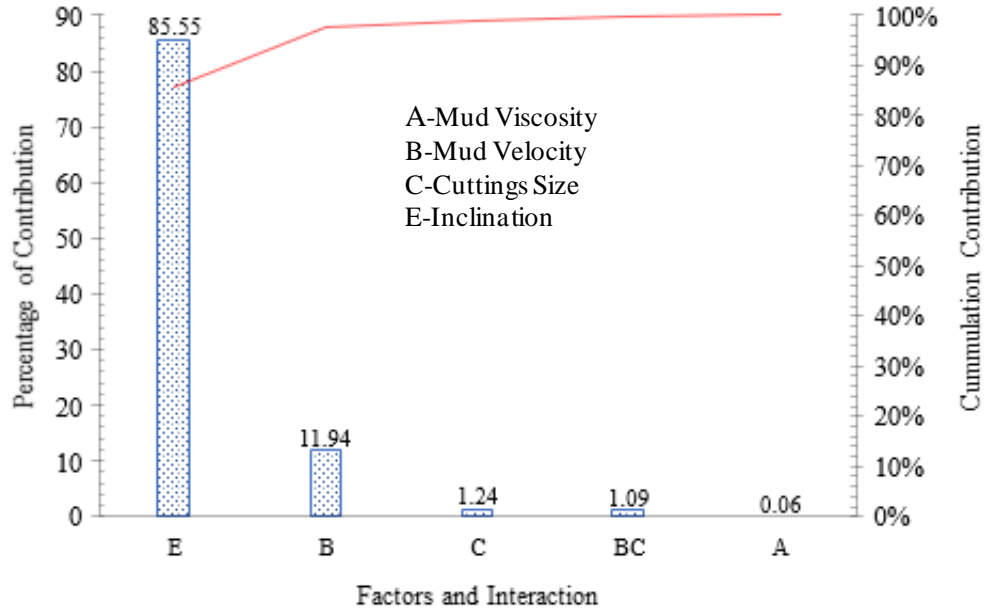


Figure 6-34: Factors and interaction contribution in pressure drop.

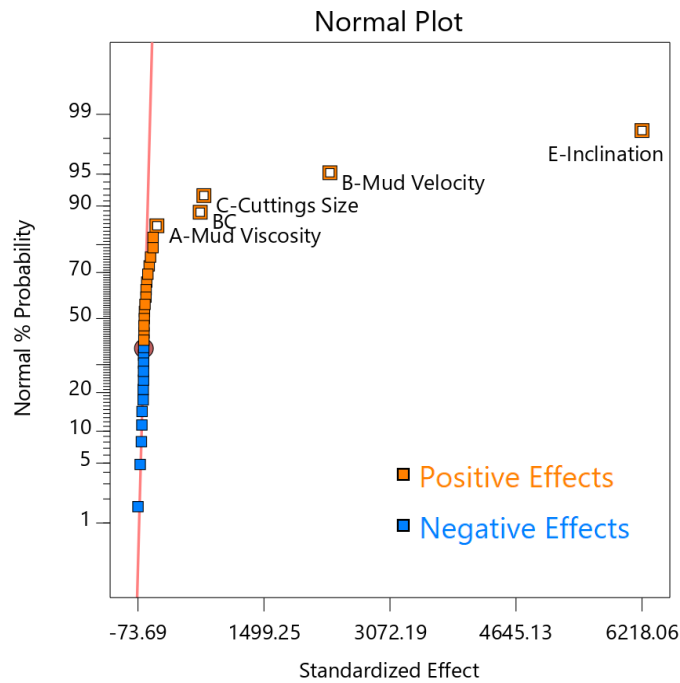


Figure 6-35: Half normal plot for pressure drop.

A positive effect indicates an increase in parameter value increase the response (pressure drop) value.

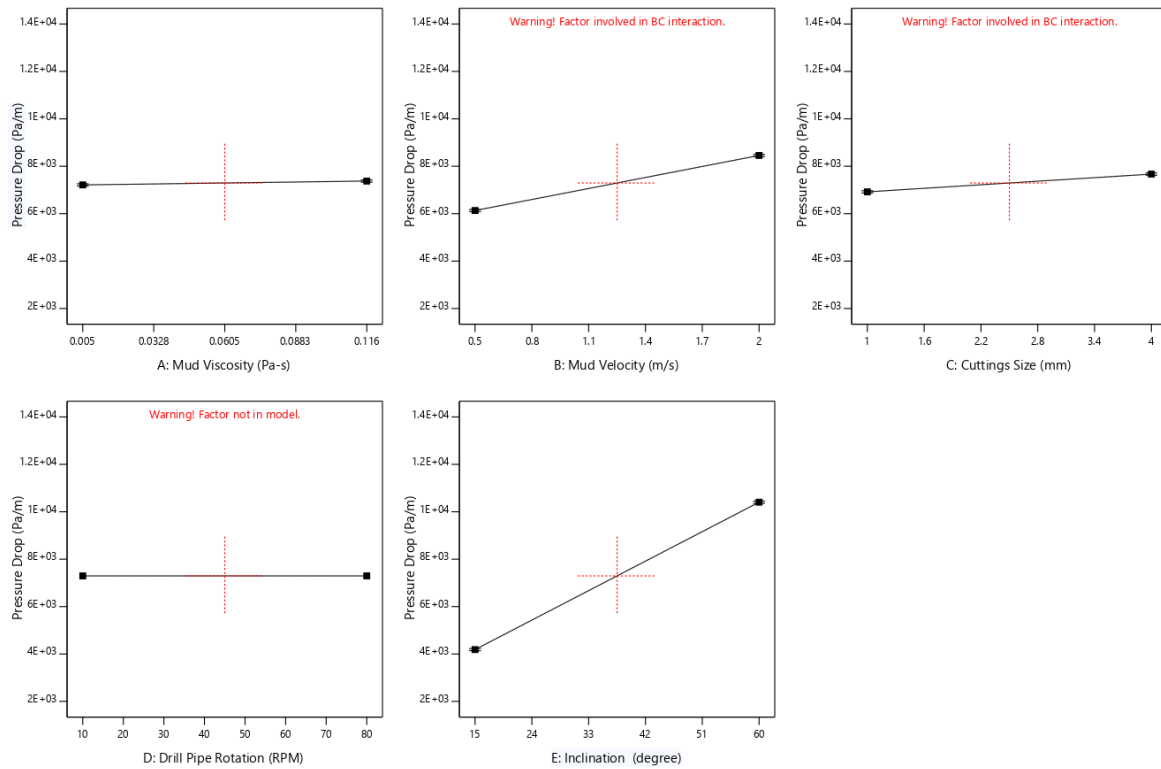
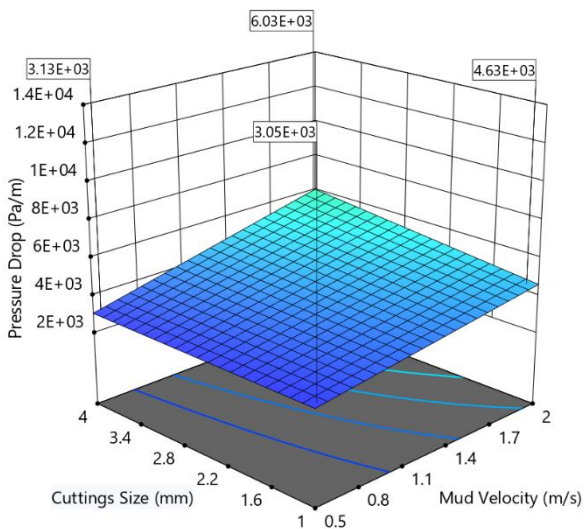
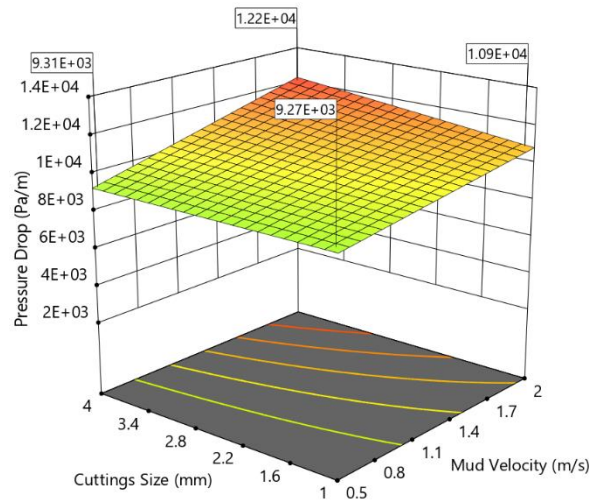


Figure 6-36: Mean dependency on annular pressure drop.



(a) 15° Inclination, 80 RPM



(b) 60° Inclination, 80 RPM

Figure 6-37: Velocity-Cuttings size interaction on pressure drop.

Chapter 7 : Conclusions and Future Recommendations

7.1 Conclusions

The current research was performed to investigate drill cuttings transport behavior in horizontal and inclined wells. The interactions among the different parameters were studied. The research work was completed in accordance with the goals defined in **Chapter 1**. Contributions and outcomes of the thesis are summarized below:

- i. A computational fluid dynamics model is developed to investigate solid transport behavior.
- ii. The interactions among different drilling parameters in the horizontal drilling operation were investigated based on a proper Design of Experiment (DOE) method. It shows that yield stress, mud circulation rate, and drill pipe rotation are the most significant parameters that can be controlled to improve the cutting transport in horizontal well.
- iii. The DOE results showed a significant negative interaction effect when mud velocity and yield stress are changed simultaneously. Therefore, increasing fluid yield stress and mud velocity concurrently may not improve the cutting transport efficiency.
- iv. Mud velocity and drill pipe rotation separately have a positive impact on the drill cuttings transport efficiency. However, DOE results revealed that there is a significant negative interaction effect to offset the individual positive effects.
- v. Three-factor interactions (i.e., the interaction between fluid yield stress, mud velocity, and cuttings size) are not significant in comparison to two-factor interactions.
- vi. It was observed that mid-size particles (i.e., 1 mm and 2 mm) were more challenging to transport. Smaller size particles (less than 1 mm) remain suspended in the fluid and are

carried along with the fluid, and larger size particles (more than 3 mm) have enough drag force acting on them to transport the particles.

- vii. A systematic experimental work was performed with state-of-the art Electrical Resistance Tomography (ERT) system and high-speed image visualization. ERT data shows inline measurement of solid volume fraction. High speed visualization analysis illustrates the mechanistic three-layer model behavior of solid cuttings transport in horizontal well section.
- viii. A flow regime map of solid transport behavior is proposed for the horizontal wells. Three different regions were identified in the flow regime map. These are: a) Region 1 - Stationary bed at the bottom, b) Region 2 - Stationary bed and moving dune, and c) Region 3 - Moving dune.
- ix. A non-dimensional number 'Transport Performance Number (TPN)' is proposed in this study to incorporate the solid bed height and solid dune moving velocity. A value of TPN > 70 is recommended for an efficient hole cleaning without forming a solid bed in horizontal well.
- x. Solid particle movement patterns was investigated in the inclined wells. A three layers concept of cuttings transport is also observed in the inclined well. Different solid particle movements were observed such as: a) particles in helical motion due to drill pipe rotation, b) rolling and suspended particles, and c) backward particles flow, transitional cuttings, and stationary cuttings bed.
- xi. Fluid velocity in the low viscous fluid has an adverse impact on hole cleaning in the inclined well, and this impact increases with the inclination. i.e., a 10° inclination from

horizontal position shows the greatest loss in cuttings transport capability with increase in fluid velocity, compared to a 5° inclination.

- xii. A CFD model for the inclined wells was developed and validated with experimental data. A transient simulation and a statistical DOE analysis were performed. A model for cuttings transport efficiency (CTE) in the inclined well was proposed. Cuttings size has the highest contribution in solid transport (55%), whereas mud velocity shows 23% and inclination exhibits 8% contribution in the CTE model.
- xiii. The artificial neural network (ANN) model shows that the parameters with even low contribution still considerably affect the CTE predictions.

7.2 Recommendations

- i. Particles with various sizes, shapes, and weight percentages can be used to simulate a more heterogeneous solid transport environment during experimental work.
- ii. Multicolor solid particles (with different characteristics) can be used to track particles movement more precisely and further understand the behavior of gravity and buoyancy effects on particle size.
- iii. High speed image technology can be integrated with particle image velocimetry (PIV) system for further investigation of particle movement trend and fluid streamlines. This can help to better explore the effect of drill pipe rotation on cuttings transport performance.
- iv. High speed visualization appears to be a great approach for water-based drilling fluids. However, it shows a limited application for an opaque drilling mud. PIV methods can be a good alternative for solid transport experimental study with opaque fluids.
- v. The concept of transport performance number (TPN) is still at infancy stage. A detailed investigation of this hypothesis through using a wide range of fluid rheology and cuttings

sizes can help to develop a nomograph of cuttings transport behaviors for different flow behaviors.

- vi. CFD simulation with discrete element methods and various solid size distributions, shapes and densities can represent more heterogeneous and realistic cases.
- vii. Hole cleaning performance of water-based mud in inclined bend section (dogleg severity) need to be investigated experimentally for different radius of curvature and annular clearance.
- viii. More experimental work is recommended at elevated pressure and temperature to investigate transport capability of water-based mud.
- ix. Effect of compressed air injection or aerated mud on cuttings transport efficiency can be investigated experimentally.

Appendix A

Investigating the Solid Transport Capability of Non-Newtonian Fluid in Annulus Bend Section

Mohammad Mojammel Huque¹, Syed Imtiaz¹, Stephen Butt¹, Sohrab Zendejboudi¹, Mohammad Azizur Rahman²

¹Memorial University of Newfoundland

²Texas A & M University at Qatar

Proceedings of the ASME 2021 40th International Conference on Ocean, Offshore & Arctic Engineering, OMAE2021, June 21-30, 2021, Virtual, Online

ABSTRACT

A directional drilling operation may include one or more bending sections along the drilling profile. These bend sections are the critical segments from the hole cleaning point of view. In this study, a computational fluid dynamic (CFD) method was used to investigate the hole cleaning behavior in annulus bending section. The Eulerian-Eulerian multiphase flow model was adopted in this study. The developed CFD model was validated with experimental data. Different non-Newtonian Herschel Bulkley fluids were used to simulate the drilling mud. Solid cuttings of different sizes (2 mm, 4 mm, and 5 mm) were used to replicate the drill cuttings. Different fluid flow rates (0.5 m/s, 1.0 m/s, 1.5 m/s and 2.0 m/s) were investigated to observe the solid settling tendency in the horizontal and bending sections. Cuttings accumulation behavior at different bending radii (10 in. and 20 in.) and bending angles (15°, 30°, and 60° from horizontal) were investigated. The simulation study shows that higher viscous fluid performs better hole cleaning at low mud velocity. Furthermore, a turbulent flow regime performs better solid transport in the

bending section. Finally, this study summarizes the hole cleaning behavior of a bend section for a range of fluid velocity, cuttings size, radius of curvature and inclination.

Keywords: Two-phase flow, Inclined well, Cuttings transport, non-Newtonian fluid

A.1. INTRODUCTION

In any drilling operation, solid cuttings tend to settle down due to significant density difference between solid cuttings and drilling mud. Continuous accumulation of solid cuttings with time initiates hole cleaning problem. Different drilling problems such as excessive torque and drag, poor rate of penetration, and stuck pipe are often associated with an inappropriate hole cleaning, leading to an increase in the overall drilling costs (Kelin et al., 2013). Although hole cleaning problem is not prominent in a vertical well drilling this is a serious issue in horizontal and deviated drilling operation. Past experimental studies (Ford et al., 1990; Sifferman et al., 1973; Tomren et al., 1986) focus on the increase in fluid viscosity and mud velocity to prevent the solid cuttings accumulation in the annular section. Other studies (Duan et al., 2008; Walker and Li, 2000) also consider additional parameters such as cuttings size, drill pipe rotation, and eccentricity.

Due to the complex cuttings transport behavior in the inclined section, solid cuttings tend to settle down in the lower annular inclined section. Furthermore, accumulated solid cuttings show a tendency to sliding down when enough mud flow rate and viscosity are not maintained. These cause a very complex transport behavior while drilling in an inclined section. Different experimental investigations (Katende et al., 2019; Peden et al., 1990; Sifferman and Becker, 1992) in the inclined well show that hole angle ranging from 20°-55° from the horizontal is more critical in cuttings transport. Moreover, most of the directional or horizontal drilling system have one or more bend sections that cannot be avoided. Cuttings transport in the bend sections were not

adequately investigated through experimental studies and computational modeling/simulation. This shortcoming of the past studies motivates the authors to further investigate the solid transport behavior in different bend sections.

Most of the previous experimental studies investigated solid transport in vertical, inclined, and horizontal sections of a well. In recent years, computational fluid dynamics (CFD) studies have been widely used in cuttings transport and hole cleaning studies. CFD approach (Huque et al., 2020a; Pang et al., 2018; Rooki et al., 2015; Siamak et al., 2015) enables researchers to investigate the phenomena beyond the experimental capabilities. An appropriate CFD model can represent the downhole drilling scenario that is often costly, and time sensitive to replicate in a laboratory environment. CFD study can help to conduct various investigations in a short period of time compared to a laboratory environment.

The objective of this study is to investigate the solid cuttings transport capability of non-Newtonian fluid in different inclined bend sections using CFD method. Several parameters such as fluid viscosity, fluid velocity, cuttings size, cuttings density, radius of curvature, and annular clearance were investigated in this study. A CFD model was proposed with experimental validation. Although a real drilling system comprises of a high length/ curvature in a directional drilling operation, a short annular bend section (7.5 feet) was chosen in this study due to the computational time and resources limitation. This manuscript is organized as follows: Section 1 covers the introduction; Section 2 presents the methodology, modelling overview in brief, and fluid rheology description; Section 3 includes the model validation, and result and discussion, and finally Section 4 summarizes the conclusions.

A.2. METHODOLOGY

Drill cuttings transport represents a two-phase flow of solid and liquid in the annular section. Cuttings transport in the annular section is modelled with the Eulerian-Eulerian multiphase flow model. Ansys Fluent v 17.2 was employed in this CFD study. A brief overview of two-phase flow modelling, test section geometry, fluid rheology and grid independency test are presented below.

A.2.1 Two-phase flow modelling

In the Eulerian model, drilling mud can be treated as a primary phase and solid cuttings are treated as the secondary phase. In the Eulerian-Eulerian multiphase flow model, solid cuttings are treated as a continuum. In solving the Eulerian model with conservation of mass and momentum equations, several assumptions were made (Huque et al., 2020a). Drilling mud is considered as an incompressible fluid and there is no interfacial mass transfer between drilling fluid and solid cuttings. Both solid and liquid phases are flowing against the gravity and have a constant density. The process is also considered isothermal.

Mass conservation. The continuity equation for the drilling mud (liquid) is given below (Fluent, 2015):

$$\frac{\partial}{\partial t}(\alpha_l \rho_l) + \nabla \cdot (\alpha_l \rho_l \vec{v}_l) = \sum(\dot{m}_{ls} - \dot{m}_{sl}) = 0 \quad (1)$$

in which, v_l is the velocity of the liquid phase; ρ_l denotes the density of the liquid phase; \dot{m}_{ls} refers to the mass transfer from the liquid phase to the solid phase; and \dot{m}_{sl} resembles the mass transfer from the solid phase to the liquid phase. Since there is no mass transfer among the phases, the summation on the right-hand side of Equation (1) is assumed to be zero. The annular volume is comprised of only two phases. The volume fraction is defined as α_l for the mud phase and α_s for

the cuttings, where $\alpha_l + \alpha_s = 1$. The subscripts l and s are used for the mud (liquid) and cuttings (solid) phases, respectively.

Similarly, the continuity equation for the solid phase is represented by the following relationship (Fluent, 2015):

$$\frac{\partial}{\partial t}(\alpha_s \rho_s) + \nabla \cdot (\alpha_s \rho_s \vec{v}_s) = \sum(\dot{m}_{sl} - \dot{m}_{ls}) = 0 \quad (2)$$

in which, v_s is the velocity of the solid phase; and ρ_s stands for the density of the solid phase.

Momentum conservation. The momentum balance for the liquid phase is given by the following equation (Fluent, 2015):

$$\begin{aligned} \frac{\partial}{\partial t}(\alpha_l \rho_l \vec{v}_l) + \nabla \cdot (\alpha_l \rho_l \vec{v}_l \vec{v}_l) = & -\alpha_l \nabla p + \nabla \cdot \bar{\tau}_l + \alpha_l \rho_l \vec{g} + \sum(\vec{R}_{sl} + \dot{m}_{sl} \vec{v}_{sl} - \dot{m}_{ls} \vec{v}_{ls}) + \\ & (\vec{F}_l + \vec{F}_{lift,l} + \vec{F}_{wl,l} + \vec{F}_{vm,l} + \vec{F}_{td,l}) \end{aligned} \quad (3)$$

in which, F_l is an external body force; $\vec{F}_{lift,l}$ represents a lift force; $\vec{F}_{wl,l}$ symbolizes the wall lubrication force; $\vec{F}_{vm,l}$ is the virtual mass force; $\vec{F}_{td,l}$ stands for a turbulent dispersion force; p introduces the pressure shared by both solid and liquid phases; and \vec{v}_{sl} is the interphase velocity defined as: $\vec{v}_{sl} = \vec{v}_s$ if $\dot{m}_{sl} < 0$.

$\bar{\tau}_l$ also introduces the stress-strain tensor for the liquid phase, as defined below (Fluent, 2015):

$$\bar{\tau}_l = \alpha_l \mu_l (\nabla \vec{v}_l + \nabla \vec{v}_l^T) + \alpha_l (\lambda_l - \frac{2}{3} \mu_l) \nabla \cdot \vec{v}_l \bar{I} \quad (4)$$

In Equation (4), μ_l and λ_l denote the shear and bulk viscosity of liquid phase, respectively. The conservation of momentum for the solid phase is expressed as follows (Fluent, 2015):

$$\begin{aligned} \frac{\partial}{\partial t}(\alpha_s \rho_s \vec{v}_s) + \nabla \cdot (\alpha_s \rho_s \vec{v}_s \vec{v}_s) = & -\alpha_s \nabla p - \nabla p_s + \nabla \cdot \bar{\tau}_s + \alpha_s \rho_s \vec{g} + \sum(K_{ls}(\vec{v}_l - \vec{v}_s) + \dot{m}_{ls} \vec{v}_{ls} - \\ & \dot{m}_{sl} \vec{v}_{sl}) + (\vec{F}_s + \vec{F}_{lift,s} + \vec{F}_{wl,s} + \vec{F}_{vm,s} + \vec{F}_{td,s}) \end{aligned} \quad (5)$$

Where p_s stands for the solid phase pressure; and \vec{R}_{sl} represents the interaction force between the solid and liquid phases. This force mainly depends on the friction and pressure cohesion and is subject to the condition that $\vec{R}_{sl} = -\vec{R}_{ls}$ and $\vec{R}_{ll} = 0$ (Fluent, 2015), as given below:

$$\sum \vec{R}_{sl} = \sum K_{sl}(\vec{v}_s - \vec{v}_l) = 0 \quad (6)$$

Here, K_{sl} ($= K_{ls}$) introduces the interphase momentum exchange coefficient; and \vec{v}_s and \vec{v}_l are the solid and liquid phase velocities, respectively.

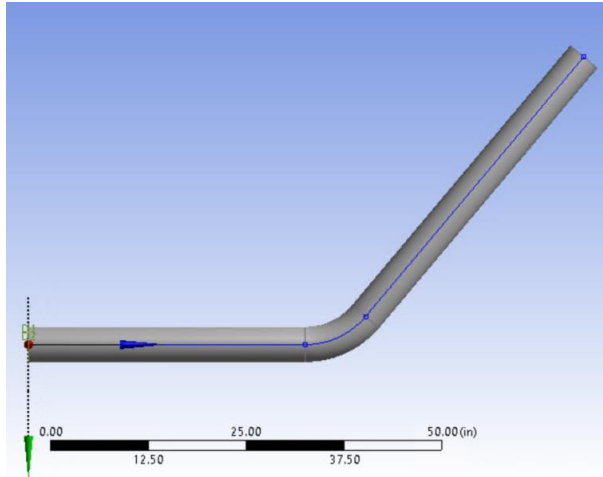
A.2.2 Test section geometry

A short annular inclined section of length of 7.5 ft is considered for this investigation with horizontal section of 3.5 ft and inclined section of 4 ft. The outer pipe diameter is 4.5 in and inner pipe diameter is 2.5 in. Three different geometrical orientations (60° , 30° , and 15°) were chosen for the analysis as shown in **Figure A.1**. In this study, all inclination angles were measured from the horizontal axis.

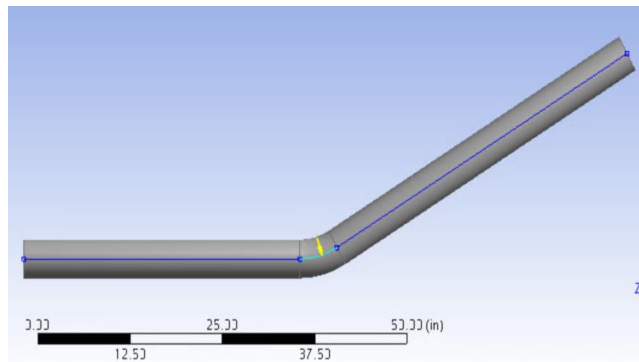
A.2.3 Fluid Rheology

Two non-Newtonian fluids (Fluid 1 and Fluid 2) were prepared with Flowzan bio polymer for this simulation study. Fluid rheology was tested with Grace 3600 viscosity meter. A non-linear curve fittings model was used to find the unknown parameter of the non-Newtonian fluid. The curve fittings model shows that both fluids demonstrate the non-Newtonian Herschel Bulkley fluid behavior with small value of yield stress as depicted in **Figure A.2**.

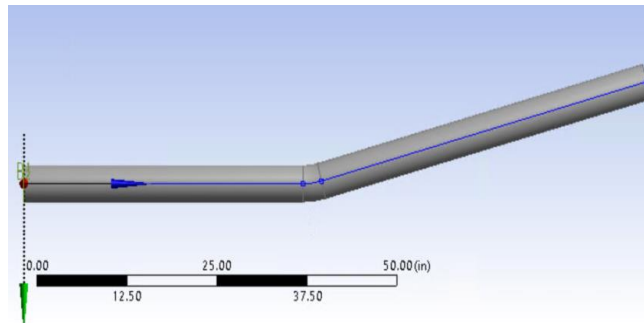
The fluid rheological parameters for both fluids are reported in **Table A.1**. Based on the rheological characteristics, Fluid 2 exhibits more non-Newtonian (lower 'n' value) and high viscous behavior (higher 'k' value) than Fluid 1.



(a) 60° inclination



(b) 30° inclination



(c) 15° inclination

Figure A.1: Geometrical orientations (60°, 30° and 15°) used in this study.
[The angle measured from horizontal axis.]

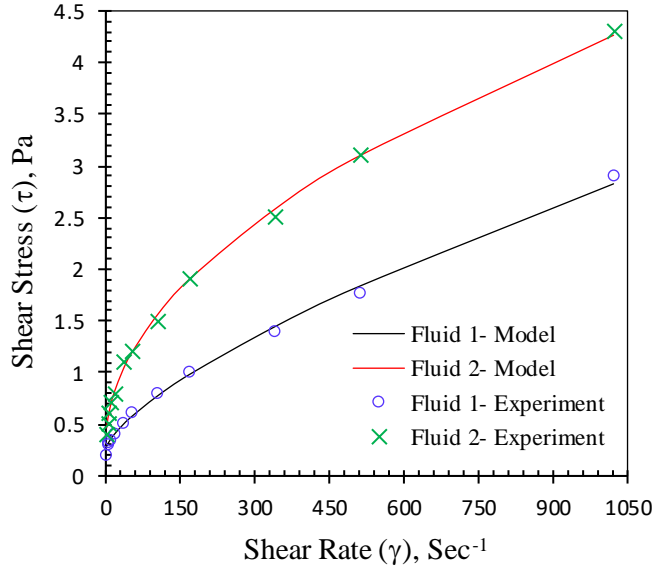


Figure A.2: Fluid rheology estimation from shear stress vs. shear rate curve.

Table A.1: Fluid properties used in this study.

Fluid Properties	Fluid 1	Fluid 2
Yield Stress, τ_0 (pa)	0.234	0.308
Consistency Index, k (Pa·s ⁿ)	0.020	0.116
Flow Behavior Index, n	0.702	0.510
R^2	0.998	0.999

A.2.4 Grid Independency Study

Meshing were performed with adjusting ‘Max Face Size’ and ‘Max Tet Size’. A grid independence test was performed with Fluid 2 at a velocity of 0.5m/s. The annular pressure drop was reported for different element sizes as shown in **Figure A.3**. The grid study shows that mesh size above 400,000 is adequate to represent an error free result. In this study, an element size of 594,504 was used. Average skewness was 0.16 and average orthogonal quality was 0.96 implying a good mesh quality for this geometry. Phase coupled SIMPLE scheme was employed for pressure velocity coupling and the momentum equations were discretized using the QUICK scheme. The convergence criteria for residuals were set as 10^{-4} for the continuity and 10^{-3} for other residuals.

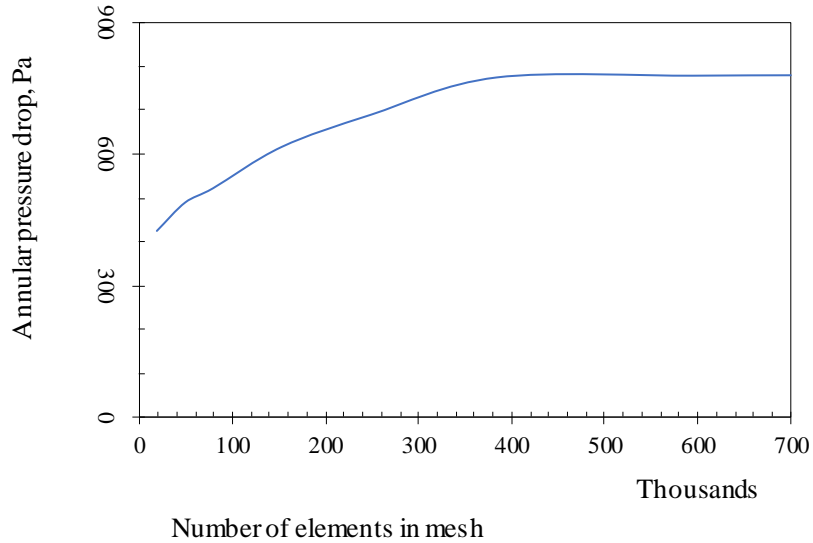


Figure A.3: Grid independence study to choose optimum element in meshing.

In this study, transient simulation was performed in each case for 60 seconds time duration with a time steps of 5 milliseconds. ComputeCanada supercomputer ‘graham’, ‘beluga’, and ‘cedar’ were used for the transient simulation. Based on the available resources (CPU, software license), a total of 96 to 128 cores of CPU were requested per simulation with 92-120 GB of RAM. The actual run time for each simulation varies between 6 - 8 hours for the given mesh size. Also, there is a certain wait time based on priority job and resources between two simulations.

A.2.5 Performance Measurement

Hole cleaning effectiveness is estimated indirectly using the parameter ‘*Annular Solid Volume Fraction*’. This is the ratio of annular solid volume accumulated over a particular time to the total annular volume, as mathematically presented below:

$$\text{Annular solid volume fraction} = \frac{\text{Volume of solid accumulated}}{\text{Total annular volume}}$$

Solid cuttings are accumulated in the annular space during drilling operation if hole cleaning is not adequate. A high annular solid volume fraction implies that more solids are accumulated over time,

and poor hole cleaning is attained. A low annular solid volume fraction is desirable throughout this study, meaning an effective hole cleaning occurs.

A.3.RESULTS AND DISCUSSION

A.3.1 Model Validation

Two phase flow experiment were conducted at Texas A & M University at Qatar (TAMUQ) fluid laboratory. The details of the experimental work is described in an earlier manuscript by the same authors (Huque et al., 2020b). The developed CFD model is validated with experimental data obtained from TAMUQ horizontal flow loop with a separate fluid ($\tau_o = 0.269$ Pa, $k= 0.064$, $n = 0.557$), flow rate of 0.72 m/s, and different ranges of drill pipe rotations. Annular solid volume fraction was estimated from the experiment and compared with the simulation results as shown in **Figure A.4**. The proposed CFD model can predict the experimental results within a margin of error of approximately 9%. Hence, it is assumed that the developed model can predict the solid flow behavior in the annular section with certain degree of confidence.

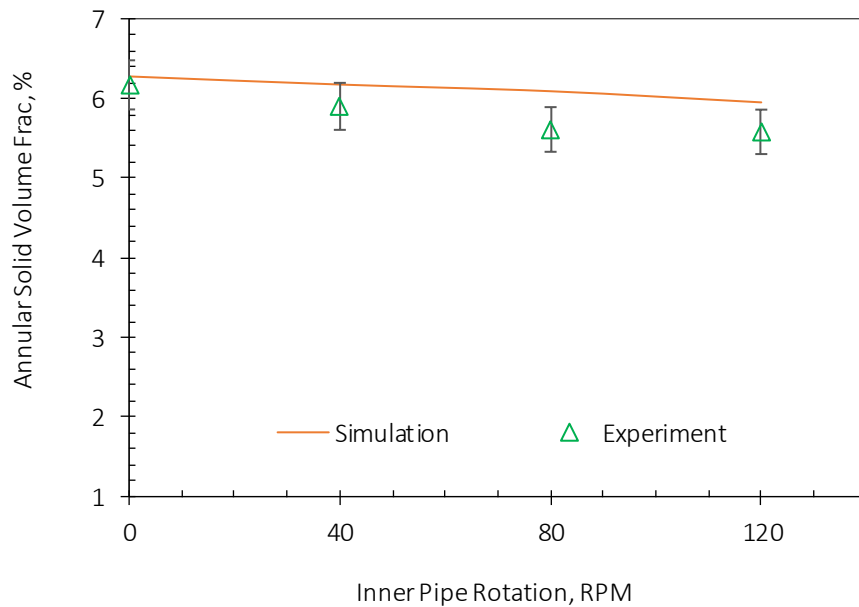


Figure A.4: Experimental validation of CFD model.

A.3.2 Transient Behavior

Transient solid movement behavior in bend section is depicted in **Figure A.5** at four different time instants (2.5 sec, 5.0 sec, 7.5 sec and 10.0 sec), where solid cuttings accumulation trend for Fluid 2 with 5 mm cuttings in a 60° well configuration is shown. The contour images show that with increasing time, the solid cuttings accumulation gradually increases in the bend section.

A.3.3 Effect of Fluid Rheology

The effect of fluid rheology on annular solid volume fraction is shown in **Figure A.6** for a 60-degree bend with 5 mm cuttings. Different mud velocities were examined, and the annular solid volume fraction was reported after each case. Fluid 2 (higher viscous, high k values) shows a gradual decrease in the annular solid volume fraction from 28.1% to 10.8% with a gradual increase in mud velocity from 0.5 m/s to 2.0 m/s. In a laminar flow regime, high viscous fluid exhibits better hole cleaning at low mud velocity. On contrary, Fluid 1 (less viscous) exhibits comparatively higher percentage of annular solids at low mud velocities such as 0.5 m/s and 1.0 m/s. However, with increase in mud velocity, annular solid percentage significantly decreases below 7%. It can be concluded that low viscous fluid at higher mud velocity generates more turbulence that helps better hole cleaning effect in the bend section.

A.3.4 Effect of Inclination

To investigate the effect of inclination on hole cleaning, 3 different angles (15°, 30° and 60° from horizontal) were investigated in this study with Fluid 2 and cuttings size of 5 mm as depicted in **Figure A.7**. According to the results, near horizontal 15° inclined well shows the highest amount of annular solid in the well at mud velocity 0.5 m/s. At the same mud velocity, increasing the inclination from the horizontal axis shows a slight decrease in annular solid volume fraction for 30° and 60°. This trend persists up to mud velocity 1.2 m/s.

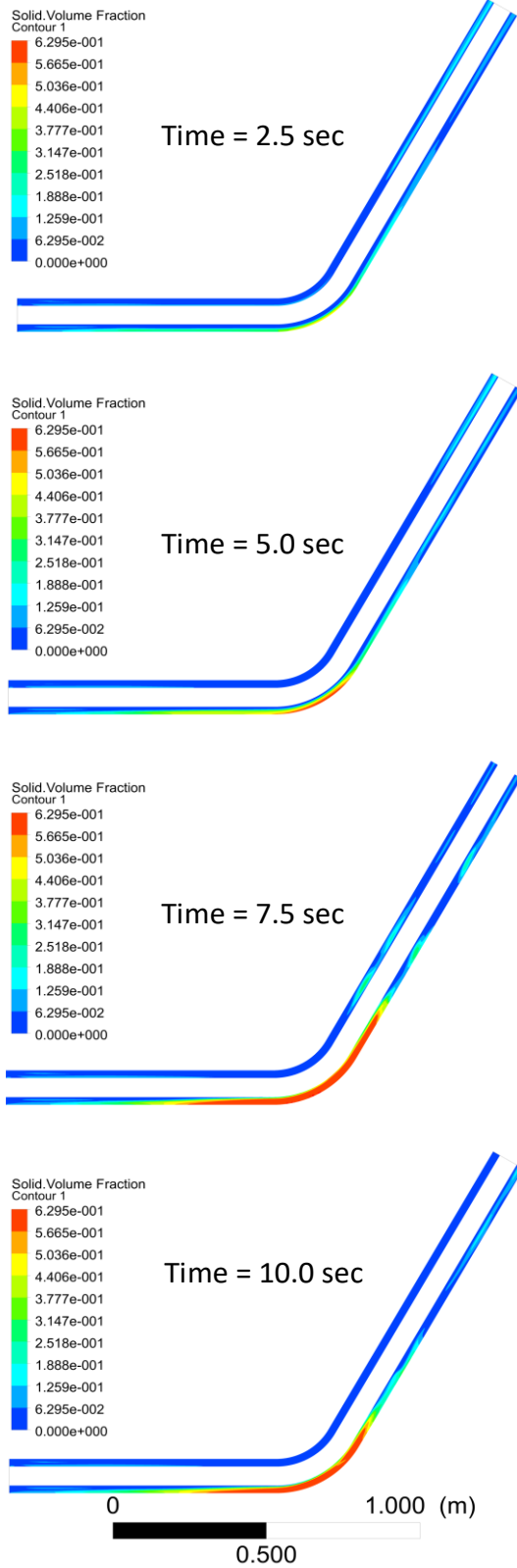


Figure A.5: Solid cuttings accumulation in the bend section with time.

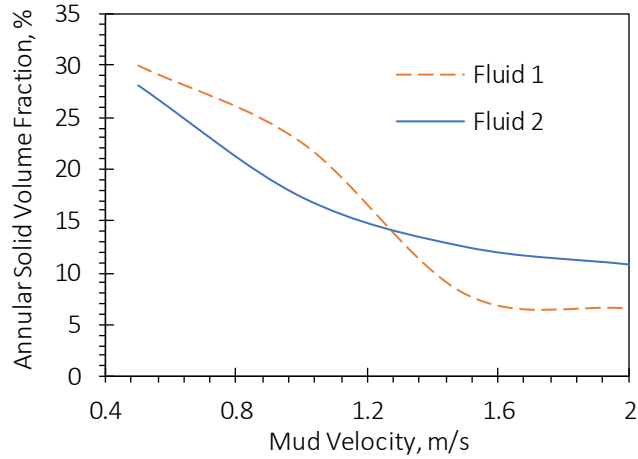


Figure A.6: Effect of fluid rheology on solid transport in bend section.

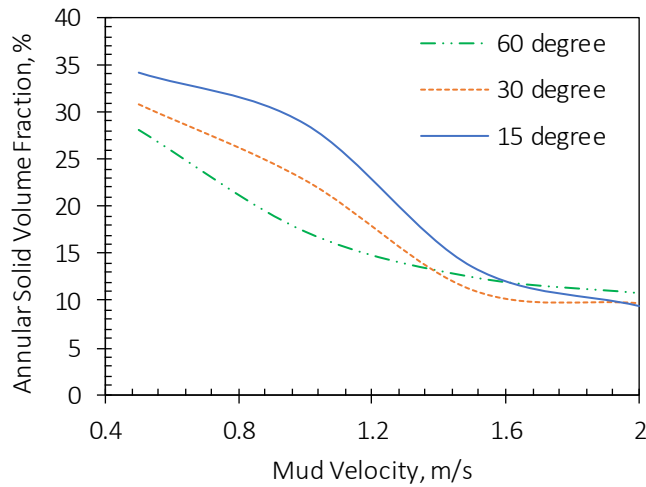


Figure A.7: Effect of inclination on solid transport in bend section.
[At higher mud flow rate, inclination effect is negligible.]

However, the annular solid volume fraction variation is almost negligible at higher mud velocity above 1.5 m/s. It can be concluded that a high fluid velocity can help in mitigating the hole cleaning problem due to inclination and bending.

The volume rendering images of solid volume fraction for 60° and 30° inclination angles are shown in **Figure A.8**. It shows that for both inclinations, the bending section is more critical in hole cleaning. Cuttings accumulation in the bend section significantly hampers the fluid flow in the

lower annular section. **Figure A.9** illustrates the mud velocity profile in the horizontal section prior to the bend for 60° and 30° inclination. It is found that there is almost zero mud velocity in the lower annular section due to solid accumulation in the bend.

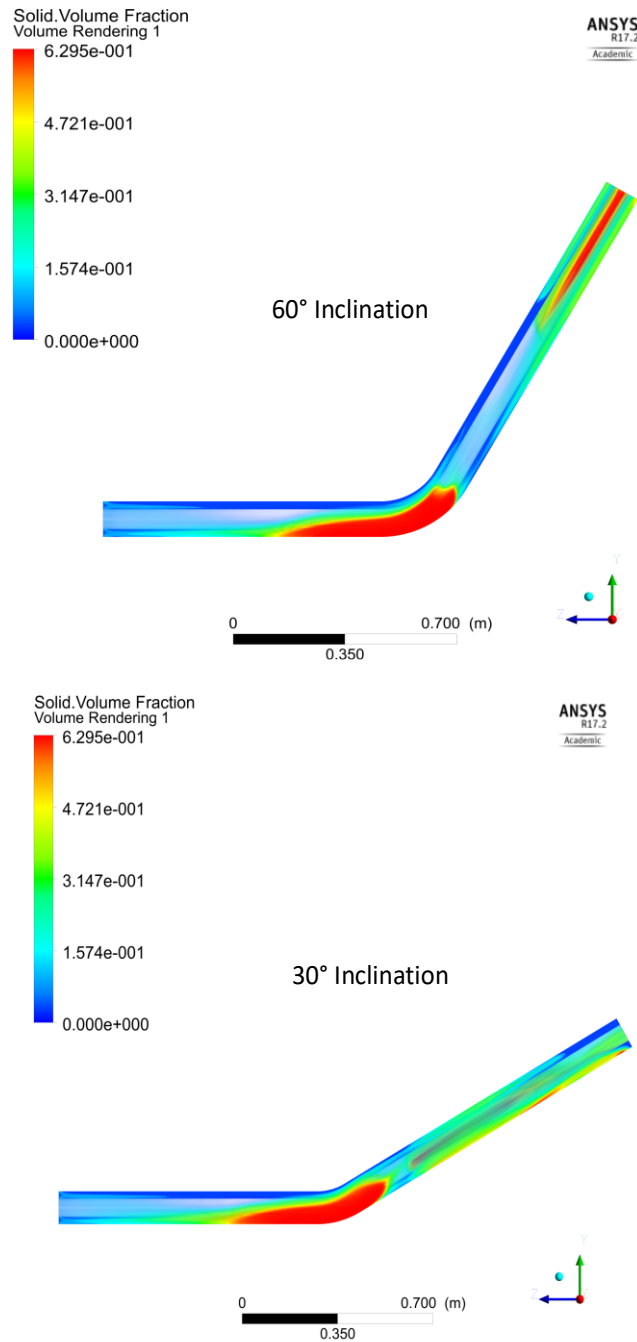


Figure A.8: Contour map of solid accumulation in inclined bend.

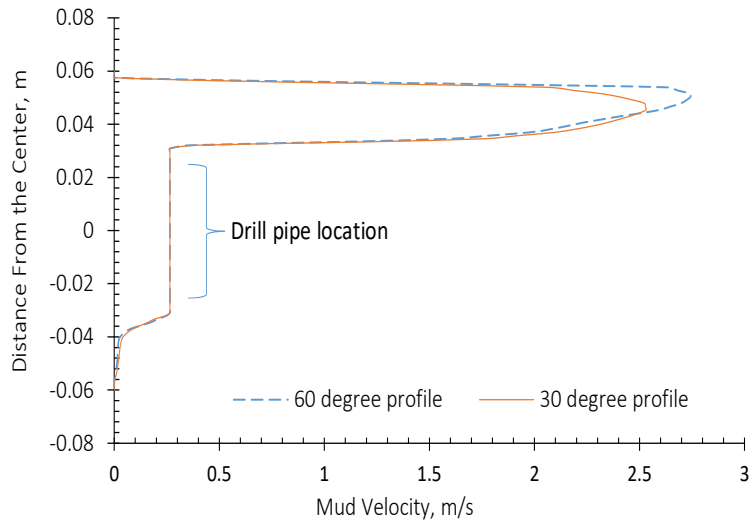


Figure A.9: Mud velocity profile in the horizontal section for 30° and 60° bend.

A.3.5 Effect of Cuttings Size

Three different cuttings sizes (2 mm, 3 mm, and 5 mm) were tested with Fluid 2 in the case of 60° inclination. For all cuttings sizes, an increase in fluid velocity decreases the annular solid volume fraction as depicted in **Figure A.10**.

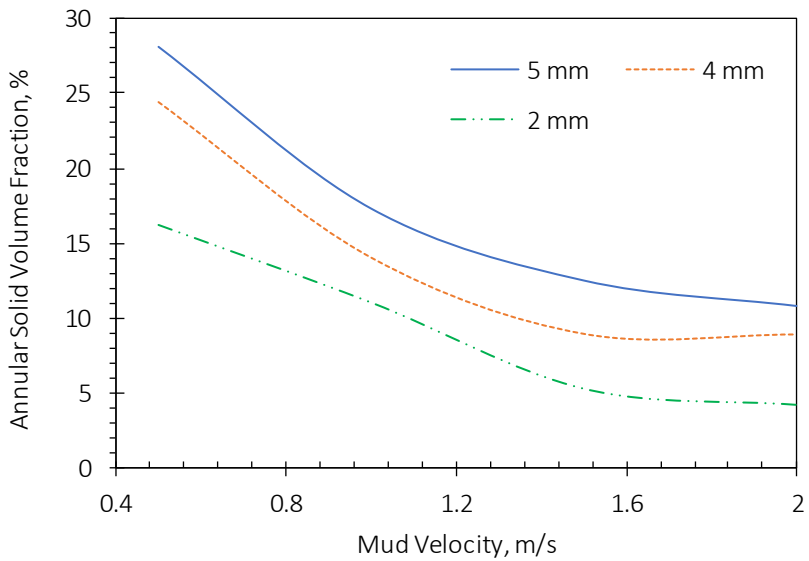


Figure A.10: Effect of cuttings size on hole cleaning. [Smaller cuttings are easier to clean from the bend.]

This study shows that smaller cuttings are easier to transport in the bending section. A smaller cutting exhibits less gravity effect and imposes less resistance to the fluid drag forces in the annular section. This is the reason for better hole cleaning with smaller cuttings size in the annular bend section.

A.3.6 Effect of Cuttings Density

Although solid cuttings density has a very minimal control from the surface during a drilling operation, the effect of solid cuttings density on cuttings transport was investigated in this study. In this phase, 5 mm cuttings were selected with two different cuttings density 2650 kg/m^3 and 2000 kg/m^3 as shown in **Figure A.11**. It was found that solid cuttings density has a significant contribution in the cuttings transport. A low-density solid lead to better hole cleaning compared to a higher density solid for the same cuttings size and mud velocity. Low density cuttings show less gravitational effect and consequently exhibit better lifting capabilities in the inclined section with less annular pressure drop due to low mixture density.

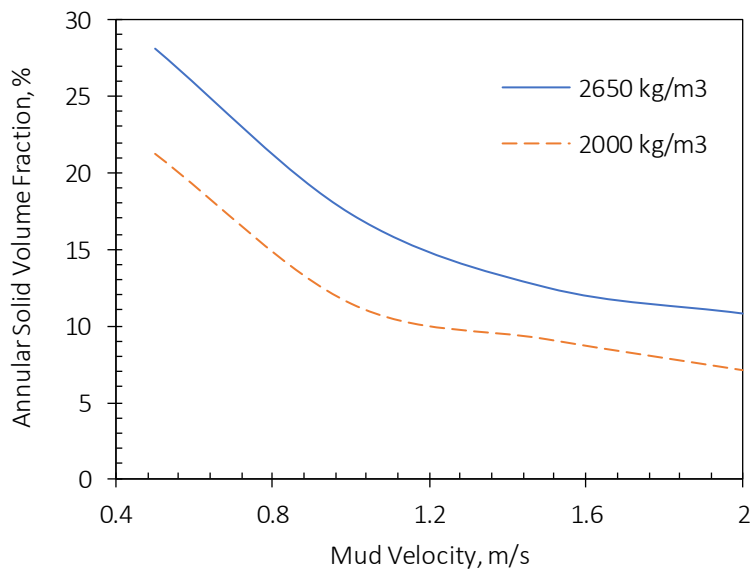


Figure A.11: Effect of cuttings density on hole cleaning.

A.3.7 Effect of Annular Clearance

Annular clearance plays a vital role in cuttings accumulation. Narrow annular slot is prone to high annular pressure drop and cuttings accumulation whereas large annular space requires a higher pumping capacity. Therefore, an optimal annular clearance is crucial during a drilling operation.

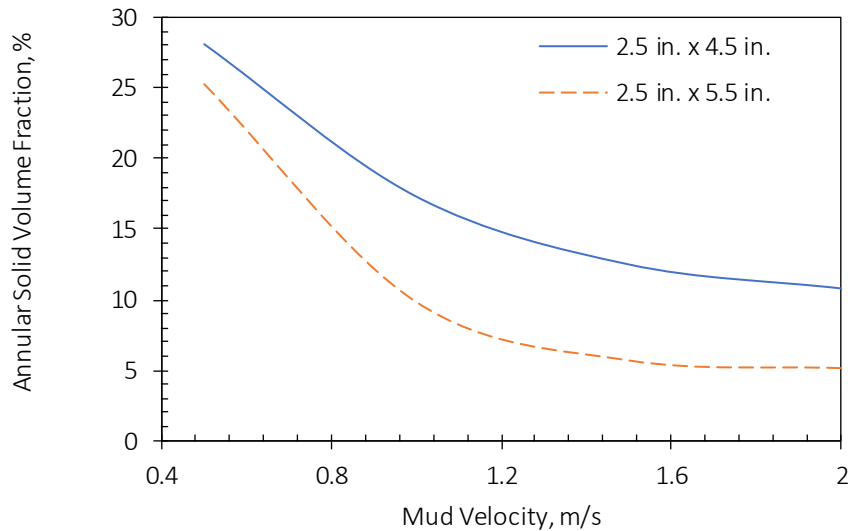


Figure A.12: Effect of annular clearance on hole cleaning.

Figure A.12 demonstrates the effect of annular clearance on solid transport. Two different annular clearances 2.5 in. x 4.5 in. and 2.5 in. x 5.5 in. were investigated in this study. At all fluid velocities, a low annular clearance exhibits a higher annular solid concentration. A higher annular clearance results in a better hole cleaning upon an increase in fluid velocity. The degree of hole cleaning shows better performance for large annular section with higher mud velocity. At the same mud velocities, large annular section shows a higher volumetric flow rate which eventually cleans hole effectively.

A.3.8 Effect of Radius of Curvature

The effect of radius of curvature were investigated with two different radius sizes (10 inch and 20 inch) for the bend section. **Figure A.13** shows the annular solid volume versus mud velocity at

two different radii of curvature for Fluid 2 and 5-mm cuttings. **Figure A.14** depicts the contour map for solid accumulation for both radius of curvature cases.

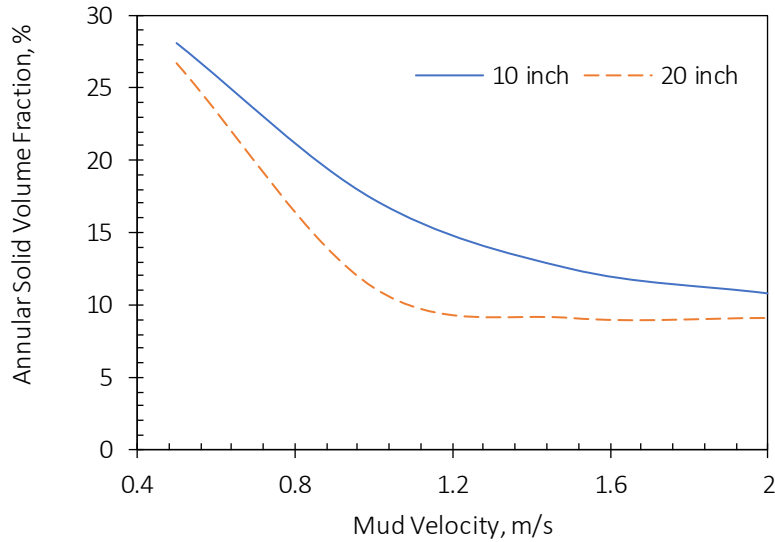


Figure A.13: Contour impact of radius of curvature in the bend section on cuttings transport.

Low radius section shows a higher annular solid volume fraction for all mud velocities. Higher radius of curvature leads to lower annular solid volume fraction.

Both radius of curvature shows almost similar amount of annular solid volume fraction at 0.5m/s and 2.0 m/s. Due to low mud velocity (0.5 m/s), the effect of higher radius of curvature is not noticeable. Both radius of curvatures shows almost similar amount of annular solid volume fraction (more than 27-28%). At higher mud velocity (2 m/s), the hole section cleans effectively and hence for both radius of curvature shows less annular solid fraction (9-11%). For the intermediate mud velocity 1.0 m/s and 1.5 m/s, there is a significant improvement in solid volume fraction with larger radius of curvature; when compared with mud velocity 0.5m/s. At the same mud velocities, the large annular section shows a higher volumetric flow rate which eventually cleans hole effectively.

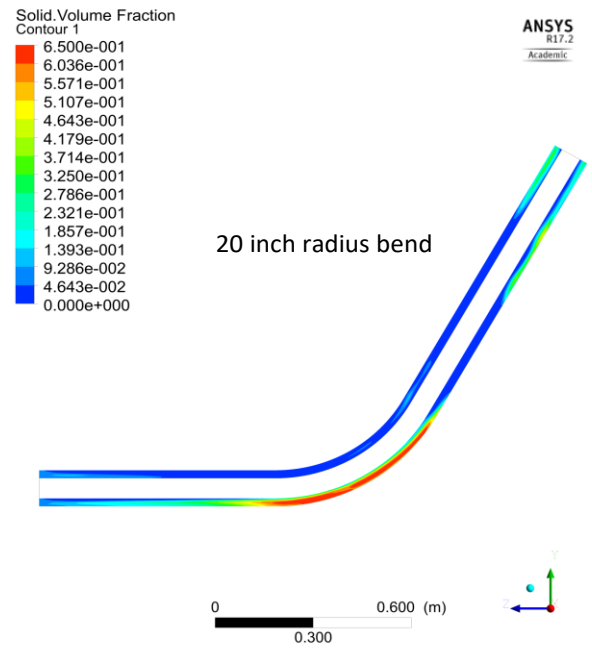
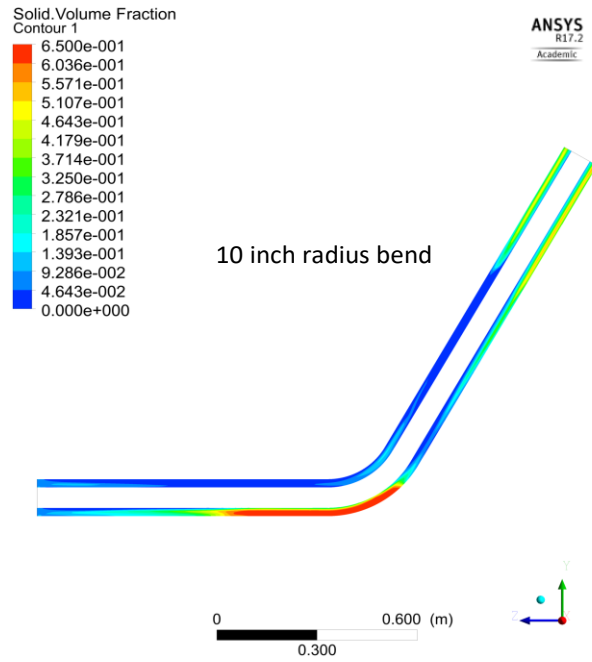


Figure A.14: Contour of cuttings accumulation on 10 in. Curvature and 20 in. Curvature.

A.4. CONCLUSION

This study investigated the hole cleaning behavior in the inclined bending section using two non-Newtonian fluid. The following remarks can be made from this study.

- Near horizontal well (15° inclination from horizontal) shows the weakest hole cleaning performance at low mud velocity. The effect of inclination diminishes with increasing the mud velocity above 1.5 m/s.
- At low mud velocity, high viscous fluid performs better hole cleaning. However, hole cleaning in the bending section is more effective with a less viscous fluid and turbulent flow.
- Cuttings size has a significant impact on hole cleaning in the inclined bend section. Larger cuttings are more difficult to clean from the bend.
- Increasing wellbore curvature shows better hole cleaning performance at intermediate velocity range of 1.0 m/s - 1.5 m/s.
- An increase in annular clearance exhibits better hole cleaning performance for all ranges of fluid velocity.

ACKNOWLEDGEMENTS

The researchers gratefully acknowledge and thank Equinor Canada, Memorial University, InnovateNL, and the Natural Sciences and Engineering Research Council of Canada (NSERC) to support this research work. This publication was also made possible by the grant NPRP10-0101-170091 from Qatar National Research Fund (a member of the Qatar Foundation).

NOMENCLATURES

Acronyms

CFD	-	Computational fluid dynamics
RPM	-	Revolutions per minute
mm	-	Millimeter
Pa	-	Pascal
ft	-	Feet
in	-	Inch

Variables/Symbols

F	-	external body force	(N, lb _f)
F_{lift}	-	lift force	(N, lb _f)
F_{wl}	-	wall lubrication force	(N, lb _f)
F_{vm}	-	virtual mass force	(N, lb _f)
F_{td}	-	turbulent dispersion force	(N, lb _f)
g	-	gravitational acceleration	(m/s ² , ft/s ²)
K	-	interphase momentum exchange coefficient	(-)
K	-	consistency index	(Pa.s ⁿ)
\dot{m}	-	mass flow rate	(kg/s, lb _m /s)
p	-	pressure	(Pa)
R	-	interaction force between phases	(-)
R^2	-	R-squared, a statistical measure	(-)
v	-	velocity	(ms ⁻¹)

Greek Letters

α	-	volume fraction	(-)
τ_o	-	yield stress	(Pa)
τ	-	shear stress	(Pa)
$\dot{\gamma}$	-	shear rate	(s ⁻¹)
∇	-	derivative	(-)
$\bar{\bar{\tau}}$	-	stress strain tensor	(-)
ρ	-	density	(kg.m ⁻³)
μ	-	shear viscosity	(ms ⁻¹)
λ	-	bulk viscosity	(ms ⁻¹)

Subscripts

l	-	liquid phase
s	-	solid phase
ls	-	liquid to solid
sl	-	solid to liquid

REFERENCES

1. Duan, M., Miska, S.Z., Yu, M., Takach, N.E., Ahmed, R.M., Zettner, C.M., 2008. Transport of Small Cuttings in Extended-Reach Drilling. *SPE Drill. Complet.* 23, 258–265. <https://doi.org/10.2118/104192-PA>
2. Fluent, 2015. ANSYS FLUENT User ' s Guide.
3. Ford, J.T., Peden, J.M., Oyeneyin, M.B., Gao, E., Zarrouh, R., 1990. Experimental investigation of drilled cuttings transport in inclined boreholes, in: *SPE Annual Technical Conference and Exhibition*. New Orleans, LA, U.S.A., 23-26 September, pp. 197–206. <https://doi.org/10.2523/20421-ms>
4. Huque, M.M., Butt, S., Zendeboudi, S., Imtiaz, S., 2020a. Systematic sensitivity analysis of cuttings transport in drilling operation using computational fluid dynamics approach. *J. Nat. Gas Sci. Eng.* 81, 103386. <https://doi.org/https://doi.org/10.1016/j.jngse.2020.103386>
5. Huque, M.M., Imtiaz, S., Zendeboudi, S., Butt, S., 2020b. Experimental Study of Cuttings Transport with Non-Newtonian Fluid in an Inclined Well Using Visualization and ERT Techniques, in: *SPE Annual Technical Conference & Exhibition*. Denver, Colorado, U.S.A. <https://doi.org/10.2118/201709-MS>
6. Katende, A., Segar, B., Ismail, I., Sagala, F., Saadiah, H.H.A.R., Samsuri, A., 2019. The effect of drill–pipe rotation on improving hole cleaning using polypropylene beads in water-based mud at different hole angles. *J. Pet. Explor. Prod. Technol.* <https://doi.org/10.1007/s13202-019-00815-1>
7. Kelin, W., Tie, Y., Xiaofeng, S., Shuai, S., Shizhu, L., 2013. Review and analysis of cuttings transport in complex structural wells. *Open Fuels Energy Sci. J.* 6, 9–17. <https://doi.org/10.2174/1876973X20130610001>
8. Pang, B., Wang, S., Wang, Q., Yang, K., Lu, H., Hassan, M., Jiang, X., 2018. Numerical Prediction of Cuttings Transport Behavior in Well Drilling Using Kinetic Theory of Granular Flow. *J. Pet. Sci. Eng.* 161, 190–203. <https://doi.org/10.1016/j.petrol.2017.11.028>
9. Peden, J.M., Ford, J.T., Oyeneyin, M.B., 1990. Comprehensive Experimental Investigation of

- Drilled Cuttings Transport in Inclined Wells Including the Effects of Rotation and Eccentricity, in: European Petroleum Conference. The Hague, The Netherlands, 22-24 October.
<https://doi.org/10.2118/20925-MS>
10. Rooki, R., Ardejani, F.D., Moradzadeh, A., Norouzi, M., 2015. CFD Simulation of Rheological Model Effect on Cuttings Transport. *J. Dispers. Sci. Technol.* 36, 402–410.
<https://doi.org/10.1080/01932691.2014.896219>
 11. Siamak, A., Mehdi, B., Majid, R., 2015. CFD-DEM approach to investigate the effect of drill pipe rotation on cuttings transport behavior. *J. Pet. Sci. Eng.* 127, 229–244.
<https://doi.org/10.1016/j.petrol.2015.01.017>
 12. Sifferman, T.R., Becker, T.E., 1992. Hole Cleaning in Full-Scale Inclined Wellbores. *SPE Drill. Eng.* 7, 115–120. <https://doi.org/10.2118/20422-PA>
 13. Sifferman, T.R., Myers, G.M., Haden, E.L., Wahl, H.A., 1973. Drill Cutting Transport in Full Scale Vertical Annuli, in: Society of Petroleum Engineers of AIME. Las Vegas, p. 5.
 14. Tomren, P.H., Iyoho, A.W., Azar, J.J., 1986. Transport in Directional Wells. *SPE Drill. Eng.* 43–56.
 15. Walker, S., Li, J., 2000. The Effects of Particle Size, Fluid Rheology, and Pipe Eccentricity on Cuttings Transport, in: SPE/ICoTA Coiled Tubing Roundtable. Houston, TX, USA, 5–6 April.
<https://doi.org/10.2118/60755-MS>

Appendix B

This section includes additional images and videos obtained from the experiment discussed in Chapter 4.

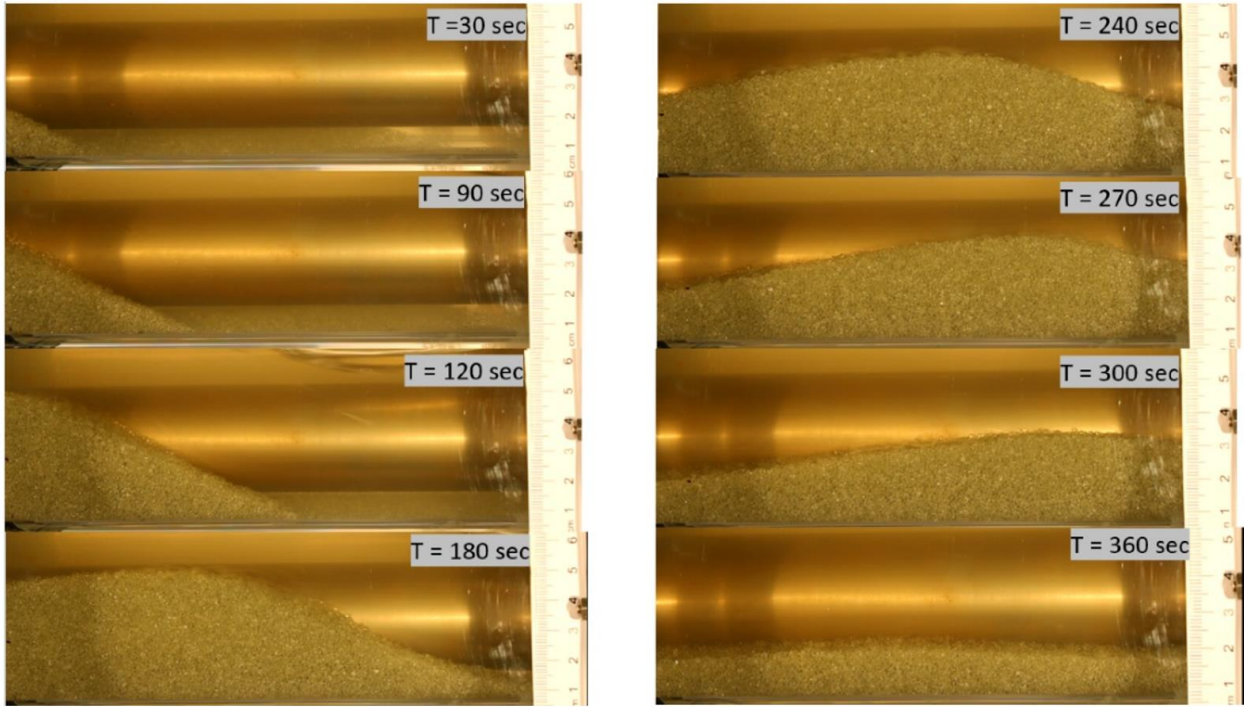
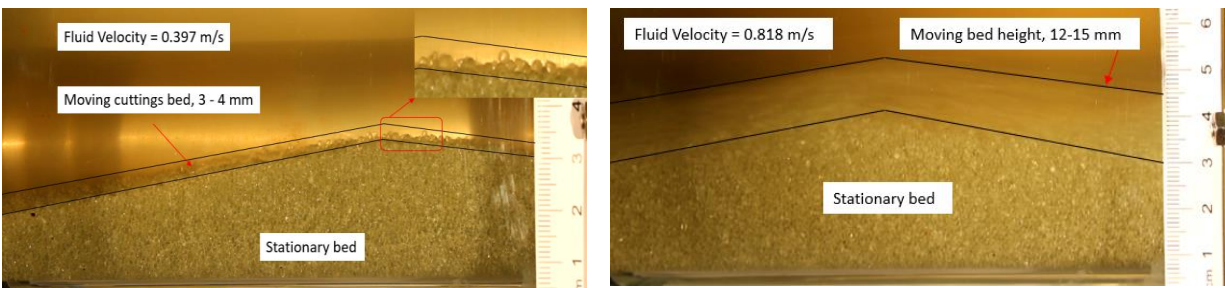


Figure B.1: Transient dune movement pattern at mud velocity 0.482 m/s with FZ 1.

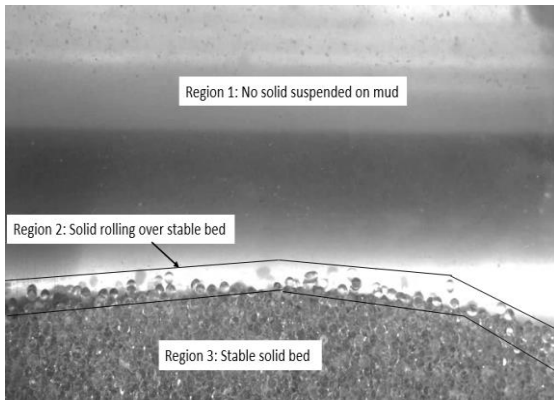


(a) $V_m = 0.397 \text{ m/s}$ ($Re = 2049$)

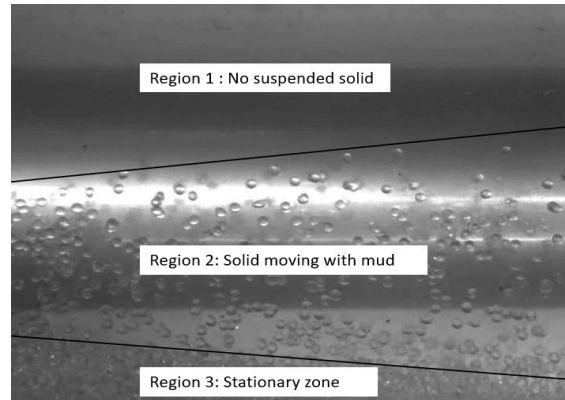
(b) $V_m = 0.818 \text{ m/s}$ ($Re = 6189$)

Figure B.2: Estimation of moving bed height at two different flow rates.

a) 3-4 mm thin moving bed for a mud velocity 0.397 m/s, and (b) 12-15 mm thick moving bed for a mud velocity 0.818 m/s.



(a) $V_m = 0.397$ m/s



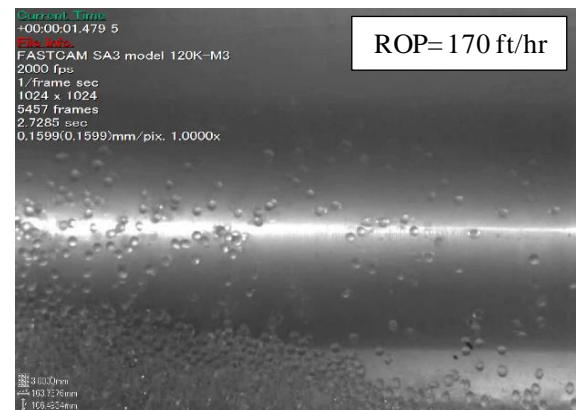
(b) $V_m = 0.65$ m/s

Figure B.3: Moving cuttings bed visualization with a high-speed camera.

a) Few rolling solids over the stationary cuttings bed at a mud velocity 0.397 m/s and no suspended solids, and (b) Significant solids moving in a suspended form at a fluid velocity 0.65 m/s with a very thin stationary bed.



(a) ROP= 85 ft/hr with a few suspended solids,



(b) ROP= 170 ft/hr with a significant amount of suspended solids

Figure B.4: High-speed camera visualization to show the effect of rate of penetration.

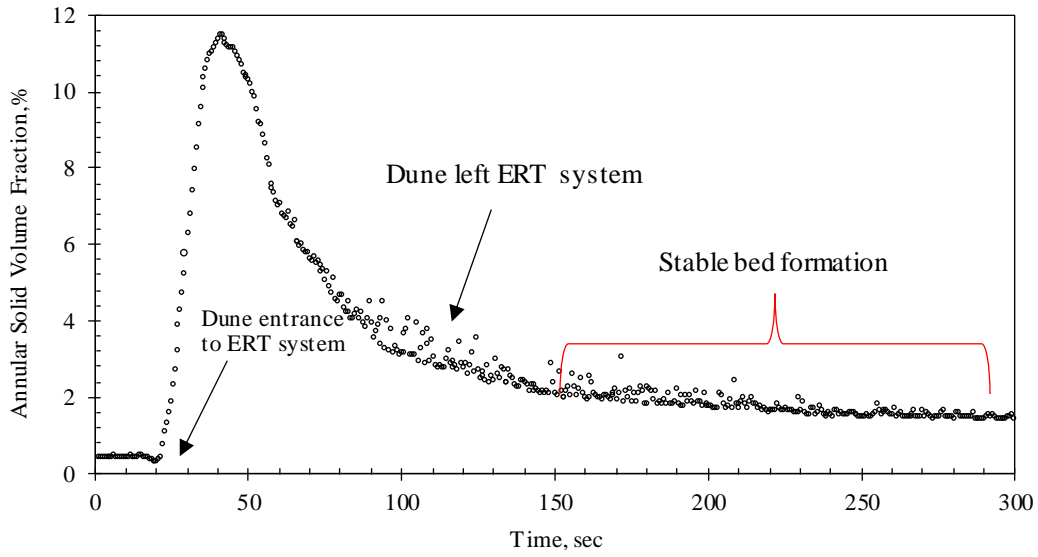


Figure B.5: ERT system shows stable solid bed profile in horizontal well.

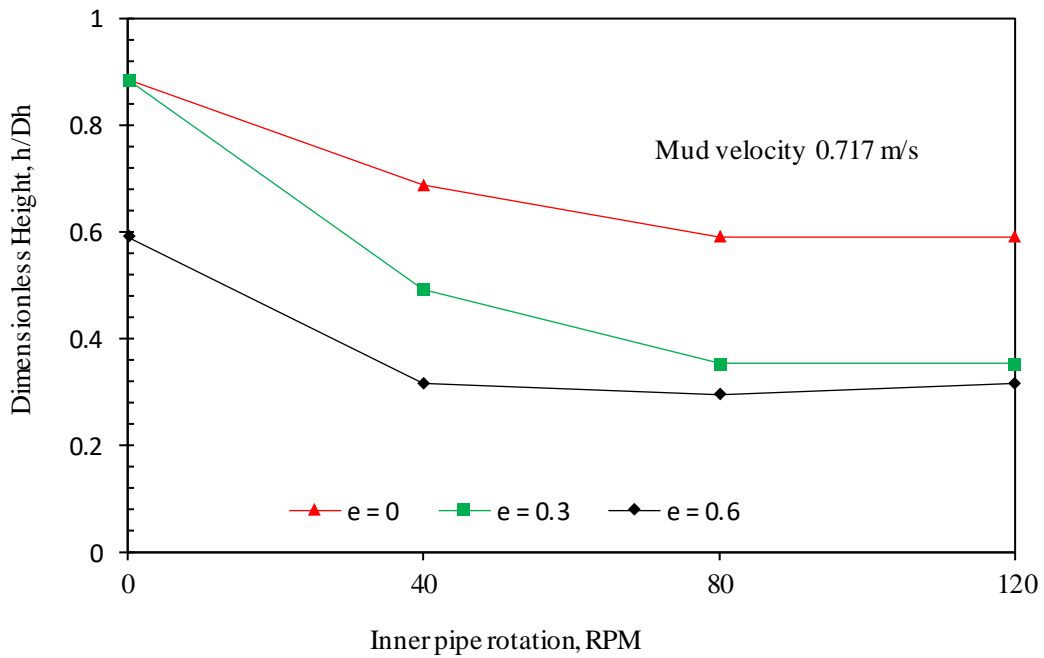


Figure B.6: Variation of bed height with inner pipe rotation for fluid FZ 1. An eccentric annular section ($e = 0.3, 0.6$) shows a less bed height, compared to a concentric annular section ($e = 0$).

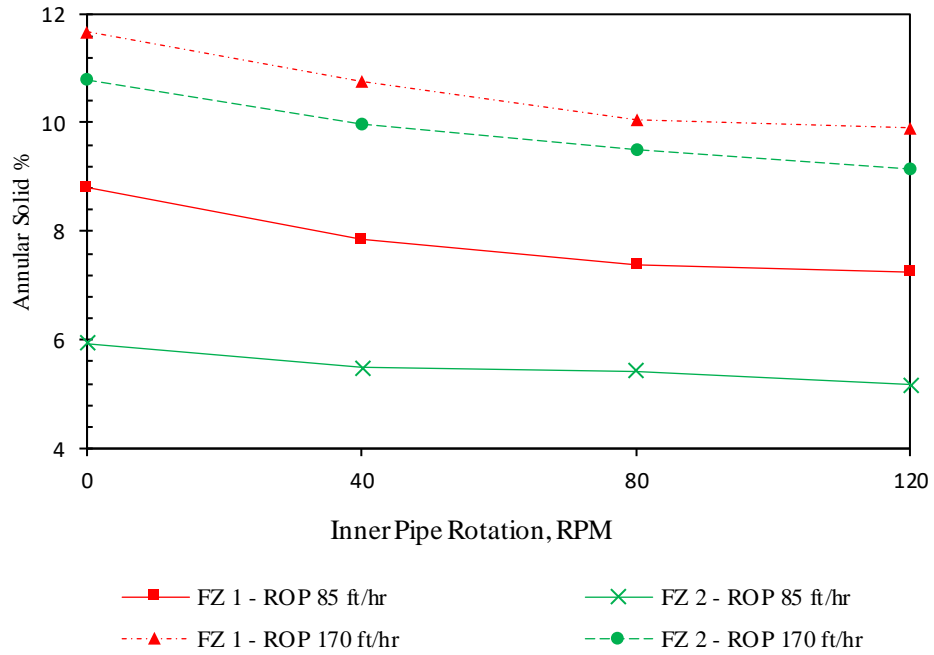


Figure B.7: Annular solid percentage as a function of drill pipe rotation.

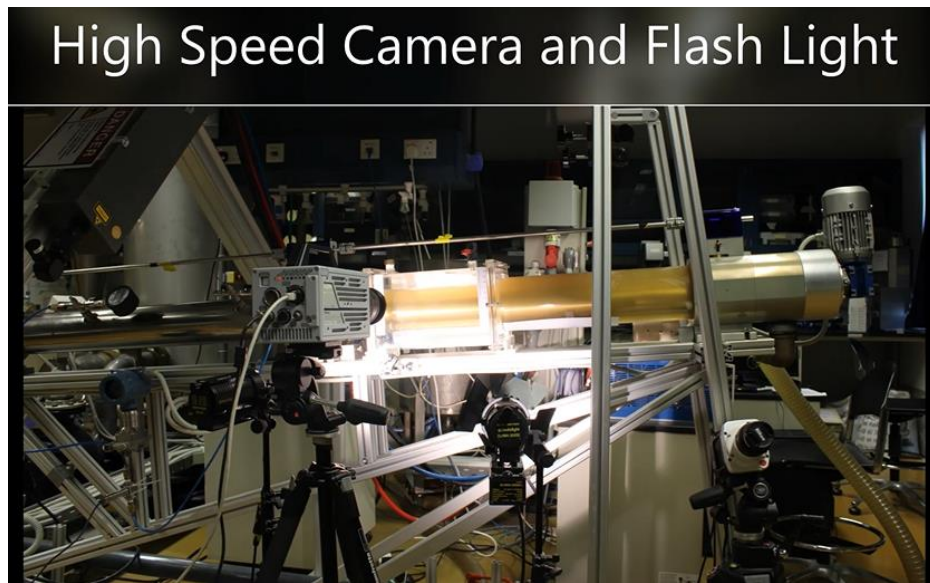
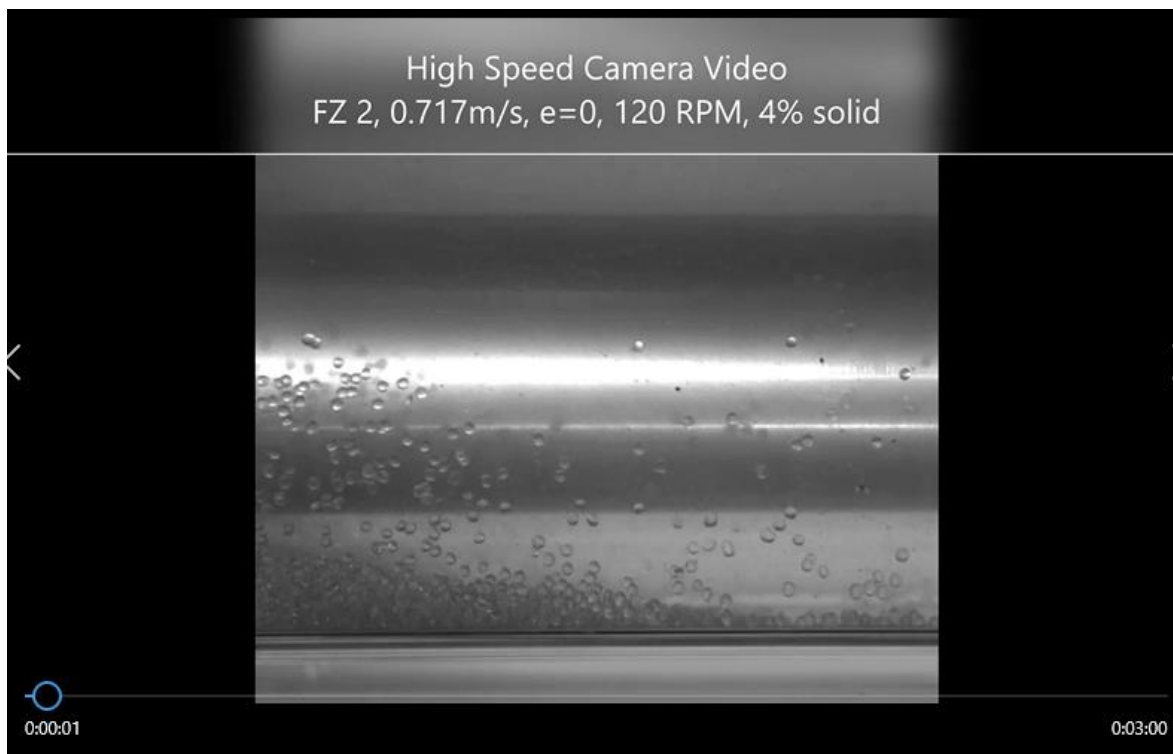


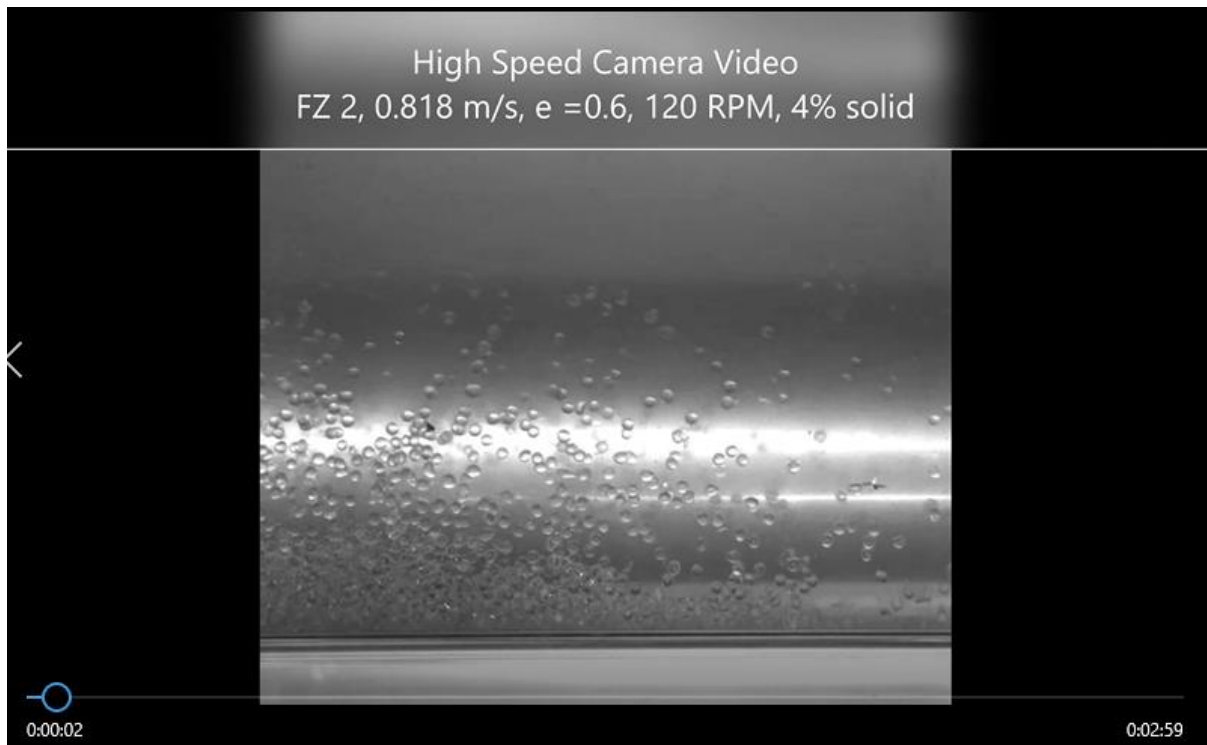
Figure B.8: Lab Image of high-speed camera and flashlight during an experiment.



Video B.1: High Speed Camera Video # 1 <https://youtu.be/0qv77fZBT0g>



Video B.2: High Speed Camera Video # 2 <https://youtu.be/Y1VwBRWrCPo>



Video B.3: High Speed Camera Video # 3 <https://youtu.be/Ib9usl8AaXQ>



Video B.4: DSLR Camera Video # 1 <https://youtu.be/y3kJSmvfdY>



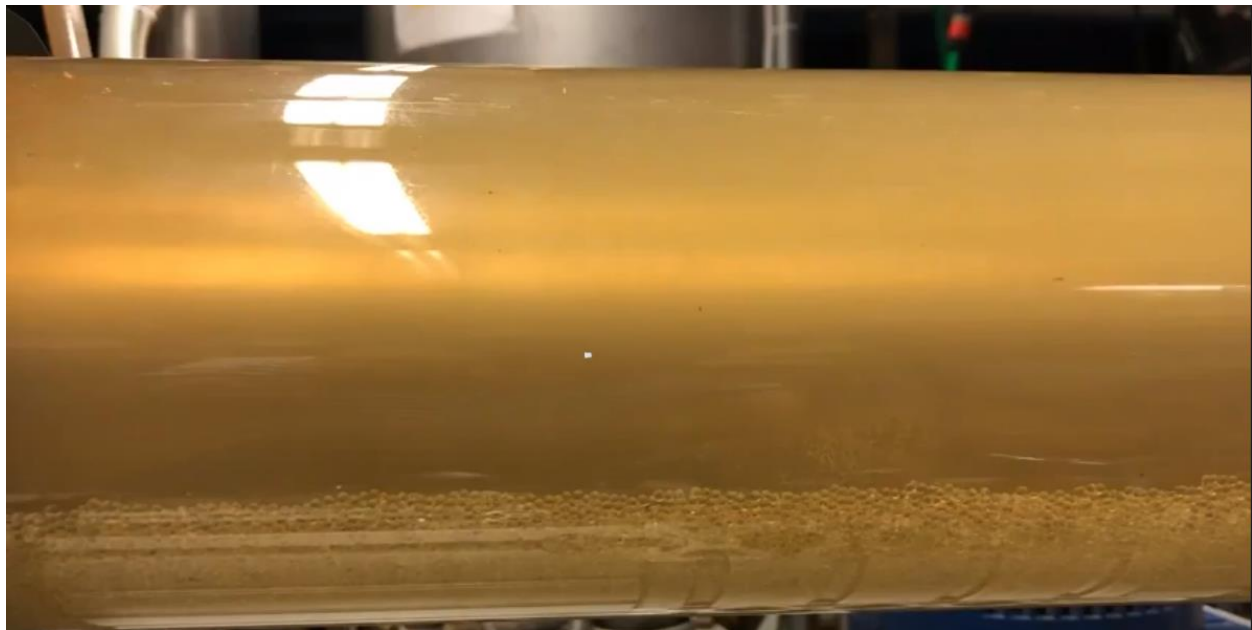
Video B.5: DSLR Camera Video # 2 <https://youtu.be/9cw3ImkSvoE>



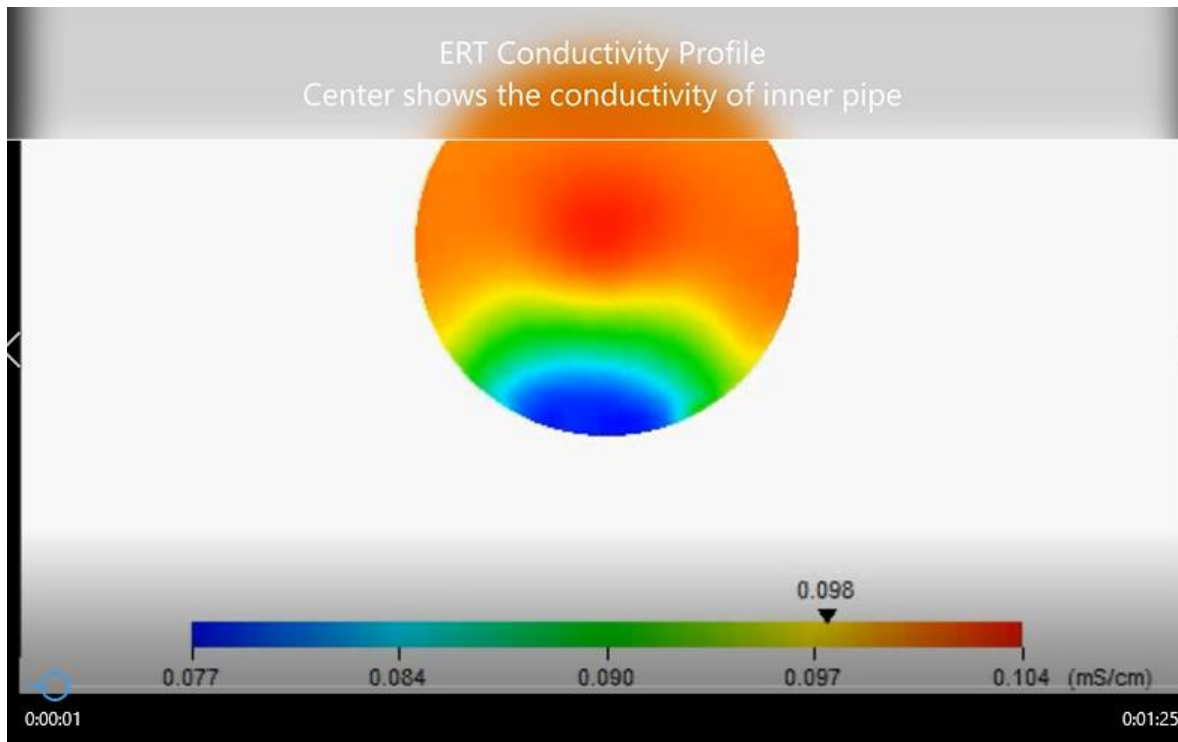
Video B.6: DSLR Camera Video # 3 <https://youtu.be/sndcVdaEmXU>



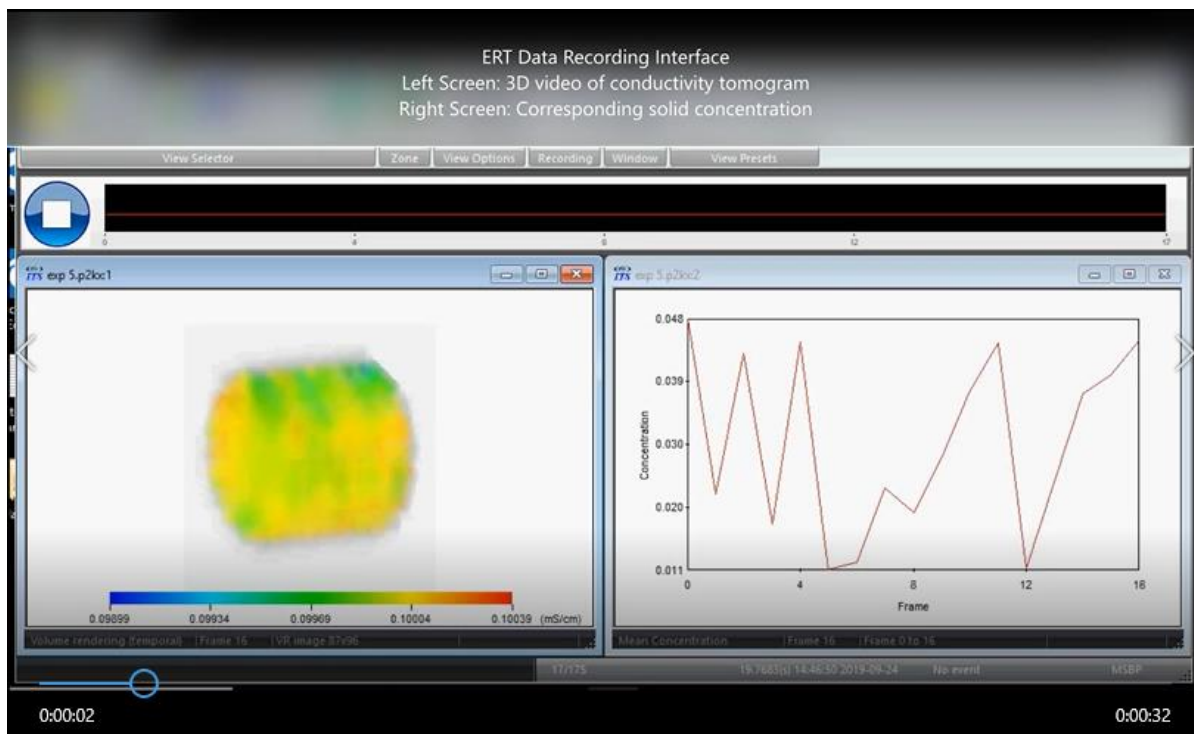
Video B.7: DSLR Camera Video # 4 <https://youtu.be/II7un1m1Agk>



Video B.8: Stationary bed formation video <https://youtu.be/hJi74QCpTM4>



Video B.9: ERT Video # 1 https://youtu.be/4q_BNLVf9AE



Video B.10: ERT Video # 2 <https://youtu.be/KhKFWWhTYki8>



Video B.11: Solid-Liquid mixing (Main Tank) Video: https://youtu.be/hCn_gNaAnT8



Video B.12: Mud preparation tank <https://youtu.be/rzZqk-7ywzc>



Video B.13: During an inclined well experiment run video <https://youtu.be/U1DLSmzAMaE>